CONTEMPORARY PROBLEMS OF POWER ENGINEERING AND ENVIRONMENTAL PROTECTION 2017

CLEAN ENERGY

TASTE OF THE FUTURE

EDITORS:
KRZYSZTOF PIKOŃ
LUCYNA CZARNOWSKA

Clean Alternative

SILESIAN UNIVERSITY OF TECHNOLOGY

Edited by Krzysztof Pikoń and Lucyna Czarnowska

CONTEMPORARY PROBLEMS OF POWER ENGINEERING AND ENVIRONMENTAL PROTECTION 2017

Gliwice, 2018

Scientific Editors: Krzysztof Pikoń, Lucyna Czarnowska

Technical Editors: Martyna Badera, Nismah Rizwan, Omais Abdur Rehman, Muhammad Ferdous Raiyan

Cover design: Muiz Sajid, Corinna Wróbel

List of Reviewers:

- prof. dr Tauseef Aized
- prof. dr Jamal Uddin Ahamed
- prof. dr hab. Teresa Grzybek
- dr hab. inż. Sylwester Kalisz, prof. nzw. w Pol. Śl.
- dr hab. inż. Sławomir Dykas
- dr hab. inż. Anna Skorek-Osikowska
- dr hab. inż. Adam Szurlej
- dr inż. Zbigniew Buliński
- dr inż. Jan Cebula
- dr inż. Lucyna Czarnowska
- dr inż. Adam Klimanek
- dr inż. Tomasz Sobotav
- dr inż. Karol Sztekler
- dr Muzaffar Ali
- dr Omar Huzain
- dr Radhika Joshi
- dr Tibor Poós
- dr Małgorzata Warwąg

ISBN 978-83-950087-1-9

Published by Department of Technologies and Installations for Waste Management

Available: http://cleanalternative.eu

Contemporary Problems of Energy and Environmental Protection

Technologies create great opportunities in the development of new ways to protect the environment and to improve the energy sector. All the problems that the new generation will have to face in the future can only be solved by investing in research and development. The challenges for future modern technologies are related to energy storage, fossil fuel economy and also better environmental performance.

Monograph “Contemporary Problems of Power Engineering and Environmental Protection” is the fifth volume of this scientific edition. It consists of manuscripts prepared by young scientists, mainly students, as well as scholars from different research fields. Their works were presented during the 5th ”Conference on Environmental Protection and Energy”. The conference took place on December 8th, 2017 in Gliwice, at the Center of New Technologies in the Silesian University of Technology. The conference was an excellent opportunity to share knowledge and ideas among participants who wanted to contribute to a better future, in harmony with the natural environment while securing energy needs of the society.

The event, as always, was organized entirely by students, as a part of the Project Management course and as one of the essential elements of the Pedagogical evolution development.

MSc Clean Fossil and Alternative Fuels Energy is focused on implantation of active learning and learning by doing methodologies. In addition to expert knowledge, the competencies in business and entrepreneurship are delivered to students. The Conference is an excellent example of shaping business and soft skills in the program curriculum. Students organized the conference using PRINCE2 project management skills acquired during Prince2 course. The organization of this event required a lot of effort, both in terms of planning and real activates. Though it was time-consuming, we believe this is a valuable experience for the students which will help them in future career.

We are proud of students’ commitment and skills, which we tried to develop and improve during the program activities.

We would like to express our appreciation to InnoEnergy for supporting MSc Clean Fossils and Alternative Fuels Energy program and the 5th Environmental Protection and Energy Conference.

Krzysztof Pikoń
Lucyna Czarnowska

Table of Contents

Supercritical power plant with CO_2 capture

Alicja Furmaniak[1], Łukasz Kiebdój[1], Mateusz Kuderski[1], Agnieszka Pociecha[1], Małgorzata Socha[1]

[1] Faculty of Energy and Environmental Engineering, Silesian University of Technology, e-mail: furmaniak.ala@gmail.com, lukasz.kiebdoj@gmail.com, mateusz300894@gmail.com, pociecha.agnieszka@o2.pl, malgorzata.sochaa@gmail.com

Abstract

The plants involved in the production of electricity are a significant emitter of harmful substances to the environment. One of these pollutions is CO_2, which is considered as emission caused the greenhouse gas effect. In today's world, hardly anyone can imagine life without electricity, so the total abandonment of the power plants is not an option. In order to reduce the carbon dioxide concentration in the exhaust gas, CCS Technology can be used. The article describes an example of a power plant with Carbon Capture and Storage Technology, which could be built in Poland. Thermodynamic analysis, the impact of it on the environment and the best place for the power plant were presented in this paper. To find the best location for the investment the region's demand for electricity, the existence of other power plants, availability of cooling water and the possibility of secure fuel delivery was taken into account. The article also describes the economic profitability of the selected power plant with CCS Technology.

Keywords: Supercritical power plant, carbon capture and storage, CCS, economic analysis, thermodynamic analysis

1. Introduction

Faced with increasing demand of electricity power industry has to implement measures that allow improving power plant engineering technologies in terms of power production growth or simultaneous harmful gases reduction, which were produced as a result of fossil fuel combustion such as: bituminous coal, lignite, peat, natural gas and natural oil.

In European Union electricity is produced in about 50% of coal and natural gas combustion. On the other hand in Poland, it is about 90%. [1] The harmful gases emission to the atmosphere could be a reason of greenhouse effect, environmental pollution and diseases. The main cause of this effect is human activity in some areas as: power plant engineering, industry or agriculture but also natural physicochemical processes which take place on earth, for example volcano eruption. Moreover, some chemical substances like NO_x, SO_2 and dust are produced during a combustion process. In this task, attention will focus on carbon dioxide reduction.

1.1 Definition of Carbon Capture and Storage

CCS (Carbon Capture and Storage) is a technology that can capture up in the best way almost from 80% to 90% of carbon dioxide emission produced from the fossil fuels combustion. The CCS chain consists of three parts: capturing the carbon dioxide, transporting the carbon dioxide and harmless storing the carbon dioxide [2] [3]. The biggest problems, which connected with this technology are relatively high costs of storing and transport. The main reason to build up and improve this kind of technology is environmental protection, because CO2 is one of the greenhouse gases, which has a harmful effect on the atmosphere.

Capture technologies allow the separation of CO_2 from gases produced in electricity and industrial processes by one of the three methods: pre-combustion, post-combustion and oxy-combustion. Firstly, pre-combustion methods take place before the coal is placed into the furnace; however, the coal should be converted into clean fossil. By contrast the post-combustion methods, where it is operated into exhaust gases. In other words, chemicals are used to purify the exhaust gases from harmful substances mainly from CO_2. The last one is an oxy-combustion and then burns the coal in an atmosphere with a higher concentration of oxygen.

This method makes that the exhaust gases have only CO_2 (90%) and water and then it is easily to separate CO_2. Even more, the oxy-fuel technique is cheapest than pre-combustion and post-combustion methods about 35% [3] [4].

1.2 Pre-combustion methods

This method is generally applied to coal-gasification. Otherwise the fuel reacts with oxygen, which was earlier separated in high temperature without combustion. The coal is gasified and product of this process is synthesis gas made from carbon monoxide and hydrogen. Then the gas is transported to shift reactor, where the synthesis gas is reacted with the water. The products such as: CO_2 and nitrogen. At the end CO_2 is captured, expanded to atmosphere pressure and stored. A hydrogen goes to combustion chamber, where is burned with oxidant and energy of exhaust gases could be used in a turbine. [5]

This method is generally applied to coal-gasification. Otherwise, the fuel reacts with oxygen. Oxygen was produced in air separation unit, and fuel was earlier separated in high temperature without combustion. The coal is gasified and product of this process is synthesis gas made from carbon monoxide and hydrogen. Then the gas is transported to shift reactor, where the synthesis gas is reacted with the water. The products such as: CO_2 and nitrogen. At the end, CO_2 is captured, expanded to atmosphere pressure and stored. A hydrogen goes to the combustion chamber, where is burned with oxidant and energy of exhaust gases could be used in a turbine. [5]

1.3 Oxy-combustion

In this method, fuel is burned with a high concentration of oxygen. After combustion, the flue gases consist CO_2 and water, which are ingredients of exhaust gases and are recycled in 80% to the combustion chamber. The main aim to recycle exhaust gases is providing a correct conditions of combustion for example: keeping a correct flame temperature, heat transfer in boiler, etc. Although the 20% of gases are used to processes such as: coal drying or fuel transporting. In this technology, the researchers are still progressing about the modernization of oxygen generator, because this component is the highly energy-intensive. [5]

1.4 Post-combustion methods

The post-combustion methods are the most popular used in CCS technology and the reasons are: relatively cheap and simple construction. The CO_2 can be captured from the flue gases by suitable sol vent. The absorbed CO_2 is liberated from the solvent and is compressed for transportation and storage. Other methods for separating CO_2 include high-pressure membrane filtration, adsorption/desorption processes and cryogenic separation. [5]

1.4.1 Chemical Absorption

In this case, it is possible to separate a carbon dioxide from the flue gas of the power station by bubbling gas through an absorber packed with liquid solvents such as ammonia, which absorbs the CO_2. In next step, the rich in CO_2 sorbent is transported from absorber to stripper, where the temperature of substance is warming up through heat transfer to a stripper. The intensification of heat transfer in this component is connected with capability of absolute separation a carbon dioxide from sorbent. Next, the CO_2 is drying, compressed and captured. Although clean sorbent comes back to absorber column. [6]

2. Thermodynamic Analysis

The plant is based on supercritical block with CO_2 capture [7]. Its simplified scheme is shown on Figure 1.

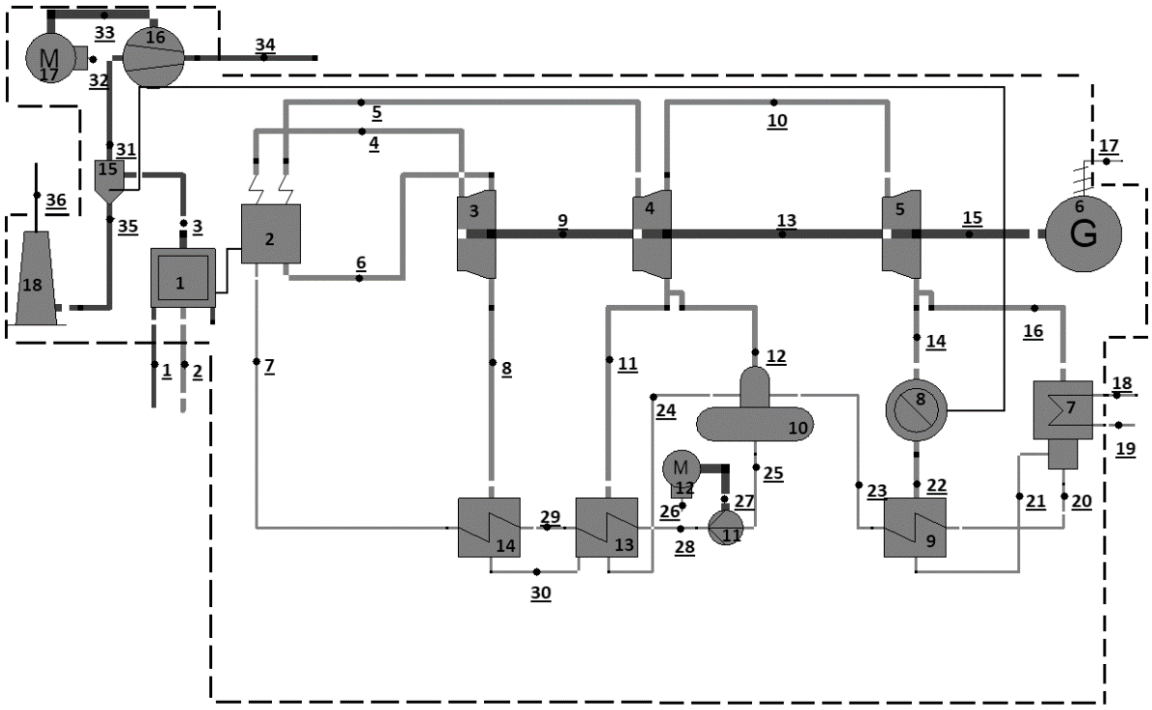

Fig. 1 Super Critical Power Plant with CCS.

Basic Information about the analysed Plant:

- Gross Plant Power: 642 MWe,
- Net Plant Power: 550 MWe,
- Net Plant Efficiency (with CCS): 32.5%,
- CO_2 Emissions: 97 kg/MWh.

For the Supercritical system feed water enters the bottom part of the economizer and passes upward through the economizer, which support the primary superheater. Water then flows upward through the furnace hopper and furnace wall tubes. From the furnace, water flows to the steam water separator. Steam flows from the separator through the furnace roof to primary superheater. From the platens, the steam flows through to the intermediate superheater. The steam then flows to the final superheater and on to the outlet pipe terminal. Steam returning from the turbine passes through the primary reheater. The crossover piping feeds the steam to the final reheater banks and then out to the turbine (3). The pulverized coal (PC) and air mixture flows to the coal nozzles at various elevations of the furnace. The hot combustion products rise to the top of the boiler and pass through the superheater and reheater sections. The gases then pass through the economizer and air preheater. The gases exit the boiler (3) and flow to CO_2-removal system (15) and stack (18).

A boiler of this capacity employs approximately 24 to 36 coal nozzles. Each burner is designed as a low-NO_x configuration, with staging of the coal combustion to minimize NO_x formation. The function of the main steam system is to transport main steam from the boiler superheater to the high pressure (HP) turbine. The function of the reheat system is to transport steam from the HP turbine exhaust to the boiler reheater and from the boiler reheater outlet to the intermediate pressure (IP) turbine (4).

The crushed coal is fed through feeders to each of the mills (pulverizers). Next, the coal is distributed to the coal nozzles in the furnace walls using air supplied by the primary air (PA) fans. The furnace bottom comprises several hoppers, with a clinker grinder under each hopper. Ash discharged from the hopper, it is transferred to trucks for offsite disposal.

The function of the extraction steam system is to transport steam from turbine extraction points through the following routes:

- from HP turbine extraction to heater 14,
- from IP turbine extraction to heater 13 and the deaerator (10),
- from LP turbine extraction to heaters 8.

The addition of CO_2 capture (15) and compression to PC case results in an efficiency 8.2 absolute percent. The efficiency is negatively impacted by the large auxiliary loads of the capture process and CO_2 compression, as well as the large increase in cooling water. The capture cases result in a 90% reduction of carbon. Carbon Dioxide Remover (CDR) (15) is used, along with compressors (16) to remove 90% of the CO_2 in the flue gas exiting. The CDR is comprised of the pre-scrubber, CO_2 absorber, CO_2 stripper, and absorbent purification unit.

The CO_2 recovery process is based on system designed by Shell Company. It consist of a few sections in the Cansolv absorber. The first are used for CO_2 absorption, and the final section is a water-wash section The flue gas enters the absorber and flows counter-current to the Cansolv solvent. Approximately, 90% of the inlet CO_2 is absorbed into the lean solvent, and the remaining CO_2 exits the main absorber section and enters the wash section of the absorber. Hot amine is collected, removed, and pumped through a heat exchanger. The cooled amine is then sent back to the absorber just above the final packing section.

The gross efficiency of electricity was calculated using the Equation 1.

$$\eta_{el\_g} = \frac{N_{el\_g}}{\dot{m}_f LHV} \tag{1}$$

Where,

$\dot{m}_f$ mass flow rate of fuel, (kg/s),

N_{el_g} gross electric power, (MW),

LHV lower heating value, $\left(\frac{MJ}{kg}\right)$.

In this paper, the Polish hard coal with the chemical composition shown in the Table 1 was used for further calculations.

Tab. 1 Capital Expenditures - CAPEX.

No.	Element	Elemental share
1	C	0.795
2	H	0.053
3	O	0.126
4	N	0.015
5	S	0.011
Lower heating value (LHV) is equal 23000 kJ/kg.		

The net efficiency of electricity calculated using the Equation 2.

$$\eta_{el\_n} = \frac{N_{el\_b} - N_{el\_AUX}}{\dot{m}_p LHV} \tag{2}$$

Where,

N_{el_AUX} Auxiliary Load Summary, (MW).

Tab. 2 Auxiliaries block with CCS.

No.	Equipment	Value	Units
1	Electrostatic precipitator	71.29	kW
2	CO_2 Compression	90.41	MW
3	Motor (12) (17)	25.83	MW
TOTAL		116.95	MW
4	Heat for CCS system	338.4	MW

For the heat supplied to the CCS installation (338.4 MW), a heat flux to the desorber was obtained at a level of 1.84 MJ/kg CO_2 removed

The unit CO_2 emission factor charged to the unit of produced energy was calculated using the Equation 3.

$$\varepsilon_{el,CO2} = \frac{\dot{m}_p LHV \cdot \varepsilon_{p,CO2}}{E_{el,n}} \tag{3}$$

Where,

$\varepsilon_{p,CO2}$ CO_2 emission unit load factor, (-),

N_{el_n} Net power, (MW).

For block with CCS, it is 141.24 $\frac{kgCO2}{MWh_n}$

3. Economic Analysis

3.1 Expenditures and revenue data

For an investor, who would like to invest in a specific plant, the proposed solution must be profitable. We want the plant reimbursement and start to make profits in the shortest possible time.

The CAPEX (CApital EXpentiture) as well as OPEX (OPerational EXpenditures) is calculated and presented in Tables 3 and 4. Using information from the NETL report (The National Energy Technology Laboratory) [7] the estimates of expenditures were made. Expenditures were updated for year 2017 using the CEPCI (Chemical Engineering Plant Cost Index) according to the Equation 4.

$$I_{2017} = I_{2011} \cdot \left(\frac{CEPCI_{2017}}{CEPCI_{2011}}\right) \tag{4}$$

Where,

I_{2017} cost in 2017, (zł),

I_{2011} cost in 2011, (zł).

$CEPCI_{2017}$ for 2017 is 562.1 and the value of $CEPCI_{2011}$ is 585.7. Dollar exchange rate is assumed to be 3.84 zł/$. This is the average exchange rate of the dollar in the period from January 2015 to November 2017. [8]

Tab. 3 Capital Expenditures - CAPEX.

No.	Description	Total Plant Cost	
		zł	zł/kW
1	Total plant cost	7 146 270.03 zł	12 990.58 zł
2	Pre-Production Costs	221 429.59 zł	401.69 zł
3	Inventory Capital	151 556.82 zł	276.40 zł
4	Other Costs as land, other owner's costs or financing costs	1 268 205.39 zł	2 314.24 zł
TOTAL:		8 787 461.84 zł	
Total CAPEX with risk multiplier (equals 1.14 - high-risk 25 year)		10 017 706.49 zł	

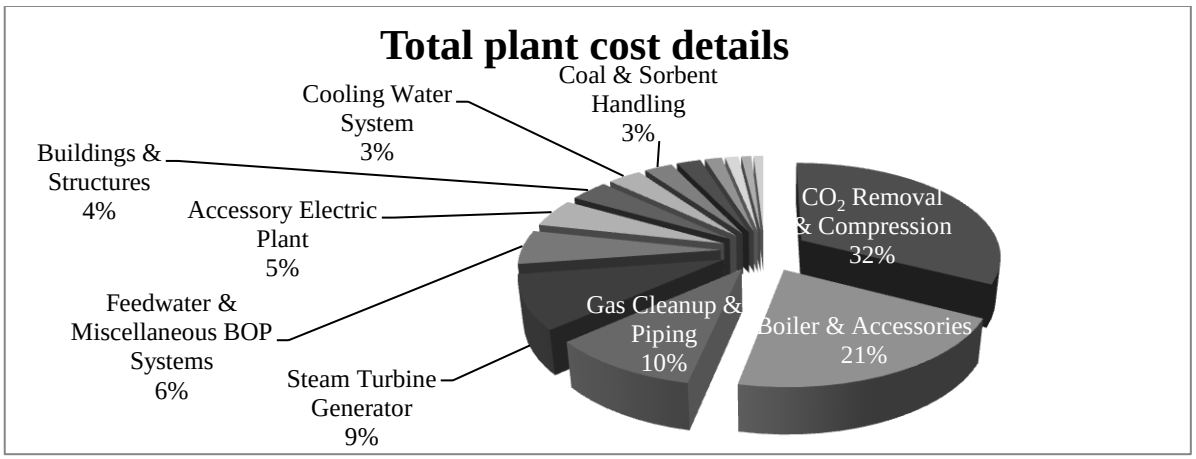

Fig. 2 Total plant cost details.

Tab. 4 OPEX - initial and annual operating and maintenance costs.

No.	Description	Cost
		zł
1	Annual Operating, Maintenance Labor and Administrative & Support Labor Costs[A]	54 096 041.56
2	Maintenance Material	63 360 292.81
3	Consumables[B]	107 921 655.87
4	Waste Disposal and Air Emission Charges (Poland)[C]	136 077 649.24
5	Fuel - Coal Cost[D]	650 891 109.39
TOTAL		1 012 346 748.88

[A] Including 11 operators, 2 skilled operators, 1 foreman, 3 accountants or secretaries, 2 lab tech's and 1 director per 8-houred shift (4 shifts per day). [9]

[B] Including, among others, water [10], makeup and waste water treatment chemicals, limestone, hydrated lime, activated carbon, CO_2 Capture System chemicals, triethylene glycol, ammonia or SCR catalyst. [7]

[C] Including Amine Purification Unit Waste, Thermal Reclaimer Unit Waste, Prescrubber Blowdown Waste [6], Polish Air Emissions and sewage disposal Charges [10] [11], EU ETS [12].

[D] Average coal price in the period from November 2015 to November 2017 from ARA is equal 83.04 $/t [13]. Final price after taking into account the charges for the coal transport is 95.50 $/t [14] [15].

Revenue, presented in Table 5, mainly came from sales of electricity energy produces by plant. Analysis made in the assumption that gypsum and ash will be sold in 100%.

Tab. 5 Revenues per year.

No.	Description	Amount per year	Cost per unit	Total cost per year
1	Electrical Energy[E]	3923974.08 MWh/year	175.00 zł/MWh	686 695 464.00 zł
By-Products				
2	Gypsum[F]	101 t/year	604.16 zł/t	61 020.16 zł
3	Ash[G]	705 t/year	20.00 zł/t	14 100.00 zł
TOTAL:				686 770 584.16 zł

The cost of plant liquidation was took as 30% of the total plant cost. Also is assumed that the financial calculation has been done using standard loan, its share in CAPEX is 70%, with the interest rate of 2.74% and inflation of 1.5% per year and it will be repaid after 15 years. Income tax was calculated according to the Polish tax rate, which was took as 19% [16]. It is paid only when revenues are positive. In addition, the analysis period is assumed 25 years.

3.2 Economic profitability

For checking profitability of the plant the NPV (Net Present Value) was calculated. It represents a profit in a particular year and it will be expressed in PLN at the present time. The NPV depends on the value of the discounted Cash Flow according to the Equation 5 and 6 and its value is shown on the Figure 3 [19].

$$NPV = \sum_{t=o}^{N} \frac{CF_t}{(1+r)^t} \tag{5}$$

$$CF_t = -J_{0,t} + S_{n,t} - K_t - P_{d,t} + L_t \tag{6}$$

Where,

Jo,t	CAPEX, (zł),
Sn,t	Revenues, (zł),
Kt	OPEX, (zł),
Pd,t	Income tax, (zł),
Lt	Liquidation cost, (zł),
r	Discount rate, (-), took as 1.48% [18].

[E] 525.85MW - calculated power, assumed 311 working days.
[F] 80% of the price of gypsum in the building wholesale [17].
[G] Based on prices of ash imported from Ukraine [18].

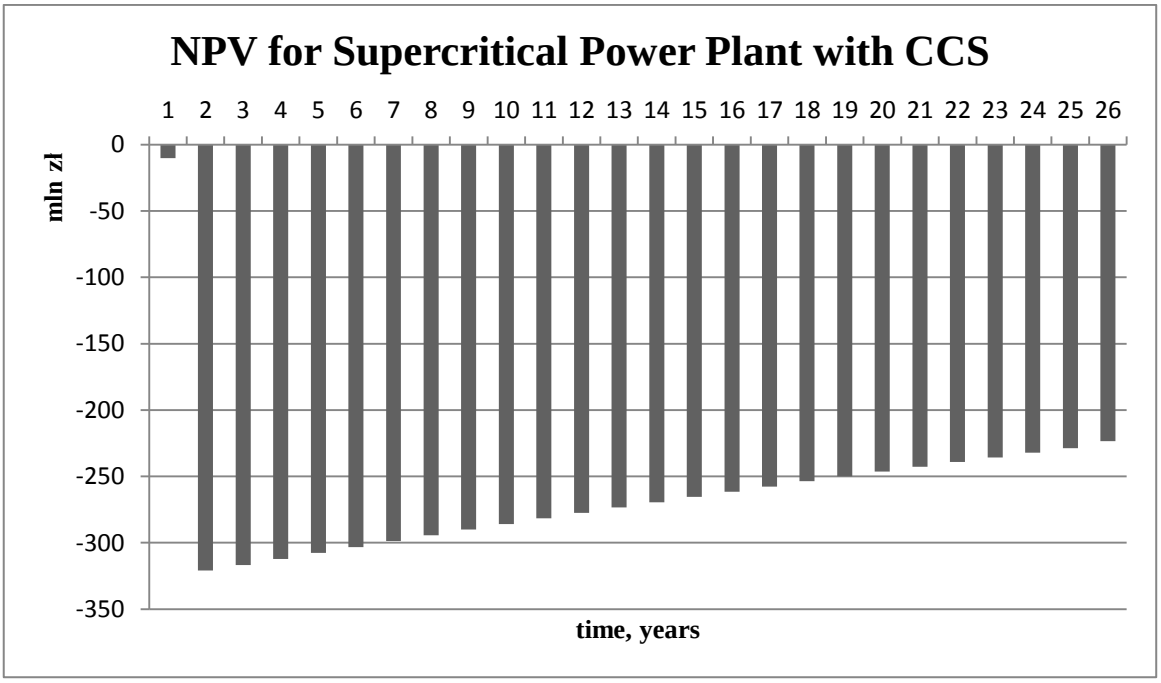

Fig. 3 NPV through Plant activity years.

The NPV is negative during all plant activity period. Every single year of its activity brings losses. The financial liquidity in 25th year shows that the plant loss is more than 8.15 billion zloty.

4. Improvement of profitability

Investing in a CCS power plant turned out to be unprofitable from an economic point of view. Although the analysed plant emits less harmful substances, due to the CCS installation, which lowered the CO_2 emission eight times, it is very unlikely that any investor will invest in this kind of power plant because it will never pay off.

In order to improve the profitability of the power plant and lead it to reimbursement at least in the last year of plant activity, the minimum price of the produced electricity was calculated. The amount received is 258.16 zł. The NPV distribution over time for this option is shown in Figure 4. By comparing the electricity price received to the market one, which average, within 2 years, is 159.08 zł [26], it is unlikely that this product will find buyers.

Some years ago there was quite similar situation with energy from renewable energy sources. It was often unprofitable so it wasn't very attractive for investors. Due to implementation of Poland's Energy Policy until 2030 Project, which is part of polish support mechanisms for electricity production in cogeneration and from renewable energy sources, production of electricity from renewable energy sources is now more profitable and therefore more popular among investors. It was mainly caused by putting the certificates of origin into effect.

If the Poland also decides to support the generation of electricity produced with reduced CO_2 emission, plants with CCS would probably start to appear more often. The minimum amount of support with certificates of origin, which will lead the plant to reimbursement in the last year of plant activity, is 83.16 zł. The NPV distribution over time for this option is shown in Figure 4.

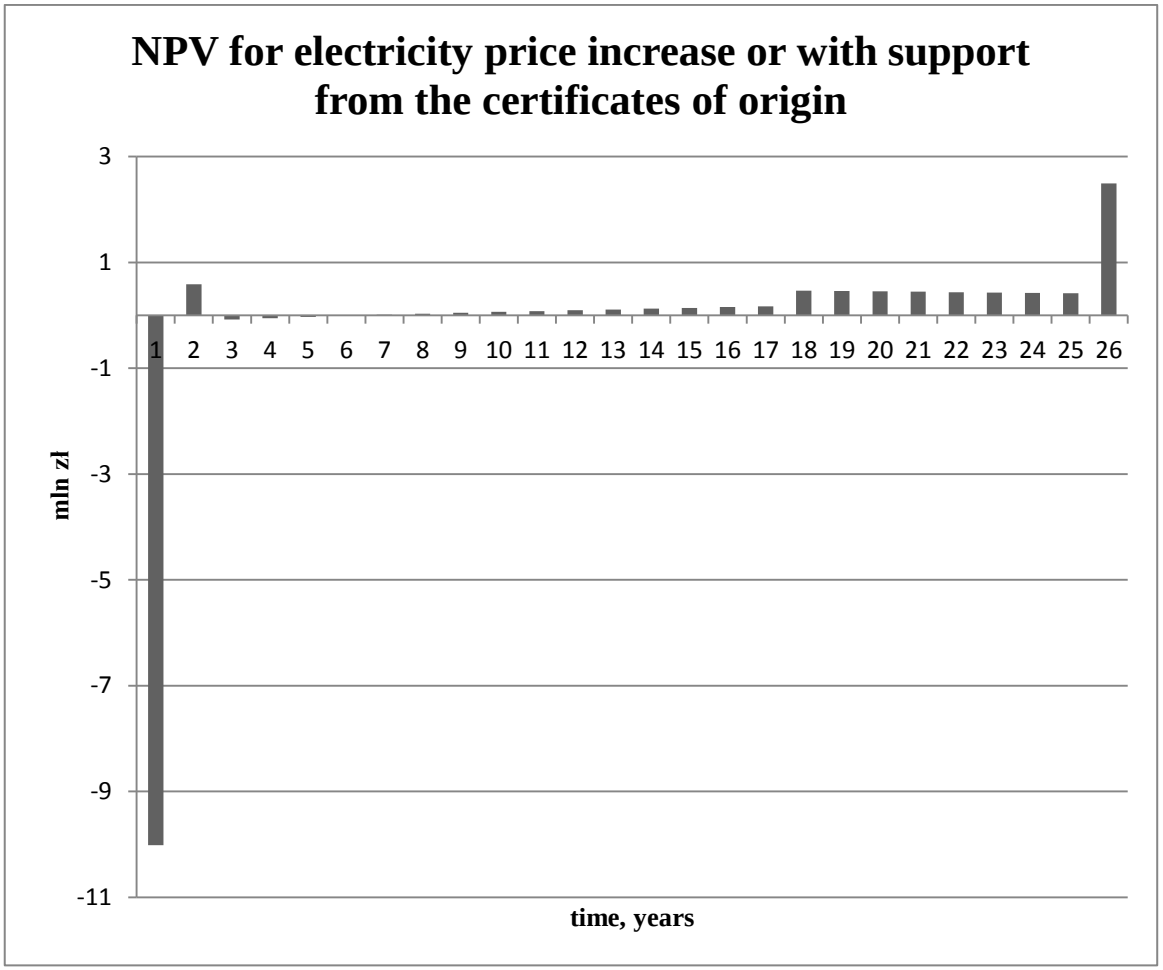

Fig. 4 NPV through Plant activity years for electricity price increase or with support from the certificates of origin.

5. Environmental Protection and Energy Policy

Nowadays, in all of the world a lot of power plants produce a significant amount of harmful gases emissions, CO_2 included. Our power plant with CCS Technology is special because it reduces most of the CO_2 emissions.

Actually, why we try to decrease harmful emissions? It is all about environmental protection. Environmental protection is crucial because we live and breathe in this area, so we want to have it clean and friendly. We do not want to have our country or planet to be dirty.

It all started when EU ETS was accepted in 1997 in Kioto. It says that we have to reduce the emission of gases, first of all, CO_2. Apart from CO_2 emissions, we have other harmful gases like: SO_2, CO, NO_x. These are generally produced by power engineering, industry, transport, civil engineering and exploitation. These cause for example smog and in some countries, people use special masks because of it (in Poland too). Harmful gases also cause acid rains, some illnesses like respiratory disease, greenhouse effect. These gradually change a climate what is dangerous for our planet. Poland had been obligated to reduce harmful gases 6% compared to 1988.

One of the most important European Union's functions in Energy Policy's scope is to reduce harmful gases, especially CO_2. As a result of coal combustion, CO_2 emission is about 34% world's emission this gas to the atmosphere. Over the years there are conducted some movements connected to low carbon economy

to counteract negative influence on the environment. There is an Energy Policy and special regulations related to reducing the emissions.

There is "Climate and Energy Package" [19] which was signed in Poland in October 2014. It says that the European Union has to increase renewable Energy sources to 27%, reduce harmful gases 43%, increase an energy efficiency about 27%. These obligations for EU are for the 2030 year which is higher compared to previous climate and energy package when these obligations were on 20% level. "Climate and Energy Package" establish nuclear power evolution, clean technologies evolution, Carbon Capture and Storage Technology evolution and renewable sources evolution. CCS and clean coal technologies could make a key role in transiting Poland to low carbon economy. Due to to implementation CCS Technology it could be possible to reduce emissions of CO_2 about 50% in next future decades.

Poland has an implement from CCS Directive, which was signed in September 2013 [21] [22]. It says that CCS Technology can be built with Plants which have the power of installation for combustion of fuels higher than 300 MW and only for the demonstration projects now because this technology for today (to the 2014 year) is only for exploration. Maybe in the future, this resolution will be used on an industrial scale. Carbon has to be storage at least 100 meters under the ground or under the sea. To transport and storage CO_2 is needed to have a special concession from the Minister of Environment.

Summarizing all facts about Energy Policy and Environmental Protection, European Union is leading to reduce harmful gases by using clean carbon technologies like CCS, oxy-combustion, combustion with biomass. They should seek to increase use of renewable sources like power from sun, water, wind and earth.

6. The best place for Power Plant in Poland

Before choosing the best place for the construction of a power plant in Poland we should reflect on the current situation of the power industry in the world. The most important issue in the analyzed subject is CO_2 emissions. The concentration of industrial emission depends on area. According to the International Energy Agency, China is on the top of ranking with the highest concentration of CO_2. Two years ago China produced 9.7 $GtCO_2$. The United States of America produced 5.6 $GtCO_2$- they were in second place. Third was India with 2.6 $GtCO_2$ to atmosphere. Fortunately, Poland was not in the top 20 in Global Carbon Atlas, although in 1960 to 1989 we ranked on 10th [23].

Poland has been a member of the European Union since 1 May 2004. In the European Union all countries emitted 3.4 $GtCO_2$ in the course of burning fossil fuels. This means that the European Union emits almost three times less greenhouse gases than China. Most of the pollutants in the European Union emit our western neighbours. Germany is responsible for 23% of total CO_2 emissions in the European Union. The United Kingdom was second (12.5%), than Italy (10.6%) and France (9.9%). In fifth place was Poland which emitted 9.2% all carbon dioxide into the atmosphere in the EU [22]. In Poland, electricity is produced by thermal power plants, water and wind power plants. Last year our total installed power was 40.14 GW. This is enough power to meet ours domestic needs. Most of the energy is produced by thermal power plants using coal and lignite.

As it is well known, to find the best location to build power plant firstly we should prepare extensive analysis of customers' needs. We considered 16 possible provinces. The most important issue during the analysis was the availability of other power plants [24]. Due to the fact a small number of power plants are located near the sea, we decided to locate our power plants in the Warmiańsko-Mazurskie Voivodeship. In this region is only one combined heat and power (CHP). The second most important aspect in choosing a power plant is the ability to deliver fuel (in this case, coal). There are two possibilities to deliver fuel to the newly built power plant.

Due to the distance of the selected region to the sea (10 km) there is a possibility of transporting coal by sea. The area was also chosen due to the availability of railway tracks. The power plant is located 3 km from the station - it is possible to build a conveyor belt transporting coal from the station to the power plant. Land development was also taken into consideration. The selected location is a green area mainly of meadows, without residential areas. In the indicated area does not run the network (gas, heat and energy). In order to reduce

operating costs, the power plant will be located near the lakes. The cooling water will be taken from Niegocin Lake.

Referring to the subject of CO_2 capture, one of the elements of selecting a specific location was also the possibility of storing CO_2 on the seabed. It is also suitable regarding a number of other power plants in this region. The largest power plants in Poland are located in central and western part of the country. The new power plant will satisfy the energy needs of customers from the north.

The location chosen is the best possible variant. It fulfils all of these assumptions. Location is shown in Figure 5.

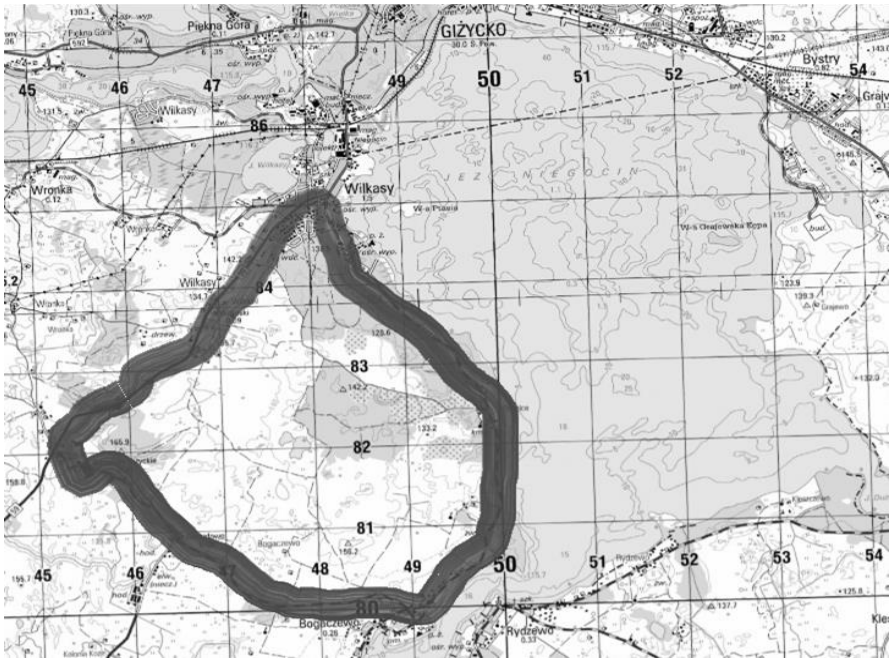

Fig. 5 Marked Power Plant localization next to Niegocin Lake in the Warmiańsko-Mazurskie Voivodeship [25].

7. Summary

We analyzed a Supercritical coal-fired Power Plant for a gross power of 642 MW with an integrated Carbon Capture Storage. The installation of Carbon Capture Storage results in a decrease in net efficiency by 9.96% in comparison to the non-CCS reference system. This is mainly due to the heat taken from the turbine tapping used in the sorbent separation and due to the high energy consumption of the carbon dioxide (CO_2) compression up to 15 MPa, which are required for transport and storage.

Economic analysis shows that the investment is unprofitable. For the electricity price of 175 zł/MWh, the investment brings losses during its entire activity. Due to the CCS, the emissions of CO_2 per MWh was nearly eight times lower than before, which contributes to environmental protection.

From the ecological point of view, power plant with CCS integration is fully reasonable. However, the economic analysis shows that it is not profitable. The economic analysis not always go hand in hand with the ecological one. Without a financial support from Polish Government or EU, for example by implementing new certificates of origin, the power plants like the analysed one have a little chance of being build.

Acknowledgment

This article was prepared within the projects Innovative Systems for Fossil Fuels Conversion and Thermoeconomic Analysis in Power Engineering carried out at Faculty of Energy and Environmental

Engineering, Institute of Thermal Technology, the field of study Power Engineering - Thermal Energy Systems. Work was conducted under the direction of Lucyna Czarnowska, PhD.

References

[1] Overview of electricity production and use in Europe, https://www.eea.europa.eu/data-and-maps/indicators/overview-of-the-electricity-production/assessment, date of access: (20/10/2017).
[2] CCS Association, http://www.ccsassociation.org/why-ccs/policy-and-regulation-for-ccs/, date of access: (17/10/2017).
[3] CCS Browser - A Guide to CO2 Capture and Storage, https://www.ccsbrowser.com/, date of access: (20/10/2017).
[4] ZEP, http://www.zeroemissionsplatform.eu/, date of access: (18/10/2017).
[5] Global Institute, www.globalccsinstitute.com, date of access: (18/10/2017).
[6] Sintef, http://www.sintef.no/en/, date of access: (18/10/2017).
[7] National Energy Technology Laboratory, *Cost and Performance Baseline for Fossil Energy Plants Volume 1a: Bituminous Coal (PC) and Natural Gas to Electricity Revision 3*, DOE/NETL-2015/1723, 2015.
[8] Kurs wymiany walut - USD, https://www.bankier.pl/waluty/kursy-walut/nbp/USD, date of access: (18/10/2017).
[9] Wynagrodzenia w Polsce, https://wynagrodzenia.pl/, date of access: (18/10/2017).
[10] Obwieszczenie Ministra Środowiska z dnia 31.08.2017 r. w sprawie wysokości stawek opłat za korzystanie ze środowiska na rok 2018
[11] Rozporządzenie Ministra Środowiska z dnia 4 listopada 2014 r. w sprawie standardów emisyjnych dla niektórych rodzajów instalacji, źródeł spalania paliw oraz urządzeń spalania lub współspalania odpadów
[12] Raport z rynku CO_2, http://www.kobize.pl/uploads/materialy/materialy_do_pobrania/raport_co2/2017, date of access: (18/10/2017).
[13] Notowania cen węgla ARA, http://gornictwo.wnp.pl/notowania/ceny_wegla/, date of access: (18/10/2017).
[14] K. Stala-Szlugaj, *Analiza kosztów transportu w cenie węgla dla energetyki*, 2012
[15] K. Stala-Szlugaj, *Koszty dostawy węgla kamiennego do wybranych użytkowników*, 2015
[16] Stawka podatku dochowego w Polsce, http://www.finanse.mf.gov.pl/cit/settlement1, date of access: (20/10/2017).
[17] Cennik budowlany, http://cennik-budowlany.pl/cement_wapno_i_gips.html, date of access: (16/11/2017)
[18] Sprzedaż hurtowa popiołu, https://pl.all.biz/, date of access: (20/10/2017).
[19] P. Gładysz, B. Melka, *Prezentacja do zajęć laboratoryjnych z przedmiotu Inżynieria Finansowa w Energetyce*, Gliwice 2016
[20] Pakiet 2012-2030, http://www.kobize.pl/pl/article/pakiet-energetyczno-klimatyczny-ue/id/389/pakiet-2021-2030, date of access: (17/10/2017).
[21] D. Dybka, *Regulacje prawne i polityka związana z wychwytywaniem i składowaniem CO_2*, http://www.pgnig.pl/documents/10184/255278/regulacjeprawneipolityka.pdf/0fbfd580-f67d-4393-8cd3-f863ec1aca13, date of access: (17/10/2017).
[22] Z. Kozłowski, K. Piotr, *Implementacja Dyrektywy CCS w Polsce*, http://www.cire.pl/item,85976,14,0,0,0,0,0,implementacja-dyrektywy-ccs-w-polsce.html, date of access: (17/10/2017).
[23] Najwięksi emitenci CO_2, http://www.green-projects.pl/2016/04/najwieksi-emitenci-co2-niechlubny-ranking/, date of access: (20/10/2017).
[24] Sektor energii w Polsce, http://www.rynek-energii-elektrycznej.cire.pl/, date of access: (20/10/2017).
[25] Geoportal Mapy, http://mapy.geoportal.gov.pl/imap/, date of access: (20/10/2017).
[26] Towarowa Giełda Energii, Dane giełdowe - Raporty Miesięczne, https://tge.pl/pl/155/raporty-miesieczne, date of access: (27/11/2017).

Design of heat exchanger for the thermoelectric module cooling

Ryszard Buchalik[1], Krzysztof Rogoziński[1], Grzegorz Nowak[1]

[1]Faculty of Energy and Environmental Engineering, Silesian University of Technology, e-mail: ryszard.buchalik@polsl.pl, krzysztof.rogozinski@polsl.pl, *grzegorz.nowak@polsl.pl*

Abstract

The paper deals with energy harvesting from the flue gases exiting the internal combustion engine by means of thermoelectric modules (TEM). It focuses on using the Seebeck phenomenon to generate electricity. This work aims at analyzing the basic factors that characterize the thermoelectric module operation, its allowable working conditions and the useful effects. Significant parameters of that cell at the current stage of their development were analyzed. A test rig for TEM performance operation was designed and optimized.

Keywords: Energy harvesting, automobile, thermoelectric module, heat transfer, temperature gradient

1. Introduction

The intensive development of civilization observed in recent decades in so-called developed countries and the enhanced dynamics of the process in developing ones involve the need to generate huge amounts of energy. Overwhelmingly, this energy is produced from fossil fuels, the combustion of which enables the production of electricity and usable heat, and provides driving energy for the transport of humans and goods [1]. An improvement in the energy use efficiency, especially in the case of energy obtained from non-renewable and continuously depleting resources of the Earth, is becoming a key issue in the era of the sustainable development of mankind. One effect of the continuous rise in the demand for different types of energy is that very soon the world will have to face the issue of the fossil fuels depletion. In addition, mankind is already struggling with the problem of huge emissions of pollutants into the environment. This results not only from industrial activity as such, but it is to a large extent related to the common use of cars (about 1.1 billion cars worldwide [2]) and machines driven by internal combustion engines.

2. The scope of consideration

The processes of the fuel chemical-to-mechanical energy conversion are usually low-efficient. Whether we want it or not, we have to cope with decreased availability of fossil fuels and their price instability caused by political reasons [3, 4]. The aforementioned emission of pollutants arising from processes of the fuel chemical energy conversion is also becoming a social, economic, ecological, research and health problem. It can be seen that even a slight improvement in the situation in this matter may have a favorable effect on many aspects of human life and activity, especially in a long-term perspective. Therefore, efforts are made worldwide to improve the unfavorable index in stationary, typically industrial plants by extending thermal cycles and adding energy recovery systems. Unfortunately, the problem is that the effect of taking such actions is very limited in transport, which, according to different sources [4, 5] accounts for large part of the overall generated energy. Large dimensions of additional heat recovery systems, high financial costs (payback period) and operating aspects (e.g. servicing) of conventional installations pose more difficulties. In the case of traction units, the mass of the entire installation also plays an important role. However, considering the magnitude of the problem and the rapid development of energy harvesting methods, especially thermoelectric technology, the issue deserves to be examined more closely. The aim of the proposed investigation is to consider the possibility and perform a quantitative assessment of the recovery of enthalpy of the hot exhaust gas arising due to the combustion process by means of a Seebeck generator, an example of which is presented in Figure 1.

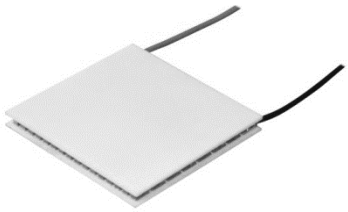

Fig. 1 Thermoelectric module.

The Seebeck phenomenon consists in generating an electromotive force [6] in a circuit composed of various types of conductors or semiconductors if their junctions are characterized by different temperatures. A thesis is proposed here that by appropriate streamlining of the exhaust gas flow, and taking account of unsteady flow phenomena, it will be possible to recover a substantial part of energy lost to the environment. In order to prove it, an experimental facility will be constructed to assess the process of hot exhaust gas heat absorption by a thermoelectric cell and conversion of the thermal energy into electricity. Thermoelectric modules are selected as the device converting waste heat to a usable effect – electricity – because they have a number of favorable characteristics. Among others, the most important are: simple and compact design, no moving parts, small size, low failure rate, ease of service, noiseless operation, long lifetime. The theory of the operation of thermoelectric devices is described in detail in many works [6, 7]. Thermoelectric cells intended for electricity generation using heat flowing through them are now available on the market. Most of them are suitable for operation at low temperatures (<100°C), but more advanced models can operate at temperatures reaching a few hundred degrees. Their use to recover the internal combustion engine waste heat seems to portend well [8, 9]. Special care should be taken to ensure an intensive heat transfer on both surfaces of the thermoelectric module as the temperature difference between the "cold" and the "hot" end is an essential factor affecting the device operation. On the one hand, it is important to obtain as much heat from exhaust gases as possible (without exceeding the thermoelectric module permissible operating temperature). But it is also necessary to cool the cold end in a manner that will ensure a possibly large temperature gradient between the thermoelectric module junctions. The heat transfer intensification will thus require the application of appropriately shaped heat exchangers and elements turbulizing the flow, which constitutes the greatest design challenge of the further works.

Based on the present state of knowledge and on the research works now being performed, it is fully justified that further research should be conducted both on the development, improvement, and adjustment of known methods of recovering energy related to exhaust gas enthalpy and on the search for new technologies in this area. Many works are now being carried out on the recovery of what is referred to as waste energy or waste heat in conventional solutions. Moreover, a rise in the significance and speed of this kind of research is anticipated [5, 8]. There are publications presenting the use of the exhaust gas heat [9], but the description usually concerns specific issues related to the research system proposed in them. Prototype systems incorporated into the vehicle structure can also be found in reference literature [10].

3. Design of test rig

Based on the above consideration a test rig for the thermoelectric modules performance was designed. Its main purpose is to comprehensively test the modules and determine the most important factors which have a crucial influence on thermal and electric parameters. As mentioned before, the key issue within the thermoelectric module performance is the heat flux passing through. So the task was to design efficient heat exchangers providing uniform temperature distribution on both sides of the thermoelectric module. The overall look of the rig is shown in Figure 2.

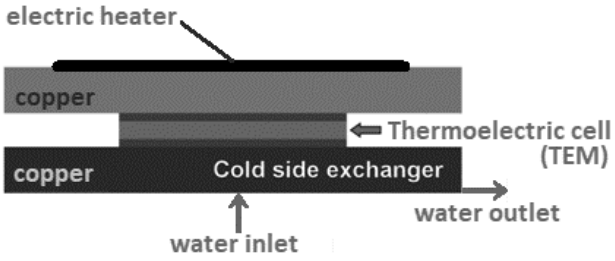

Fig. 2 Test rig diagram

The most basic aspect to make assessment and calculations relatively easy, reliable and credible is providing homogenous temperature distribution on the surface of the thermoelectric cell at every of its both sides (hot and cold). Copper was selected as an intermediary material, which is in contact with thermoelectric module, according to its high thermal conductivity. The facility consists of two electric resistance heaters placed on the top surface of upper (hot) block of copper. The first one heats the upper surface nearly uniformly, whereas the other is focused in the middle of the surface. Both of them are powered by an independently adjustable source, autotransformer or pulse width modulation. The block has a base dimension of 100 mm x 100 mm, which allow investigation of thermoelectric modules up to 100 mm x 100mm. The numerical simulations were made in Ansys Mechanical software for an exemplary thermoelectric module of 50 mm x 50 mm (contact surfaces) x 4 mm. This cell is similar to that one, which has been used in previous investigations [11]. Heat flow through the module (declared by manufacturer) is around 440 W for cold side temperature 30 °C and hot side 250 °C. This value was used to calculate mean thermal conductivity for the whole thermoelectric module, in the normal direction to the contact surface, using relation (1). For those data, $\lambda_z = 3{,}2\,\frac{W}{mK}$.

$$\lambda_z = \frac{h*Q}{a^2*\Delta T} \tag{1}$$

Where,

- λ_z Thermal conductivity (W/m/K),
- h Height of TEM (m),
- P Heat flow (W)
- a width of TEM (m),
- ΔT Temperature difference (K).

The thermoelectric module usually consists of two thin ceramic plates and vertically oriented columns of metallic material between them, with air gaps separating them. This probably has a significant influence on thermal flow. Therefore, the thermal conductivity of the material was set to orthotropic, and in the other two directions was assumed small, $\lambda_x = \lambda_y = 0{,}1\ W/mK$. This parameter has a negligible impact on simulation results. Its higher value helps to achieve homogenous temperature distribution. The numerical calculations showed that using only the first heater (nearly uniformly heating the top surface of the upper copper block) it is impossible to achieve uniform temperature distribution at the contact between copper and thermoelectric cell. The middle part is significantly cooler. This is the reason why two independent heaters were implemented. The height of upper copper block cannot be too small, because of the influence of heterogeneous heat distribution from the electric heater (the first one, placed at the whole surface). The resistive element of this heater (spiral) is not perfectly distributed, it is represented in the numerical model by four rectangles measuring 10 mm x 80 mm, with 10 mm distance between them, placed symmetrically. At their surface, constant and homogenous heat flow was assumed. The height of upper copper block also cannot be too large. Firstly because of the decline of the possibility of controlling the temperature distribution at TEM contact area by changing the ratio of power supplied to both heaters. Secondly because of the heat capacity of this block. The test rig should ensure the possibility of relatively fast operating condition change. The calculations were made for arbitrary height hot copper block. When the height is low, the shape of the electric heater is clearly visible at the contact surface with TEM, it makes it non-homogenous, which is undesirable. To make an assessment of temperature distribution the

temperature difference parameter was used, which represents the difference between the hottest and coldest points of TEM contact surface. When increasing the height, the temperature difference at contact area (between module and copper block) becomes smaller. However, when it is larger than 20 mm the difference stays at nearly the same level. Obtained results are presented in Table 1. In the real situation, the temperature difference should be smaller than calculated because of existing copper material between the spirals of the heater, which also conducts heat. The height of 15 mm was chosen as the most appropriate solution based on previously described assumption. This means that the grove in which resistive heater will be placed will be made in copper no closer than 15 mm to the cell. Grove will have a depth of about 5 mm and will be covered with thin, bolted copper plate, so the overall height of the copper block will be around 20 mm. The temperature distribution for the height from the heat source (surface heater) of 15 mm is presented in Figure 3.

Tab. 1 Characteristic temperatures at the contact area of the TEM

Height of copper block, mm	**Minimum temp. at contact area, $°C$**	**Maximum temp. at contact area, $°C$**	**Temperature difference, K**
5	244,48	259,60	15,12
10	247,19	255,34	8,15
15	247,95	254,39	6,44
20	248,23	253,91	5,68
40	248,35	253,84	5,49

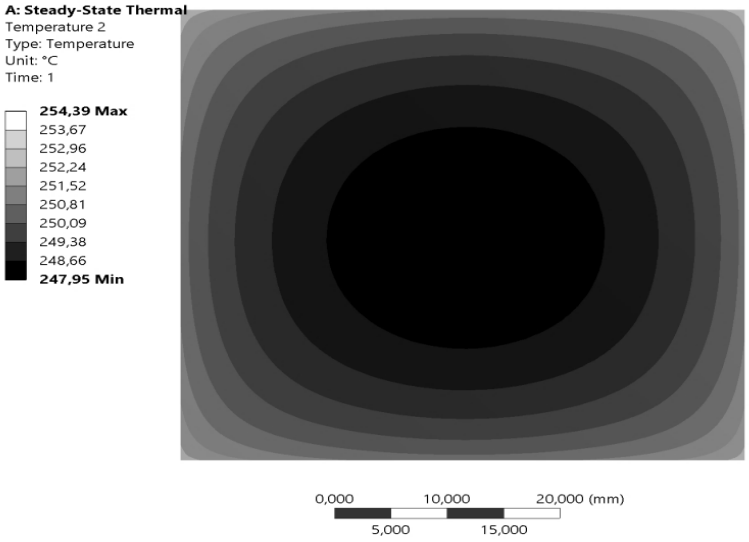

Fig. 3 Temperature distribution at hot TEM side at 15 mm block height.

The thermocouples will be used to control the temperatures at many particular points close to TEM to correctly set the power ratio between two heaters and confirm the uniform temperature distribution, on both sides of the cell (both hot and cold block). The next important aspect is appropriate treatment of the contact surface. It should be polished to reach a good level of smoothness. The thermal grease will additionally be used and tested in many configurations. The clamping force seems also to be a crucial issue to consider, with will probably significantly influence the thermal resistance at the contact surface. It will be controlled via a mass placed at the top of the assembly. The dimensions of the whole test facility were established due to TEMs available on the market, to allow testing of the vast majority of them. Power generated on a sliding potentiometer resistor will be used as the useful effect. A heat flow through the TEM will be determined by calculating firstly the power of electric heater and secondly the power received by cooling medium at the lower part of the test rig. Both these values are supposed to be very close to each other. All unused surfaces of lower and, particularly, the upper copper block will be covered with thermal isolating material. In numerical model, they are assumed to be

thermally isolated. Water will be used to cool the cold copper block via a set of internal passages whose configuration has been optimized.

4. Numerical optimization of cold heat exchanger

The main idea of the cold heat exchanger was that it should have provided a fairly uniform temperature distribution at the contact surface, and its manufacturing ought to be cheap. The developed solution is a copper plate, with drilled channels for coolant distribution. From the inlet, which is placed at the center of the plate and perpendicular to the surface, four channels were emitted radially distributing the coolant. Along the sides of the plate are four discharge manifolds, which discharge the coolant from the exchanger. Between the distribution channels and the discharge manifolds, there are four channels of smaller diameter, which are designed to distribute the heat uniformly. The shape of the exchanger has been planned so that it meets the criteria of cyclic symmetry. With this solution, the numerical model can be simplified to a quarter of the volume of the entire exchanger without affecting the calculation result. The heat exchanger is cooled with water whose inlet and outlet parameters are measured.

Appropriate simulations were made in the Ansys Workbench environment using the Fluent software. Numerical mesh was created in Ansys Meshing with use of tetrahedral mesh with a maximum element size of 1.5 mm. The contact surface of both liquid and solid was refined using 0.5 mm elements. The boundary layer was reproduced with a minimum element thickness of 0.01 mm, which resulted with y^+≤1.5. Compliance of mesh nodes on surfaces defined as the cyclic condition was maintained.

The CFD model was solved using the pressure-based solver in steady state with the k-epsilon turbulence model adopted. The model uses two materials available in the Fluent database; a solid copper and liquid water. The boundary conditions are shown in Fig. 4. At the inlet, a velocity-inlet boundary condition was used, with a constant temperature of 300 K. The outlet used pressure-outlet condition with a gauge pressure of 0 Pa. On the contact surface of water and copper, the interface condition enabling the exchange of heat was defined. A heat flux of 200 $\mathrm{kW/m^2}$ was assumed on the contact surface of the exchanger with the cell, which according to the cell dimensions corresponds to 500 W of thermal power. Other walls of the exchanger were adiabatic. On the Periodic 1 and Periodic 2 (Figure 4) surfaces, the rotational periodicity condition was assumed with the axis of rotation in the axis of the exchanger. During the calculations, pressure-velocity coupling SIMPLE and Spatial Discretization Second Order were used for pressure, momentum, and energy.

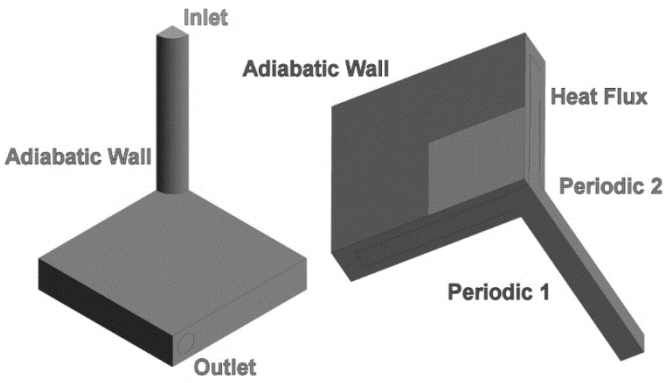

Fig. 4 Boundary conditions.

The shape of the exchanger was optimized using the Direct Optimization of the Ansys Workbench. Optimization was based on the Screening algorithm (Shifted-Hammersley Sampling) [12]. This is the basic way of optimization implemented in the Workbench environment. The algorithm generating a set of n combinations of input parameters, so as to evenly cover the range of their variation. Input can be defined as a range of variables or finite sets of numbers. The algorithm makes it also possible to define many independent criteria (with different weights) that determine the direction of optimization.

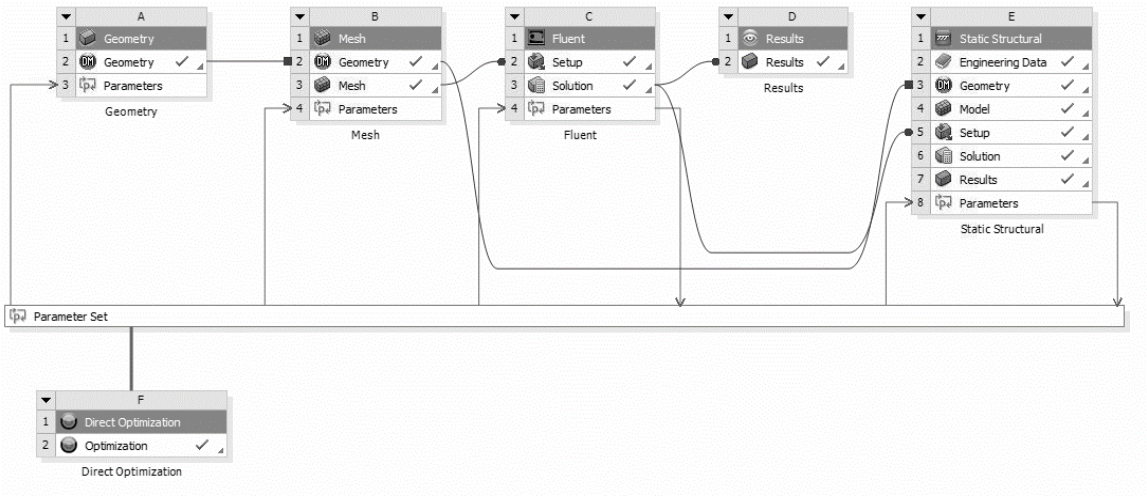

Fig. 5 Calculation scheme.

The following optimization criteria were adopted:

- Minimizing the maximum temperature on the contact surface of the cell
- Minimizing the maximum temperature on the remaining surface of the exchanger
- Minimizing the average temperature on the contact surface of the cell
- Minimizing the average temperature on the remaining surface of the exchanger

The same weights were assumed for each criterion. In the geometric model, the diameter and distance between each of the four heat-receiving channels were optimized (Figure 6).

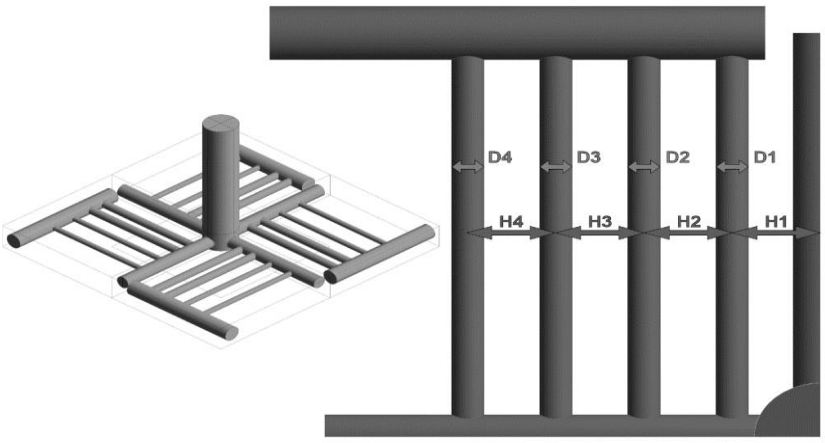

Fig. 6 Design variables of the optimization problem.

CFD calculations were used to optimize the water velocity at the inlet to the exchanger in the range of 0.4 to 1.1 m/s in the increments of 0.1 m/s. For each case, the highest von Mises stress was also determined, but it was not used as an optimization criterion. The optimization task was solved for 200 cases, of which the best solution was chosen. The results are summarized in Table 2.

The Figure 7 shows the temperature distribution on the bottom surface of heat exchanger. The analyzed exchanger allows for uniform heat transfer from the cell. The temperature difference between the warmest and the coldest areas does not exceed 6 K.

Tab. 2 Dimensions and characteristic temperatures for optimized solution.

Parameter	**Value**
H1, mm	11,0
H2, mm	6,0
H3, mm	8,0
H4, mm	9,0
D1, mm	3,0
D2, mm	3,0
D3, mm	2,0
D4, mm	2,0
v, m/s	1,1
$\mathrm{TH_{avg}}$, K	305,17
$\mathrm{THF_{max}}$, K	305,99
$\mathrm{TAW_{avg}}$, K	301,59
$\mathrm{TAW_{max}}$, K	303,71

Where:

- THF_{avg} - average temperature at the interface with the cell
- THF_{max} - maximum temperature on the contact surface of the cell
- Taw_{avg} - average temperature on the remaining surface of the bottom exchanger
- TAW_{max} - maximum temperature on the remaining surface of the bottom exchanger

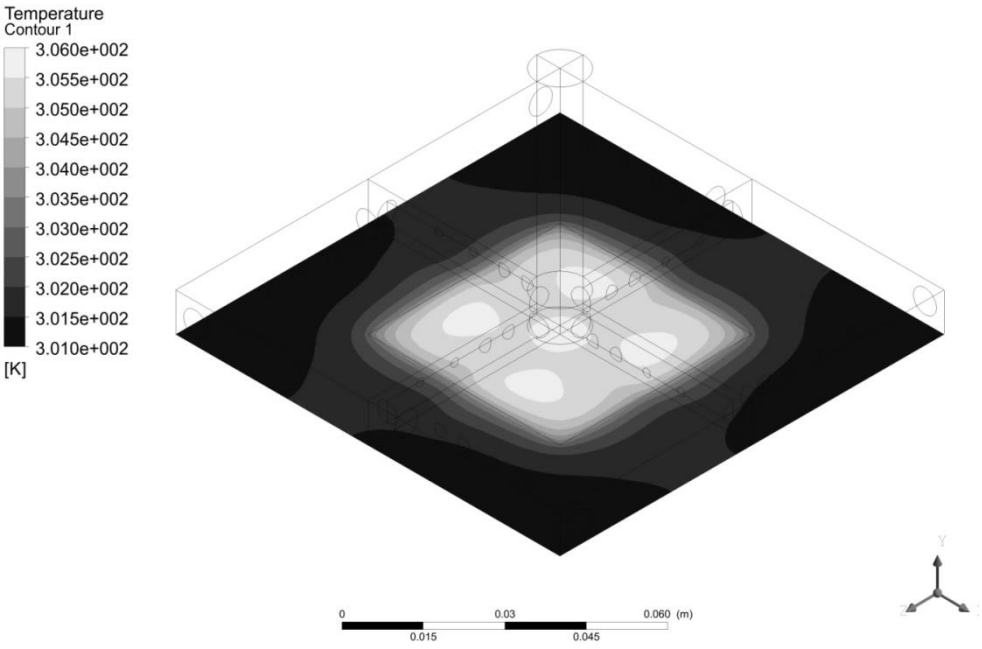

Fig. 7 Temperature distribution on hot side.

5. Summary

The paper discusses the problem of waste energy harvesting form hot flue gases with use of thermoelectric modules. The key issues of the TEM performance have been mentioned. At the very initial stage of research, a test rig for TEM performance was designed. Both hot and cold heat exchangers were optimized in order to provide uniform temperature distribution at the whole surface of the module. Selected measurements will make it possible to get module's operational parameters and in consequence its performance characteristics.

Acknowledgment

The authors gratefully acknowledge the financial support provided by the National Science Centre of Poland through project no. UMO-2016/23/B/ST8/03133.

References

[1] H. Hao, Y. Geng, J. Sarkis. Carbon footprint of global passenger's car: Scenarios through 2050, Energy, 101, 2016, pp. 121-131.

[2] D. Sperling, D. Gordon. Two Billion Cars - Transforming a Culture, TR News 259, November–December 2008.

[3] E. Brutschin, A. Fleig. Innovation in the energy sector – The role of fossil fuels and developing economies, Energy Policy 97, 2016, pp. 27–38.

[4] Global Transport Scenarios 2050, World Energy Council, 2011.

[5] R. Saidur, M. Rezaei, W.K. Muzammil, M.H. Hassan, S. Paria, M. Hasanuzzaman. Technologies to recover exhaust heat from internal combustion engines, Renewable and Sustainable Energy Reviews 16, 2012, pp. 5649–5659.

[6] S. Lineykin, S. Ben-Yaakov. Modeling and Analysis of Thermoelectric Modules, IEEE Transactions On Industry Applications, 2007, 43(2).

[7] C. L. Izidoro, O. H. Ando Junior, J.P. Carmo, L. Schaeffer. Characterization of thermoelectric generator for energy harvesting, Measurement, 2016.

[8] M. Karvonen, R. Kapoor , A. Uusitalo , V. Ojanen. Technology competition in the internal combustion engine waste heat recovery: a patent landscape analysis, Journal of Cleaner Production 2016, 112, pp. 3735-3743.

[9] K. M. Saqr, M. K. Mansour, M. N. Musa. Thermal Design Of Automobile Exhaust Based Thermoelectric Generators: Objectives And Challenges, International Journal Of Automotive Technology, 2008, 9(2), pp. 155-160.

[10] X. Liu, Y.D. Deng, Z. Li, C.Q. Su. Performance analysis of a waste heat recovery thermoelectric generation system for automotive application, Energy Conversion and Management, 2015, 90, pp. 121–127.

[11] R. Buchalik, D. Buczkowski, G. Przybyła,, G. Nowak. Investigation of Waste Heat Recovery for Automobile Application Based on a Thermoelectric Module, Journal of KONES Powertrain and Transport, 2016, 23(4).

[12] M. Ali, R. Dapoigny. Advances in Applied Artificial Intelligence: 19th International Conference on Industrial, Engineering and Other Applications of Applied Intelligent Systems, IEA/AIE 2006, Annecy, France, June 27-30, 2006.

Experimental investigation of waste heat recovery through surface of rotary kiln

Nouman Akram [1], M. Usman Moazzam [2], Hafiz Muhammad Ali [2], Ashar Ajaz[2], Arslan Saleem2[2]

[1]Faculty of Energy and Environmental Engineering, Silesian University of Technology, e-mail: nouman293@gmail.com
[2]Department of Mechanical Engineering, University of Engineering and Technology, Taxila, Pakistan

Abstract

Heat loss that occur from the surface of rotary kilns is a major source of waste heat in cement industries. Extent of waste heat recovery using a multi shell heat exchanger is experimentally determined. The experimental setup consisting of two concentric steel shells is thermally insulated by glass wool. The designed system uses ambient air as working fluid for waste heat recovery, and to facilitate the passage of air between the shells for heat transfer, a variable speed centrifugal fan (for variable flow rate) is installed. The results show that the proposed system extracted as much as 79.6 % of the total heat loss. It is also observed that the proposed design do not increase the kiln temperature which also proves its feasibility.

Keywords: Heat exchanger, waste heat recovery, rotary kiln, heat loss, experimental setup

1. Introduction

The rotary kilns are used all over the world by different industries to produce variety of products like Cement, Lime, Alumina, Vermiculite, Magnesia and Iron ore pellets. They are also used for roasting a wide variety of sulfide ores prior to metal extraction. Cement production is one of the most energy demanding industrial processes. Thus, the amount of heat wasted in the process is high ranging from 8-15% of the total heat input [1]. There are various works available on waste heat recovery in the cement sector which includes waste heat recovery from flue gases and recovering waste heat from the surface of rotary kilns. While the former has attracted much of the attention of the industries and waste heat recovery plants for flue gases are installed by cement production units all over the world[2], the latter remained unpopular due to some practical and technical issues regarding function of the kiln. The Kiln in a cement plant rejects considerable amount of heat to the atmosphere through its surface. So, by suitably designing and installing the waste heat recovery system over the kiln shell, heat can be extracted. Recently, a model of rotary kiln used for calcination of dolomite in magnesium production in which a heat exchanger is proposed by Karamarković et al. [3]. It uses both convective and radiant heat loss from the surface of kiln shell and prevents overheating, does not require air tightness and is implementable over rotary kilns with analogous surface temperature distribution. In this paper, the concept used for experimental model proposed and designed for cement production process is somehow similar to the system proposed for magnesium production. However, our model employed different geometrical, thermal & airflow conditions necessary for cement production.

Therefore, the model presented in this paper considers a heat exchanger, consisting of two concentric annular thermally insulated shells which surround the rotary kiln. The model gives us the solution of different equations determining the heat loss from the bare kiln both convective and radiant heat loss. It also evaluates the amount of recoverable waste heat from the surface of the kiln shell for a designated mass flow rate of the working fluid which is air in this case, and computes the surface temperature distribution. The paper discusses the design, fabrication and experimental investigation of a prototype rotary kiln, along with the heat exchanger. This setup contains thermally insulated suction pipes as well which are connected to the outermost shell and their other ends are connected to the input of variable speed centrifugal fan in order to achieve different flow rates. To further increase the efficiency of the waste heat recovery system, we have installed glass wool as insulating material for secondary shell, as it has lower thermal conductivity as compared to mineral wool resulting in

increased overall system efficiency. This paper is committed to the waste heat recovery through surface of a rotary kiln by the use of a heat exchanger installed above the kiln that efficiently extracts the heat loss; radiant and convective.

2. Mathematical modelling

The total heat loss from the surface of bare kiln is the sum of convection and radiation heat transfer i.e. $Q_{kiln} = Q_{conv.} + Q_{rad.}$

$$Q_{kiln} = hA_k\Delta T + \text{€}\sigma A_k[T_1^4 - T_2^4] \tag{1}$$

Where,

- h Convective heat transfer coefficient,
- A_k Area of the kiln,
- ΔT Temperature difference,
- € Emissivity of the surface,
- σ Stefan Boltzmann Constant

Following are the formulas required to solve equation (1)

$$A_k = 2\pi rl \tag{2}$$

Where,

- r Radius of the kiln shell,
- l Length of the kiln shell.

$$h = \frac{(Nu)*(K)}{L} \tag{3}$$

Where,

- Nu Nusselt number,
- k Thermal conductivity.
- L Characteristic length, which is equal to the outer diameter of the kiln.

The relationship that applies to the average dimensionless heat transfer co-efficient for free convection around a horizontal cylinder [4] is

$$Nu = \{0.60 + 0.387[Raf3Pr^{1/6}]^2\} \tag{4}$$

The characteristic length L from which the Nusselt and Rayleigh numbers are calculated is

$$L = D \tag{5}$$

The function f_3 (Pr) describes the effect of the Prandtl number over the entire range 0 <Pr< ∞ and is given by

$$f_3(Pr) = \left[1 + (\frac{0.559}{Pr})^{\frac{9}{16}}\right]^{-\frac{16}{9}} \tag{6}$$

Rayleigh number can be computed by the relation presented in [5]

$$Ra = g \times l^3 \times ß \times \frac{(Ts - Ta)}{k \times v} \tag{7}$$

Following equation is used to find out total heat extracted

$$Q_{out} = \dot{m} \times Cp \times \Delta T \tag{8}$$

Where,

C_p Specific heat and constant pressure,
$\dot{m}$ Mass flow rate.

$$= \rho \times V \times A \tag{9}$$

Where,

ρ Density of air,
V Velocity,
A Area of the fan outlet.

2.1 Calculations

Tab. 1 Dimensions of the experimental setup

Parameter	Value	Unit
Length of kiln shell	0.609	Meter
Diameter of kiln shell	0.254	Meter
Length of secondary shell	0.550	Meter
Diameter of secondary shell	0.267	Meter
Length of tertiary shell	0.550	Meter
Diameter of tertiary shell	0.280	Meter

Tab. 2 Parameters for calculation

Parameter	Value	Unit
Rayleigh number	2.913×10^{8}	Dimensionless
C. of thermal expansion	3.3184×10^{-3}	K^{-1}
Kinematic viscosity	161.8×10^{-7}	m^2/s
Thermal diffusivity	228.7×10^{-7}	m^2/s
Prandtl number	0.70	Dimensionless
Nusselt number	78.538	Dimensionless
Characteristic length	0.254	M
Convective heat transfer coefficient	8.2	W/m^2K
Surface temperature	231.2	°C
Ambient Temperature	29	°C

Equation (2) has been solved for area of kiln using dimensions provided in Table 1 which is equal to $0.4864m^2$. To solve equation (3), equations (4) to (7) are solved. All the values for dry air have been obtained at the working fluid ambient temperature from the properties tables presented in [6], [7] and [8]. These obtained values are shown in the Table 2.

Nusselt number in equation (4) thus calculated has value 78.53. The characteristic length used is the diameter of kiln shell equation (5) for the calculation of convective heat transfer co-efficient in (3). The calculated value for convective heat transfer coefficient at a surface temperature of 231.2°C is 8.2 W/m^2K which is in range as per calculation carried out at similar surface temperature of 241 °C presented in [3] having the value of 8.19 W/m^2K. The length of section for which the values are compared is 1m being close to length of kiln shell being considered in this paper. Now that all the required parameters are established for calculation of equation (1), the heat loss from the surface of bare kiln is thus determined. This heat loss is compared to the total heat input to find out percentage heat loss of the input through kiln surface.

In order to find out heat extracted mass flow rate and temperature difference is calculated. The value for specific heat at constant pressure i.e. 1.005 KJ/ (kg K) is obtained from [6] at given ambient temperature. Mass flow rate is calculated using the relation shown in equation (9). The obtained value for density of dry air at ambient temperature is 1.13 kg/m^3 and heat extracted at different flow rates is thus calculated at fan outlet area of $0.00316m^2$.

Heat loss because of convection from the surface of kiln; $Q_{conv.} = 806.47$ W

Heat loss because of radiation from the surface of kiln; $Q_{rad.} = 1087.04$ W

Total heat loss of the bare kiln; $Q_{total} = 1893.51$ W

The heat loss thus obtained is 94.67 % of the total heat input to the system i.e. 2000 W.

3. Experimental Investigation

3.1 Experimental Setup

A prototype rotary kiln was designed and tested. Mild steel sheets having gauge 18 thickness were used in the fabrication of steel shells. The core component in the experimental setup was the heating source. The heating requirements of the setup were fulfilled by electric heating rods. Two rods having a power of 1000W each providing total heat input to the system of 2 kW were suspended inside the kiln shell along the central horizontal axis. To hold the rods inside the hollow kiln shell steel fixtures of minute thickness and width were used, and to prevent the inner shell from conducting electricity ceramic holders were used holding the rods.

The inner shell was riveted by forming a lap joint. The length of the kiln shell was 0.6096 m, and its diameter is 0.254 m. The shell was sealed from both the ends and inside the shell was the heating source.

A secondary shell (also made up of mild steel) having larger diameter than inner shell was used to cover it. This shell was different than inner shell in terms of dimensions and provision of holes for air delivery as shown in Figures 1, 2 and 3. The air suction holes were formed on the outer shell over the section of the kiln where temperature was higher than other sections of the kiln. The shell had a length of 0.558m and diameter of 0.2677m. There was thus an intentionally provided gap between inner and outer shell to allow flow of ambient air.

In order to insulate the outermost shell glass wool insulation was used. This allowed prevention of radiation heat loss from outer shell's surface. (Figure 1)

The whole assembly was placed over a wooden stand, care was taken to ensure proper designing of the stand to ensure equidistant gap between inner and outer shells. (Figure 2)

A variable speed centrifugal fan was used, connected to the apparatus via insulated flexible pipes. Each pipe had 1.8m length, with one end connected to the fan inlet and the other end connected to the secondary shell's air outlet. (Figure 3)

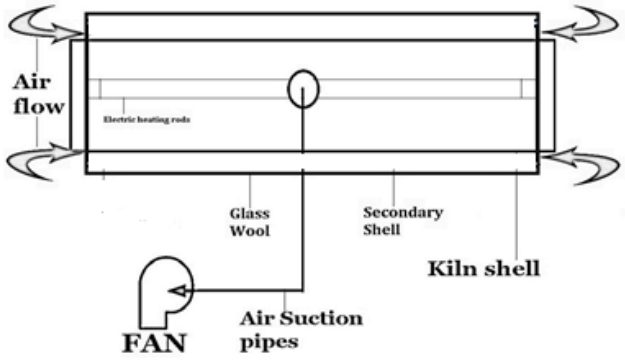

Fig. 1 Experimental Setup drawing

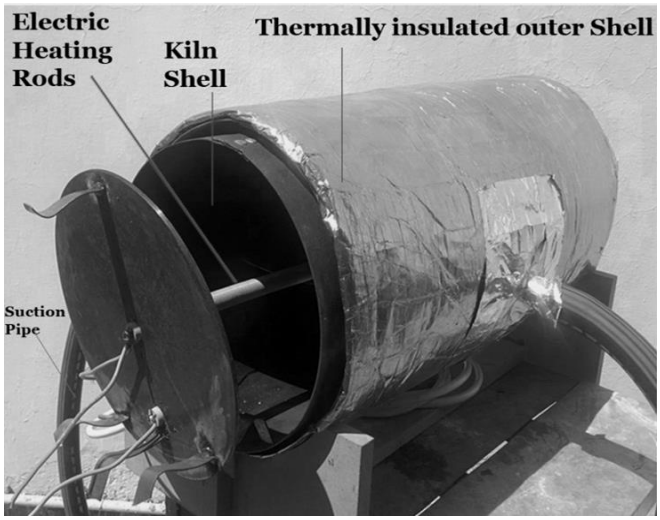

Fig. 2 Experimental Assembly

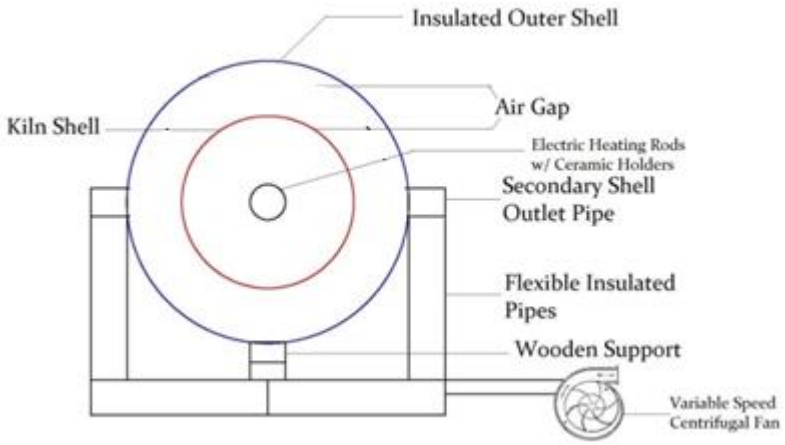

Fig. 3 Experimental Setup Cross sectional view

3.2 Experimental Procedure

Power was provided to the electric heating rods. Kiln shell was continuously monitored for rise in temperature from the start till the steady state conditions were achieved. It was observed that after 50 minutes of operation there was no more rise in temperature for the kiln shell. The peak temperature recorded was 254°C and average surface temperature was found out to be at 232°C.

The second step in the procedure was covering the kiln shell, as it was the main purpose of the experimentation. Kiln surface temperature was monitored periodically. To prevent heat transfer via conduction it was ensured that no part of the inner shell comes in contact with the outer shell.

Blower was switched on using ambient air as the working fluid, it created suction between the two shells. Air swept over the outer surface of the inner shell, as well as the inner surface of the outer shell simultaneously and carried along the entrapped heat via forced convection to the outlet of the centrifugal fan. With the help of anemometer fan's air velocity was found out and with the help of temperature sensors fan's outlet air temperature was monitored.

Surface temperatures of the kiln, ambient temperature, and the fan's outlet temperatures at different speeds of the fan were noted down. The temperature of glass wool insulation was measured as well, along with the inner wall temperature of the secondary shell. All these readings were used for calculations using the mathematical model.

Steady state conditions were achieved in 50 minutes. In order to note down temperatures for different sections along the length of the kiln five test points were chosen, the kiln was divided into four sections each having length of 0.15 meter. The temperatures were noted down using K type probe thermometer. It was observed that the temperature for bare kiln averaged around 231.2°C and with secondary shell 236.1°C.

Tab. 3 kiln surface temperature

Kiln Length (in.)	Temp. °C for Bare Kiln	Temp. °C with Secondary shell
Start	204.4	209
6	252.4	258.1
12	248.6	254.2
18	252.9	258.5
24	198.4	201

A small increase in kiln surface temperature as mentioned in table 3 was observed with secondary shell installation; the reason for this increase was that airflow was not provided for the first 50 minutes. Later on as the steady state conditions were achieved the blower was turned on the kiln shell outer surface temperature became constant. This also proves the usefulness of the proposed secondary shell design which does not allow for continuous increase in temperature because of entrapped waste heat in the gap between the two shells.

4. Results and Discussion

The overall inner shell temperature increased by 4.9 °C and then became constant without varying further. This satisfy an important requirement of the industry by not varying kiln temperature which otherwise can affect the production process. The dimensionless numbers used in calculations for the current system have their values in accordance with the specified geometry of the prototype.

Recovered waste heat at various mass flow rates was calculated. It can be shown in terms of percentage of total heat loss from bare kiln as shown in table 3. It was observed that heat extracted and mass flow rate had a direct relation. By varying air speed optimal conditions for maximum heat extraction were found. The proposed system extracted as much as 79.6 % of the total heat loss.

The results obtained for the prototype can be used for full sized rotary kilns. The proposed solution for waste heat recovery is backed by set of governing equations, which can be used for calculating heat loss and extraction for industrial kiln.

Tab. 4 Heat extracted from the kiln

Obs.	Outlet air temp. (°C)	Air Speed (m/s)	Mass flow rate (Kg/s)	Heat extracted (W)	% Extraction
1	72.2	9.7	0.0347	1506	79.6
2	72.0	9.4	0.0337	1456	76.9
3	71.4	8.7	0.0312	1329	70.2
4	71.2	8.4	0.0312	1329	70.2
5	70.8	7.7	0.0270	1134	59.9

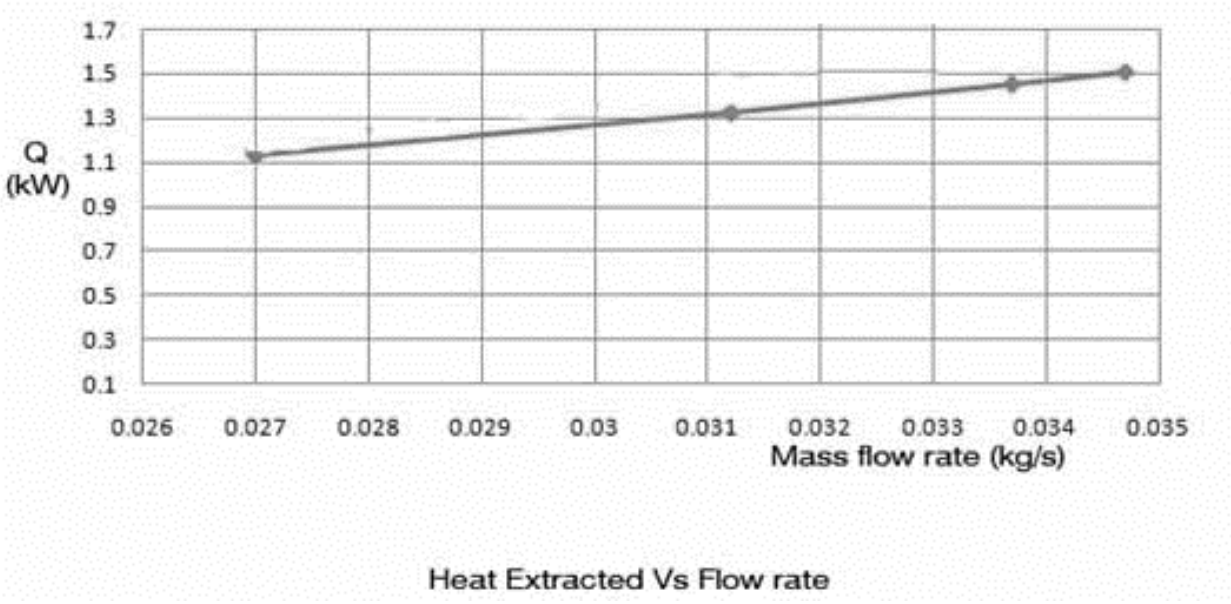

Fig. 4 Heat Extraction comparisons at different mass flow rates

5. Conclusion

The paper focused on experimental investigation of waste heat recovery through the surface of kiln. It was observed that the proposed arrangement extracted waste heat from surface of kiln shell and prevented rise in kiln temperature because of controlled ambient airflow. A lot of research has been conducted on waste heat recovery throug flue gases in cement industries but attention was required to be provided over this significant portion of surface heat loss, thus this paper is a step forward in this direction and will pave way for practical application of the proposed solution.

Acknowledgment

The authors of this paper would like to acknowledge the support of Department of Mechanical Engineering, University of Engineering and Technology Taxila Pakistan.

Nomenclature

A_k	Area of the kiln [2πrl], (m^2),
ß/h	Convection heat transfer coefficient [(Nu)* (k)/L], ($Wm^{-2}K^{-1}$),
K	Thermal Conductivity, ($Wm^{-1}K^{-1}$),
L	Characteristic length [D], (m),
Nu	Nusselt Number [0.60+0.387[Raf3$Pr^{1/6}$]^2], (Dimensionless),
f_3Pr	Function of Prandtl Number [f_3Pr= [1+ (0.559/Pr)$^{9/16}$]$^{-16/9}$], (Dimensionless),
Ra	Rayleigh Number [$gl^3ß$ (T_s-T_a/Kv)], (Dimensionless),
T_a	Ambient temperature, (K),
T_m	Mean surface temperature, (K),
T_s	Kiln Surface Temperature, (K).

References

[1] AC, Caputo. Performance modeling of radiant heat recovery exchangers for rotary kilns, *Applied Thermal Engineering*, 2011, 31, pp. 2578-2589.

[2] Waste Heat Recovery for the Cement Sector: Market and supplier analysis, a report by International Finance Corporation, World Bank Group, June 2014.

[3] V. Karamarković. Recuperator for waste heat recovery from rotary kilns, A*pplied Thermal Engineering*, 2013, 54, pp. 470–480.

[4] W. Churchill, HHS. Chu. Correlating equations for laminar and turbulent free convection from a horizontal cylinder, *International Journal of Heat and Mass Transfer*, 1975, 18, pp. 1049–1053.

[5] W. Kast. Heat transfer by free convection: external flows, *VDI-Gesellschaft, VDI Heat Atlas*, second ed., Springer, Heidelberg, 2010, pp. 667-672.

[6] R. Span. Properties of Dry Air, *VDI Heat Atlas*, Second ed., Springer Science, pp 195-214, 2010.

[7] EW. Lemmon. Thermodynamic properties of air and mixtures of nitrogen, argon, and oxygen from 60 to 2000 K at pressures to 2000 MPa, *Journal of Physical and Chemical Reference Data*, 2000, 29, pp. 331–385.

[8] EW. Lemmon, RT. Jacobsen. Viscosity and thermal conductivity equations for nitrogen, oxygen, argon, and air, *International Journal of Thermophysics*, 2004, 25, pp. 21–69.

Thermal Processing of Biomass Using Solar Energy

Szymon Sobek [1], Sebastian Werle [1]

[1] Institute of Thermal Technology, Silesian University of Technology, email: szymon.sobek@polsl.pl, sebastian.werle@polsl.pl

Abstract

To follow European Union (EU) and national legislations in the renewable energy sector, biomass is continuously gaining in importance. Until 2020 EU Member States are obliged to increase the share of renewable energy to 20% in total EU energy consumption, along with a 20% decrease of greenhouse gas emissions and overall energy consumption. Thermal methods of biomass conversion are the most popular ways of utilizing its energy potential. Among these methods it can be specified: combustion and co-combustion, gasification and pyrolysis. The process that distinguishes itself by the highest rate of converting biomass energy is pyrolysis. Conventional implementation of mentioned earlier processes, based on the heat generated from the combustion of non-renewable fuels, results in significant emissions of greenhouse gases, which contradicts the concept of eco-friendly and green energy production. The idea of using solar energy as a source of heat in pyrolytic reactors opens up new opportunities for efficient energy production from biomass. In this paper review of the pyrolysis process fundamentals and assumptions for designing and constructing of experimental solar-thermal pyrolytic reactor is presented.

Key words: Pyrolysis, Biomass, Utilization, Solar-Thermal, Renewable Energy Sources (RES).

1. Introduction

Right now more than 80% of the world's overall energy needs are provided by non-renewable fuels [1]. If the economy and population growth continue, global energy demand is expected to increase by 37% in 2040. International Energy Agency (IEA) analysis proves that without decisive action, energy related greenhouse gas (GHG) emissions could more than double by 2050 [35]. In awareness of 2020 Climate & Energy Package limitations, more and more renewable energy sources, such as solar energy and biomass should be implemented. Between 2010 and 2040 significant development in renewable energy will be noticed for biomass (from 45 217 to 136 950 PJ) and solar energy (from 184 to 55 768 PJ) [3]. The European Environment Agency (EEA) has estimated that around 9838 PJ per year of biomass could be obtained without any harmful impact on the natural environment [4]. In this matter key suppliers are: agriculture 95 Mtoe (Megatonne oil equivalent; 1Mtoe = 42GJ), waste 100 Mtoe and wood industry 30 Mtoe [5]. Due to this fact, in EU countries, biomass is right now one of the leading renewable energy sources in heat, electricity and biofuel production [6]. Only in Poland, annual biomass energy potential is equal to: >20 million Mg of waste straw, approx. 4 million Mg of waste wood and approx. 6 Mg of sewage sludge [8]. Thermal methods of utilizing waste biomass are continuously gaining on importance with each year. The main reason for that are requirements of the European Commission (EC), which order to increase share the of renewable energy sources in overall energy consumption to 20% by 2020 [9, 10]. In addition within the Biomass Action Plan [11], which was published at the end of 2005, the EC encourages the EU Member States to harness the potential of all cost effective forms of energy generation from biomass. The thermal processes include combustion, co-combustion, gasification and pyrolysis [12]. The most common is direct combustion of biomass material. The biggest problems with biomass-fired plants are in handling and pre-processing the fuel. This is the case with both small grate-fired plants and large pulverized coal power plants. Drying the biomass before combustion improves the overall process efficiency, but due to its relatively high humidity and significant amounts of conventional powered heat required may not be economically motivated in many cases. Despite the observed ecological, economic and social benefits, the use of biomass creates many technical problems, as follows:

- A wide range of humidity causing difficulty in combustion stabilization.
- Biomass fuels have ash that is more alkaline in nature, which may exaggerate the fouling problems.
- Low density makes it difficult for transportation and storage.
- High volatile content causing combustion process to be rapid and difficult to control.
- The relatively low the lower heating value.
- Heterogeneity and diversity of composition, including the content of chlorines lead to process during which hydrogen chloride, dioxins and furans are formed [13].

These problems cause that co-combustion of biomass with fossil fuels (mainly hard coal) gained importance. This process can be advantageous with regard to substitution of fossil fuels, reducing fuel cost and emissions of NO_x and CO_2 minimizing waste and reduce soil and water pollution and increasing boiler efficiency. However, attention must be taken to increase deposit formation in the boiler and limitations in ash use due to compositions in biomass, especially alkali metals, which may disable the use of ash in building materials. Due to undesired changes of ash compositions, the share of biomass is usually limited to approximately 20% of the fuel input [14]. Additionally, there are other barriers of co-combustion biomass with coal. These barriers include:

- Biomass procurement practices to obtain low-cost fuels in a long term reliable manner; the impact of co-combustion on ash composition and ability to sell fly ash.
- The trade-off between the impact of biomass on emissions and fuel cost [15].

All presented facts because that new pioneer and innovative thermal solutions for biomass conversion are needed. An example of such technology is pyrolysis. There are many other important advantages of pyrolysis in comparison to combustion, as follows:

- Pyrolysis can be performed at a relatively small scale and at remote locations which enhance the energy density of the biomass resource and reduce transport and handling costs.
- Due to lower temperature of the process corrosion problem is reduced – the maintenance costs of the installation are lower.
- Due to the lower temperature of the process, recovery of the selected elements (mainly non-ferrous metals) from solid products is possible.
- Due to the endothermic nature of the pyrolysis, control of the process is easier in comparison to combustion.
- Pyrolysis is characterized by high level of the fuel flexibility.
- The pyrolysis products can be stored and later used for energy purposes [20].

Despite its advantages, pyrolysis has the disadvantage of requiring an external energy input to reach the operating temperature [21]. This external energy input is generally derived from a non-renewable source that has a negative impact on the environment. A possible solution to this problem is to use solar energy to heat the reactor to achieve conditions appropriate for solar pyrolysis initialization. In such process the concentrated solar radiation supplies high temperature heat for biomass pyrolysis reaction [22]. Then biomass and solar energy can be converted into transportable and dispatchable solar fuel [23]. Solar processes have the potential to produce higher calorific value products with lower CO_2 emission compared with conventional process [24]. The biomass energy upgraded through solar energy providing pyrolysis reaction enthalpy transferred into products. Solar pyrolysis is an endothermic process of converting a biomass in an inert atmosphere in which the required heat is provided by concentrated solar energy. The direct solar radiation is concentrated and redirected to the pyrolytic reactor and the biomass to reach pyrolytic temperatures. Solar pyrolysis of carbonaceous materials leads to the formation of gases, pyrolytic oil and char. Gas products can be applied for heat and power production or precursors for chemicals [25]. Pyrolytic oil can be transported and stored for further use in boilers or engines for energy and heat generation [26]. Char can be used as a fuel or adsorbent [27]. Compared with the conventional pyrolysis process, solar application provides some advantages such as [28]:

- Faster system start up and shutdown time.
- Possibility of storing solar energy in the form of chemical energy.

- Minimized risk of secondary reactions due to high and low temperature zone in the reactor.
- Highly concentrated solar radiation provides higher peak temperatures and faster heating rates.

2. Pyrolysis Reaction Model and Process Conditions

Biomass pyrolysis is defined as a thermal decomposition of the biomass polymers present in the organic matter under and inert oxygen-free atmosphere [17]. The ambient reaction atmosphere is provided by a flow of chemically inert gas, most often nitrogen or helium, which main role is to remove oxygen from the reaction zone and transport the volatile components. Inert gas flow brought to pyrolytic reactor mainly depends on reaction area as well as feedstock and estimated volatile product quantity. In pyrolysis reaction three products are always produced (solid, liquid and gaseous) and its proportions can be varied over a wide range by adjustment of the process parameters [18]. The theoretical pyrolysis reaction was presented by Piatkowski et al. 2011 as follow [28]:

$$C_xH_yO_zS_uN_v \xrightarrow{heat} CO + CO_2 + H_2 + CH_4 + C_nH_m(n \geq 2) + H_2O + Oil + Char \quad (1)$$

The final course of the reaction depends on the parameters listed below:

- Mean outlet temperature of the process, referred here as t_{out}.
- Heating rate β, which is described as temperature increase of feed biomass in a specified time period, most usually seconds $^oC \cdot s^{-1}$, or minutes $^oC \cdot min^{-1}$, for lower heating rates.
- Residence time of biomass, τ.

Based on these parameters, the classification of the pyrolysis process has been divided into three main technologies [28]:

Tab. 1 Pyrolysis technology and process conditions [28]

Pyrolysis technology	**Process conditions**		
	Residence time	**Heating rate**	**Temperature, °C**
Slow	5-30 min	< 50 ºC·min^{-1}	400-600
Fast	< 5 s	10-200 ºC·s^{-1}	400-600
Flash	< 0.1 s	~1000 ºC·s^{-1}	650-900

3. Products Yield

Pyrolysis besides physical approach, can be also described a heterogeneous chemical reaction [33]. From the heat transfer point of view, proper process begins when the reactor reaches its operational temperature after relatively short non-steady state while reaching it. From thermochemical point of view reaction begins as soon as the heat is supplied. Pyrolysis can be divided on three steps (Figure 1) [28]. First, when sample reaches temperature of 100-200 °C drying process begins, with some internal rearrangements, such as bond breakages and free carbonyl and radical group formation, along with a small release of water, CO and CO_2. Proper pyrolysis starts at 250 °C and approximately ends at 500 °C, producing primary products. During primary pyrolysis solid biomass decomposition occurs with significant weight loss. Products after formation can further participate in secondary reactions as heating continues.

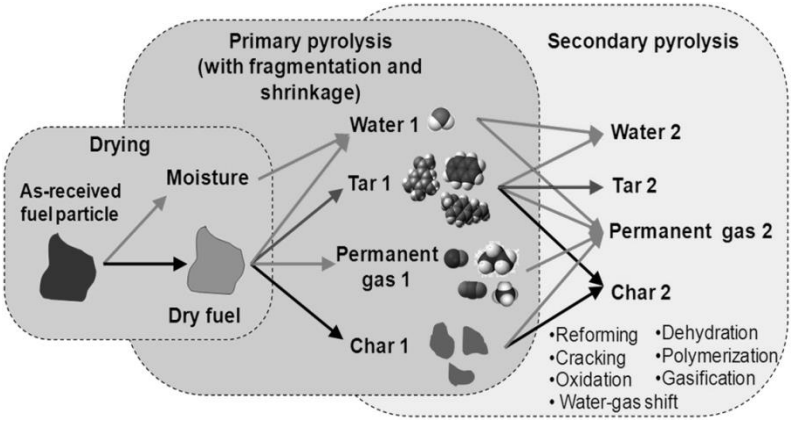

Fig. 1 Steps of thermal decomposition of solid biomass under oxygen-free atmosphere: drying, primary and secondary pyrolysis [30].

As mentioned before, the final product yield highly depend of reactor operating conditions [28], and characterization of feedstock. Table 2 presents the main products yield in order to pyrolysis technology.

Tab. 2 Pyrolysis technology and product distributions [28]

Pyrolysis technology	**Product yields**		
	Liquid , %	**Solid, %**	**Gas, %**
Slow	<30	<35	<40
Fast	<75	<25	<20
Flash	<20	<20	<70

Data collected in Table 1 and 2 shows that increase of heating rate and temperature of the process is followed by the downfall of solid products in total yield due to a higher intensity of decomposition. Slow pyrolysis is used most likely to produce char, with the lowest temperatures and heating rates along with the longer residence time of biomass. Fast pyrolysis is getting attention in producing liquid organic compounds, mostly phenols and lower hydrocarbons. Oil formation demands plenty of time for secondary pyrolysis reactions (Figure 1) with moderate thermal power directed into the reaction zone. Higher heating rates, thus energy supply, direct pyrolysis reaction into more gas production orientated yields. Flash pyrolysis, being the fastest process occurring the highest heating rates results in the highest pyrolytic gas yield along with smaller char and oil production. According to the topic of the following article, such high power supply can be efficiently obtained through concentration of solar radiation with accordingly designed set of mirrors (concentrators) or lenses. Exact influence of temperature on the product yields has not been determined so far, thus the authors of this paper intend to explore this issue in the future.

4. Estimation of Heat of Pyrolysis

As a highly endothermic process, pyrolysis requires a significant amount of heat delivered to the reactor. Estimation of the amount of heat, referred as Q, necessary to provide desirable reaction is a key role in designing a reliable pyrolytic reactor. In case of solar pyrolysis, thermal power must be appropriately collected and concentrated at the reaction area (Figure 2). This is possible by concentrating solar radiation with a set of mirrors or lenses which focal point coinciding with the biomass residence place. Moreover, thanks to the proper operation of the active surface of the mirrors operator can control the density of the heat flux, thus control the whole process.

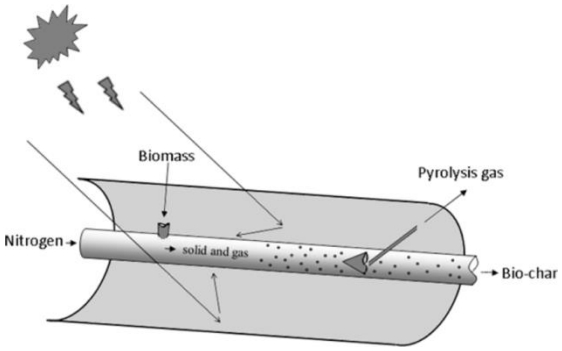

Fig. 2 Parabolic through solar concentrator used in solar pyrolytic reactor [34]

The amount of energy necessary to carry out pyrolysis reaction was estimated by the authors of publication [32]. In this paper the equation is presented after simple transformation considering the reactants enthalpy streams to estimate necessary thermal power $\dot{Q}$ expressed in watts:

$$\dot{Q} = \dot{H}_{char}(t_{out}) + \dot{H}_{liquid}(t_{out}) + \dot{H}_{gas}(t_{out}) - \dot{H}_{biomass}(t_{in}) \tag{2}$$

where,

t_{in} Temperature of biomass at the inlet of reactor, (°C),
t_{out} Temperature of the products at the outlet, (°C),
$\dot{H}_i$ Total enthalpy stream of a product *i* or the biomass, ($J \cdot s^{-1}$).

Stream of total enthalpy of *i* reactant is calculated as a product of reactants mass flow and specific enthalpy as following:

$$\dot{H}_i = \dot{m}_i \cdot h_i \tag{3}$$

where,

$\dot{\mathbf{m}}_\mathbf{i}$ Mass flow of *i* reactant, ($kg \cdot s^{-1}$),
$\mathbf{h_i}$ Specific enthalpy of the *i* reactant, ($J \cdot kg^{-1}$).

Mass flows of reactants can be calculated based on principle of mass preservation from feedstock biomass flow and estimated product yields depending on pyrolysis technology (Tab.2). Enthalpy of each product can be described as a sum of physical enthalpy, which is a heat capacity $C_{p,i}$ as a function of temperature, and standard enthalpy of formation $\Delta_f H^{\Theta}$ referenced to mass units as follows [32]:

$$h_i = \Delta_f H_i^{\theta} + \int_{298,15}^{T2} C_{p,i}(T)dT \tag{4}$$

Enthalpies of specific product fractions can be estimated as a temperature function, if only yields of individual products are known. Standard enthalpy of formation of char is calculated directly from the higher calorific value, or ultimate composition. In case of pyrolytic gas, thermodynamic databases provide all necessary data to calculate total enthalpy as a mass average of individual enthalpies of products: CO, CO_2, H_2, N_2, H_2O and lower hydrocarbons. The steam in gaseous products is vaporized moisture, so heat of vaporization ca be estimated accurately from technical analysis of the biomass. The real problem starts when it comes to estimating enthalpy of pyrolytic oil. Pyrolytic oil consists of hundreds or thousands of organic compounds, which precise identification is almost impossible. With that in mind, the total enthalpy of formation of pyrolytic oil has to be calculated, just like for char, from HHV or ultimate composition. What has to be mentioned is that enthalpy of the "liquid" is in fact enthalpy of vaporized pyrolytic oil, if only T_{out} is high enough to avoid condensation of the liquid [32].

5. Biomass Pyrolysis Kinetics

The main role of examination of reaction kinetics is to understand and know the course of the reaction in time. Virtually each kinetic model proposed obeys fundamental Arrhenius rate expression:

$$k(T) = A\exp\left[\frac{-E_a}{(MR)T}\right] \tag{5}$$

where,

T	Absolute temperature, (K),
(MR)	Universal gas constant, ($J \cdot kg^{-1} \cdot K^{-1}$),
k(T)	Temperature-dependent reaction constant, (s^{-1}),
A	Pre-exponential factor, (s^{-1}),
E_a	Global activation energy of the reaction, ($J \cdot mol^{-1}$).

Temperature dependence of Arrhenius equation comes from exponential term. This model describes well volatile homogenous reactions, based on molecular collision theory. Pre-exponential factor *A* describes a measure of the frequency at which all molecular collision appear notwithstanding on their energy level, thus reaction constant *k(T)* represents the frequency of successful molecule collisions. Energy of activation can be interpreted as amount of energy, necessary to allow molecules to get close enough to collide and form products. Another rule, transition state theory, tells that activation energy is a difference between the average energy of system and the average energy of reactants. In work [33] *et al.* authors criticized the present methodology of evaluating biomass pyrolysis kinetics parameters. The authors rightly pointed out the fact, that biomass pyrolysis kinetic, being heterogeneous process, cannot be appropriately approximated by oversimplificated and false reaction models. At their opinion adoption homogeneous reaction kinetic theory to describe heterogeneous reactions is unacceptable. It is plausible, that inconsistency arising in biomass kinetic data among the literature is a result of using kinetic expressions, barley modifications of those used in homogeneous models that hardly can be applied to describe solid state nature of biomass.

5.1. Experimental methods of kinetic analysis

When analytical methods started to raise controversies, scientist found a way of an experimental evaluation of reaction kinetics. Kinetic data are usually acquired through a series of experiments under isothermal conditions, with a slight element of non-isothermal behaviour during heating and dynamic, non-isothermal kinetics estimation methods, which main advantage is investigation of sample behaviour in wide a range of temperatures expeditiously. Dynamic methods use modern thermobalances that subjects sample to a programmed heating rate, ensuring no temperature regions are omitted, what can happen during a sequence of isothermal experiments. From among the most used and popular methods of estimation kinetic parameters of biomass thermal decomposition we can specify:

- Thermogravimetric analysis (TGA) – is the most commonly applied analytic method in solid state thermal decomposition studies, which gained prominence in studies of biomass pyrolysis. TGA measures sample mass drop caused of realise of volatile products during applied heating rate in function of temperature or time. In this method maximum reaction rate can be obtained from the first derivative of mass drop over time $-dm/dt$.
- Differential scanning calorimetry (DSC) – this method is based on comparison of heat flux into or out of the sample against comparative inert material, as the two are simultaneously heated (or cooled) at a constant rate. The integral of DCS peak is directly proportional to the enthalpy change of the reaction.
- Differential thermal analysis (DTA) – method uses the temperature difference ΔT between the sample and inert reference material subjected to identical temperature alteration along with plotting it in function of time $\Delta T(t)$.Reaction rate can be calculated directly from temperature difference in derivative of time and height of the slope ΔT, at any temperature.

5.2. Kinetic expressions for biomass pyrolysis

Biomass decomposition kinetics are usually predicted to a single reaction, which under isothermal condition can be presented as:

$$\frac{d\alpha}{d\tau} = k(T)\, f(\alpha) = A \exp\left[\frac{-E_a}{(MR)T}\right] f(\alpha) \tag{6}$$

where,

τ Time, (s),

α Degree of conversion, or reaction extent,

dα/dτ Rate of isothermal reaction,

f(α) Conversion function.

Conversion function *f(α)* estimates reaction model specific to the used method of mechanism control. Reaction extent *α* can be defined as the mass fraction of initial biomass decomposed as well as the mass fraction of volatile products released as decomposition continues:

$$\alpha = \frac{m_0 - m}{m_0 - m_f} = \frac{v}{v_f} \tag{7}$$

where,

m Mass of biomass present at time τ, (kg),

m_0 Initial substrate mass, (kg),

m_f Final mass of pyrolysis solid products, (kg)

v Mass of volatile products in function of time τ, (kg)

v_f Total amount of gas products, (kg).

In case of non-isothermal methods the additional parameter that has to be taken into consideration is heating rate *β*. Rate of reaction under such conditions can be expressed as a function of temperature at a linear heating rate through a simple transformation:

$$\frac{d\alpha}{dT} = \frac{d\alpha}{d\tau}\frac{d\tau}{dT} = \frac{d\alpha}{d\tau}\beta^{-1} \tag{8}$$

where,

β heating rate, (°C·s^{-1}).

An expression of rate of reaction law for non-isothermal condition can be presented as following:

$$\frac{d\alpha}{dT} = \frac{k(T)}{\beta} f(\alpha) = \frac{A}{\beta}\left[\frac{-E_a}{(MR)T}\right] f(\alpha) \tag{9}$$

Presented equations still do not adequate reflect heterogeneous nature of biomass pyrolysis due to the fact, that reaction constant *k(T)* is calculated from equation 6 for homogeneous kinetic model. Yet this problem can be improved by introducing to the equations reaction order. With this model reaction rate is proportional to amount of unreacted substrate *(1-α)* raised to exponent *n* determined by specific reaction order:

$$\frac{d\alpha}{dT} = k(T)(1-\alpha)^n \tag{10}$$

Dynamics of biomass pyrolysis are usually expressed as first order decomposition process in the production of discrete gaseous fractions:

$$\frac{dv_i}{d\tau} = k_i(T)(v_i^* - v_i) \tag{11}$$

where,

$k_i(T)$ Reaction constant for an specific volatile fraction *i*, (s^{-1})

v_i Total mass of gas released corresponding to fraction *i* through time τ, (dm^3),

v_i^* Effective volatile content for fraction *i*, (dm^3).

For such specified expressions, total rate of decomposition reaction can be presented as a sum of all particular volatilization rates for each fraction, which are weighted accordingly to respective component in unreacted solid substrate.

6. Concept of solar powered pyrolytic reactor

Gathering all the information, first assumptions of pyrolytic reactor project can be made. Study of solar biomass pyrolysis process can only be carried out on suitably constructed apparatus, which allows to monitor and control reaction parameters as well as observations, as the reaction goes on. As a feedstock wooden, straw and sludge waste pellets where chosen as in order to a properties consistency and supply availability. Inert atmosphere is provided by nitrogen mass flow, which amount is related to the mass flow of feedstock and reaction area accordingly. Heat should be supplied by a xenon lamp concentrated by focusing lens on the tubular reactor containing biomass pellet. Heat can be delivered in two ways:

- Direct – radiation is focused on pellet surface,

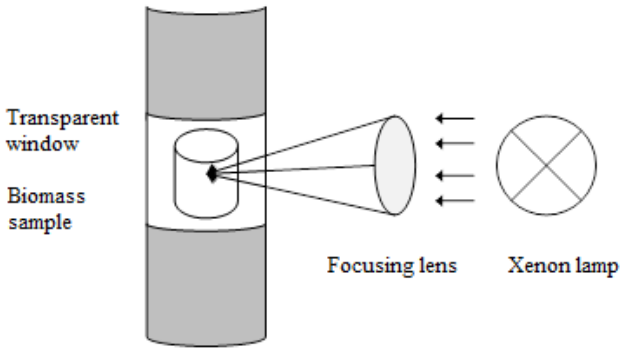

Fig. 3 Direct heating of biomass sample

- Indirect – radiation falls on the reactor wall, heat is supplied to the pellet through conduction and convection.

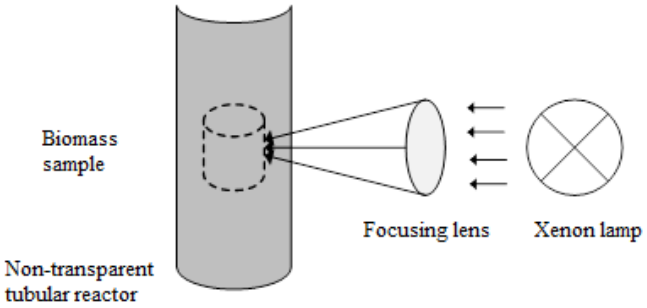

Fig. 4 Indirect heating of biomass sample

In case of direct heating, heat is transferred through a highly transmissive reactor wall or window (Fig. 3), to minimize radiative heat losses as well as provide isolated oxygen free atmosphere. In this solution temperature increase of biomass is caused directly by the radiative heat flux emitted by the lamp.

Indirect heating involves highly conductive, non-transparent wall between lamp and biomass sample (Fig. 4). In this case the heat is conducted through the wall into the reactor, where biomass sample is located. High conductivity of the wall material, provides equal temperature field, which generates uniform heat flux delivered along the length of the sample.

Volatile products of the reaction are transported with inert gas to condenser, where liquid products gather for later analysis. Gaseous products pass through to be kept and sealed in Tedlar Bag. When reaction ends, solid product is removed from the reactor and prepared for analysis and weighting.

Pyrolysis of single biomass sample in presented theoretical reactor can be carried out in many cases thanks to ability of controlling heat flux, heating rate, the temperature of the process, all for different type of feedstock.

7. Conclusions

Solar powered pyrolysis of biomass is promising way of renewable energy production in the time of incoming energy sector reforms. Obviously, not every country can boast of considerable potential in the field of solar energy. However the application of the mentioned method does not require high implementation cost, and its simplicity enables to open up new prosumer prospect to even small holders of potential biomass fuel. What's more pyrolysis of waste biomass allows to utilize waste disposal, even as problematic as sewage sludge, and exploits its energetic potential in the form of useful chemical energy of oil gas and pyrolysis char. Such a solution can not only significantly reduce the cumbersome sewage disposal costs, but even bring a profit. Among the pyrolysis products applicability oil and gas can be used as a fuel in furnaces as well as an organic reactant source in chemical and petrochemical industry. Char, thanks to its porosity, after proper examination can be used as eg. a filter feed. The solar powered pyrolysis process significantly lowers CO_2 emission, thus lower the cost of energy production and it's a new, original way of storing solar energy in a stable form of pyrolysis products.

Acknowledgments

The paper has been prepared within the frame of the project "*Study on the solar pyrolysis process of the waste biomass",* financed by the National Science Centre, Poland (registration number 2016/23/B/ST8/02101).

References

[1] IEA, World Energy Outlook, 2014, IEA.
[2] T.V. Ramachandra, *Solar energy potential assessment using GIS*, Energy Edu Sci Technol 2007;18:101–14.
[3] JL. Sawin, F. Sverrisson, K. Chawla, C. Lins, R. Adib, M. Hullin, et al. Renewables 2014, *Global status report*; 2014.
[4] European Environment Agency, *How much bioenergy can Europe produce without harming the environment*, 2006, p. 6.
[5] *Eurostat Main Tables*, IEA, WEO 2011, Annexes, p. 26.
[6] C. Marculescu, *Comparative Analysis on Waste to Energy Conversion Chains Using Thermal-Chemical Processes*, Energy Procedia 2012;18:604-611.
[7] A. Magdziarz, M. Wilk, *Thermal characteristics of the combustion process of biomass and sewage sludge*, J. Therm. Anal. Calorim. 2013;14:519-529.
[8] S. Werle, R.K. Wilk, *A review of methods for the thermal utilization of sewage sludge: the Polish perspective*, Renewable Energy. 2010;35:1914–1919.
[9] *Refuse derived fuel, current practice and perspectives – Final Report*, European Commission – Directorate General Environment 2003.
[10] *Directive 2009/28/EC* of the European Parliament and of the Council of 23 April 2009 on the promotion of the use of energy from renewable sources.
[11] *Communication from the Commission* of 7 December 2005 – Biomass Action Plan.

[12] S. Werle, *Impact of feedstock properties and operating conditions on sewage sludge gasification in a fixed bed gasifier*, Waste Management and Research. 2014;32:954-960.
[13] J. Werther, M. Saenger, E-U. Hartge, T. Ogada, Z. Siagi, *Combustion of agricultural residues*, Progress in Energy and Combustion Science, 26;2000:1-27.
[14] A.A. Khan, W. de Jong, P.J. Jansens, H. Spliethoff, *Biomass combustion in fluidized bed boilers: potential problems and remedies*, Fuel Processing and Technology.2009;90:21–50.
[15] L.D. Smoot, *International research centers activities in coal combustion*, Progress in Energy and Combustion Science, 1998;24:409–501.
[16] *Act of the renewable energy sources* (Dz. U. 2015 poz. 478) 20 February 2015r.
[17] P. Rutkowski, A. Kubacki. *Influence of polystyrene addition to cellulose on chemical structure and properties of bio-oil obtained during pyrolysis*, Energy Conversion and Management. 2006;47:716-731.
[18] S. Yaman, *Pyrolysis of biomass to produce fuels and chemical feedstock*, Energy Conversion and Management. 2004;45:651-671.
[19] P. Basu, *Biomass gasification and pyrolysis*, Practical design and theory. Elsevier, 2010.
[20] K. Zeng, D.P. Minh, D. Gauthier, E. Weiss-Hortala, A. Nzihou, G. Flamant, *The effect of temperature and heating rate on char properties obtained from solar pyrolysis of beech wood*, Bioresource Technology. 2015;182:114-119.
[21] S. Morales, R. Miranda, D. Bustos, T. Cazares, H. Tran, *Solar biomass pyrolysis for the production of bio-fuels and chemical commodities*, Journal of Analytical and Applied Pyrolysis. 2014;109:65-78.
[22] N. Piatkowski, C. Wieckert, AW. Weimer, A. Steinfeld, *Solar-driven gasification of carbonaceous feedstock—a review*, Energy and Environmental Science. 2011;4:73–82.
[23] W.C. Chueh, C. Falter, M. Abbott, D. Scipio, P. Furler, SM. Haile, A. Steinfeld, *Highflux solardriven thermochemical dissociation of CO_2 and H_2O using nonstoichiometric ceria*, Science, 2010
[24] A. Nzihou, G. Flamant, B. Stanmore, *Synthetic fuels from biomass using concentrated solar energy - a review*, Energy, 2012;42:121–31.
[25] E Grieco, G. Baldi, *Analysis and modelling of wood pyrolysis*, Chemical Engineering Science, 2011;66:650–60.
[26] N. Özbay, E. Apaydın-Varol, BB. Uzun BB, AE. Pütün, *Characterization of bio-oil obtained from fruit pulp pyrolysis*, Energy, 2008;33:1233–40.
[27] U. Moralı, S. Sensöz, *Pyrolysis of hornbeam shell (Carpinus betulus L.) in a fixed bed reactor: characterization of bio-oil and bio-char*, Fuel;150:672–8, 2015.
[28] K. Zeng, D. Gauthier, J.Soria, G. Mazza, G. Flamant, *Solar pyrolysis of carbonaceous feedstocks: A review*, Solar Energy 156, Elsevier, 2017.
[29] Y. Yang, J.G. Brammer, A.S.N. Mahmood, A. Hornung, *Intermidiate pyrolysis of biomass energy pellets for producing sustainable liquid, gaseous and solid fuels*, Bioresource Technology, 2014.
[30] D. Neves, H. Thunman, A. Matos, L. Tarleho, A. Gomez-Barea, *Characterization and prediction of biomass pyrolysis products*, Progress in Energy and Combustion Science, 2010.
[31] S. Morales, R. Miranda, D. Bustos, T. Cazares, H. Tran, *Solar biomass pyrolysis for the production of bio-fuels and chemical commodities*, Journal of Analytical and Applied Pyrolysis 65-78, 2014.
[32] H. Yang, S. Kudo, H.P. Kuo, K. Norinaga, A. Mori, O. Masek and JI. Hayashi, *Estimation of Enthalpy of Bio-Oil Vapor and Heat Required for Pyrolysis of Biomass*, Energy Fuels 27, p.2675-2686, 2013.
[33] J.E. White, W. Catallo, B. Legendre, *Biomass pyrolysis kinetics: A comparative critical review with relevant agricultural residue case studies*, Journal of Analytical and Applied Pyrolysis 91, p.1-33, 2011.
[34] M. Bashir, X. Yu, M. Hassa and Y. Makkawi, *Modeling and Performance Analysis of Biomass Fast Pyrolysis in Solar-Thermal Reactor*, ACS Sustainable Chem. Eng., p.3795−3807, 2017.
[35] A. Eisentraut, *The Biofuel and Bioenergy Roadmaps of the International Energy Agency*, Bioenergy and Water, 2013.

Materials and technology for the construction of high steam parameters boilers

Agata Widuch [1], Katarzyna Żelaznowska [1]

[1]Silesian University of Technology, e-mail: agataa.widuch@gmail.com, zelaznowska.k@gmail.com

Abstract

The purpose of this paper is to present the development of boiler for supercritical (SC) and ultra-supercritical (USC) steam parameters. The issues related to materials and technologies used in boilers for supercritical and ultra-supercritical steam parameters will be discussed. Special attention will be paid to the effect of supercritical steam on specific materials and on the requirements they must meet. In addition, the planned development and improvement of the supercritical boilers will be described.

Keywords: Supercritical boilers, ultra-supercritical boilers, advanced Ultra-supercritical boilers, materials, technology

1. Introduction

Possibility of building new coal-fired boilers for high steam parameters and development of energy technology based on high efficiency systems and low emission of pollutants cannot take place without the development of material engineering. In recent years there is visible and rapid progress related to the improvement of materials and technology that meet the high requirements of the main elements the boiler. These actions can only be implemented with cooperation and coordination of several entities. Technology improvement is demanded from manufacturers of materials, designers and users. Naturally knowledge, skills gained from past experience and role of research organization, cannot be ignored.

The reluctance of global societies to utilize nuclear power as well as the penalties of using oil in the 1970s have led to a renewed focus on the use of highly efficient carbon technologies in the United States, Japan, and Western Europe. As a result, the energy industry has begun to focus on increasing the efficiency by improving steam parameters and developing new types of ferritic and austenitic materials. In the decade of eighties and nineties the number of activities initiated by individual countries or international initiatives were flourishing.

The first major project related to the development of components with 9-12% chromium steel content began in the United States at the Electric Power Research Institute (EPRI). The same project was joined by European countries and Japan, which allowed the creation of materials such as T91 and T92. The main goal was to improve the security of energy storage, supply and also reduction in carbon dioxide emissions. There are currently many projects in different parts of the world and at different stages that involve the development of materials that can handle steam temperature of up to 760°C and achieve a thermal efficiency approaching 50%.

2. Materials for the construction

2.1 Low-alloyed steel grade

Despite long history of usage, low-alloy steels are all the time common material for boiler construction and also are constantly refined. They are used to create welded and resistant for high temperature components such as furnace water wall, superheat and reheat tubing not only for SC boilers, but also for USC boilers operating at temperatures below 560°C. However, usage of these materials caused problems in the preparation and production, that resulted from design elements with a sufficiently large wall thickness. From the years 1980-1990, numerous were carried out at the same time regarding improving the development of low-alloy steel, 9-12% Cr steel with increased strength and austenitic steels. Thanks to that, USC boilers have been made of low-

alloy steels with increased creep strength, including T23 and T24 steels. The use of these steels has allowed improvement in the formation and production of furnace water with thinner walls. By comparing the T23 and T24 to the most resistant of conventional low-alloyed steel, T22, we can see that their strength is increased twice. Reduction in the amount of carbide in the steel has directly contributed to the improvement in weldability and reducing the probability of cracking of refined steel. Disadvantage of these materials is the occurrence of cracks at higher temperatures and the possibility of cracks caused by corrosion, but small changes of chemical composition of steel and improving the environmental conditions during production, are carried out in order to cope with these problems. T23 and T24 steels are commonly used in boiler production worldwide, mainly due to low production costs.

2.2 High-alloyed martensitic steel grade

High-alloy martensitic steels containing 9-12% Cr, owing to their high-temperature resistance have been used in the SC and USC boilers in building elements having the highest temperature, such as superheater. These steels have many advantages such as increased strength for wiredrawing and creep. They are also highly resistant to the adverse oxidation, corrosion, thermal expansion and allow for rapid heat conduction. In addition these steel are cost-efficient. However, usage of these materials involves limitation in boiler efficiency. In the eighties, the first SC boiler was built, by using the martensitic steel CrMoV 12%. Over the next two decades steels Grade 91 having a composition of 9% CrMoVNb and Grade 92 with the composition of 9% Cr 2% WVNb were introduced. These are examples of currently used steels that can be used for temperature above 600°C. Welding of these steels is carried out only after prior heating to 200°C, and the joints in the next step are heated to a temperature of 760°C.

2.3 Austenitic steels and advanced austenitic stainless steels

For the construction of boilers with improved efficiency, it is necessary to create materials that meet the strength requirements of a suitable creep resistance, corrosion and oxidation. These conditions can be met by increasing the Cr content in the alloy, as well as adding components such as niobium and titanium, whose carbides are more stable. Therefore, austenitic alloys, due to their characteristics, are most suitable for the construction of high-temperature, thin-walled components. Superheater tubes are mainly constructed from austenitic steels.

In the past, many austenitic steels have been developed, such as Esshete 1250, AC 66, Super 304 HCu, TP347HFG, HR3C, A-3, NF 709, SAVE 25. They contain different contents of elements such as niobium, silicon, manganese, molybdenum, titanium, tungsten. Because of insufficient resistance to cracking, corrosion and oxidation they have not been popularized. Studies of these alloys allowed for improvement their properties and increased the strength of the newly formed materials. The main problem was the corrosion resulting from the combustion of coal containing sulfur. Most progress in research on austenitic steels are associated with the formation of steel Sanicro 25. This steel was invented by Sandvik in the European project AD700. Thanks to its properties, Sanicro 25 is comparable to nickel-based steels and can be used for construction of boilers beyond 50% efficiency. Modern austenitic steel brings economic benefits because it reduces the cost of construction of boilers USC and USC-A compared to those produced nickel steel. Sanicro 25 is currently the most resistant to creep among austenitic stainless steel, and can operate at temperatures reaching 700°C. The discussed steel was tested in many laboratories and boilers in power plants throughout Europe. It can be used in A-USC units to build superheater. Sanicro 25 exhibits excellent resistance to oxidation and corrosion, and also is a material relatively easy to manufacture and welding. The austenitic steels mentioned above can only be used up to 650°C and in addition the superheater components made of them have thick walls, the ideal replacement can be the Sanicro 25. It is designed to create high-pressure superheater with thinner walls.

2.4 Nickel base alloys

The use of nickel-based alloys would increase the efficiency of the power plant by more than 50% and increase the steam temperature above 700 ° C. Research on these steels has been conducted mainly over the last decade, so be aware that knowledge of the properties of these materials is not yet complete. The basic property

of these alloys which is checked is the creep resistance. In many projects, these steels are constantly being developed so that they can be used at temperatures much higher than 700 ° C.

Nickel-based alloys are divided into two groups: precipitation hardened alloys and solid solution-strengthened alloys. The first ones show better plasticity, but they have a worse creep resistance. However, precipitation hardened alloys have higher requirements for heat treatment. Easy production goes down proportionally with lowering resistance: in that case the size of produced elements is smaller.

Listed below are the nickel-based alloys that are solid solution strengthened. Elements such as chromium, cobalt, molybdenum and tungsten are in big amount, they have a nickel matrix, and their purpose is to provide hardening. Alloy 230 (Haynes 230) by Haynes International, has excellent heat resistance, resistance to oxidation, not only to 1149°C, but also in the presence of high-nitrogen environment, additionally it is very thermally stable. Alloy 617 (INCONEL alloy 617) has a high oxidation resistance up to 980°C. Studies of this alloy have proven that it is suitable for the construction of large-sized components.

Precipitation hardened nickel alloys contain in their structure, elements such as aluminum and titanium that cause deformation of the material, but they exhibit significant increase in creep strength. Alloy 263 (NIMONIC alloy C263) is a Rolls-Royce developed steel that has improved welding capabilities compared to 80A steel. Alloy 282 (Haynes 282 alloy) has a relatively low content of aluminum and titanium. To obtain good strength values of the material it is necessary to perform two-stage temperature reduction. Initially for two hours at 1010°C and then for further eight hours at temperature of 788°C. The Alloy 718Plus (Allvac 718Plus) steel prototype was Alloy 718, used only till 649°C. The improved steel is simpler in heat treatment and additionally has improved creep strength. The last already is nickel alloys Alloy 740 (INCONEL alloy 740), which was developed by Special Metals Corporation. The steel is constantly being developed for use in boiler casing, and research is focused on welding and production methods.

It has already been proven that nickel-based alloys may be suitable for the construction of boiler elements for advanced supercritical steam parameters, but the risk of financial constraints prevents manufacturers from building A-USC blocks. As we know, the quality of materials is associated with an increase in production costs, but more resistant materials allow reduction in the thickness of the wall elements. The chart below shows how the steam parameters need to change and 100 000h of work.

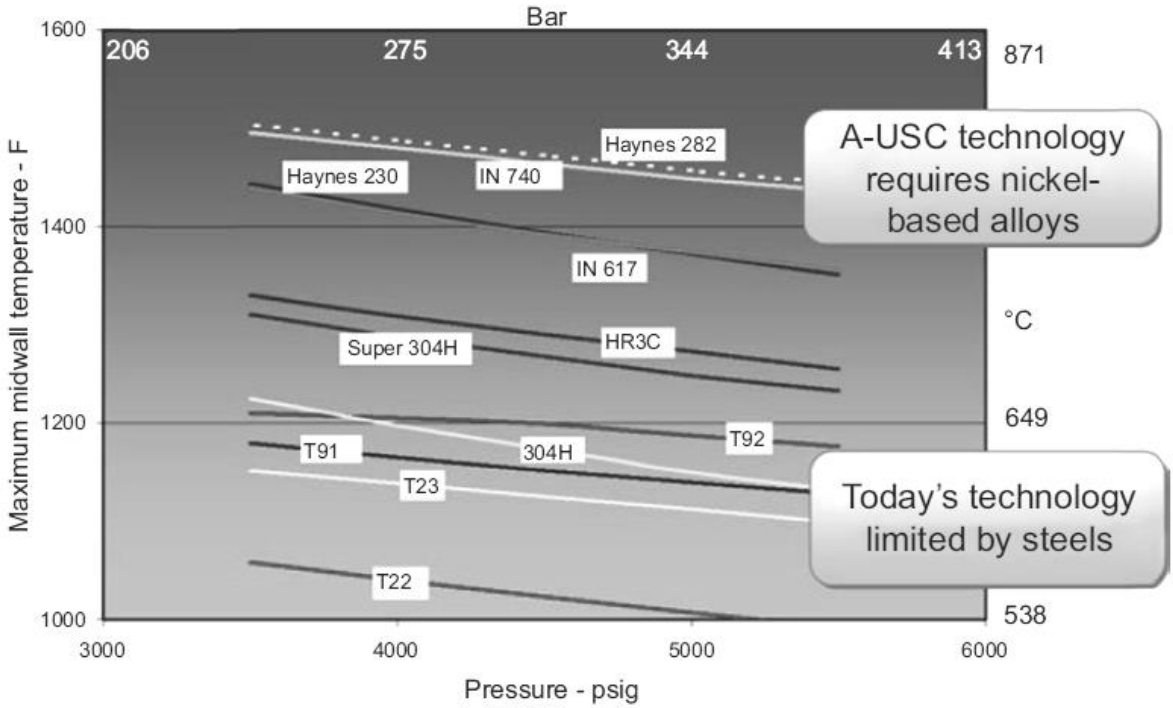

Fig. 1 Maximum operating temperature and pressure of the different materials [2]

3. World research programs on the development of modern materials for the power industry

3.1 United States Department of Energy US DOE

Since 2001, a program has been developed for the improvement of materials and technology for the construction of boilers capable to operate in supercritical conditions. The program involves few different enterprises. The scope is to increase efficiency of the power plants by increasing steam parameters to t=760°C and p=35MPa. For now materials and processes appropriate to achieve those parameters were defined.

In comparison to coal burnt in Europe and Japan, coal from USA contains more sulphur and moisture. This causes the need to find alloys with a higher resistance to corrosion. Due to project conducted in USA the further research started in Europe and Japan.

This project consists of two consortia: the USC Steam Boiler Consortium and the USC Steam Turbine Consortium. USC Steam Boiler Consortium result of a common effort of the US DOE, the energy research organizations, major equipment suppliers for the development of new materials, also for A-USC combustion. The consortium has developed several superalloys that are currently in need of testing in terms of simplicity of manufacturing, weldability, creep and oxidation resistance and corrosion resistance. The basic task is to create a database of mechanical properties of materials.

In supercritical steam power plants, a great progress has been made according to newly developed materials such as Inconel 740 and Haynes 282. Further tests are planned to confirm corrosion and oxidation resistance. Tested alloys are 304H, HR3C, HR6W, Haynes 230, Inconel 617, Inconel 740 and Haynes 282.

Laboratory tests include preservation of material for a temperatures higher than 760°C. The research study, if financially viable, should be closed in 2019 in the United States. It would include design, construction and testing. There are no plans for new technologies in the industry, such power plants could be put into use in 2025.

3.2 Thermie 700 Advanced Power Plan (AD700)

More than thirty European manufacturers have joined forces to construct the A-USC power plant with efficiency exceeding 50% and reduced emissions of harmful chemical compounds. The power of the plant was planned to be around 400MW, while the steam parameters were set at t=700°C÷720°C and p=35MPa. The plan is to finish the project in 15 years, which will comprise of six stages.

The first stage (1998-2004) was successfully completed. It involved the determination of the research feasibility and the development plan for the new materials.

The second stage (2002-2006) of the work was to design the basic structure and auxiliary elements and to present the properties of materials used in the power plants - 700°C (COMTES). The main obstacle was the development of materials resistant to rupture and lifetime of at least 100 000h. It was sufficient to study new materials mainly nickel-based steels, because they are more resistant to creep. In addition, these improved materials must be suitable for manufacturing and, above all, for welding pipes.

The third stage (2004-2009) was run in parallel to the second and fourth. Iits scope was to investigate the operational aspects of the newly manufactured components.

The fourth stage (2006-2010) involved the construction of a demonstration plant on a large scale. German company E.ON. Wilhelmshaven took up the construction of the first power plant based on the AD700, with a power of 550 MW. As per schedule, the first boiler working with advanced ultra supercritical parameters was to be put into operation in 2014. Unfortunately, due to the operational difficulties in heavy-walled components of alloy 617 it was not successful. However, European countries participating in the AD700 program, led by E.ON. decided to introduce two additional projects that have come into effect for the demolition of COMTES700. Projects such as HWT11 and ENRIO were responsible for the control repair construction. This work have helped to reduce the cost of production of demonstration plant and reduce the risk of using unrecognized technology. The improved alloy 617 (renamed 617B), with welds and alloy 263, was tested in the Italian company ENEL Andrea Palladio near Venice. Another challenge for the European energy sector is the production of clean fossil

fuel energy that can compete with the rapidly growing renewable energy industry. Coal power plants will therefore have to be designed to work both at low and high loads. For manufacturers, this will be a huge technological challenge, due to thick-walled and welded components with high requirements and the economic challenge resulting from not many hours of electricity transmission. Due to such a large number of unsolved issues, it is anticipated that A-USC power stations in Europe will be commercially available not earlier than 2020.

3.3 Japanesse 700 ° C program

Although Japan is in the third place in the world economy, it is paradoxically lacking in its own sources of fossil fuel. After the 1970, when the use of fossil fuels was banned, the Japanese industry had to become independent of oil supplies, thus extending the use of coal and nuclear energy. The energy sector in Japan is associated with increased costs resulting from the continual import of energy sources, according to that more attention is paid to increasing the thermal efficiency of coal blocks. Many individual manufacturers, of power plant elements, have joined forces to introduce the A-USC, because the government in this country has not introduced any refinement program. As a result of these activities, the Japanese have launched ISOGO power plants with a power of 600MW and operating at t=605°C÷620°C and p=27.2 MPa, using commonly known construction materials. At the same time, the country started to work on the use of technology such as A-USC power plants.

In cooperation with other countries, in March 2008, the "Cool Earth" program was launched, which aims to reduce greenhouse gases. This program includes 21 major technological improvements, ex. the commercialization of the A-USC (t=700°C and p=35MPa), the burning of coal dust and the rising the efficiency of power plants: 46% by 2015 and 48% by 2020.

"Before 2020" is the name of the Japanese A-USC boiler development project, which consists of two stages:

- stage I (700 ° C / 700 ° C - single superheated boiler)
- stage II (700 ° C / 700 ° C / 650 ° C - double superheated boiler)

Japan has been among the top nations with good power plant technology, but its development programs do not use nickel alloys (to reduce costs), although it is planned to expand the use of ferritic and austenitic steels so that they can work at higher temperatures, but the assumed vapor pressure will be lower than those achieved in other A-USC programs.

Between 2014 and 2016, new generation components were tested in existing boilers, including superheater panels, safety valves and turbine bypass. Materials for these items were tested for their creep resistance, fatigue, oxidation and corrosion. The tests included material HR6W, HR35, 617, 263, 740 and 141.

The massive earthquake in 2011 and the closure of a large number of nuclear power plants have unfortunately altered the hierarchy of nationwide operations in the power industry. At the same time, A-USC boilers have been trying to build power plants based on gas generation, hence it is unlikely that the “Before 2020” will be completed in the current decade.

3.4 Chinese A-USC program

China put an effort to increase the efficiency of its power units as early as 1980, which resulted in the first two supercritical boilers with a power of 600MW. The following steam parameters were reached t=540°C÷566°C and p=24.2 MPa. They were implemented in Shidongkou in 1992. The next two boilers of similar parameters started work 12 years later at the Huaneng Qinbei power plant. 2004 was year for new power plants in China, as they created two additional units of 900MW and with steam parameters: t=538°C÷566 C and p=25MPa. Since 2005, China has begun commercializing USC power plants, since utility power from supercritical power plants has already reached 27GW. Over the next four years (2006-2010), 72 additional USC boilers, with power of 600MW and 1000MW, were created. It allowed additional 60GW to be delivered to the transmission line.

In Beijing, in June 2010, a national alliance was launched by the National Energy Resources Office to work on A-USC 700 ° C carbon fired technologies. Several research laboratories, manufacturers of machinery and equipment involved in the construction of power plants and companies dealing with the exploitation of such facilities were involved in the work. The Chinese program assumes the fulfillment of three basic goals: achieving a steam pressure above 35MPa, a rise in steam temperature above 700°C, assuming that the boiler output will exceed 600MW. This program included many separate tasks to meet, including the A-USC power plant project, the search for and development of new high temperature resistant materials, the strength testing of new materials, and finally the use of new technology in a demonstration power plant. The main objective of the program was to develop own alloys resistant to high temperatures and to improve the properties of borrowed materials. The Chinese research focused on G115 and 740H steel. Research centers are required to acquire the necessary experience in the field of production, assembly and subsequent operation of components, as well as to increase reliability and reduce the cost of the resulting investment. European COMTES 700 is a project similar to the Chinese CTH 700, in which the steam parameters would be t=725°C and a pressure of p=25MPa.

3.5 Indian A-USC program

In 2003 a bill was passed in India to clarify the laws governing all electricity trading, with the main goal of reducing power shortages on lines and increasing competition on the market in order to provide consumers with continuous electricity supply.

By the end of 2012, the Indian government committed to create additional units with a power of at least 100 000 MW. The Ministry of Energy together with organizations such as the CEA and the PFC have joined forces to launch a research program on the construction of SCs based on coal combustion. The Indian climate change group, pointed that it would be necessary to build USC boilers in conjunction with IGCC technologies to benefit from clean coal technologies. Opening of India's first 800 MW A-USC power plant is planned for 2017. However, as a result of minor delays stemming from the lack of approvals of construction steps by the government, the opening of the plant this year is in question. These plants are built in collaboration with many companies and manufacturers, and it’s cost is expected to be $ 1.5 trillion. The A-USC program in India is similar in design to other types of projects around the world. It assumes the creation of a research knot that controls primarily the degree of corrosion of metal components formed during the combustion of native coal. Boilers and turbines, according to the exact European tests, are made in this case with alloy 617, but for the production of thicker components is used steel 740. Future plans focus on investigating 800MW power generation and commercialization of A-USC technology.

4. Summary

The aim of the study was to demonstrate that increase in the steam parameters in power units must be accompanied with progress in the field of material engineering. The high thermal requirements posed by advanced ultrasupercritical boilers, make that worldwide progress in continually research on the use of new technologies. Programs are often executed internationally in cooperation with companies and research laboratories. One of the most active projects is the European program AD700, under which a power plant is scheduled to complete in the next three years with efficiency over 50%. Average efficiency of boilers in Europe is now about 37 percentage.

References

[1] A. Shibli: *Coal Power Plant Materials and Life Assessment. Development and Applications*, Woodhead Publishing Series in Energy: Number 62, Wielka Brytania 2014.
[2] A. Di Gianfrancesco: *Materials for Ultra-Supercritical and Advanced Ultra-Supercritical Power Plants*, Woodhead Publishing Series in Energy: Number 104, Wielka Brytania 2017.
[3] Dongke Zhang FTSE: *Ultra-supercritical coal power plants*, Woodhead Publishing Series in Energy: Number 41, Indie 2013.
[4] R. Blum, J. Bugge, S. Kjaer : *Development of a PF Fired High Efficiency Power Plant (AD700)*, DONG Energy Generation, Denmark 2007.
[5] M. Lis: Powyżej punktu krytycznego, www.energetykajutra.pl, 2016.
[6] *Siemens* advertisement materials.

[7] *Babcox&Wilcox* advertisement material.
[8] A. Hernas : *Materiały i technologie do budowy kotłów nadkrytycznych i spalarni odpoadów*, Wydawnictwo Stowarzyszenia Inżynierów i Techników Przemysłu Hutniczego w Polsce, Katowice 2009.

Hydrogen Production from Bagasse

Moeez Ahmed[1], Miguel Santos Silva[1]

[1]Faculty of Energy, Silesian University of Technology, email: moeezahmed92@hotmail.com, santossilva.miguel@gmail.com

Abstract

The paper is about Hydrogen Production, with Bagasse as primary feed source. The process consist of implementation of a novel Two Stage Pyrolysis-Gasification Reactor followed by hydrogen extraction via Carbon Membrane Shift Reactor. The study shows that this process is feasible and an environmental friendly way of recycling the by-product of the sugarcane by producing hydrogen, which can be utilized in many applications, in particular as a renewable fuel.

Keywords: Bagasse, hydrogen, pyrolysis, gasification, membrane, reactor

1. Introduction

Most of the bagasse produced in Pakistan is either utilized for feeding livestock or for cooking purposes and the rest of it is wasted. We hope to utilize the bagasse in a more productive manner. The purpose of the study was to design a process which will convert bagasse to hydrogen gas, emitting carbon dioxide as by-product, which in turn will be stored instead of being released into the atmosphere. Both gaseous compounds are in high demand within Pakistan's agro based economy and this process serves as a potential to cater those requirements. Hydrogen is a clean and environmentally friendly fuel and the process employed in manufacturing in this case is much cheaper than conventional electrolysis of water.

2. Process Description

Pyrolysis and Gasification are processes that convert organic or fossil fuel based carbonaceous materials into carbon monoxide, hydrogen and carbon dioxide. This is achieved by reacting the material at high temperatures (>700 °C), with a controlled amount of steam and air incurring oxidation in the fuel. We are going to utilize this mechanism to design a Hydrogen Production plant based in Pakistan. Bagasse is the by-product of sugarcane and is readily available in Pakistan. The cost is relatively low due to the fact that most of the bagasse goes unused and its cost is roughly about Rs. 4500/ton or 152 PLN/ton. Pakistan is the 6th largest producer if sugarcane and the total production of bagasse in Pakistan is approximately 30-32 million tons per year.

The following Table showcases the composition of Bagasse

Tab. 2 Composition of Bagasse

Composition	Weight (%)
Cellulose	45-55
Hemicellulose	20-25
Lignin	18-24
Ash	1-4
Waxes	<1

The following process flow diagram illustrates our proposed design from the preparation of bagasse to the final extraction of Hydrogen and its storage.

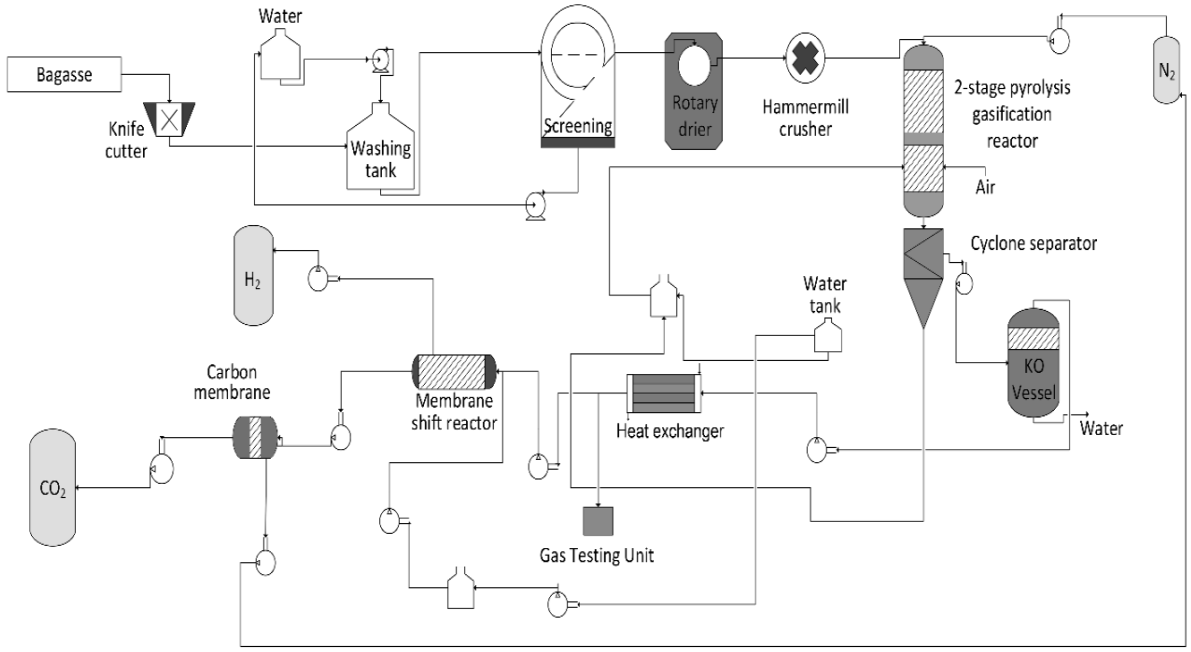

Fig. 1 Process Flow Diagram.

2.1 Feed Preparation

Bagasse is taken from different areas of Pakistan and is fed to knife cutter section where the size of bagasse is shortened to about 5cm. Then this is shifted to washing tank where washing of bagasse is carried out and then passes through screening section to remove the excess water out. The moisture content in bagasse after screening section is about 50%. This moisture should be reduced below 5%. Feed is passed through rotary drier, where the moisture content of bagasse is reduced to about 2%. After drying, the size of bagasse is ground to about 5mm.

2.2 Pyrolysis & Gasification

The feed enters the pyrolysis section where bagasse is heated and thermally decomposed in a non-reactive atmosphere. Thermal decomposition of bagasse is carried out at 500 °C [1,3]. Biomass pyrolysis is endothermic, and requires considerable amount of heat. The whole process is carried out in the absence of oxygen to avoid any chemical reaction. For this, nitrogen is purged through the section to eliminate air. The biomass consists of long chains of hydrocarbons that break down to small molecules containing gases, condensable liquids and char. Condensable vapour known as bio-oil, bio-crude, etc., and non-condensable gases known as CO, CO_2, H_2, CH_4 are generated by the pyrolysis process. We are carrying out slow pyrolysis at 500 °C with residence time of about 10 minutes [4]. Most of our product will be in the form of gases. The product from pyrolysis section goes to gasification section. In the gasification section temperature raised to 850 °C [6]. The result of the gasification is a fuel gas (called syngas) consisting mainly of carbon monoxide (CO), hydrogen (H_2), carbon dioxide (CO_2), water vapor (H_2O), methane (CH_4), nitrogen (N_2), some hydrocarbons in very low quantity and contaminants, such as carbon particles, tar and ash.

2.3 Cyclone Separator & KO Vessel

In this section, char and other solid particles are separated from gases. Char is the intermediate solid residue which is formed in reactors during pyrolysis and gasification processes. The gases from cyclone separator are shifted to the knock out vessel, where gases are separated from liquids most notably bio-oils. The gravity is utilized to remove liquids from gases in vertical vessel.

2.4 Heat Exchanger

The purpose of the heat exchanger is to cool down the gaseous mixture to the desired temperature for further operations. The heat exchanger used for this purpose is a shell and tube heat exchanger. The gaseous mixture is being kept on the tube side while the cooling water flows on the baffle side. The shell and tube heat exchanger has the baffle side of single pass and tubular side has double pass [10]. The tubes are made of cupronickel alloy which is made of a mixture of copper and nickel [7-8]. The temperature of the gases at inlet is at 850 °C (1123K) and has to be reduced to around 350 °C (623K). The temperature difference on tube side arises to be 500 °C. The flow of water at the cooling water inlet is at room temperature around 25 °C. The outlet temperature of water is at 80 °C at the exit of the heat exchanger on the shell side. The temperature difference on shell side arises to be 55 °C. The heat exchanger has a total number of 12 tubes which provide sufficient surface area for temperature reduction of gases. The flow of water required for the reduction in temperature is 1091 kg / hr. While the mass flow rate on the tube side for gases is 83.56 kg/hr which is the combined mass of nitrogen plus products of the gasifier. Triangular pitch was used for our heat exchanger.

2.5 Membrane Shift Reactor

The membrane acts as a semi-permeable barrier and separation occurs by the membrane controlling the rate of movement of various molecules between two gas phases in this case. The cooled gaseous mixture from the shell and tube heat exchanger is directed towards the membrane shift reactor. A commercial application of the water gas shift (WGS) reaction is in raising the concentration of hydrogen in gas mixtures produced via steam reforming or partial oxidation of hydrocarbons. Thus, a commercial process of the WGS reaction usually operates at high temperatures, between 623K and 673 K, with an iron and chromium based catalyst having high thermal stability to suppress the concentration of carbon monoxide. Further, ultra-high-purity hydrogen is produced directly, since silica membrane is permeable only to hydrogen. The catalysts are divided on weight basis of 92% in favor of iron catalyst to the remaining 8% weight of chromium catalyst [2]. The silica membrane used in the production of hydrogen is in the form of a hollow fiber. This module resembles a shell and tube heat exchanger. Thousands of tubes are bundled together. It is also in asymmetric shape with a dense coating of silica membrane on top over a glass support. The membrane has a pore size of 3°A (Angstrom). The design of the reactor is in a tubular shape with the gaseous mixture entering from the central tube. Hydrogen which is present in the mixture and the evolved hydrogen due to the water gas shift reaction are separated through permeation while the remaining carbon dioxide is carried further onwards. The membrane is divided into three stages, where each stage removes hydrogen from the mixture on a subsequent level. The permeated hydrogen is collected in the storage tank. The remaining gases are passed on to the carbon membrane. The permeance of hydrogen at 350°C is 1.2 x 10^-6, permeance of carbon dioxide is 1.24 x 10^-8 and permeance of nitrogen in silica membrane is 3.6 x 10^-9[9]. The selectivity (α) of hydrogen over carbon dioxide is 100 and selectivity (α) of hydrogen over nitrogen is 344 respectively. The pressure ratio is of 0.1 between permeate and reject phase.

2.6 Carbon Membrane

The carbon membrane is used to separate the carbon dioxide and nitrogen. The carbon membrane used is in the form of a hollow fibre. It is also in asymmetric shape with a dense coating of carbon membrane on top over a glass support. The membrane has a strong affinity towards carbon dioxide. The selectivity is around ($\alpha = 14.3$) for carbon membrane of carbon dioxide over nitrogen. The design of the reactor is in a tubular shape with the gaseous mixture entering from the central tube. The permeated carbon dioxide is collected in the storage tank. The remaining nitrogen is collected in a storage tank and is being recycled and directed back to the gasifier for nitrogen purging.

3. Chemical Equations

The following chemical reactions take place inside the two stage Pyrolysis and Gasification Reactor and inside the Carbon Membrane Shift Reactor [5].

Water Gas Phase Reaction:

$$C + H_2O \leftrightarrow CO + H_2 \tag{1}$$

Boudouard Reaction:

$$C + CO_2 \leftrightarrow 2CO \tag{2}$$

Water Gas Shift Reaction:

$$CO + H_2O \leftrightarrow CO_2 + H_2 \tag{3}$$

Methane Reforming:

$$CO + 3H_2 \leftrightarrow CH_4 + H_2O \tag{4}$$

Partial Oxidation:

$$C + \frac{1}{2}O_2 \leftrightarrow CO \tag{5}$$

4. Material Balance

4.1 Pyrolysis and Gasification Unit

Flow Rate of Bagasse entering the gasifier unit = 713 kg/ hr

1 g of bagasse produces 18 mmol of H_2 [6]

$$\left(713\frac{Kg}{hr}\right)x(1000\frac{gm}{kg}) = (\frac{713000gm}{hr})$$

$$(\frac{713000g}{hr})x(18\frac{mmol}{g}) = (1.28\,x\frac{10^7g}{hr}H_2)$$

$$(1.28x10^7mmol\frac{H_2}{hr})\,x\,(\frac{2g}{mol}) = (2.567\,x\frac{10^4g}{hr}H_2)$$

$$(2.567x\frac{10^4g}{hr}H_2)\,x\,(\frac{1kg}{1000g}) = (\frac{25.67kg}{hr}H_2)$$

Flow Rate of Hydrogen exiting the gasifier unit = 25.67 kg/hr

4.2 Carbon Membrane Shift Reactor

Flow Rate of Hydrogen entering the membrane shift reactor = 25.67 kg/hr

1 g of bagasse produces 18 mmol of H_2 [4]

Carbon monoxide produced in the gasifier unit = 13.82kg/hr

Carbon monoxide produced through Steam Reforming = 2.59 kg/hr

$$CO + H_20 \rightarrow CO_2 + H_2$$

$$(\frac{13.82kg}{hr}) + (\frac{2.59kg}{hr}) = (\frac{16.41kg}{hr})$$

$$(\frac{16.41kg}{hr}) \, x \, (\frac{1}{28})(\frac{mol}{kg}) = (\frac{0.586mol}{hr})$$

$$(\frac{0.586mol}{hr}) \, x \, (\frac{2kg}{mol}) = (\frac{1.172kg}{hr})$$

$$(\frac{25.67kg}{hr} H_2) + (1.172 \frac{kg}{hr}) \, H_2 = (27.40 \frac{kg}{hr} H_2)$$

Flow Rate of Hydrogen exiting the membrane shift reactor = 27.40 kg/ hr

5. Conclusion

Bagasse, being an abundant by-product of sugarcane industry in Pakistan, provides an efficient and effective method for the production of clean hydrogen. The project entails successful integration of pyrolysis and gasification processes as one inline unit process. Theoretical hydrogen yield for the feedstock used in the study was determined to be 27.40 kg H_2/713 kg of bagasse. In conclusion, almost complete gasification of bagasse could be accomplished at a temperature around 850 ^oC, and the process was evaluated to be suitable for hydrogen production.

This design is not specifically dedicated to Bagasse as major biomass feed source. It can be modified for various forms of biomass feed from all over the world, with major examples including; cotton, wheat husks, coffee, fibers, stalks, coconut shells, lentils, corn husks, among others.

The production of clean hydrogen can be used in many industries including Fertilizer, Petrochemical and Oil Refineries. Hydrogen can also be utilized in energy production through electrochemical reaction in Fuel Cells. The byproduct, Carbon Dioxide, can also be used for various industrial purposes like Petrochemical and Beverage Industries.

Overall, the design and production process of Hydrogen through this novel two stage Pyrolysis – Gasification reactor resulted to be very successful and has great potential of being employed in the upcoming years.

Acknowledgment

This project is dedicated to all the support received from the School of Chemical and Materials Engineering, National University of Sciences and Technology. We are highly thankful to Dr. Iram Mehmood for the supervision of the project and her severe dedication towards its completion. We would also like to thank Sir Muhammad Ahsan for his precious time and help during the course of the project. Muhammad Usman Yousaf and Mohammad Saim Bin Farooq deserve a lot of praise for their support throughout its conclusion.

References

[1] MI. Jahirul, MG. Rasul, AA. Chowdhury, N. Ashwath. Biofuels Production through Biomass Pyrolysis —A Technological Review, *Energies*, 2012, 5, pp. 4952-5001.

[2] Purifying hydrogen with inorganic silica membranes at high temperatures. *The University of Queensland, Brisbane* Qld 4072, Australia.

[3] S. Sivakumar, N. Ranjithkumar, S. Ragunathan, Design and Development of Down Draft Wood Gasifier, *International Journal of Mechanical Engineering*, 2013, 2(2), pp. 1-10.

[4] A.Basile, E.Driolia, F.Santell, V.Violante, G.Capannelli, G.Vitullie. A study on catalytic membrane reactors for water gas shift reaction, *Gas Separation and Purification*, 1996, 10(1), pp. 53-61.

[5] SC. Rabelo, H. Carrere, R.M Filho, AC. Costa. Production of bioethanol, methane and heat from sugarcane bagasse in a biorefinery concept, *Bi resource Technology*, 2011, 02(17), pp. 7887-7895.

[6] W. Chunfei, TP. Williams. Hydrogen production by steam gasification of polypropylene with various nickel catalysts. *Applied catalysis B: Environmental*, 2009, 87, pp. 152-161.

[7] Lenntech, https://www.lenntech.com/stainless-steel.htm, (20/05/2015).

[8] Thomasnet, https://www.thomasnet.com/articles/chemicals/corrosion-resistant-coatings, (16/04/2015).

[9] D. Tsay, S. E. Weiss and T. C. Tsay, Single stage membrane reactor for high purity hydrogen production, 2007, US20070157517.

[10] R. K. Sinnot, *Chemical Engineering Design*, 4th Edition, Volume 6, Elsevier butterworth heinemann, pp. 34-490, 2005.

Thermoeconomic analysis of the supercritical power plant located in the USA and Poland

Zaręba Patrycja[1], Dyrlaga Izabela[1], Gaweł Aleksandra[1], Wysocka Alicja[1], Jezioro Aleksandra[1]

[1]Power Engineering, Silesian University of technology, pat.zareba13@gmail.com, dyrlagaizabela@gmail.com, aleksandra.gawel94@gmail.com, awysocka94@gmail.com, ola.jezioro@op.pl

Abstract

Nowadays, most of the electricity is produced in conventional power plants fed by a hard coal. The article presents a thermoeconomic analysis of the real existing power plant. The object is situated in the northern part of the United States of America in Montana state, additionally, the theoretical location in Poland was taken into the consideration to make the comparison between the costs and incomes generated by the power plant in both location. From authors points of view, the following article covers four main aspects, which describes interesting issues of running the power plant. (1) The financial aspects, which contains the sensitivity analysis for the specifying parameters - the cost of the hard coal and cost of sale for the electricity. (2) The political aspects, as the base for economy and ecology. (3) The innovative aspects to describe what actions were taken in order to improve the system and (4) the informative which provides rest of useful information. To find the locations where the efficiency could be increased the exergy analysis was done, as it reveals the places of biggest exergy loses.

Keywords: Supercritical power plant, energy balance, exergy balance, thermoeconomics analysis, hard coal fuel, innovations, digital twins, ecology, sensitivity analysis

1. Introduction

Nowadays most of total electric power is produced in conventional power plants. Annually all people around the world consume 19 099 Mtoe (Million Tonnes of Oil Equivalent)[3]. Usage of one Mtoe is a spending of almost 6 850 barrels of oil or 1 162 790 dm^3 gasoline.

In 1995 people consumed only 12 417 Moe, 2 194 Mtoe in the USA. Everywhere, but in the European Union, that tendency increased since then. In the EU consumption was 966 Mtoe back then, and in 2015 it was 775 Mtoe. In 2015 people in Poland used 117,4 Mtoe and in 1995 it was 122,98 Mtoe. In the meantime, the usage in the USA increased to the 2 578 Mtoe.

To produce electricity we usually use fossil fuels, mostly coal. In 2015 more than 65% electricity was produced from fossil fuels and more than 40% from coal, followed by hydroelectric plants(16%), nuclear plants (10,6%), biofuels and waste (2,2%), and geothermal, solar, wind and other sources make up the remaining (4,9%)[1]. Two countries: People's Republic of China (24%) and the United States (18%) dominate the electricity production in the world. In the United States, 67% electricity production comes from fossil fuels. As in China, where this value is 73%. In Poland 86% total electricity productions comes from fossil fuels.

Coal still plays a significant role in the world electricity production. Conventional power plants fed by coal provide stabilization in an electrical grid. Now, when energy industry develops renewable energy sources, this is the most important feature.

2. Analysed power plant

The analysed power plant has really existed in the United States of America. The power plant is situated in the north of USA, in Montana state. To make power plant energy and exergy balance real cycle was simplified. The analysed cycle is shown in Figure 1.

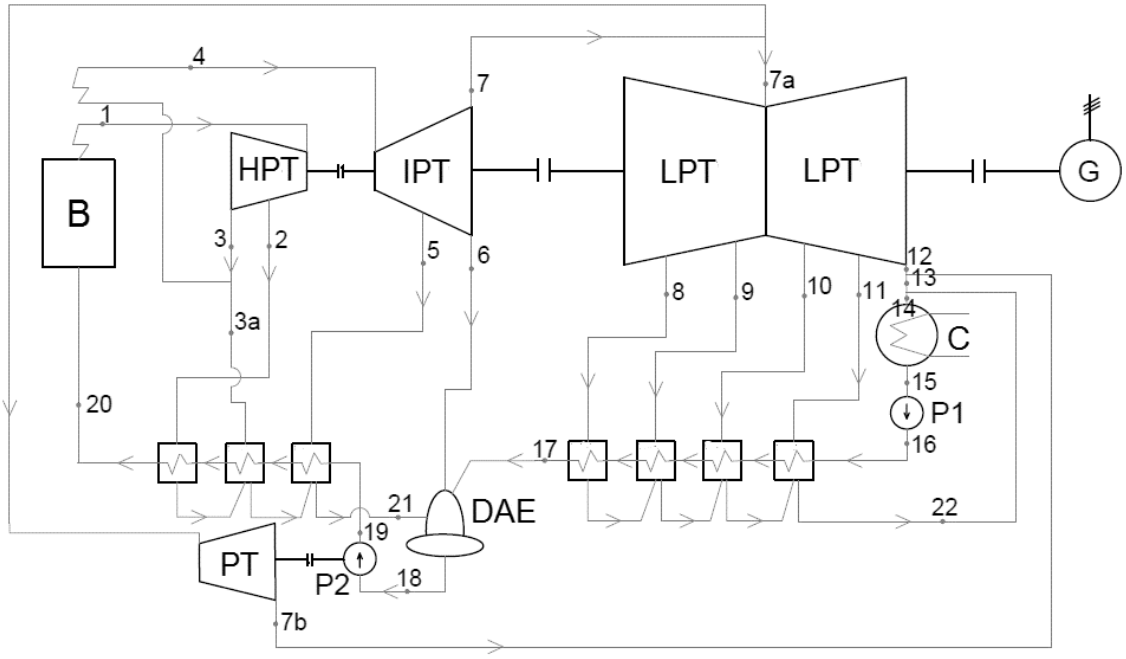

Fig. 1. Analysed power plant scheme

The system is composed of the boiler (B) which is feed by the hard coal. It is the fluidized bed boiler. In the boiler is produced high-pressure and high-temperature steam. The stem is directed to the steam turbine, where the steam expands. Three different stages of the steam turbine are distinguished: the high-pressure turbine (HPT), the intermediate-pressure turbine (IPT) and the low-pressure turbine (LPT). After the high-pressure turbine steam is directed to the reheater where we can increase temperature. Then steam is directed to the intermediate-pressure turbine. Next, the steam condenses in the condenser (C). Additionally, two different sections of heat recovery are presented. The high-pressure before the boiler and low-pressure after condenser. Between heat recovery sections is deaerator (DEA). In addition, the small steam turbine(PT) which is used to power water supply pump (P2) is one of the parts of the system.

3. Power plant's basic parameters

The power plant operates on supercritical steam parameters (pressure above 22,115 MPa and temperature above 647,27 K). Parameters in main points are shown in Table 1. Points designation correspond to the points in Figure 1.

Tab. 1 Basic steam parameters

Point	Temperature, K	Pressure, MPa	Enthalpy, kJ/kg	Mass flow, kg/s
1	866.5	24.2	3476.67	447.93
4	866.5	4.5	3652.29	377.23
7a	637.3	0.9	3188.48	314.61
14	305.4	0.005	1927.09	343.89

\The general form of power plant energy balance takes shape:

$$N_{iT} = \dot{m}_{in} \cdot h_{in} - \sum_{i=1}^{n} (\dot{m}_{out} \cdot h_{out}) \tag{1}$$

where:

N_{iT} - Turbine internal power
$\dot{m}_{in}$ - Mass flow in the inlet of the turbine
$\dot{m}_{out}$ - Mass flow in the outlet of the turbine
h_{in} - Enthalpy in the inlet of the turbine
h_{out} - Enthalpy in the outlet of the turbine

After calculations, total turbine internal power is 604,38 MW and the efficiency is 44,4 %. This particular power plant exists in the USA, although in order to choose the best option in terms of energetic and economic aspect, the assay includes an alternative to building such power plant in Poland. In Table 2 can be seen compared calculated parameters with parameters of polish supercritical power plants. As we can see, analysed power plant has nearly the same steam parameters as supercritical power plants located in Poland.

Tab. 2 Comparison of power plants

Power plant	**Power output, MW**	**Temperature of primary/secondary steam, K**	**Pressure, MPa**	**Efficiency, %**
Analysed power plant	**550**	**866.5/866.5**	**24.23**	**40.41**
Łagisza	460	833.15/855.15	27.5	43.0
Pątnów	464	813.15/838.15	25.0	41.0
Bełchatów	858	828.15/855.15	25.0	42.0

4. Exergy analysis

The exergy analysis is one of the tools to verify the efficiency of industrial heat processes. This analysis allows checking in which of the components of the system the exergy loss is the biggest. This permit to find the locations where the efficiency could be increased. The reason why the exergy analysis is used instead of the energy analysis is that the exergy, as opposed to energy, is not subject to the law of conservation. It answers more questions than the simple energy analysis.

Tab. 3 Exergy flow analysis

Process	**Fuel exergy, MW**	**Product exergy, MW**	**Exergy loss, MW**
Boiler	1454.2	688.5	765.7
High Pressure Turbine	198.5	183.6	14.9
Intermediate Pressure Turbine	184.2	173.3	10.9
Low Pressure Turbine	254.3	229.1	25.2
Generator	586.1	550.0	36.1
Pump	0.79	0.598	0.192
Condenser	19.6	19.6	0.0

The Table above presents the results of exergy analysis. Exergy losses were calculated as a difference between the fuel exergy and the product exergy. For example. for a steam turbine. the product is the mechanical

energy of the shaft and the fuel is the difference between input and output exergy streams. Enthalpy and entropy in each point for environmental parameters were calculated for T_{ot} = 298 K and p_{ot} = 0.1 MPa.

$$B = \sum_{i=1}^{m} (h_i - h_{ot} - T_{ot}(s_i - s_{ot})) \tag{2}$$

5. Fuel of the power plant

The boiler which produces the steam in the power plant is fed with the pulverized coal. Due to the lignite mines located nearby the power plant. the comparison of the profitability of using both types was done.

The differences in the composition of both substances. hard coal and lignite. are clearly visible. The concentration of carbon is ten percentage points lower in lignite than coal for which the value is 50%. Instead. there is more moisture in that component - it is slightly above one third. while in the latter one it is one fourth. Coal also contains the chlorine - the amount is just a jot but is visible. The ash contribution in lignite is slightly higher than in coal.

Besides that. rest of the composition is similar. In both components. there are hydrogen. nitrogen. sulfur. and oxygen. The values are really close to each other. What is worth mentioning. amount of oxygen varies around 10% in both components.

If the hard coal came from the mines situated in Poland. it would contain three times more ash. than the one that comes from the USA. Rest of the components would be on a similar level. That disadvantage was strong argument against building such power plant in Poland.

Taking into consideration problematic aspect of the lignite. which refers to the combustion process. transportation. and emission of undesirable products. the coal was chosen as the main fuel. In further paragraphs. more details about this choice will be given.

The calorific value of the fuel is based on the Dulong's formula given below

$$LCV = 1100(33\,900c + 121\,040\left(h - \frac{o}{8}\right) + 10\,500s - 2\,500w) \tag{3}$$

The letters correspond to the substances contained in the carbon written above. The formula requires percentage values of the contamination. Low Calorific Value calculated for the analysed system is 18.82 MJ/kg.

Knowing that value. the High Calorific Value could be calculated as

$$LCV = HCV - rf \tag{4}$$

Where r is the enthalpy of evaporation of water and f is the amount of water vapour obtained by burning one kilogram of solid fuel. The result for the considered power plant is 20.19 MJ/kg. The reason why the LCV is recalculated into the HCV is that in American nomenclature the efficiency is calculated by using the HCV. whereas in EU the LCV is used. This aspect should be taken into consideration while comparing data from different sources.

Those calculation has permitted to assess the usage of fuel. The power plant uses 70.9 kg/s of fuel. It gives more than six thousand megagrams (tonnes) per day. On an annual basis. it is two and a quarter of millions of Megagrams. It could fill the volume of the Great Pyramid in Giza and still around 240 000 Mg would left. That is why the storage of fuel area has to be huge. For example. in Bełchatów power plant the size of the power plan itself is relative to the size of its storage area.

6. Political and ecology

When it comes to the environmental protection the attitude of having all hands on deck is important. If one of the countries refuse to take care of the environment. the rest suffers. In 2015 the USA had the second place in a ranking of annual carbon dioxide emissions from burning fossil fuels [3]. after China and before India. Americans produced more than fifteen tonnes of CO_2 per capita.

Comparing to the year 2016. the decision concerning environmental protection in the USA changed significantly. Currently. it is not so demanding like it was a few years ago [4]. The USA signed out from the Paris Climate Agreement (Clean Power Plan). which results not only in the lack of control of CO_2 emission. but also abandons the restrictions about the ground chosen to become a foundation for a new mines. This decision scratches off the work of previous four years.

The main goal now is to create cheap energy for Americans. The cost of the systems responsible for purifying the exhaust gases is included in the price of the energy. Now. when the priority is to reduce the price. it will not be required to decontaminate the exhaust gases. This will effect in an increase of CO_2 and greenhouse gases emissions [4].

Nonetheless. the analysed power plant was built before the changes in law. so it has all required systems which purify the exhaust gases. Those are the SNCR system for reduce the sulphur oxides. and thanks to the secondary air inlet and ammonia inject the NO_x are reduced. The fly ash is diminished by the baghouses. After all of the stages of the processes. the final emission of NO_x is on the zero level. the same as SO_2. The emission of CO_2 is almost 3 and half of million Mg/year.

According to the current law. there is no necessity to pay any additional fees for the emission. so it is not included in the financial aspect.

7. Innovations

There is a variety of innovations implemented in order to increase the efficiency of the power plant. If the whole cycle was looking like on the T-s scheme the same as the Rankine cycle. the efficiency would be the highest. The Rankine cycle is the comparative cycle for power plants. it presents the ideal processes with given parameters. Reality is naturally different. there are plenty of ideas how to approach the ideal one.

Not mentioning the supercritical parameters. reheating systems. heat regenerations systems. there are three things worth getting a closer look because nowadays most of those are regular things. Those are the fluidized bed boiler. air cooled condenser and Digital Twin system.

The boiler in the analysed power plant is a fluidized bed boiler (CFB). It is a relatively new technology. The boiler is fed with the coal dust. the oxidizer (in analysed case it is air) supply is from under the bed at high-pressure. The air lifts the bed material and the coal particles and keeps it in suspension. Then the coal is combusted.

This technology helps with mixing fuel with air because fine particles of partly burned coal. bed material and ash are moved along with the exhaust gases to the upper areas of the boiler and then into a cyclone. In addition that reduces losses by avoiding incomplete combustion.

The most important advantage of the fluidized bed boiler is the flexibility of firing a wide range of coal (wide range of calorific heating value). By using CFB is reduced the emission of harmful substances. There is no additional requirement of separate NO_x capturing devices because the combustion temperature for fluidized bed boiler is less than in pulverized coal (PC) boilers. Sulphur Dioxide is converted the SO_2 to sulfates during the combustion and circulation which leaves with the ash. On the other hand. fluidized bed boiler is less resistant to corrosion and it requires high-pressure air in the furnace. Additionally. CFB has long startup time from a cold state.

It is required to use the air-cooled condenser simultaneously with the water-cooled one. It is caused by the fact that in some time during the year the lack of water force power plant to use only air in order to cool the factor. It has the advantages and disadvantages. the biggest of the latter one are certainly two issues: that it requires more of energy input and has lower heat transfer coefficient - which means it is less effective.

The pluses of such solution are for example fact that there are no dead zones because the heat is transmitter homogeneously. the resistance to corrosion is way higher as there is no water and these are more environmentally friendly. The last one is induced by the fact that smaller usage of water from the ambient means the smaller restoration of warmed up water to it - so smaller influence for the environment. Not the most important. but still worth noticing is the appearance of that type of a condenser - those looks like the roofs of Scandinavian houses. so definitely local inhabitants are not hostile about that.

One of the aims of the article was to indicate innovative solutions of applied technology. The processes described above are already implemented in the present solutions. although they can be classified as innovative. The most modern and therefore innovative aspect is described below. The idea is to replace the SCADA system with the Digital Twin (DT).

SCADA system collects the data and is able to visualize those. It can also control the processes. raise the alarm if necessary and archives all the data. It all sounds great. though nowadays it is required more from the system. Those new needs are covered by Digital Twin - it can adapt to changing working conditions because it is able to learn. and so predict the behaviour of the system. One of the greatest capabilities of the DT is to provide the optimization in order to improve productivity. It can also be a great assistance for an operator. as it suggests solutions to the occurring problems.

8. Informative

The transmission grid in the United States is not homogeneously distributed. The west and the middle part is noticeably less developed. The analysed power plant is located in that part. therefore it has to be ready to guarantee the energy delivery in different stages of daily and monthly demand. It also has to be reliable. in case of any unexpected emergency occurred. Although. when everything works fine. the power plant works in the basic. as it requires a lot of time to change the power output of the plant.

These days it is very popular to describe our mother planet as the Global Village. It has a lot of advantages and disadvantages.

The North American Electric Reliability Corporation is one of the better sides of the foregoing statement. As is receives all information from all power plants in the USA. it can send the guidelines to each of those. It can control the energy production and prevent the blackouts.

By dint of the Internet. the information gets from one point to another within the blink of an eye. Unfortunately. most of them are treated without any scepticism. therefore it is commonly seen that people are repeating falsehood sentences. That problem happens also to the power plants. There were a lot of situations when the Greenpeace. and similar to it institutions. were painting signs "Stop CO_2 emission" on the chiller chimneys and were convincing people that what is coming out of those. is really harmful. Nowadays. with the existing technology. the exhaust gases are sometimes directed to the cooling tower instead of going to the stack. It does not mean that each nimbus above the cooling tower includes injurious substances.

In order to prevent such situations. the company does not only has to try to increase the awareness in people but also work on the PR (Public Relations). There are dozens of ways how to be positively associated.

One of the suggestions is to make a better first impression and outlook in the neighbourhood. As impressive huge chimneys are not the best view. the idea is to paint them in a nice looking way. There are some power plants which already are implementing this - in Poland it is Opole and Jaworzno and even in Africa there is one in Johannesburg.

Another way is to promote sports events. sponsor players. and stadiums. There are many examples of it. In Poland. this approach is quite common. For example one of the best Polish volleyball teams. PGE Skra Bełchatów is mainly sponsored and owned-by Polska Grupa Energetyczna. This company controls the majority of polish power plants. such as Bełchatów which was mentioned in the beginning of this article. Polish national team in handball is sponsored by Polskie Górnictwo Naftowe i Gazownictwo - the largest company in Poland engaged in exploration and production of natural gas and crude oil. These are just a few examples that could be mentioned.

Such instances outside of Poland can be also pointed out. In 2016 in the Summer Olympic Games in Rio de Janeiro (Brazil) one of the main partners was GE (General Electric) company. GE also support the Team USA - national teams in many different sports. Russian Gazprom will be one of the main sponsors of the upcoming World Cup in Moscow (2018). Stadiums built by companies like PGE and Tauron in Poland and NRG in the USA are very impressive and worth seeing. Not only sport but also some cultural events are happening there. and not only there. When it comes to the cultural happenings. the Narodowa Orkiestra Symfoniczna Polskiego Radia (NOSPR). which is the National Symphony Orchestra of Polish Radio is sponsored by Tauron company.

The charity events deserve to be mentioned. A lot of companies are reinforcing marathons and similar actions. to collect money for children. or to perform the renovation of the buildings and buy specialist equipment which is necessary for therapeutic activities. Not only so noble goals are taken into the consideration but also the ideas how to improve the neighbourhood. So did the group of workers of PGE. who had built the playground for children and also arranged the outdoor bookcrossing shelves.

Taking all of above into consideration. in the financial aspect of the power plant. it is settled to spend a great amount of money per year for such actions. It raises the morale of employees and gives the company better outlook.

9. Financial Analysis

The analysed power plant is already existing. and so the financial analysis will not include the investments costs such as building permission. loans. and equipment. The financial analysis included only costs and profits since the return of the investments costs of the power plant.

Annual income for power plants comes from electricity selling. To calculate this should multiply annual average. daily produced energy by annual working time and the average price for electricity sell. For calculations. the annual operating time of the power plant was assumed as 7000 hours. what gives almost 291 days. Nearly 73 days have been deducted for necessary repairs and unscheduled failures. These numbers were chosen as similar option to Poland. where coal-fired power plants work on average 7000 hours a year [8]. It was also assumed that the power plant works all time on the nominal parameters and produced the constant amount of electricity.

$$S_n = N_{el} c_{el} \tau \tag{5}$$

N_{el} - daily average produced energy
τ - annual working time
c_{el}- average price for electricity sell [9][10]

The cost structure is more complex. They can be divided into several categories. In the analysis distinguished: maintenance costs. cost of purchase and preparation of fuel. administrative costs. cost of environmental protection. cost of purchase and preparation of water and other costs such as accessory electric plant and improvements to the site. The cost structure of the power plant is shown in the chart below.

It is clearly visible that the main two types of the costs are fuel and administrative. Even though the latter one may seem too high. it merits noticing that costs related to the PR and lawyers are also included in this part. The third main cost is the maintenance cost. as this is the active power plant.

The difference in costs and incomes is generated profit. In order to verify how susceptible is that profit for any change in the price of coal. electricity and carbon dioxide emission. the sensitivity analysis has been made. The results. for power plant situated in the USA. can be seen in the picture number 3. As there are no loans more to pay off. the profit is on really high level. Only remarkably reduced price of the electricity could harm the profitability of the power plant. as this factor is the most influential.

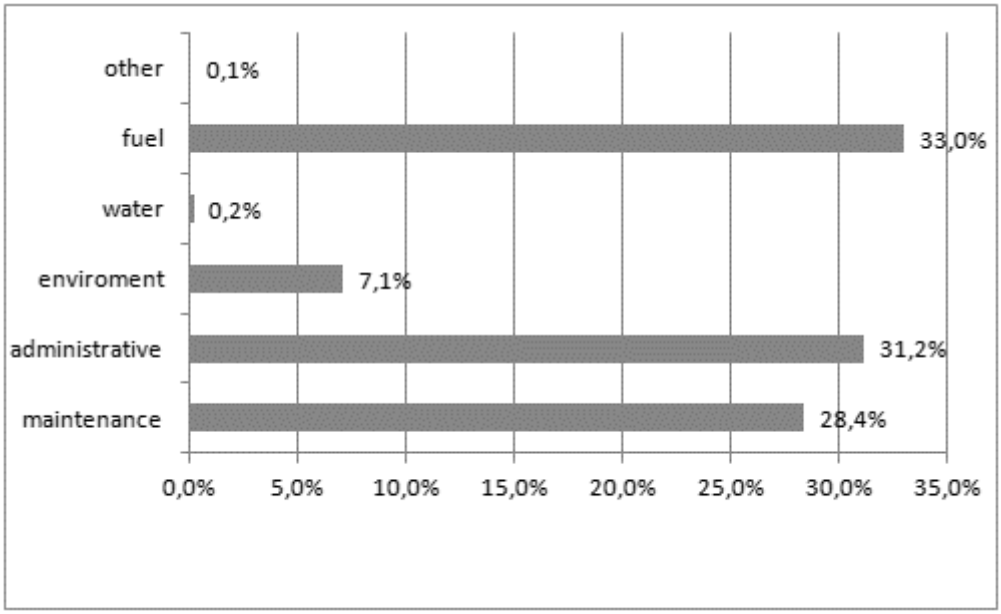

Fig. 2 Cost structure graph plot

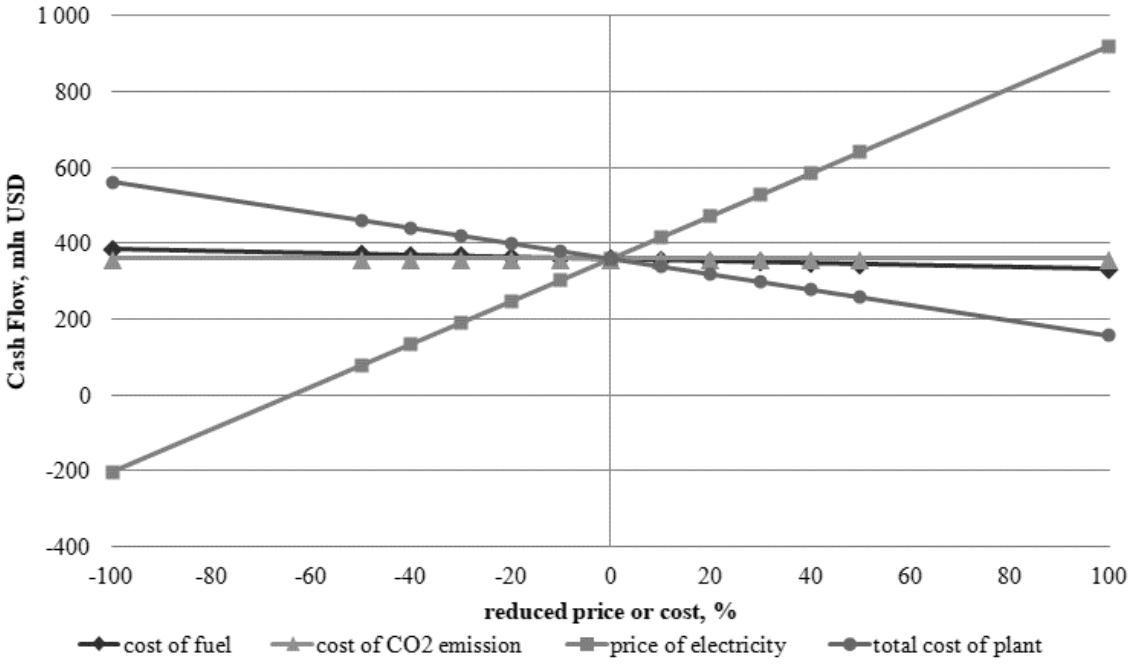

Fig. 3 Cash flow sensitivity – USA

The results for power plant situated in Poland was shown in the picture below. The most sensitive to changes is the price of electricity. Even slight change in electricity sales price can significantly affect cash flow. It is also visible. that price of CO_2 emission has not serious influent of cash flow. The effect of change of fuel price is similar to the USA example.

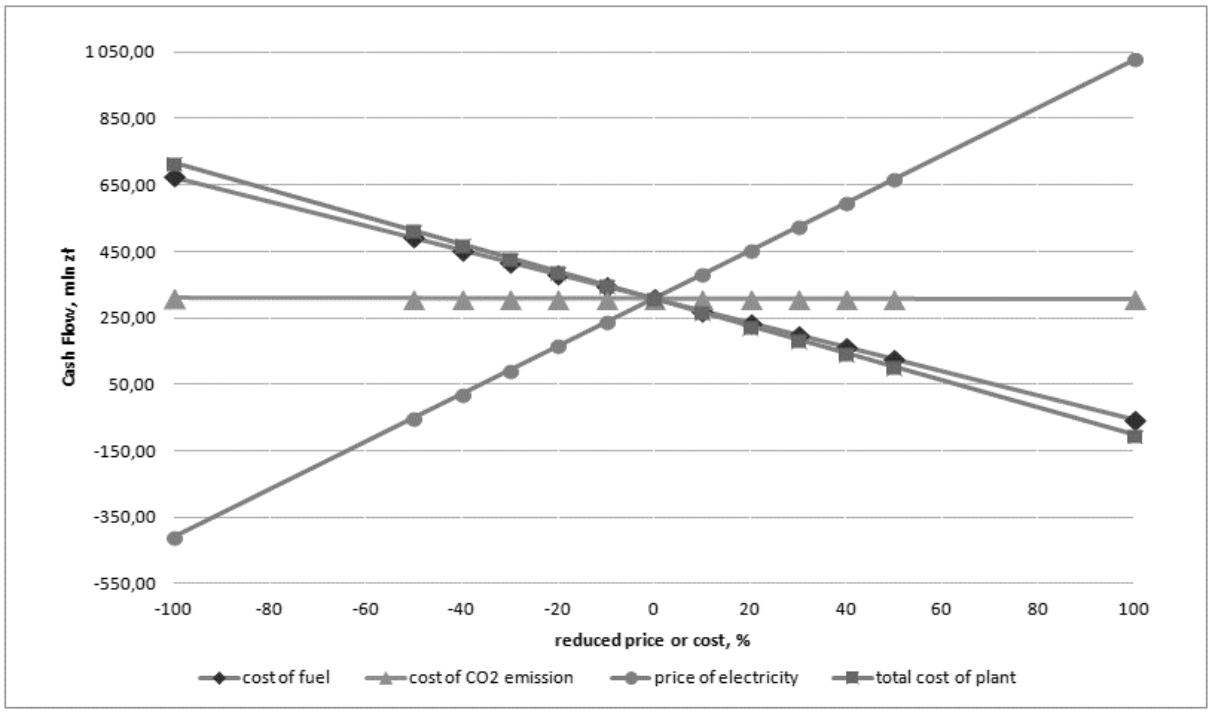

Fig. 4 Cash flow sensitivity – Poland

10. Summary

After the analysis. it was found that better location is in the USA. as the quality of used coal is higher and the coal is cheaper. Also. the requirements of the CO2 emission are not so restrictive as it is in European Union. What is more. the price of the sale of the energy is higher. Therefore. these aspects lead to higher incomes and that location was chosen.

The power plant is really innovative. as it has the fluidised bed and works on supercritical parameters. However. an additional idea was suggested. which not improves the efficiency of the power plant. but optimizes the way the power plant works.

Another important point is fact. that the biggest loses of exergy takes place in the boiler. This loses consist of the processes which occurs in the boiler. There are two most important elements in all loses. The highly irreversible combustion process which is one-third. and the heat transfer which is one quarter. As the loss of exergy causes a reduction in the useful effects of the process. hence any future improvements should aim to reduce this loss. especially in the boiler as it provides with the most useful process in the whole power plant.

The biggest impact on the cash flow has the change in the price of energy sales. while the lowest has the cost of CO2 emission. This tendency occurs independently of location. In general. what can also be seen. the location in the USA is less vulnerable to changes in costs of fuel and total costs of the power plant. Nonetheless. it should be underlined that such incomes are not possible. as for the sake of calculations. assume work with the nominal parameters and average work time.

Power plant management is not only about the technical aspects. it is also about the people and their opinion about the company. The key is to be positively associated and to create a trustworthy brand in human minds.

Acknowledgement

This article was prepared within the projects Innovative systems for fossil fuels conversion and Thermoeconomic Analysis in Power Engineering carried out at Faculty of Energy and Environmental Engineering. Institute of Thermal Technology. the field of study Power Engineering - Thermal Energy Systems. Work was conducted under the direction of Lucyna Czarnowska. PhD.

References

[1] J. Szargut. *Termodynamika*. Państwowe Wydawnictwo Naukowe. Warszawa 1985.
[2] T. Chmielniak. *Technologie energetyczne.* Wydawnictwo Naukowo – Techniczne. Warszawa 2008.
[3] Energryatlas. http://energyatlas.iea.org/#!/tellmap/-1118783123/2 (29/11/17).
[4] Green Project. http://www.green-projects.pl/2016/11/donald-trump-program-ekologia (29/11/17).
[5] M. Pawlik. Zaawansowane technologicznie bloki energetyczne – Nowe wyzwania. Elektroenergetyka". nr 8/2013 .
[6] Process Modeling Design Parameters In NETL Studies. 2014.
[7] M. Matuszewski. Cost and Performance for Low-Rank Pulverized Coal Oxycombustion *Energy Plants. 2010.*
[8] Narodowe Centrum Badań Jądrowych http://ncbj.edu.pl/niezalezna-ocena-kosztow-produkcji-energii-elektrycznej (29/11/17).
[9] Urząd regulacji energetyki. https://www.ure.gov.pl/pl/rynki-energii/energia-elektryczna/srednie-ceny-energii-i (29/11/17).
[10] OVO Energy. https://www.ovoenergy.com/guides/energy-guides/average-electricity-prices-kwh.html (29/11/17).
[11] M. Mieczyński. *Egzergia w termodynamice teoria i zastosowania*. Oficyna Wydawnicza Politechniki Wrocławskiej. Wrocław 2013.

Waste treatment technologies - A review

Abdul Rehman[1]

[1]*Department of Power Engineering, Silesian University of Technology Poland, email: abdul.me17@gmail.com*

Abstract

As the population on the earth increased, the waste generated by humans also increased proportionally. This waste varies from organic in nature, produced directly by people, to the industrial waste. When this waste started to effect environment, many new ways to treat the waste were invented. A number of possible ways to make waste less harmful are discussed in this article along with their pros and cons. At the end there is a description of different waste collection and transportation methods which are being used around the globe.

Keywords: Waste treatment technologies, incineration, waste collection methods, recycling, history of waste treatment

1. Introduction

Waste management is the collection, transport, processing or disposal, managing and monitoring of waste materials. The term usually relates to materials produced by human activity, and the process is generally undertaken to reduce their effect on health, the environment or aesthetics. Waste management is a distinct practice from resource recovery which focuses on delaying the rate of consumption of natural resources. All waste materials, whether they are solid, liquid, gaseous or radioactive fall within the remit of waste management.

Waste management practices can differ for developed and developing nations, for urban and rural areas, and for residential and industrial producers. Management of non-hazardous waste residential and institutional waste in metropolitan areas is usually the responsibility of local government authorities, while management for non-hazardous commercial and industrial waste is usually the responsibility of the generator subject to local, national or international authorities.

2. History

Throughout most of history, the amount of waste generated by humans was insignificant due to low population density and low societal levels of the exploitation of natural resources. Common waste produced during pre-modern times was mainly ashes and human biodegradable waste, and these were released back into the ground locally, with minimum environmental impact. Tools made out of wood or metal were generally reused or passed down through the generations.

However, some civilizations do seem to have been more profligate in their waste output than others. In particular, the Maya of Central America had a fixed monthly ritual, in which the people of the village would gather together and burn their rubbish in large dumps [1].

There has been a significant rise in municipal solid waste (MSW) generation in the last few decades due to rapid urbanization and industrialization. Municipal solid waste is being generated at a rapid pace and is expected to reach about 2.2 billion tonnes globally by 2025 due to urbanization and industrialization.

3. Methods of treatment

3.1 Landfills

Disposal of waste in a landfill involves burying the waste and this remains a common practice in most countries. Landfills were often established in abandoned or unused quarries, mining voids or borrow pits. A

properly designed and well-managed landfill can be a hygienic and relatively inexpensive method of disposing of waste materials. Older, poorly designed or poorly managed landfills can create a number of adverse environmental impacts such as wind-blown litter, attraction of vermin, and generation of liquid leachate. Another common product of landfills is gas (mostly composed of methane and carbon dioxide), which is produced as organic waste and breaks down anaerobically. This gas can create odor problems, kill surface vegetation and is a greenhouse gas.

Design characteristics of a modern landfill include methods to contain leachate such as clay or plastic lining material. Deposited waste is normally compacted to increase its density and stability and covered to prevent attracting vermin (such as mice or rats). Many landfills also have landfill gas extraction systems installed to extract the landfill gas. Gas is pumped out of the landfill using perforated pipes and flared off or burnt in a gas engine to generate electricity.

Fig.1 A landfill in Poland

3.2 Incineration

Incineration is a disposal method in which solid organic wastes are subjected to combustion so as to convert them into residue and gaseous products. This method is useful for disposal of residue of both solid waste management and solid residue from waste water management. This process reduces the volumes of solid waste to 20 to 30 percent of the original volume. Incineration and other high temperature waste treatment systems are sometimes described as "thermal treatment". Incinerators convert waste materials into heat, gas, steam and ash.

Incineration is carried out both on a small scale by individuals and on a large scale by industry. It is used to dispose of solid, liquid and gaseous waste. It is recognized as a practical method of disposing of certain hazardous waste materials (such as biological medical waste). Incineration is a controversial method of waste disposal, due to issues such as emission of gaseous pollutants.

Incineration is common in countries such as Japan where land is scarcer, as these facilities generally do not require as much area as landfills. Waste-to-energy (WtE) or energy-from-waste (EfW) are broad terms for facilities that burn waste in a furnace or boiler to generate heat, steam or electricity. Combustion in an incinerator is not always perfect and there have been concerns about pollutants in gaseous emissions from incinerator stacks. Particular concern has focused on some very persistent organic compounds such as dioxins, furans, and PAHs, which may be created and which may have serious environmental consequences [2].

Fig. 1.Spittelau incineration plant in Vienna

3.3 Recycling

Recycling is a resource recovery practice that refers to the collection and reuse of waste materials such as empty beverage containers. The materials from which the items are made can be reprocessed into new products. Material for recycling may be collected separately from general waste using dedicated bins and collection vehicles, a procedure called curbside. In some communities, the owner of the waste is required to separate the materials into various different bins (e.g. for paper, plastics, metals) prior to its collection. In other communities, all recyclable materials are placed in a single bin for collection, and the sorting is handled later at a central facility. The latter method is known as "single-stream recycling."

The most common consumer products recycled include aluminum such as beverage cans, copper such as wire, steel from food and aerosol cans, old steel furnishings or equipment, polyethylene and PET bottles, glass bottles and jars, paperboard cartons, newspapers, magazines and light paper, and corrugated fiberboard boxes.

PVC, LDPE, PP, and PS (see resin identification code) are also recyclable. These items are usually composed of a single type of material, making them relatively easy to recycle into new products. The recycling of complex products (such as computers and electronic equipment) is more difficult, due to the additional dismantling and separation required. [3]

The type of material accepted for recycling varies by city and country. Each city and country have different recycling programs in place that can handle the various types of recyclable materials. However, certain variation in acceptance is reflected in the resale value of the material once it is reprocessed.

3.4 Biological reprocessing

Recoverable materials that are organic in nature, such as plant material, food scraps, and paper products, can be recovered through composting and digestion processes to decompose the organic matter. The resulting

organic material is then recycled as mulch or compost for agricultural or landscaping purposes. In addition, waste gas from the process (such as methane) can be captured and used for generating electricity and heat (CHP/cogeneration) maximizing efficiencies. The intention of biological processing in waste management is to control and accelerate the natural process of decomposition of organic matter. [4]

Fig.3.A community-level composting plant in a rural area in Germany

3.5 Energy recovery

The energy content of waste products can be harnessed directly by using them as a direct combustion fuel, or indirectly by processing them into another type of fuel. Thermal treatment ranges from using waste as a fuel source for cooking or heating and the use of the gas fuel (see above), to fuel for boilers to generate steam and electricity in a turbine. Pyrolysis and gasification are two related forms of thermal treatment where waste materials are heated to high temperatures with limited oxygen availability. The process usually occurs in a sealed vessel under high pressure. Pyrolysis of solid waste converts the material into solid, liquid and gas products. The liquid and gas can be burnt to produce energy or refined into other chemical products (chemical refinery). The solid residue (char) can be further refined into products such as activated carbon. Gasification and advanced Plasma arc gasification are used to convert organic materials directly into a synthetic gas (syngas) composed of carbon monoxide and hydrogen. The gas is then burnt to produce electricity and steam. An alternative to pyrolysis is high temperature and pressure supercritical water decomposition (hydrothermal monophasic oxidation). [5]

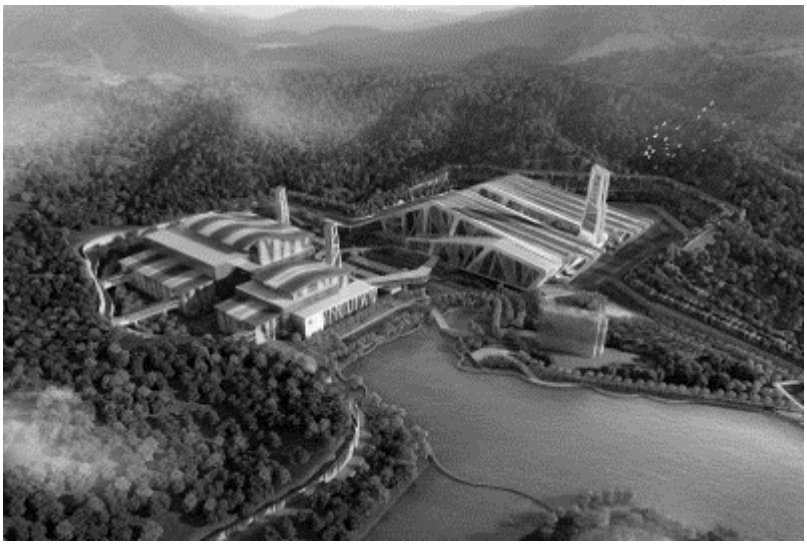

Fig. 4 Baoan Waste-to-Energy Facility in Shenzhen, China

4. Waste handling and transport in world (Recommendations)

Waste collection methods vary widely among different countries and regions. Domestic waste collection services are often provided by local government authorities, or by private companies in the industry. Some areas, especially those in less developed countries, do not have a formal waste-collection system. Examples of waste handling systems include:

- In Europe and a few other places around the world, a few communities use a proprietary collection system known as Envac, which conveys refuse via underground conduits using a vacuum system. Other vacuum-based solutions include the MetroTaifun single-line and ring-line automatic waste collection system, where the waste is automatically collected through relatively small diameter flexible pipes from waste collection points spread out up to a distance of four kilometers from the waste collections stations.
- In Canadian urban centers curbside collection is the most common method of disposal, whereby the city collects waste and/or recyclables and/or organics on a scheduled basis. In rural areas people often dispose of their waste by hauling it to a transfer station. Waste collected is then transported to a regional landfill.
- In China, Plastic pyrolysis or Tire pyrolysis is: the process of converting waste plastic/tires into industrial fuels like pyrolysis oil, carbon black and hydrocarbon gas. End products are used as industrial fuels for producing heat, steam or electricity. Pyrolysis plant is also known as: pyrolysis unit, plastic to fuel industry, tire to fuel industry, plastic and tire recycling unit etc. The system is used in USA, California, Australia, Greece, Mexico, the United Kingdom and in Israel. For example, RESEM pyrolysis plant that has been operational at Texas USA since December 2011, and processes up to 60 tons per day.
- In Taipei, the city government charges its households and industries for the volume of rubbish they produce. Waste will only be collected by the city council if waste is disposed in government issued rubbish bags. This policy has successfully reduced the amount of waste the city produces and increased the recycling rate.
- In Israel, the Arrow Ecology company has developed the ArrowBio system, which takes trash directly from collection trucks and separates organic and inorganic materials through gravitational settling, screening, and hydro-mechanical shredding. The system is capable of sorting huge volumes of solid waste, salvaging recyclables, and turning the rest into biogas and rich agricultural compost. The system

is used in California, Australia, Greece, Mexico, the United Kingdom and in Israel. For example, an ArrowBio plant that has been operational at the Hiriya landfill site since December 2003 serves the Tel Aviv area, and processes up to 150 tons of garbage a day.

- In Saudi Arabia there is the world's largest AWCS now being built in the vicinity of Islam's holiest mosque (Mecca). During the Ramadan and Hajj 600,000 kilos, or 4,500 cubic meters, of waste is generated each day, which puts a heavy demand on those responsible for collecting the waste and litter. In the MetroTaifun Automatic Waste Collection System, the waste is automatically collected from 74 waste feeding points spread out across the area and then transferred via a 20-kilometre pipe network to a central collection point, keeping all the waste collecting activities out of sight and below ground with the central collection point well away from the public areas.
- Waste hierarchy, which refers to the "3 Rs" reduce, reuse and recycle, which classify waste management strategies according to their desirability in terms of waste minimization. The waste hierarchy remains the cornerstone of most waste minimization strategies. The aim of the waste hierarchy is to extract the maximum practical benefits from products and to generate the minimum amount of waste.

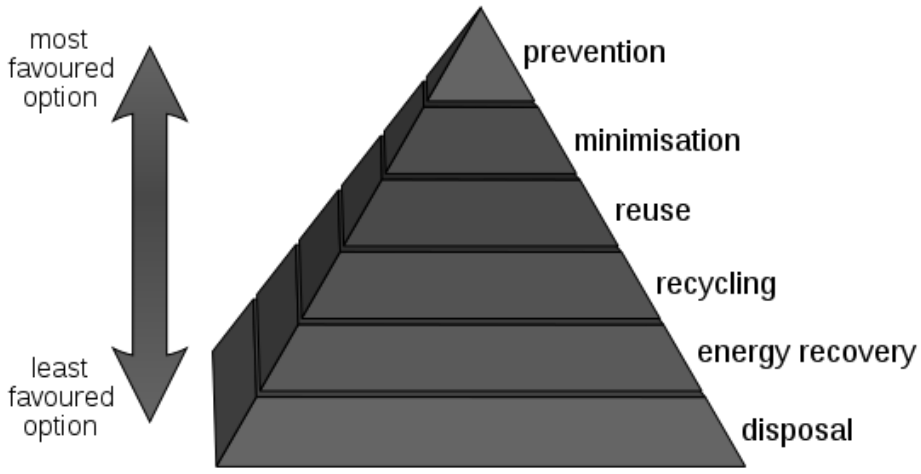

Fig. 5 The waste hierarchy.

References

[1] Rathje William and Cullen Murphy, Rubbish! The Archaeology of Garbage, Harper Collins Publishers, 1992.

[2] S.Silva, AM Lopes. Environmental aspects and impacts of a waste incineration plant, *4th international conference on energy and environment research ICEER 2017*, 2017, pp. 239-244.

[3] N. Singha, D. Hui, R. Singh, I.P.S.Ahuja. Recycling of plastic solid waste: A state of art review and future applications, *In Composites Part B: Engineering*, 2017, 115, pp. 409-422.

[4] M.T. Alexis, R.M. James, Sustainable recycling of municipal solid waste in developing countries, *Waste Management*., 2009, 29, pp. 915-923.

[5] A. Kumar, S.R. Samadder. A review on technological options of *waste* to *energy* for effective management of municipal solid waste, *Waste Management*, 2017, 69.

Flue Gas Cleaning Systems - A Review Paper

Maja Zagala[1], Hesham Abdelaal

[1]Faculty of Power and Environmental Engineering, Silesian University of Technology, e-mail: majazagala@gmail.com, heshabd658@student.polsl.pl

Abstract

The combustion of fuel results in the production of a mixture of gases containing pollutants such as carbon dioxide, sulphur dioxide, dust and soot, as well as nitrogen oxides, heavy metal bearing fumes and unburned hydrocarbons. The pollutants can be removed from the flue gases by using the latest flue gas cleaning systems, so that harmful organic and inorganic substances are no longer discharged into the atmosphere. These substances are partly incorporated in the reaction-neutral slag or concentrated in the filter dust as end product of the flue gas cleaning process, allowing them to be deposited safely underground. Pollutants are therefore continuously removed from the environmental cycle.

Keywords: Desulphurization, denitrogenation, dust, adsorption, absorption

1. Introduction

The purpose of a flue gas cleaning system is to reduce atmospheric emissions of substances hazardous to the environment and health. This includes e.g. heavy metals, dioxins and substances that cause acidification and eutrophication. Because many of the substances are toxic and carcinogenic, it is important to reduce their emissions. The acidification of forests and lakes has been reduced substantially by removing sulfur dioxide and oxides of nitrogen from flue gas.

2. Desulphurization units

There are several critical technological and regulatory challenges facing Flue Gas Desulphurization (FGD) projects that are common to all regions. These are discussed below.

2.1 Mechanism of sulphur removal

SO_2 conversion to easily removable form from exhaust gases. Decision to build desulphurization unit is made to guarantee accomplishment of European standards about SO_2 emission. To choose right desulphurization method is very complicated task because not each method can be applied in specific energetics condition [1].

Classification of desulphurization method:

- Type and character of process: absorption, adsorption, catalysis
- Applied sorbent: regeneration, non-regenerative
- Received product: wastage, semi-wastage, non-wastage
- Procedure of sulphur removal: wet, semi-dry, dry

SO_2 absorption: Capture from exhaust gases through dissolution in solution or in water suspension connected with chemical reaction. There are different types of absorbers. Features that decide of chosen absorber:

- Flow volume
- Gas, liquid features
- Pollutants present in exhaust gases
- Size of needed diffusion surface

- Flow resistance and power usage
- Corrosion possibility

SO_2 adsorption: Gas compound capture on the solid material surface (adsorbent).

Effectiveness of adsorption depend on:

- Surface interphase contact
- Adsorption Capability of deposit– type, size, sorbent structure
- Absorb gas property and intensity
- Process temperature

While designing process based on adsorption it has to be taken into account:

- Cleaning effectiveness
- Gas and sorbent physicochemical properties
- Stream of cleaning gas and sorbent quantity
- Energy usage and others like sorbent regeneration
- Ability of by-product usage

Wet method: Substances used for desulphurization and products drain away from reactor in wet conditions. Based on absorption process. Most famous method of desulphurization. Calcium compounds are mostly used as absorbent (available and cheap). Process without regeneration. SO_2 transformed to sulphate and calcium sulphate. Desulphurization process take place at scrubber. Exhaust gases are cooled to 50-70 C degree, due to contact with water.

Wet calcium method:

- Most common method. Many commercial systems installed in: Jaworzno III, Bełchtów, Opole, Kozienice, Pątnów, and Rybnik
- Non-regenerative method – SO_2 absorption in suspension of water and finely ground $CaCO_3$ or $Ca(OH)_2$
- Reactor is usually a spraying counter-current absorber – made from materials resistance from corrosion, abrasion
- Method guarantee >90% of desulphurization rate
- Strict rules about pH control
- By-product –gypsum – with proper conversion can be used in civil engineering.

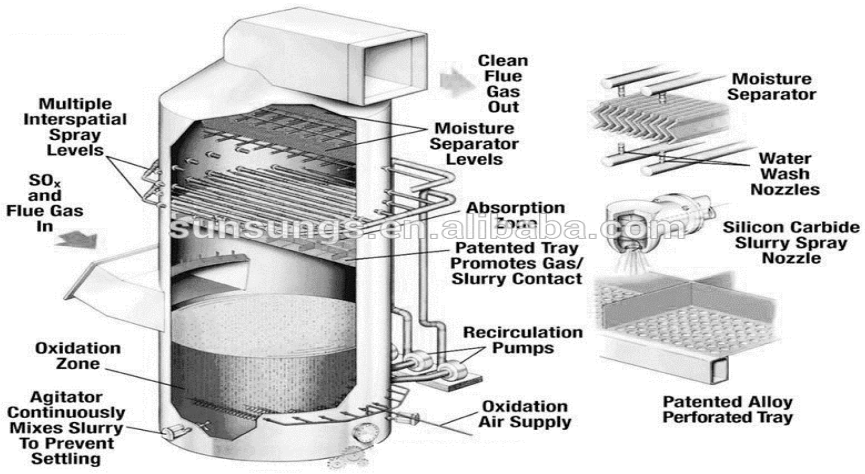

Fig. 1 Absorber

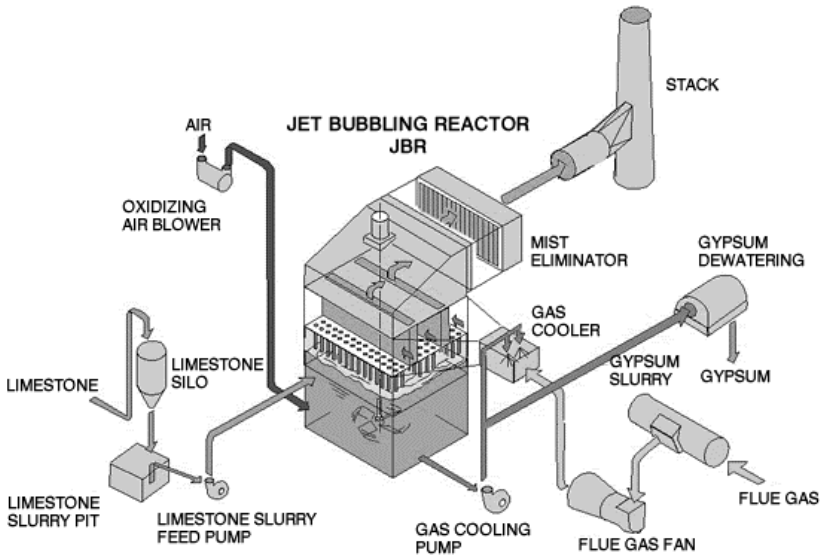

Fig. 2 Wet method

Dry-scrubbing method: Based on absorption process. Substances used to exhaust gases desulphurization are feed in wet basis. Products transported from reactor in dry basis. Moreover, it is based on similar processes that wet methods. Exhaust gases with temperature equal 130-170 ˚C flow through scrubber in which solutions are sprayed. SO_2 is absorbed on the drop surface then is absorb inside the drops by sulphates reaction and sulphites are formed. The amount of the water is adjust that during process all will evaporate, as to make sure product will be dry. After dry-scrubbing method temperature is equal around 70-80 C degrees [1]. Exhaust gases should be around 5-15 seconds inside scrubber to obtain high effectiveness. Usually combined with particulate collector. Desulphurization efficiency between 60-90 %.

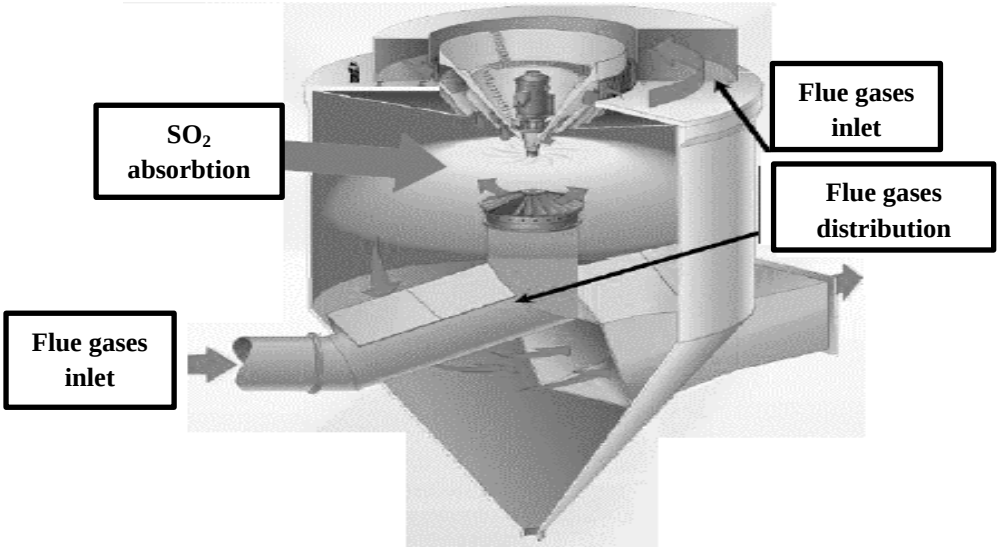

Fig. 3 Scrubber

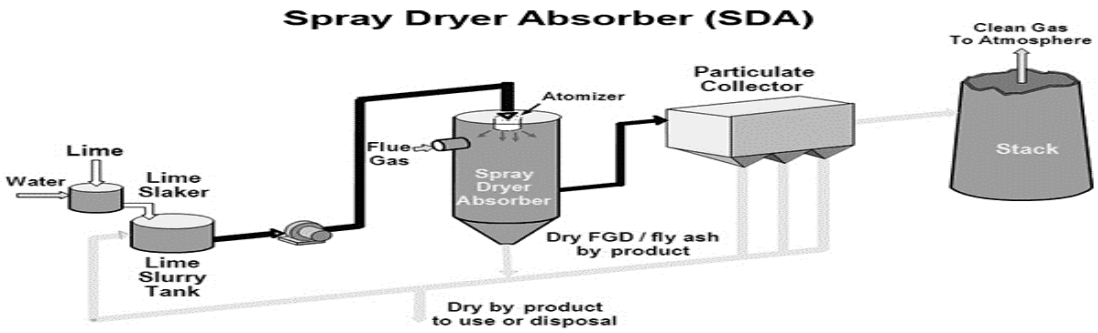

Fig. 4 SO_2 Dry Absorbing Method

Dry methods: SO_2 removal are carry out in dry basis. Based on adsorption process. Low desulphurization efficiency equal between 30-40 %. Low sorbent costs. Simple technology.

FSI method-Sorbent is mixed with coal and then delivered straight to combustion chamber. Sorbent is blown to different smoke ducts, desulphurization process it taking place there and also in particulate collectors [2].

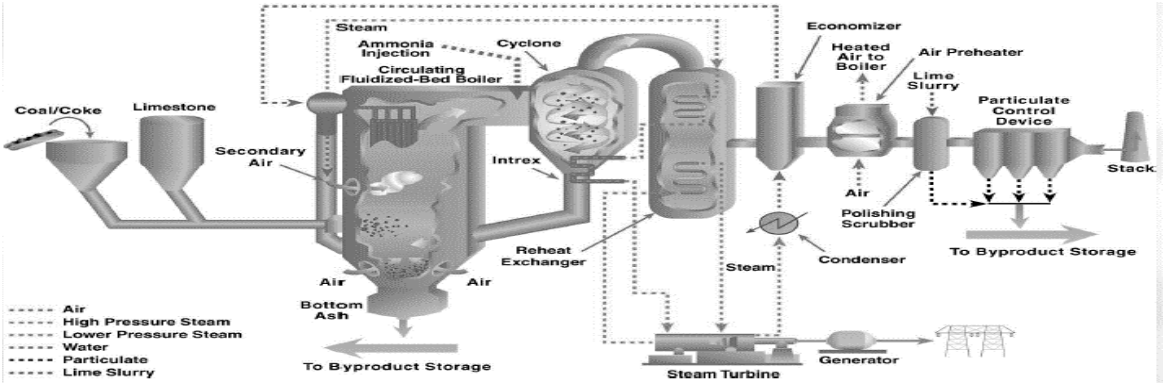

Fig. 5 FSI method

Tab. 1 Comparing different methods

Parameter	Unit	Method		
		Wet	Semi-dry	Dry
Desulphurization effectiveness	%	>95	80-85	30-50
SO_2 concentration in cleaned flue gases	mg/m_n^3	200-400	400	800-1000
Dust concentration in cleaned flue gases	mg/m_n^3	10-30	5-30	high increment
Liquid by-products	-	slurry	none	none
Solid by-products	-	gypsum	mixture of combustion products and sorbent	mixture of combustion products and sorbent

3. De-nitrification units

Creation of NO_x in combustion chamber is controlled by

- Excess air ratio
- Fuel physical and chemical properties- nitrogen content, volatiles content, reactivity.
- Temperature
- Way of heat collection
- NO_x reduction methods

3.1 Mechanism of NO_x removal

Combustion process modification. Flame temperature and excess air ratio reduction. Proper organization of combustion. The aim is to obtain maximum quantity of N_2 in exhaust gases.

Air staging: Air is division into 2 or more stages. First stage is combustion with excess air ratio below one $\lambda<1$ and the second is afterburning stage with excess air ratio above one $\lambda>1$. Unfortunately, there is a high risk of big amount of under-stoichiometric combustion products creation. CO emission is higher, carbon presence in the ash, slag [3]. On the other hand second stage is created to avoid creation of all those situations mentioned above. The secondary air is fitted to quantity that excess ratio will be above one, to make sure CO and carbon will be after-burn.

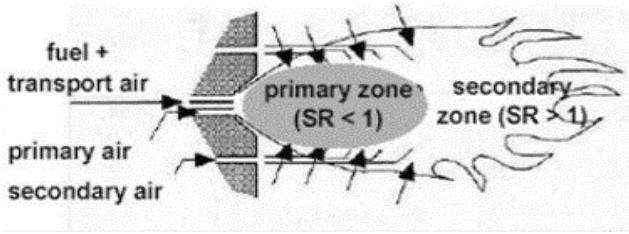

Fig. 6 Combustion Air Staging

Fuel staging: Fuel and air are divided for two or more stages. First stage is combustion with excess air ratio above one $\lambda>1$. Next stage is with excess air ratio below one $\lambda<1$ and with re-burning fuel injection. Last stage is again with excess air ratio above one $\lambda>1$ and with after-burning air injection [3].

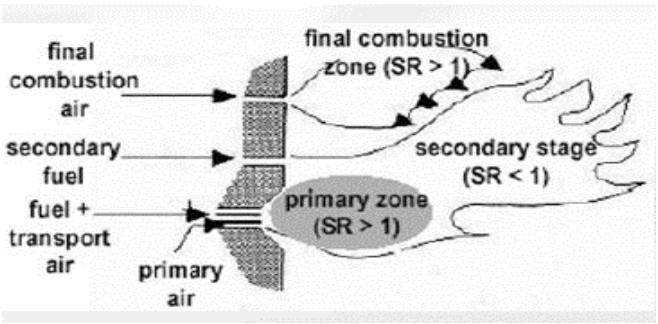

Fig. 7 Combustion Fuel Staging

Exhaust gases recirculation: Exhaust gases return to burner. Recirculation lower the temperature and decrease oxygen content. In pulverised boilers exhaust gases are recirculating to mills to combustion chamber and secondary air.

SNCR (Selective Non-Catalytic Reduction): Reactant feed into combustion chamber. The most common reactant is ammonia working with temperature between (850-1000 ºC). This method is very sensitive to temperature and fuel property changes. Possibility of ash pollution with NH3. The effectiveness of NO_x reduction is between 30-60%. Unfortunately this is the most expensive installation, it also demand lot of work with catalyst building on boiler. High operation costs [2].

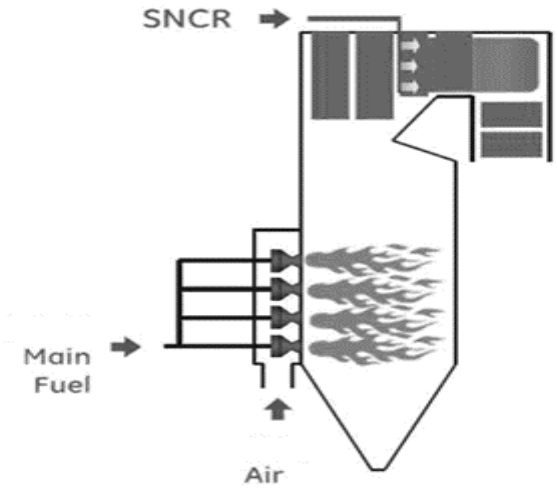

Fig. 8 Selective Non-Catalytic Reduction Method [3]

SCR (selective Catalytic Reduction): Delivery of reactant to separate reactor. Most popular reactant is ammonia. Temperature in reactor is between 250-400 ºC. The effectiveness is between 80-95%.

SCR-High dust system: Most common system. There is no need to reheat exhaust gases before catalyst. Problems with additional space for reactor [2].

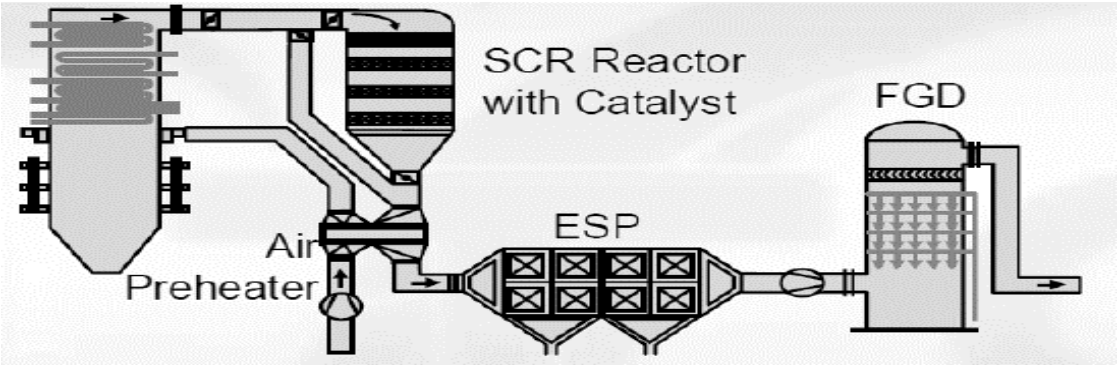

Fig. 9 Selective Catalytic Reduction High Dust Method

SCR-Low dust system: No problems with exhaust gases pollination, demand of high temperature in dust collection.

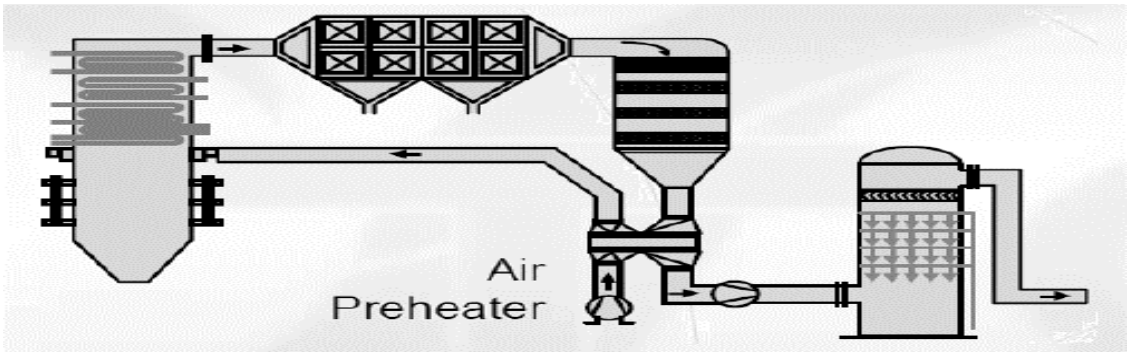

Fig. 10 Selective Catalytic Reduction Low Dust Method

4. Dust Collection

Important parameters for proper operation of installation:

- Effectiveness of dust extraction.
- Flow resistance.
- Power requirement indicator.
- Energy requirement indicator.
- Filtration costs (investment and operation).

4.1 Methods of Dust Collection

Cyclone: Most common method. Usually used for stoker boilers. Based on centrifugal force. Flue gases are spinning, bigger particles are throw to walls direction and then they are drop to the bottom of cyclone. There can also be combination of few connected cyclones –multi-cyclone. It is for systems with higher amount of flow.

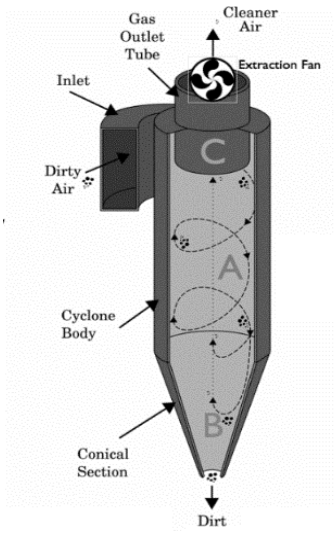

Fig. 11 De-dusting: Cyclone Method

Electrostatic participation: Very common method. The aim is to remove particles from flowing flue gases, caused by electrostatic field interaction on electrically charged particles. Potential difference is produced between negatively charged cumulative electrode and grounded corona electrode. Cumulative electrode produce electrons which are moving to corona electrode direction and at the same time they are passing electric charge to

ash particles. Thanks to that ash is also attract to corona electrode. After that particles are settle on electrode they discharged and going down cause of vibration to lock-hopper.

Dust collector: Ash particles are settle in porous medium. In dust collection filtration through fabrics are applied. Ash is catch on the material surface. Flue gases go through filters and dust is stop cause of size this is the filtration phase. After that in regenerative phase air is blown to filters to clean it surface from dust.

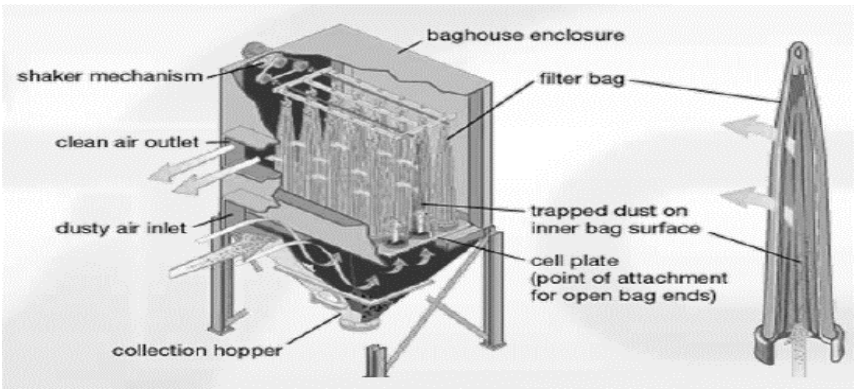

Fig. 12 Dust Collector

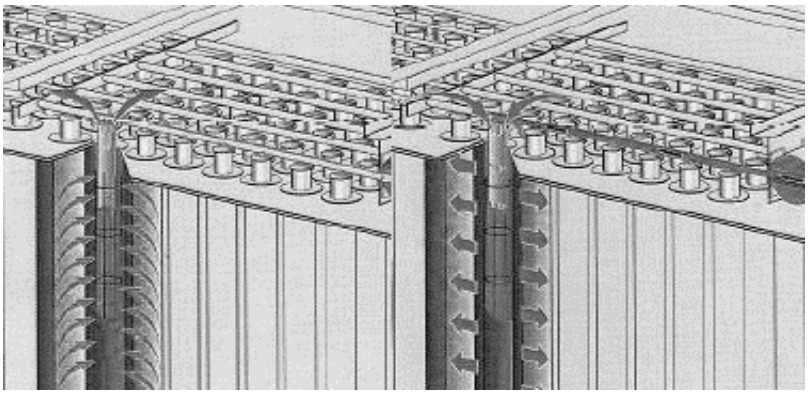

Fig. 13 Dust Collector: Regenerative Phase

5. Conclusion

There are many methods but we should always select the one that is most efficient and suitable for our installation. That is why you have first to analyses the problem in your project and which method will be beneficial for that purpose. This will help in selecting the methods that are proper with each other. Moreover, we should have an economic overlook at the flue gases and then decide in which invest more money. Nowadays in Europe there are legal limits that we have to follow, so the market for this kind of technologies is growing.

References

[1] CARMEUSE, http://www.carmeusena.com/markets/flue-gas-treatment/dry-scrubbing, (4/12/2017).
[2] Kaitian environmental tech, http://www.kaitiangroup.com/en/index.html, (4/12/2017).
[3] Cyclone Dust Collection System, https://mastslav.weebly.com/, (4/12/2017).
[4] X. Ma, T. Kaneko, G. Xu, K. Kato. Influence of gas components on removal of SO2 from flue gas in the semidry FGD process with a powder–particle spouted bed, *Fuel*, 2001, 80 (5), pp. 673.
[5] VGB POWERTECH, https://www.vgb.org/en/, (5/12/2017).

Harvesting Energy from Agricultural Residues for Small Scale Combustion Applications in Pakistan

Nismah Rizwan [1], Sara Noor Ehsan[2]

[1]Silesian University of Technology, Poland, e-mail: nis.riz96@gmail.com
[2]National University of Sciences and Technology, Pakistan, email: sara.n.ehsan@gmail.com

Abstract

Being an agrarian country, Pakistan holds the potential to bring its biomass resources into use and contribute towards its development. Therefore, the purpose of this study was to explore the fuel potential of 3 major crop residues in Pakistan: Cotton-gin by-product, Wheat straw, and Rice straw. Physical and chemical properties of individual residues were analyzed, which include: particle size distribution, proximate analysis, and calorific value. Based on the results, multiple binding agents and processing conditions were experimented with for optimum pelletization of the biomass. Analyzing the mechanical strength, proximate analysis, and calorific value of the pelletized fuel revealed that cotton-gin by-product, in combination with paper pulp as binding agent, was the most effective fuel.

Keywords: Binding agent, biomass fuel, combustion, crop residue, pelletization

1. Introduction

Currently, the world, particularly Pakistan, faces a number of issues that are directly linked to deterioration of the environment. The most critical of these is indoor air pollution. On a global scale, around 4.3 Million premature deaths occur annually in association with indoor air pollution [1]. In Pakistan, the major source of this pollution is sub-standard and unsafe cooking practices, particularly in the rural areas. These practices are commonly linked to the occurrence of eye and pulmonary illnesses. These stoves are mostly run on wood as fuel, which is a major reason for their high pollution potential.

Large scale deforestation is another direct result of the high consumption of fuel wood. Owing to the fact that around 70% of Pakistani households depend on fuel wood for energy [2], the already deficient forest cover (less than 4% currently) is depleting further. In addition to this, the instable economic situation of the country is increasing the difficulty in shifting from conventional to modern sources of fuel. So, since the use of traditional fuels cannot be ceased immediately, the exploration of alternatives is necessary.

Keeping in view the current situation of the country, the best possible alternative to fuel wood is agricultural residue biomass. Pakistan is an agrarian country, with vast areas of land being cultivated with a variety of crops. These crops produce approximately 114 Million tonnes of field-based residues, with an equivalent energy potential of about 1.6 MTJ every year [3]. More than 90% of these residues is burned in open fields. Globally, biomass fuel provides 11% of the energy demand, while more than 3 billion people use it for cooking. So, if the agricultural residues in Pakistan are brought in to use as well, they are sufficient to considerably alleviate the burden on current energy resources. This will simultaneously provide an efficient means of waste management, as otherwise these residues are burned in open fields leading to air pollution.

In Pakistan, three of the major crops are cotton, rice, and wheat. Around 10 Million tonnes of rice, and 25 Million tonnes each of cotton and wheat by-products are generated annually, and their combined equivalent energy potential is estimated at 3.4 MTJ/year [3]. These residues also provide the advantage of being inexpensive. Therefore, they can conveniently be used in domestic energy intensive activities, such as cooking. However, the adaptability of such fuel and technology is a major concern and needs to be addressed to ensure effectiveness.

This study explores Cotton, Rice, and Wheat by-products as potential sources of inexpensive and environment friendly fuel. These residues were combined with only readily available binding materials, such as paper pulp and starch to form fuel pellets. The pelletization process took place under ambient conditions of temperature and pressure, which are two of the most crucial process parameters. However, due to experimental difficulties they could not be varied and were kept constant within the ambient range. Also, the time of compression for each pellet was kept constant to allow standardization and better comparison.

2. Materials and Methods

2.1 Raw Material Properties and Pre-processing

Residues of Cotton, Wheat, and Rice were acquired with the aid of World Wide Fund for Nature Pakistan (WWF-Pakistan). The residues were taken from parts of lower-Punjab, Pakistan. Before pelletization, the size of these residues was reduced in order to increase uniformity of particles. More uniform particles result in better pelletizability and relatively less energy consumption. A particle size in the range 600 – 850 μm (between sieve # 20 and 30) was used for wheat and rice straw. Cotton-gin by-product cannot be passed through a sieve due to the agglomerating nature of its particles. So, it was only cleaned out to remove excess dirt and other contaminants.

2.2 Binding Agent

The choice of additive was based on a number of considerations, which are elaborated in Table 1. Water was added to each of the binding agents before use in order to attain moisture in the desired range, and to enhance their lubricating abilities and reduce energy consumption during processing.

Tab. 1 Comparison and Analysis of different Binding Agents

Evaluating Parameters	**Paper Pulp**	**Starch**	**Waste Engine Oil**
Accessibility	Easily accessible	Varies with region	Varies with region
Cost	12 Rs/kg (≈ 12 ₡/kg)	235 Rs/kg (≈ 2.35 ₡/kg)	35 Rs/litre (≈ 35 ₡/litre)
Binding Characteristics	Improves mechanical strength	Improves mechanical strength	Reduces mechanical strength
Environmental Impacts	Low Sulphur Content Low NO_x emissions	High CO emissions	High CO emissions
Effect on Calorific Value of fuel	Enhancement	Reduction	Minimal Enhancement

Upon comparison between the three as binding agents in the pelletization of the agricultural residues, paper pulp was chosen as the most effective and feasible one. Old and used newspapers, otherwise wasted, represent a valuable source of energy mainly due easy separation from the waste stream. It is relatively homogeneous and mostly free from non-combustible and toxic contaminants. Moreover, the pulp formation process is relatively simple and quick. It is easily combustible and has a calorific value of over 17 MJ/kg. So, it plays a role in enhancing the calorific value and flammability of the fuel pellet, as a whole. In addition to this, paper pulp has high lignin content; therefore it acts as an effective binding agent for the pellets. Paper pulp, used in the pelletization process, was made using the process depicted in Figure 1.

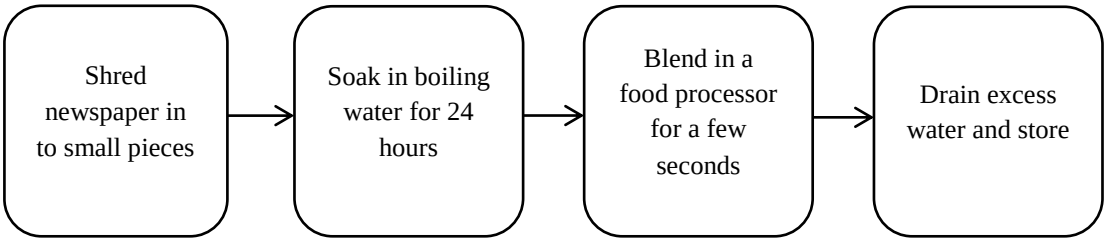

Fig. 1 Schematic of Pulp Making Process [4]

2.3 Analysis of Raw Material

2.3.1 Proximate Analysis

Proximate analysis of the agricultural residue was done in order to determine its chemical properties. The analysis involves heating the residues at various conditions to determine 4 components: moisture content, volatile matter, fixed carbon, and ash content [5]. For the analysis, a 2 gram sample of each residue was taken. First the moisture content was determined using the Standard Oven Drying method and heating the sample in an oven at 105°C for 1 hour. The residue was then subjected to a temperature of 925°C, in a muffle furnace, under anaerobic conditions, for 7 minutes. This residue was then heated at 550°C, in the presence of Oxygen, for 1 hour. The masses at the beginning and end of each phase were measured to determine the required parameters.

2.3.2 Calorific Value

A Differential Scanning Calorimeter (NETZSCH DSC 404C) was used to determine the energy content of agricultural residue. The instrument measures the change in heat required to increase temperature of the sample in relation to a reference substance. It works on the principle that when a sample undergoes phase transformation, heat flows to or from it. This transfer of heat depends on the properties of the reference substance used, as the main goal is to maintain the two at the same temperature. A small sample, 0.5-100 mg in size, was heated under an inert Nitrogen atmosphere (to allow improved heat conductivity), and a thermocouple was used to detect the difference in temperature [5]. The results were displayed as a curve of 'specific heat' against 'temperature', providing quantitative and qualitative data on endothermic and exothermic processes.

2.4 Compression Assembly and Equipment

For the pelletization assembly, a piston-type compression mechanism, made of mild steel, was fabricated [4]. The assembly included a hollow cylindrical die, with an inner diameter and height of 3 cm, along with a solid-filled cylindrical rammer with a height of 8 cm. The material to be compressed was filled in to the die and the rammer placed on top. This assembly was then pressed between the plates of a hydraulic press (12-Tonnes; manually operated) to compress the waste in to a pellet. A CAD Drawing of the compression assembly is shown in Figure 2.

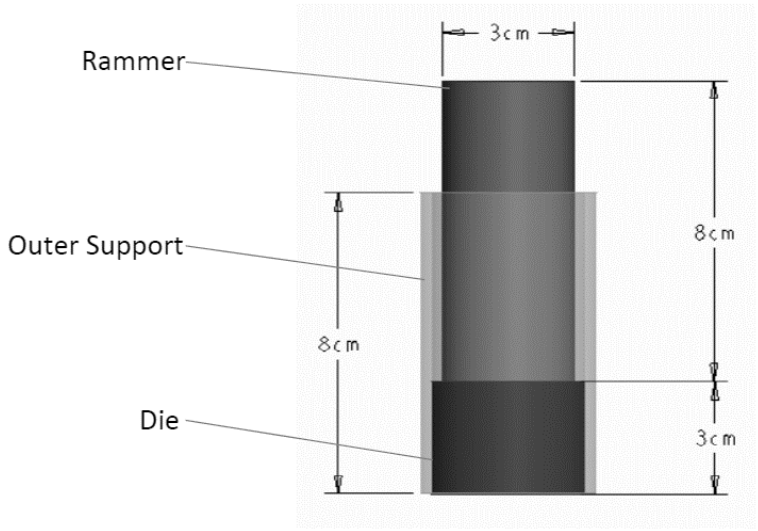

Fig. 2 CAD Drawing of Compression Assembly

2.5 Experimental Matrix

The pelletizability of the biomass pellets was assessed in two stages: first by varying moisture content of the binding agent and then by varying binder concentration in the pellets. Deductions on the optimum conditions from each stage were based on the mechanical strength of the pellets. The compression pressure and time were kept constant at 21 bars and 3 minutes, respectively, for each stage.

For the first stage, the moisture of the paper pulp was manually adjusted to obtain pulp of two consistencies, one dry and the other wet. The moisture contents of these were determined by the standard oven drying method [5]. The pelletization process was then carried out with both the pulps, while keeping the binder concentration constant at 50%. The pellets were tested for mechanical strength to determine the optimum binder moisture content. For the second stage, the binder concentration was varied while keeping the binder moisture content constant at the value determined in the first stage. The concentrations were varied at 30% and 50% by weight. These pellets were also tested for mechanical strength to determine the optimum concentration.

2.6 Pellet Testing

2.6.1 Mechanical Strength

Hardness is used as a measure of a material's resistance to permanent deformation. It is an important parameter in determining a pellet's handling and transport properties. Hardness of the pellets was tested in terms of its compressive, or mechanical, strength, and a Universal Testing Machine (Shimadzu AG-Xplus Series) was used for the purpose. During the test, the pellet was pressed between two flat plates and the applied load was gradually increased. The load applied per unit deformation was measured and displayed as a stress-strain curve. The Universal Testing Machine had a load capacity of 20 kN and a strain rate of 1 mm/min was used [6]. Mechanical strength of the pellets was also used as an indicator of the optimum parameter in each phase of the experimental matrix. For each phase, the pellets were tested for their mechanical strength. The binder moisture content and concentration for which the strength was greatest was taken as the optimum value for that parameter.

2.6.2 Proximate Analysis

After going through all stages of the experimental matrix, and deciding the optimum pellet parameters, the produced pellets were tested for their chemical properties using proximate analysis. The procedure of the analysis was similar to the one used in Section 2.3.1 [5].

2.6.3 Calorific Value

Calorific values for the produced pellets could not be determined using DSC analysis, due to a limitation of sample size. So, the values were interpolated based on the amount of each material present and its individual energy content.

3. Results and Discussion

3.1 Biomass Fuel Pellets

The pellets formed as a result of the compression process are shown in Figure 3. The images clearly show that pelletization of cotton-gin by-product gave the best results as the pellets formed were more compact. With wheat and rice straw, the pellets formed were fragile and fell apart the moment they were touched.

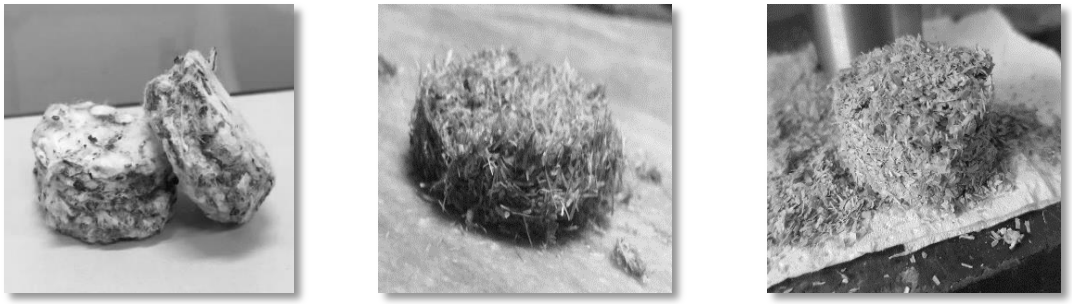

a b c

Fig. 3 Biomass Fuel Pellets (a – Cotton-gin by-product, b – Wheat straw, c – Rice straw)

3.2 Analysis of Raw Fuel

3.2.1 Proximate Analysis

The proximate analysis of an individual 2 gram sample of the pre-processed residues of cotton, wheat, and rice revealed that moisture content was within the desirable limit of 5% for all three. The ash contents were also found to be quite low in case of cotton-gin and wheat straw. Similarly, the volatile matter for all three residues was found to be high, with the highest for wheat. The results (Table 2) indicate a greater suitability of cotton-gin by-product and wheat straw, as fuel sources, in comparison with rice straw.

Tab. 2 Proximate Analysis of Raw Agricultural Residue

Agricultural Residue	**Moisture Content (%)**	**Volatile Matter (%)**	**Fixed Carbon (%)**	**Ash Content (%)**
Cotton-gin By-product	5.33	52.64	32.13	9.90
Wheat Straw	6.11	55.71	29.39	8.79
Rice Straw	4.86	47.41	29.43	18.30

3.2.2 Calorific Value

Results of the DSC analysis (Table 3) of the three pre-processed residues showed a mostly exothermic peak for cotton-gin by-product in comparison with relatively more endothermic peaks for wheat and rice straws. This indicates that wheat and rice straws require more energy to burn than they give off during combustion. On the other hand, cotton-gin by-product releases a significant amount of heat, while requiring much less activation energy. Comparing the specific heats at a fixed value of temperature revealed that the calorific values of cotton-gin by-product and wheat straw were higher than rice straw.

Tab. 3 DSC Results of Raw Agricultural Residue

Agricultural Residue	Nature of Peak	Calorific Value(kJ/kg)
Cotton-gin By-product	Exothermic	16323.18
Wheat Straw	More Endothermic	16950.00
Rice Straw	More Endothermic	15300.00

3.3 Analysis of Pelletized Fuel

3.3.1 Proximate Analysis

Proximate analysis (Table 4) of the residues after undergoing pelletization indicated a significant increase in volatile matter and a decrease in ash content, thus highlighting the success of the process in improving combustion characteristics of the fuel. The moisture content of the pellets was relatively high initially, as shown in Table 4, but it was reduced to less than 5% by sun drying before use. Since pelletization of rice straw could not be achieved, its proximate analysis was not conducted.

Tab. 4 Proximate Analysis of Pelletized Fuel

Agricultural Residue	Moisture Content (%)	Volatile Matter (%)	Fixed Carbon (%)	Ash Content (%)
Cotton-gin By-product	11.80	82.90	12.60	4.40
Wheat Straw	17.40	81.00	13.10	5.90
Rice Straw	Pelletization not achieved			

3.3.2 Calorific Value

The calorific value of the cotton-gin by-product showed a slight increase whereas that for wheat straw showed a decrease upon addition of the binder and pelletization, as shown in Table 5. This indicates a greater suitability of cotton-gin by-product for use as pelletized fuel in comparison with wheat straw. Again, rice straw could not be pelletized, so no results were obtained.

Tab. 5 Interpolated Calorific Values of Pelletized Fuel

Agricultural Residue	**Calorific Value (kJ/pellet)**
Cotton-gin By-product	165.21
Wheat Straw	117.19
Rice Straw	Pelletization not achieved

3.3.3 Mechanical Strength

Mechanical strength of the pellets was considered as the criteria upon which all other process parameters were tested. When using stress-strain curves, a higher mechanical strength is exhibited by the material that undergoes minimum change in length (strain) upon maximum applied stress. Therefore, the material for which the curve extends to a higher value of stress and breaks off at a lower value of strains has the higher mechanical strength, which is desired.

Rice straw could not be pelletized so, no results were obtained for it. For the first phase of the experimental matrix (stated previously), the highest mechanical strength was observed for the pellets formed using paper pulp with a moisture content of 74%. Generally, the mechanical strength was seen to increase with an increase in moisture content of the binder, after which it started to decrease (Figure 4). This may be attributed to increased lubrication due to excess water.

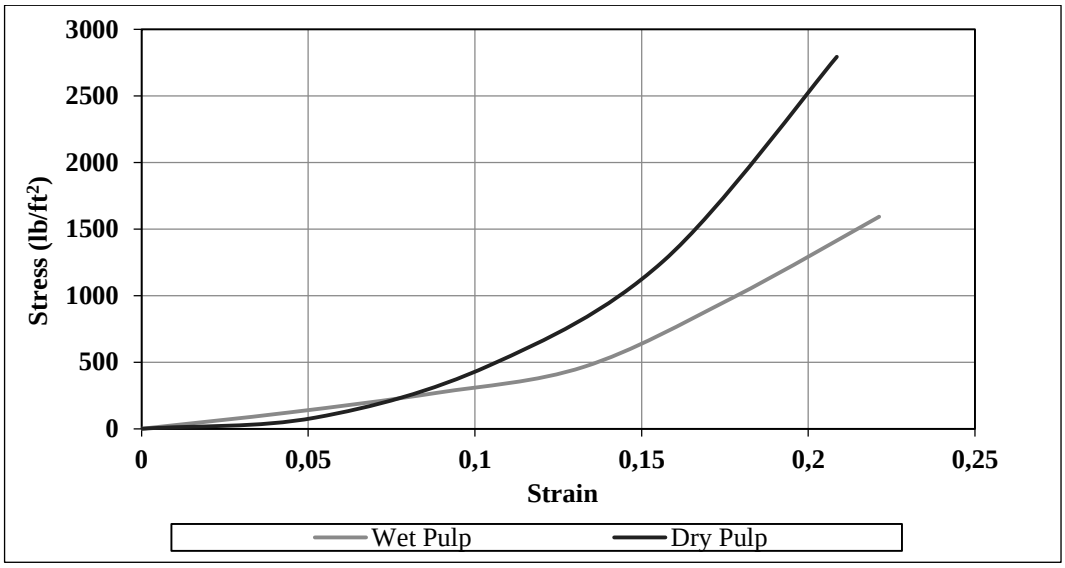

Fig. 4 Stress-Strain Curves of Varying Moisture Contents of Paper Pulp

For the second phase of the matrix, binder concentration in the pellets was varied. The mechanical strength increased when the binder concentration was increased from 30% to 50% for cotton-gin by-product and wheat straw (Figures 5-6). This indicates that a higher binder concentration results in more efficient pelletization of the biomass.

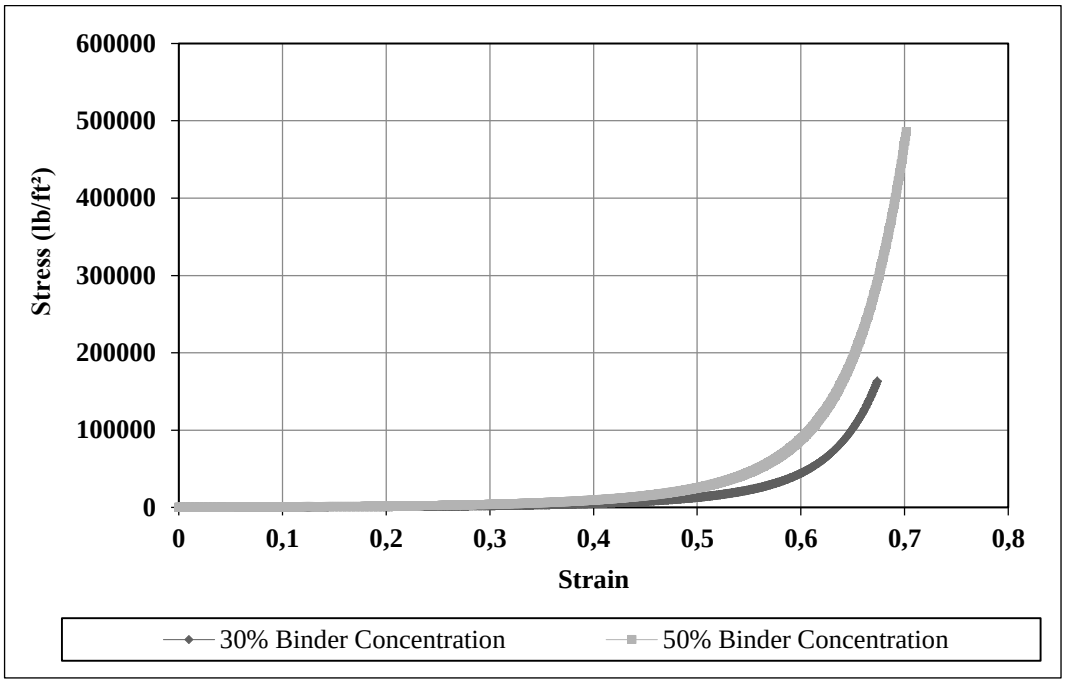

Fig. 5 Stress-Strain Curves of Varying Binder Concentration in Wheat Pellets

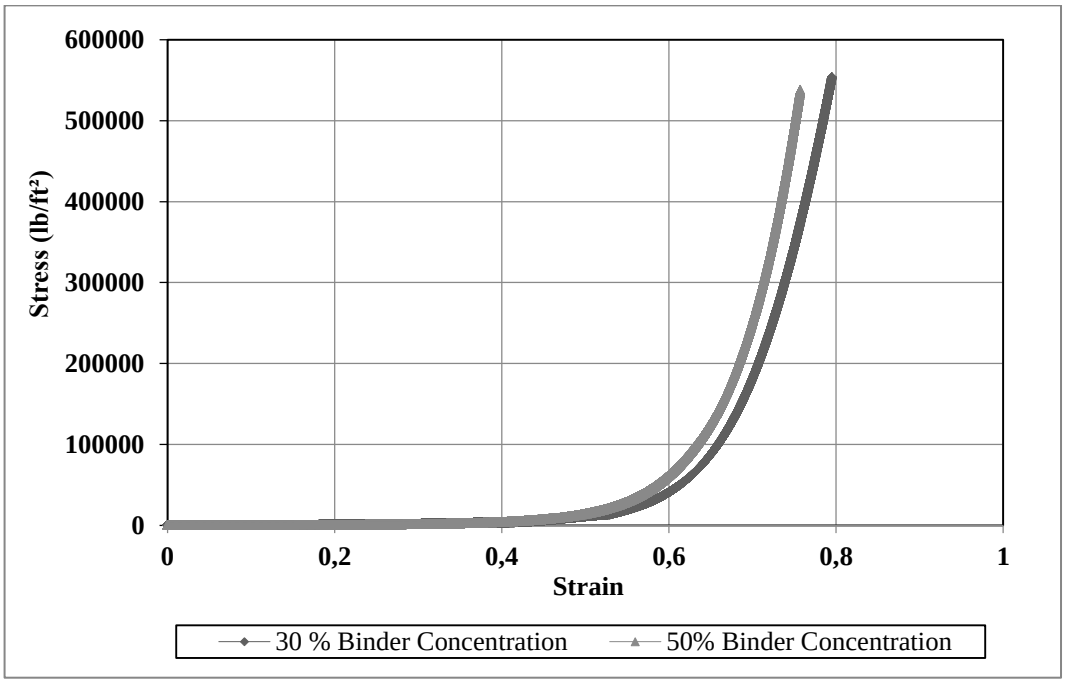

Fig. 6 Stress-Strain Curves of Varying Binder Concentration in Cotton-gin by-product Pellets

Once the optimum pellets for both, cotton-gin by-product and wheat straw had been identified, mechanical strengths of the two were compared (Figure 7). The results showed a greater strength for pellets of cotton-gin by-product in comparison with wheat straw, as they had a higher density and better binding characteristics at ambient temperature.

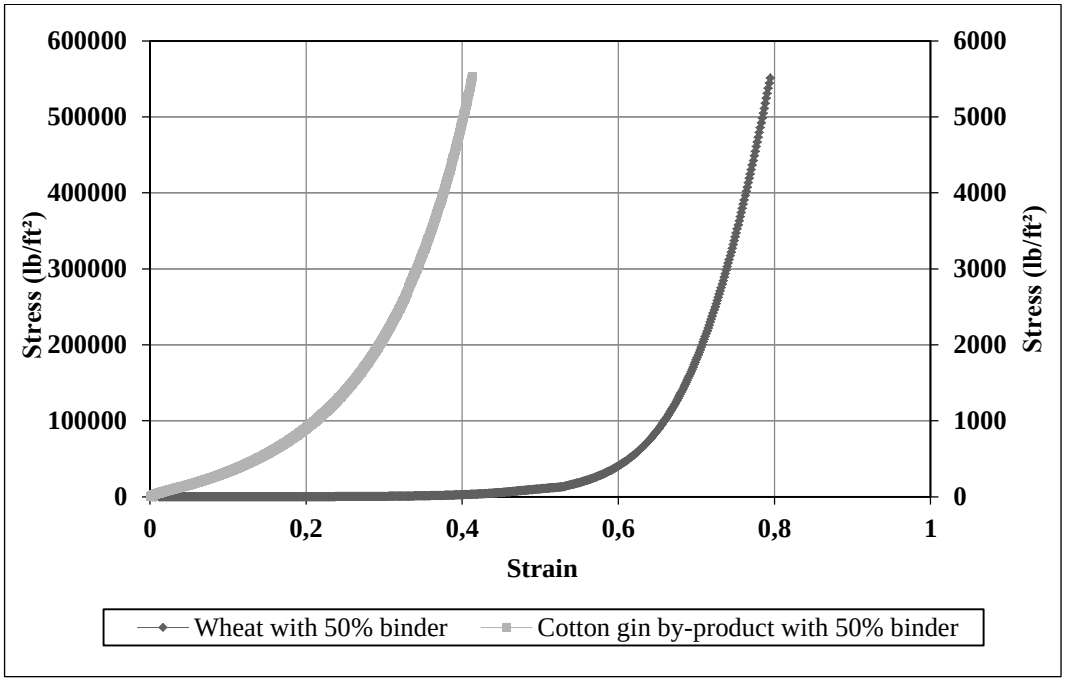

Fig. 7 Comparison of Mechanical Strength of Optimum Cotton-gin by-product and Wheat Pellets

4. Summary

This research was conducted with the key objective of exploring alternate fuel sources for small scale combustion applications, such as cooking. The agricultural residues were selected based on their availability and fuel potential. For selection of the additive to be used, the criteria observed included: accessibility, cost, binding characteristics, environmental impacts, and the effect on calorific value. Waste newspaper, used as raw material for pulp formation, is readily available throughout Pakistan, in contrast with starch or waste engine oil, which are accessible according to the region. Variation in cost of binders provided a comparison for feasibility analysis. The binding characteristics, as per previous studies, show that paper pulp and starch improve mechanical durability of the pellets while the waste engine oil reduces it. Paper pulp enhances the calorific value, while starch additives tend to reduce it side-by-side significantly increasing CO emissions. Observations made during the experimentation process, concluded paper pulp as the most feasible and suitable option to be used as a binder. However, paper pulp alone was not sufficient to yield high quality wheat and rice straw pellets, under ambient conditions. In order to compare the products of the complete process of pelletization for both cotton-gin by-product and wheat residue, their fuel characteristic analysis was done along with testing their mechanical strength. According to the experimental matrix set up to vary moisture content of the binder and its concentration for both the residues, the resultant of each variation was tested for mechanical strength to enable the next variation. The optimum moisture content of paper pulp (74%) in combination with the optimum binder concentration (50% by weight) exhibited higher compressive strength for both residues. This is backed by the literature on pelletization as addition of binder enhances the calorific value of pellets while simultaneously increasing the mechanical durability needed for their handling and transport. For the optimum choice of sustainable fuel, a comparison between both types of residues was made based on compressive strength. The results indicated a higher compressive strength for pellets composed of cotton-gin by-product with paper pulp as additive. Combustion analysis and calorific value determination of the fuels also supported this choice. Overall

combustion characteristics of cotton-gin by-product pellets indicated their effectiveness in small scale combustion applications, also contributing towards healthier operating conditions.

Acknowledgment

This research was conducted at and supported by National University of Sciences and Technology, Islamabad, Pakistan. Additionally, technical assistance and raw materials were provided by World Wide Fund for Nature, Pakistan.

References

[1] World Health Organization. Clean Household Energy for Health, Sustainable Development, and Wellbeing of Women and Children, *WHO Guidelines, 2016*.

[2] M. Hamayun, S.A. Khan, A.L. Khan. Wood as a Fuel Source in the Hindukush: A Case Study of Utror and Gabral Valleys, Northren Pakistan, *Pakhtunkhwa J. Life Sci.*, 2013, 1(2), pp. 94–99.

[3] The World Bank, Final Report on Biomass Atlas, 2016.

[4] D. Shyamalee, A.D.U.S. Amarasinghe, N.S. Senanayaka. Evaluation of different binding materials in forming biomass briquettes with saw dust, *International Journal of Scientific and Research Publications*, 2015, *5*(3), pp. 1–8.

[5] ASTM International, https://www.astm.org, (15/12/2017).

[6] Y. Huang, M. Finell, S. Larson, X. Wang, J.L. Zhang, R. Wei, L. Liu. Biofuel pellets made at low moisture content – Influence of water in the binding mechanism of densified biomass, *Biomass and Bioenergy*, 2017, *98*, pp. 8–14.

Carbon Neutral University – A Case for AGH University of Science and Technology

Hamid Iftikhar[1], Łukasz Wojnicki[1], Sara Vieira[1]

[1]Faculty of Energy and Fuels, AGH University of Science and Technology, email: hamidiftikhar90@gmail.com, lukaszwojnicki1@gmail.com, s.cvieira@sapo.pt

Abstract

Carbon Neutral or Net Zero Carbon energy is a concept wherein you produce the same amount of energy from renewable (green) energy sources as much as you consume from non-renewable (brown) energy sources to offset your carbon footprint. According to an IEA report Poland produced 86% of its electricity from non-renewable energy sources (coal oil and gas thermal power plants); which translates into the fact that the electricity consumed at AGH UST constitutes a hefty share from brown energy sources. To counter the intensive carbon emissions from university's electricity usage, it has been proposed to use energy efficiency measures and commercially feasible renewable energy technologies such as solar photovoltaic and wind energy to achieve carbon neutrality by the year 2030 which also shall also translate into CO_2 savings of 1,580 tonnes/annum.

Keywords: Carbon neutral university, net zero energy, PLGBC, AGH UST Krakow, Poland

1. Introduction

Energy plays a critical role in a country's economic development. It is linked to residential, commercial, agricultural and industrial growth. The nexus between energy and environment gets profound in the way energy is produced. Carbon intensive ways of producing energy (electricity) deteriorate environment by increasing greenhouse gases. Figure 1 shows various greenhouse gases which are direct result of industrial emissions where CO_2 has the highest greenhouse gas index [1].

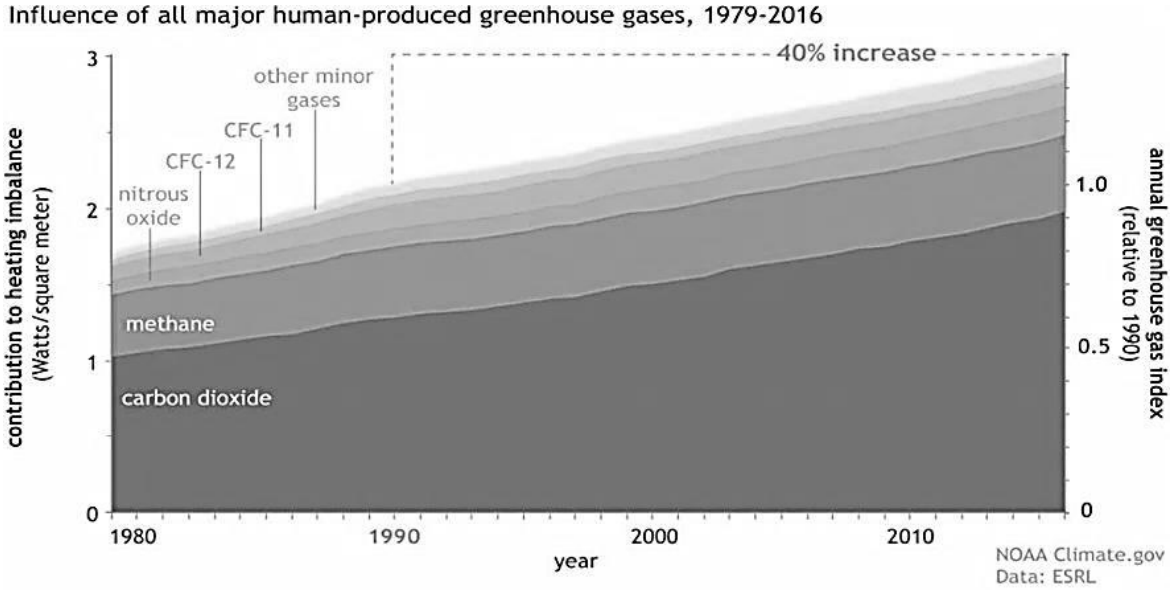

Fig. 1 Greenhouse Gas Index (1979-2016)

In case of Poland, the situation is getting worse as the greenhouse gases emitted by brown energy technologies are creating smog leading to major health issues across the country. Figures 2 and 3 show the Particulate Matter (PM) concentration in the air in Krakow. For PM 2.5, 25 micrograms per cubic meter is the permissible range and it can be seen in the figure that in the month of November 2017, the value reached 93 micrograms per cubic meter which is almost 4 times the permissible range. Similarly for PM 10, the permissible range is 50 micrograms per cubic meter and it reached 115 micrograms per cubic meter in November, 2017 [2].

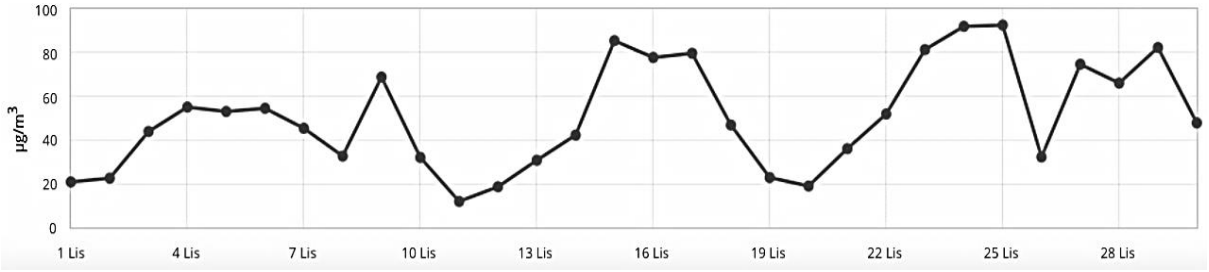

Fig. 2 Particulate Matter 2.5 Concentration in the Air

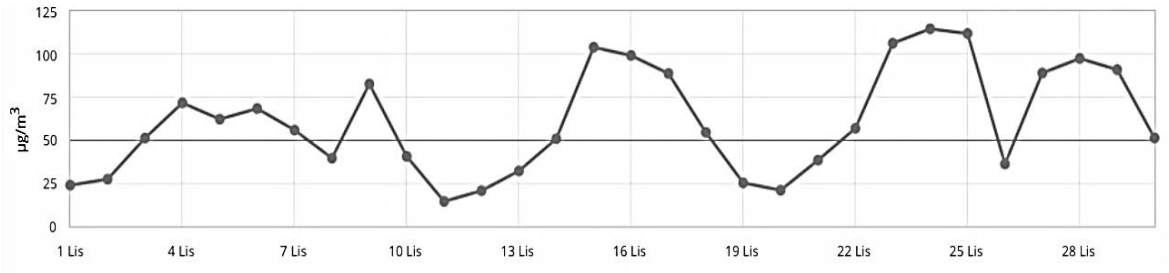

Fig. 3 Particulate Matter 10 Concentration in Air

The need of the hour is to shift towards renewable energy technologies to reduce our carbon footprint. In this regard, the authors suggest taking an initiative of making AGH UST carbon neutral by 2030. This initiative can help reduce CO_2 emissions, improve image of the university, develop research and development in the field of energy & environment, and provide internships and job placements to students of the university. Moreover there is a legal requirement for Poland to produce its energy from renewable energy sources by 2020 which Poland has been falling short of and IEA has been warning Poland of this matter [3; 4].

Such an initiative from university can also help bring more investors to the country and complete Poland's global commitments. Various other universities have also worked on carbon neutrality concept and have made commitments to go carbon neutral at various period of time [5; 6; 7; 8].

Tab. 1 Carbon Neutrality Commitments by various Universities

No.	University	Country	Commitment for Carbon Neutrality (Years)
1	Cornel University	United States of America	2035
2	University of Bristol	United Kingdom	2030
3	University of Florida	United States of America	2025
4	University of California	United States of America	2025

Carbon neutrality is achieved by eliminating carbon at three major energy intensive sectors

- Electricity Consumption
- Space Heating and Cooling
- Transportation

For this paper we have only taken the electricity consumption sector while the rest can be looked in detail in future research on the subject.

2. Electricity Generation in Poland

As per IEA's recent key energy data report published in 2015, electricity generation in Poland stood at 166.2 TWh which was mainly generated through non-renewable energy sources (coal 80%, gas 5% and oil 1%) and meagre 14% share was taken up by renewable energy sources [9].

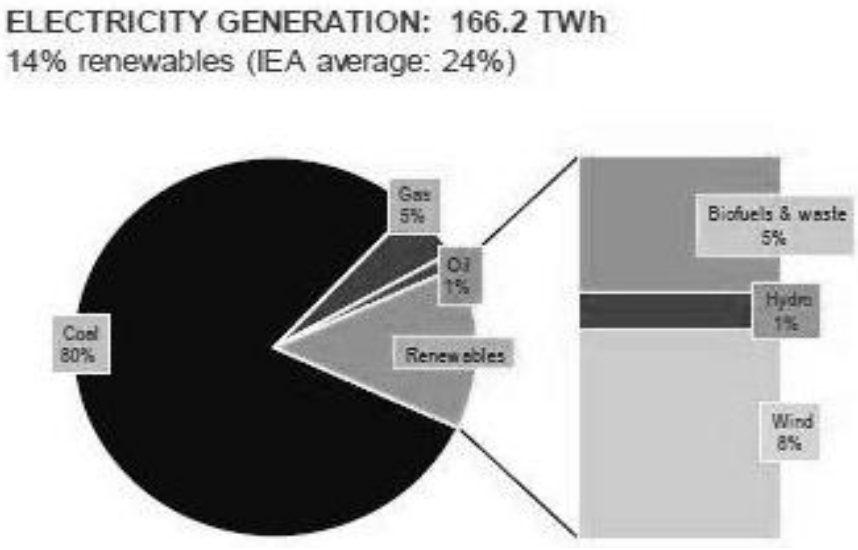

Fig. 4 Electricity Generation in Poland

3. Carbon Neutrality at AGH UST

Detail in Figure 4 explains the fact that electricity consumed at AGH UST is composed of 86% carbon intensive energy and the way forward to move towards carbon neutrality and going towards net zero electricity consumption is to work on two principles:

- Incorporating Energy Efficiency Measures
- Installation of Renewable Energy Technologies

3.1 Electricity Consumption at AGH UST

As per the official university reports, the annual electrical consumption of AGH UST stands at 2,182,107 kWh [10]. As per Figure 4, 14% is already coming from renewable energy sources, therefore we need to eliminate 86% of the total electricity consumption to go carbon neutral. In this paper we propose that we reach the net zero figure by incorporating energy efficiency measures that reduce 16% of current consumption and the rest of 70% to be covered by renewable energy technologies.

Tab. 2 Electricity Consumption at AGH UST

No.		Energy (kWh)
Annual Consumption		
1	AGH – Annual Electricity Consumption	2,182,107
2	Carbon Intensive Electricity (86%)	1,876, 612
Strategy to go Carbon Neutral		
3	Energy Efficiency Target (16%)	349, 137
4	Renewable Energy Deployment (70%)	1,527,475

3.2 Energy Efficiency Measures

Various energy efficiency measures can be incorporated to reduce the consumption considerably without incurring huge investment costs such as:

- Changing Consumer Behavior
  - Switching off lights and electrical appliances right after usage
  - Motivating people into using the stairs and avoiding the elevator
  - Motivating people into opening the windows in order to ventilate the room instead of turning on the air conditioners
  - Reducing Phantom Loads
- Daylight Harvesting
- Unoccupied Setback
- Occupancy Sensors

Furthermore, other steps can be taken which are less intensive but reduce energy consumption considerably such as:

- Replacing fluorescent light bulb with LED bulbs
- Improving building capsule's thermal insulation
- Solar-thermal and Geo-thermal systems installation for space and water heating.
- Ventilation on Demand
- Hot Water Resets

3.3 Renewable Energy Technologies

Various renewable energy technologies can be incorporated to go carbon neutral such as solar photovoltaic, wind energy, bio fuels and fuel cells etc. For current paper we have considered solar photovoltaic and wind energy to be the favorable technologies as they are market compatible and commercially feasible.

Simulation for 1 MW of both solar photovoltaic and wind energy technologies were performed as per Krakow's weather conditions to determine the number of units produced by each technology.

3.3.1 Solar Photovoltaic

National Renewable Energy Lab's solar PV simulation software was used to determine the units of electricity produced on annual basis by 1 MW fixed solar PV system in Krakow at various tilt angles and the best result was found to be at a tilt angle of 30^0 [11]. Table 3 shows the results of different tilt used for the simulation of solar PV system.

Tab. 3 Solar PV Tilt Angle Results

Tilt Angle	0^0	15^0	**30^0**	45^0	60^0
Yield (kWh)	797,952	859,772	**884,356**	869,687	816,758

At a tilt angle of 30^0 the system gives the maximum annual yield of 884,356 kWh/annum. Tables 4 and 5 show the specifications and results obtained by the simulations performed.

Tab. 4 Solar PV System Specifications

Location and Station Identification	
Requested Location	Krakow, Poland
Weather Data Source	(INTL) BIELSKO BIALA, POLAND – 41 mi
Latitude	49.67˚ N
Longitude	19.25˚ E
PV System Specifications (Commercial)	
DC System Size	1000 kW
Module Type	Standard
Array Type	Fixed (Roof Mount)
Array Tilt	30˚
Array Azimuth	180˚
System Losses	14%
Inverter Efficiency	96%
DC to AC Size Ratio	1.1
Economics	
Average Cost of Electricity Purchased from Utility	No Utility Data Available
Performance Metrics	
Capacity Factor	10.1%

Tab. 5 Solar PV System Results

Month	**Solar Radiation (kWh/m^2/day)**	**AC Energy (kWh)**	**Energy Value ($)**
January	1.20	32,493	N/A
February	2.05	49,574	N/A
March	2.87	75,221	N/A
April	3.57	87,580	N/A
May	4.63	114,704	N/A
June	4.57	107,875	N/A
July	5.02	118,566	N/A
August	4.27	101,906	N/A
September	3.13	74,877	N/A
October	1.94	50,248	N/A
November	1.51	38,142	N/A
December	1.26	33,171	N/A
Annual	**3.00**	**884,357**	**0**

3.3.2 Wind Energy

For calculating wind energy from same name plate capacity (1 MW), software produced by DR Zaber LLC was used. DR Zaber LLC is a company located in Krakow which also manufactures wind energy turbines [12]. Simulations were performed at their largest manufactured turbine (100 kW). For 1 MW 10 such turbines were used.

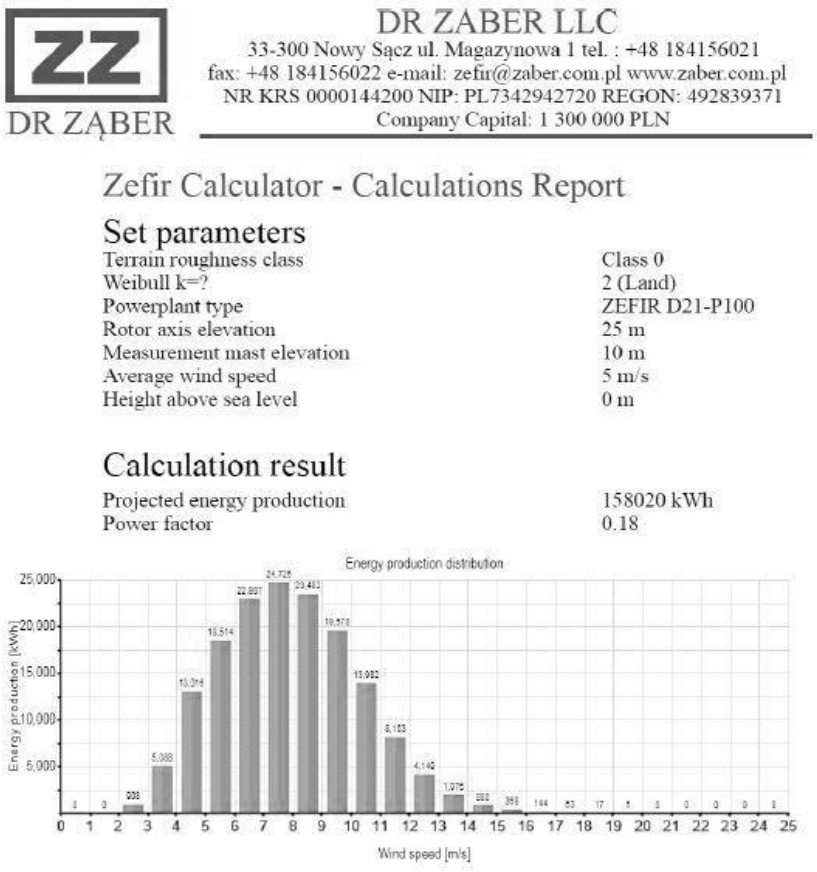

Fig. 5 Simulations Results of Wind Energy Simulation

One 100 kW wind turbine produced 158,020 kWh/annum. 10 such turbines (1 MW) would produce 1,580,200 kWh/annum.

4. Economic Analysis

Economic analysis was performed to determine the feasibility and calculate the payback period of both technologies.

$$Payback\ Period = Years\ prior\ to\ full\ recovery + \frac{Unrecovered\ cost\ at\ start\ of\ year}{Cash\ flow\ during\ full\ recovery} \quad (1)$$

4.1 Solar Photovoltaic

Annual yield of solar photovoltaic reduces by 0.7 % because of deterioration of cells by weather, which means that annual yield from the solar PV system decreases on annual basis [13].

Table 6 shows the annual solar yield and annual earning based on the earnings and the tariff for solar provided by the Polish government [14].

Table 6 Annual Solar Yield and Annual Earnings

Year	**Annual Solar Yield**	**Annual Earning**
	kWh	**€**
1	884,356	88,436
2	878,166	87,817
3	872,018	87,202
4	865,914	86,591
5	859,853	85,985
6	853,834	85,383
7	847,857	84,786
8	841,922	84,192
9	836,029	83,603
10	830,176	83,018
11	824,365	82,437
12	818,595	81,859
13	812,864	81,286
14	807,174	80,717
15	801,524	80,152
16	795,913	79,591
17	790,342	79,034
18	784,810	78,481
19	779,316	77,932
20	773,861	77,386
21	768,444	76,844
22	763,065	76,306
23	757,723	75,772
24	752,419	75,242
25	747,152	74,715

Table 7 presents the total investment, annual solar yield, tariff for sale of electricity to the utility company, payback period of the investment and total solar PV required the 70% university's electricity demand to make it carbon neutral.

Table 7 Economic Analysis of Solar PV Power System

Economic Analysis	
Investment (1 MW)	€ 1,040,000
Annual Solar Yield (kWh) – 1st Year	884,356
Tariff (c/kWh)	0.1
Payback Period (Years)	12.19
Solar PV Required to Offset Demand	1.72 MW
Total Investment Required	€ 1,788,800

4.2 Wind Energy

Wind energy farms do not have annual reduction in the energy yield hence it has been assumed that each year they shall produce the same amount of energy i.e. 1,580,200 kWh. Based on the annual solar yield and tariff provided by the Energy Regulatory Office of Poland [15], the economic analysis has been performed and provided in Table 8.

Table 8 Economic Analysis of Wind Power System

Economic Analysis	
Investment (1 MW)	€ 1,774,267
Annual Solar Yield (kWh) – 1st Year	1,580,200
Tariff (c/kWh)	0.082
Payback Period (Years)	13.53
Solar PV Required to Offset Demand	1 MW
Total Investment Required	€ 1,774,267

4.3 Discussion

Comparison of Tables 7 and 8 reveal that investment cost to cover the 70% of electricity of university through renewable energy technologies shall be lower in case of wind technology but solar PV has an advantage with lower payback period. On the other hand wind energy has an advantage that only ten wind turbines of 100 kW each shall be required to be installed whereas huge amount of land shall be required to produce 1.72 MW Solar PV power plant. In this regard wind energy shall be deemed a more feasible solution.

4.4 Investing Agencies

A number of agencies across the globe invest in innovative initiatives related to renewable energy technologies. Three of them have been mentioned as follows [16; 17; 18].

- National Fund for Environmental Protection and Water Management
- European Union
- International Renewable Energy Agency (IRENA)

5. CO_2 Emissions Reduction

According to Polish government estimates CO_2 produced per unit of electricity generated from non-renewable resources is 812 grams/kWh [19]. As per this rate, an annual CO2 reduction of 1,524 tonnes/annum can be achieved.

Table 9 CO_2 Emissions Reduction

Electricity from Non–Renewables (86%)	1,876, 612 kWh/annum
CO_2 Emission per Unit of Electricity Produced	812 g/kWh
CO_2 Emission Reductions	1,524 tonnes/annum

6. Conclusions and Discussions

The paper provides a possible road map for universities to play an important role towards green energy transition and go carbon-neutral providing certain commitments and timeframes. In this paper the authors have proposed AGH UST to go carbon neutral by 2030 by implementing energy efficiency measures and installing renewable energy technologies. Solar PV and Wind Power have been considered as two possible alternatives for renewable energy installation and wind has proved to be an alternative as it has lesser investment cost and requires lesser space for installation.

For this paper we have only taken the electricity consumption sector while space heating and cooling, and transportation sector can be looked in detail in future research on the subject.

Acknowledgment

The authors would like to thank Mr. Karol Sztekler for providing the university's electricity consumption data, without which the manuscript wouldn't have been completed.

References

[1] Climate.gov., https://www.climate.gov/news-features/understanding-climate/climate-change-annual-greenhouse-gas-index, (02/12/2017).
[2] Malposkie - Air Quality Monitoring System, http://monitoring.krakow.pios.gov.pl/dane-pomiarowe/automatyczne/stacja/6/parametry/1711-44-46-202-43-42-45/miesieczny/11.2017, (02/12/2017).
[3] National Action Plans, https://ec.europa.eu/energy/en/topics/renewable-energy/national-action-plans, (02/12/2017).
[4] Wind Power Monthly, https://www.windpowermonthly.com/article/1422518/iea-urges-poland-opt-cleaner-coal-renewables, (02/12/2017).
[5] Cornell Sustainable Campus, http://www.sustainablecampus.cornell.edu/initiatives/climate-action-plan, (02/12/2017).
[6] University of Bristol, Green Campus, http://www.bristol.ac.uk/green/pledges/, (02/12/2017).
[7] Office of Sustainability, University of Florida, http://sustainable.ufl.edu/topics/neutralufcoalition/, (02/12/2017).
[8] Carbon Neutrality Initiative, https://www.universityofcalifornia.edu/initiative/carbon-neutrality-initiative, (02/12/2017).
[9] Agency International Energy, *IEA – Most Recent Key Energy Data*, 2015.
[10] J. Bielewicz. Analiza zapotrzebowania mocy elektrycznej oraz sposób zakupu energii elektrycznej dla obiektów Uczelni, http://www.smartgrid.agh.edu.pl/documents/prezentacje/2016/1.03.2016_J.Bielewicz.pdf, (02/12/2017).
[11] NREL PVWatts, http://pvwatts.nrel.gov/pvwatts.php, (02/12/2017).
[12] ZZ DR Zaber, http://zaber.com.pl/zefir/, (02/12/2017).

[13] G.T. Klise, J.L. Johnson, S.K. Adomatis. *Standardizing appraisals for PV installations. in Photovoltaic Specialists Conference (PVSC), 2013 IEEE 39th*, 2013 .
[14] Energy Regulatory Office, https://www.ure.gov.pl/en/, (02/12/2017).
[15] Energy Regulatory Office, https://www.ure.gov.pl/pl/rynki-energii/energia-elektryczna/aukcje-oze/dokumenty/6539,Ceny-referencyjne.html, (02/12/2017).
[16] National Fund for Environmental Protection and Water Management, https://www.nfosigw.gov.pl/en/, (02/12/2017).
[17] European Union, http://www.buildup.eu/en/explore/links/nfepwm-polish-national-fund-environmental-protection-and-water-management, (02/12/2017).
[18] International Renewable Energy Agency, www.irena.org, (02/12/2017).
[19] The reference rate of carbon dioxide emission per unit for the production of electricity to determine the baseline for JI projects implemented in Poland, http://www.rynekinstalacyjny.pl/artykul/id3856,emisja-co2-z-energii-elektrycznej-w-polsce, (02/12/2017).

A review of anaerobic membrane bioreactors

Szilveszter Gábor Kéki [1], Guanghua Yang[1]

[1]Department of energy and environmental engineering, Silesian University of Technology, email: keki.szilveszter@gmail.com, superyangguanghua@me.com

Abstract

During the last decade, anaerobic membrane bioreactor (AnMBR) technology have been developed and applied in biogas production due to the significant advantages over conventional anaerobic treatment. Referring to both conventional and advanced configurations, this review presents a comprehensive summary of AnMBRs for biogas production in recent years, including the types of AnMBR and its application. The potential of biogas production from AnMBRs cannot be fully exploited, since certain constraints still remain and these can cause low methane yield. The characteristics of AnMBR and aerobic MBR for wastewater treatment is also compared. AnMBR technology appears to be suitable for treatment of various streams, especially for food industrial wastewater and municipal wastewater.

Keywords: Anaerobic membrane bioreactor, biogas production, methane, wastewater, methanogenesis

1. Introduction

During the biogas production, conventional reactors often struggle with the leaching of active sludge. Since methane-producing methanogenic bacteria have a very low propagation rate, reactor start times are high and sensitive to external influences. Although increasing the solid retention time (SRT), it is possible to reduce the leaching of microorganisms, but this entails an increase in hydraulic retention time (HRT), which results in a larger design size of the reactor. With nano or ultrafiltration, almost all of the reactor's solid content can be retained, so SRT can be infinite, but with the membrane filter HRT is no longer dependent on SRT, thus significantly reducing the design size of the reactor. Thus, concentration of degrading organisms can be increased, compared to the general reactors, which leads to gain biogas yield and methane concentration, also reduces the amount of sludge produced and makes the reactor more resistant to environmental changes. Due to increased bioactivity and the use of membrane filters, the quality of outcoming water is excellent. Now days, clogging of the membranes is one of the main obstacle of wide spread using, however with recent technological improvements, the number of applied AnMBRs is growing. The aim of this article is showing the available AnMBRs systems, and the possible applications.

2. Types of AnMBRs

In most cases, studies with AnMBRs are laboratory and rarely pilot sizes. One of which works in industrial scale, called "Kubota Submerged Anaerobic Membrane Bioreactor (KSAMBR)" designed by Japanese Kubota Company. The reactor can process distillation residues (mash) or food waste. First, the residue is pretreated, chopped and riddled, then it is stored in a buffer tank for dissolving purposes where the nutrients are well mixed. After the liquid is introduced into the methane fermentation tank (MF), where rapid thermophilic degradation occurs. The MF tank includes a separate container that seats the membrane filter units. The anaerobic sludge is concentrated in the immersed membrane filter container from where it is circulated back into the MF tank or drained for further treatment. The resulting biogas contains ~ 60% methane, ~ 40% carbon dioxide, and minimal other gas. The collected biogas is used for power generation and boiling. With this construction they could recover 12 GJ of energy per day mean while the reactor's electricity and heat consumption were less than 5 GJ.

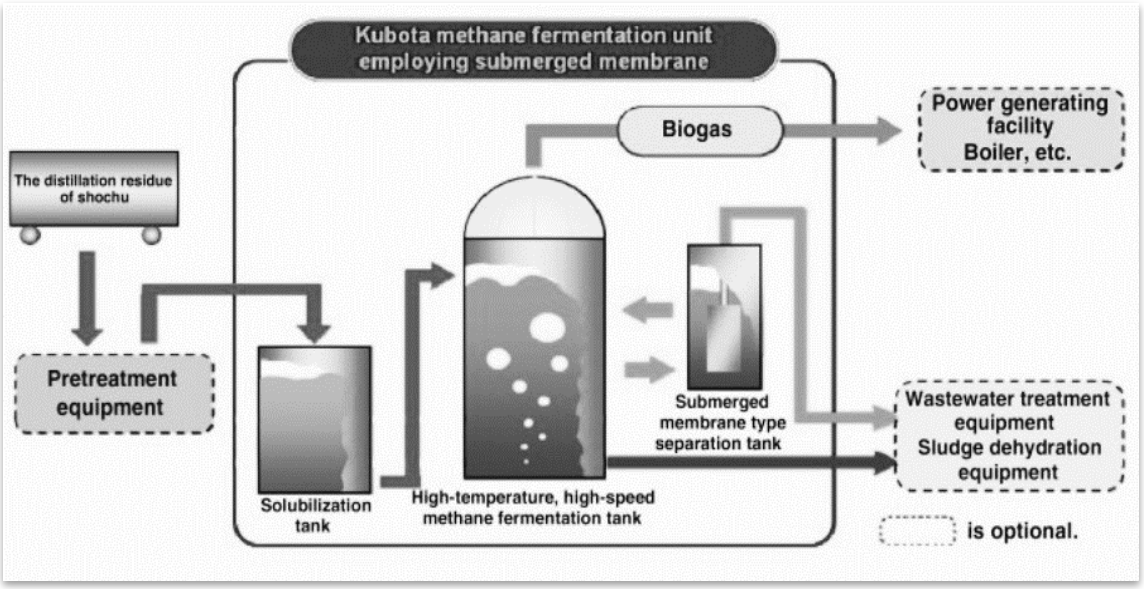

Fig. 1. KSAMBR process.

2.1 Basic AnMBR types

2.1.1 Completely stirred tank reactor (CSTR) AnMBRs

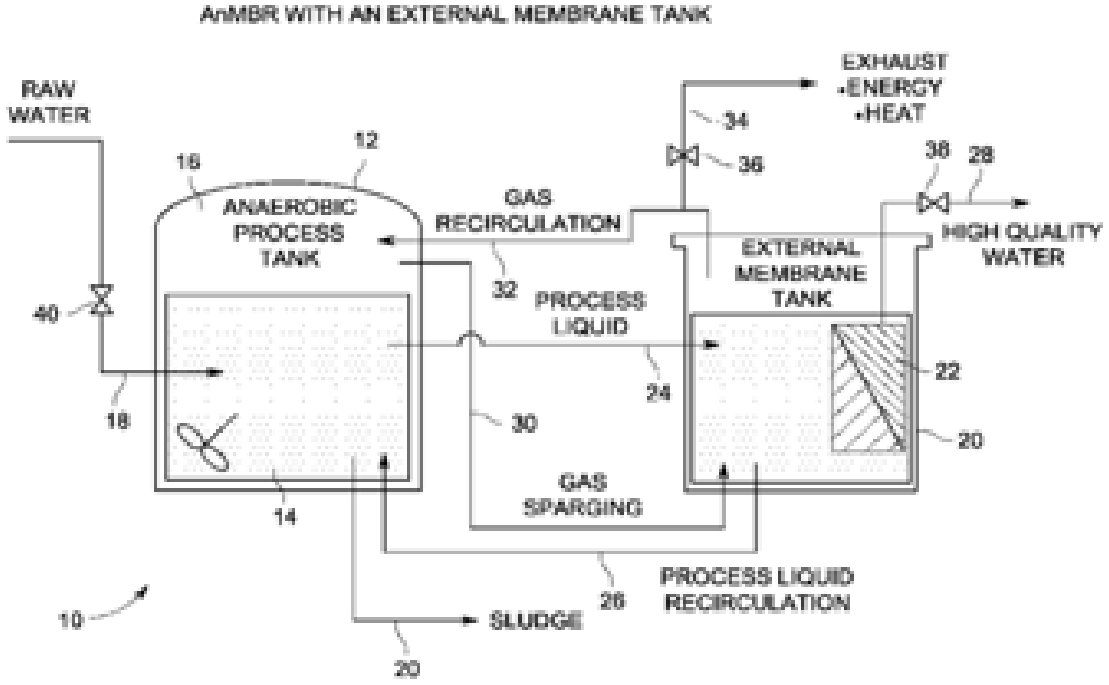

Fig. 2 A schematic diagram showing the comprehensive processes of biogas production from anaerobic processes [11].

Completely stirred tank reactors (CSTRs) are the most common and most popular reactors thanks to their simple construction and operation. Their tank could be cylindrical or square, and the mixing turbine is placed in this tank. The advantage of the reactor is that the mixing of the total amount of liquid is solved, so the substrate

distribution is completely homogeneous, providing adequate methane production. Among the CSTRs, for energy reasons, the use of the submerged membrane is becoming more popular as cleaning is simpler. In laboratory and pilot tests, generally promising 0.23 (STP) CH_4/g COD $_{removed}$ methane yields are achieved with 85% methane content. CSTR is often used for hydrogen fermentation research, where they are able to produce biohydrogen by inhibiting methanogenic bacteria. This requires control of partial hydrogen pressure and pH, as well as the feeding of chemical inhibitors and the establishing of iron-reducing environment. The results so far resulted from 2.5 to 66 hydrogen yields [dm^3 H_2/dm^3 feed] with 62.6% hydrogen content. Nonetheless, the reactor requires continuous mixing, in addition, continuous pumping will result in a reduction in particle size, which increases membrane clogging and complicates the interaction between acetogens and methanogens, leading to an increase in volatile fat acids (VFA) concentration, thus process leads to inhibition. CSTRs generally operate with lower organic loading rate (OLR) (<5 g/L MLSS) to reduce membrane contamination [2].

2.1.2 Up-flow anaerobic sludge blanket reactor UASB AnMBR

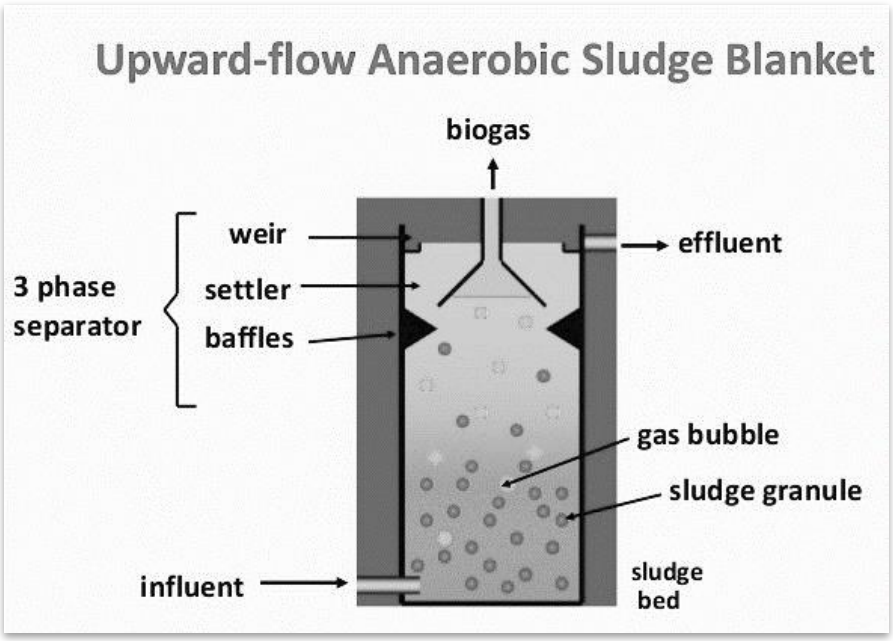

Fig. 3 Upward-flow Anaerobic Sludge Blanket reactor

The UASB reactor consists of a high tank with a granular sludge bed at the bottom, above a tall column includes the mixture of gas bubbles and granulated sludge particles. At the top of the reactor is the gas cap and the weir that realize the three-phase separation. The gas bubbles generated inside the reactor are directed by baffles to the gas cap, where biogas is educed. The advantage of the construction is that the methanogenic sludge granulate is able to settle in a dense and thick sludge bed. With additional filtration, this construction was used to treat kraft evaporator condensate at mesophilic temperature, which lead to 0.35 L CH_4/g COD $_{removed}$ methanol yield at 90% methane concentration. In a general UASB which treats wastewater with low organic matter content, due to poor mixing, a decrease in biogas yield occurs as COD removal efficiency decreased. Using a membrane in the UASB may vary. In Beijing, setting-up a biofilter layer on top of the sludge bed was achieved with excellent sludge activity (21.5g/L MLSS), which lead to a 0.42 [L/L] biogas yield with a 66% methane content. Controversially, the direct implementation of the membrane eliminates the hydraulic selection of the granules thus quality of the sludge getting worst, which affects methane production [3].

2.1.3 Anaerobic fluidized-bed AFB MBR

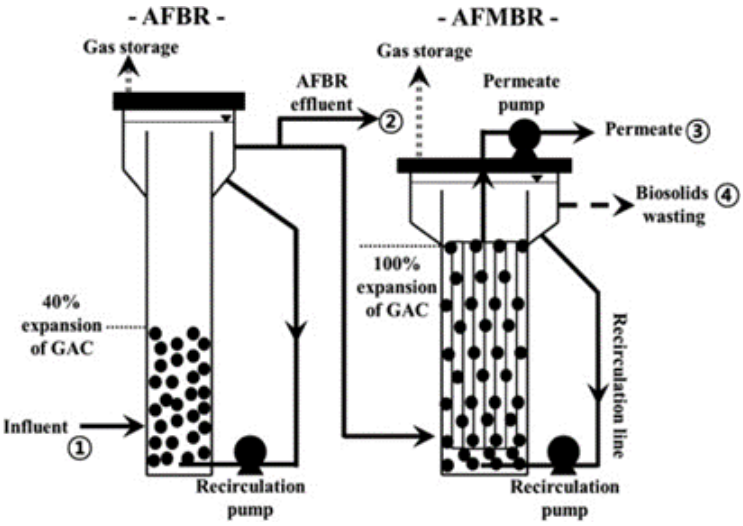

Fig. 4 AFBR process.

The advantage of this type is a very intense mass flow, high MLSS, and so on that the fluidization of granular activated carbon (GAC) can so reduce the clogging of the membrane by scrubbing the membrane, leading to direct reduced operating costs. Several studies have also conducted staged anaerobic fluidised (SAF) MBR systems. The SAF-MBR consists of a general AFBR and an AFMBR whose main role is methane recovering. The system reached of 92.1 (Ndm3) CH_4 / m^3 methane yield with 86% methane content. According to the study, only 30% of the energy produced by methane can be covered the energy demand in the process. According to another study, the SAF-MBR system has great potential as cost-effective bioenergy recovery system with low energy demands, high efficiency. One of the most significant problem that a considerable part of the methane yield, up to 63% being dissolved, is lost in the outcoming fluid. There are other lab-scale constructions called integrated anaerobic fluidized-bed membrane bioreactor (IAFMBR), where the AnMBR part is settled inside of the general AFBR in purpose of minimizing foot-print. The system was able to produce biogas with 80% methane content by converting 50% of the COD into methane. However, 25% of methane has "passed away" with the outcoming fluid [4].

2.1.4 Two-phase anaerobic digestion TPAD

In the system, the first reactor is a fixed bed reactor which give place for the acidogenesis process. From here, the liquid flows into a jet flow AnMBR, where it is injected through a nozzle which provide an excellent circulation of the liquid, therefore homogenization and material transfer are realized. The two separate phases provide the opportunity to optimize acetogenesis and methanogenesis separately, to overcome VFA accumulation, and to increase biogas yield. In the study, slaughterhouse wastewater was treated with 0.27 L CH_4/g COD $_{removed}$ methanate yield [1].

2.2 Modified AnMBR

2.2.1 Anaerobic ammonium 0ixidation (Anammox) AnMBR

One disadvantage of AnMBR is that they are not capable of nitrogen separation. This can be offset if the technology is supplemented by ammonia removal. The advantages of the Anammox process: a) higher nitrogen removal than general nitrogen removal processes, b) smaller footprint because aeration is not required. In the anammox process, nitrite react with ammonia, and finally nitrogen gas produced. Municipal waste water was treated by the combination of CANON (completely autotrophic nitrogen removal over nitrite process) MBR and AnMBR technology. The process achieved 0.206 L CH_4/g COD $_{removed}$ methane yields with 85% total nitrogen

separation, which can provide a promising solution for the complete treatment of wastewaters including energy recovery. However, methane dissolving in the permeate is still a problem [5].

2.2.2 Anaerobic dynamic membrane bioreactors AnMBR

To solve the two biggest issue, cost and clogging of membranes, a new type of membranes called dynamic membranes could resolve these problems. In that case the filtration media is a cake layer formed on cheap carrier or support materials (e.g., Dacron mesh or macro porous textiles) which perform membrane filtration. The cake layer can easily be removed after clogging, and after the cleaning phase, the cake-membrane layer is re-formed. The frequency and mode of cleaning depend on the type of support material and their chemical resistance. Recent observations mentioned, that because of the bigger pore size, the cross-flow velocity (CFV) of the membrane is lower, therefore shear stress on the biomass was reduced, which contributed to better methanogenic activity. Also, methane yields close to the theoretical maximum, are reported, even treating raw landfill leachate 0.30 L CH_4/g $COD_{removed}$, and from concentrated synthetic waste water 0.3 L CH_4/g $COD_{removed}$, where methane concentration was between 70 and 90 %. Methane losses through permeate is still a problem [6].

2.2.3 Anaerobic membrane distillation bioreactor (AnMDBR)

This technology requires mesophilic or thermophilic temperature to provide the required heat for membrane distillation. In the process the vapor phase is separated by high hydrophobic PP, PVFD or PTFE membranes. There is a temperature difference between the two sides of the membrane, so at higher temperature on the reactor side, the partial pressure of the water vapor, will be higher than on the colder side. That partial pressure difference is the driving force of the mass transport [5]. The biogas generated in the reactor is used for scrubbing the membrane and for heat and energy production. It is assumed that during heat-driven membrane distillation, methane flows into the permeate by gas diffusion and as the gas diffusion process is slower than the pressure-driven transport in a general AnMBR. Through the pores of the membrane by the Poiseuille flow, the amount of dissolved methane could be reduced [7].

2.2.4 Gas-lifting AnMBRs (Gl-AnMBR)

In both the external and the flooded AnMBR, the gas scrubbing requires considerable energy. Using biogas accumulated in the headspace as lifting gas, sustainable membrane flux could be achieved with minimum energy consumption. The blending of biogas further promotes methane stripping, thus reducing methane dissolving. A tube module with a pore size of 0.03 μm was used, where the biogas was mixed at the bottom of the module to the sludge, and then through the two-phase (liquid gas) passed through the vertically mounted tube module. Injected biogas increased shear stress on the surface of the membrane and effectively reduced clogging, also rising gas bubbles helped filterability of the sludge by reducing average density. However, the increase in shear stresses again reduced the activity of the methanogens [8].

2.2.5 Anaerobic membrane Sponge bioreactors (AnMBRs)

In a laboratory experiment, a membrane module was placed in the reactor between two rotary plates. Polyurethane sponges were also placed in the reactor. The sponges had two major roles. On the one hand, they bound the bacteria to promote their growth, protecting them from shear stresses, on the other hand, the sponges continually wiped the surface of the membrane, which effectively prevented the formation of the cake layer. However, the study investigated only the low density media and the direction of water flow in the light of them effect on cleaning the surface of the membrane. The configuration requires further experiments, for example: what is the optimal density, shape, size of the sponge, and how the rotational shear stress has an effect on bioactivity and biogas production [9].

3. Application of AnMBR

As the required quality of discharged effluents is rising, and as the efficiency of water consumption is becoming more and more important, because of potential energy recovering, and excellent effluents quality, AnMBRs are getting more and more competitive.

When AnBMRs are used for industrial applications, most attempts have been made to treat food wastewater because in most cases they do not contain toxic substances or high solids content. The most common type in this field is CSTR, which reactors operate with smaller OLRs than High Rate Anaerobic Reactors (High Rate Anaerobic Reactors HRARs), but they are still able to break down more organic matter than traditional CSTRs. Their COD removal is outstanding at about 90%. In paper industry, the COD content of the kraft distillate condensate has been successfully reduced by 93% to 99% efficiency with both mesophilic and thermophilic methanogens. However, the high temperature of the condensate causes the presence of higher concentrations of soluble microbial products (SMP), which leads to frequent membrane clogging. In the oil industry, AnMBR was also used to treat waste water generated by the Fischer-Tropsch process. The reactor produced complete solid separation with high OLR up to 25[kg COD/m^3/d], and the released COD remained steadily below 500 mg/L. During 320 days of operation, no deterioration was observed in membrane performance with a low flux from 1.5 to 3.5 LMH. In the textile industry, a submerged AnMBR was used with the addition of poudered active carbon (PAC). The average colour removing ability was 94%, the COD removing capability was 90%. The industrial usage of AnMBRs is low and often needs additional anaerobic or aerobic membrane treatments. Combined procedures have been tested for textiles, medicines and oil waste waters, and the efficiency of cleaning has always improved. Although if a wastewater can be treated in traditional anaerobic way, in theory it could be treated by AnMBR too, but improvements in the membrane performance is inevitable in order to AnMBRs become widespread [10].

For wastewater with high organic matter content, anaerobic processes are mostly developed. Although for waste waters with low organic matter content - such as urban wastewater - AnMBRs are much less applied because of the slow growth of anaerobic microorganisms, long hydraulic retention time (HRT) required, and the quality of released water rarely reaches the required quality. However, with the help of membrane, the entire suspended solids matter can be retained and the quality of the permeate is adequate. For example, each AnMBR is able to separate more than 85% of the COD and 99% of the total suspended solids (TSS). In comparison, a general UASB reactor has a BOD separation capability of 80% and the effluent COD generally ranges from 100 to 220 mg/L and TSS is from 30 to 70 mg/L. The outstanding COD and TSS removal is achievable due to the small pore size of the membranes (0.01 to 0.45 μm), therefore if the pore size is increased by the released COD and the TSS values are increased. The disadvantages of AnMBRs that they are not able to handle the nitrogen and phosphorus content of wastewaters as they should have an anoxic or aerobic zone. However, combined anaerobic and aerobic sewage treatment is hindered due to low COD:N and COD:P ratios. Partial nitration / nitrification can be a solution since ammonium ion can act as an electron donor, so no additional carbon source or other electron donor is needed. In addition, reverse osmosis membrane can be used to achieve full phosphorous and nitrogen separation. Then, physical/chemical separation techniques may be considered, although these are considerably more expensive than biological methods. Some medically active substances (acetyl salicylic acid, ibuprofen, fenofibrate) can be degraded using long HRT (30 days). The main weakness of AnMBR is that the sustained flux of the membranes is generally below 15 LMH. Comparison, in an aerobic MBR, this is 25-144 LMH for the outer membranes and 3.7 to 85 LMH for the submerged membranes. However, the costs of an AnMBR and an aerobic MBR are almost the same, but the anaerobic reactor's operating costs only one-third of an aerobic one's, and moreover this can be reduced by the biogas production. SAnMBRs, with the growth of membrane performances, can offer a promising solution to urban wastewater treatment [10].

Overall, it can be mentioned that when sewage is characterized by its organic matter content, solids content, and extreme conditions (high temperature, pH, etc.), then AnMBRs are used for high organic rates, low-solids content and without extreme conditions, waste water it is not worth using because the specifically designed HRARs are equally suitable and have a much lower investment and operational cost [10].

4. Conclusions

The biggest problem that haven't solved so far is the methane dissolution with permeate. This has caused problems in almost every study. It is worth testing the membrane distillation design. In my opinion, the price of membranes can be most effectively reduced using the dynamic membrane. By separating acetogenesis and methanogenesis, both methane yields and the stability of degrading processes can be increased. The membrane purification was best achieved in AFBR by GAC granules and in the sponge AnMBR by the rubbing of

polyurethane cubes, and even in the case of sponge cake there was no need for a separate membrane purification phase, further examination of the design is recommended. According to my research, CANON-MBR provides a better solution than nitrogen removal as reverse osmosis since it does not cause ammonia accumulation and can therefore be used to treat high ammonia-containing effluents. In my view, due to the increasing water purity requirements and the growing membrane technology, the AnMBRs will be widespread. They properly purify sewage and are more resistant to environmental changes and the fluctuation of feed quality due to retained microorganisms, and can therefore be used for continuous biogas production.

References

[1] DC.L. Mao, Y.Z. Feng, X.J. Wang, G.X. Ren, *Review on research achievements of biogas from anaerobic digestion, Renew. Sust. Energy Rev*. 45 (2015) 540e555.

[2] C. Cheng, G. Wenshan, N. Huu Hao, L. Duu-Jong, T. Kou-Lun, J. Pengkang, W. Jie and W. Yun, "*Challenges in biogas production from anaerobic membrane bioreactors*," Renewable Energy, 1. 1998, pp. 120-134, 2016.

[3] H.Ozgun,R.K.Dereli,M.E.Ersahin,C.Kinaci,H.Spanjers,J.B.vanLier,*A review of anaerobic membrane bioreactors for municipal wastewater treatment: integration options, limitations and expectations*, Sep. Purif. Technol. 118 (2013) 89e104.

[4] R. Yoo, J. Kim, P.L. McCarty, J. Bae, *Anaerobic treatment of municipal waste- water with a staged anaerobic fluidized membrane bioreactor (SAF-MBR) system*, Bioresour. Technol. 120 (2012) 133e139.

[5] Z.Y. Li, X.D. Xu, X.C. Xu, F.L. Yang, S.S. Zhang, *Sustainable operation of sub- merged Anammox membrane bioreactor with recycling biogas sparging for alleviating membrane fouling*, Chemosphere 140 (2015b) 106e113.

[6] M.E. Ersahin, H. Ozgun, Y. Tao, J.B. van Lier, *Applicability of dynamic mem- brane technology in anaerobic membrane bioreactors*, Water Res. 48 (2014) 420e429.

[7] S. Goh, J.S. Zhang, Y. Liu, A.G. Fane, *Membrane Distillation Bioreactor (MDBR) e a lower Green-House-Gas (GHG) option for industrial wastewater recla- mation*, Chemosphere 140 (2015) 129e142.

[8] J.B. Gimenez, N. Marti, J. Ferrer, A. Seco, *Methane recovery efficiency in a submerged anaerobic membrane bioreactor (SAnMBR) treating sulphate-rich urban wastewater: evaluation of methane losses with the effluent*, Bioresour. Technol. 118 (2012) 67e72.

[9] J. Kim, J. Shin, H. Kim, J.Y. Lee, M. Yoon, S. Won, B.C. Lee, K.G. Song, *Membrane fouling control using a rotary disk in a submerged anaerobic membrane sponge bioreactor*, Bioresour. Technol. 172 (2014) 321e327.

[10] L. Hongjun, P. Wei, Z. Meijia, C. Jianrong, H. Huachang and Z. Ye, "*A review on anaerobic membrane bioreactors: Applications, Membrane Fouling and Future Perspective*," Desalination, 1. Volume 314, pp. 169-188, 2013.

[11] H. Youngseck, B. Reid Allyn, S. Domenico, C. Jeffrey Ronald, S. David Eaton and C. Sheng, „*Method for utilizing internally generated biogas for closed membrane system operation*". Patent number: US8580113 B2.

Carbon Capture and Storage: Technology of the Future - A Review Paper

Ryszard Górnowicz [1], Hesham Abdelaal [1]

[1]Faculty of Power and Environmental Engineering, Silesian University of Technology, e-mail: rysiek.gornowicz@gmail.com, heshabd658@student.polsl.pl

Abstract

Carbon capture and storage can play a unique and decisive role in mitigation strategies in the coming decades. A practical legal and regulatory framework is needed to develop a quality control system on the road to meeting promises to substantially reduce carbon emissions. Different approaches are being considered in countries with social and economic services activities. However, the current legal framework is often unclear, mainly because most have not been formulated for the climate control system, and there are numerous gaps and overlaps in legal issues that may hinder the design of a food safety control system. This paper presents a current study of a number of existing legal and regulatory aspects of the classification of chemicals. Instead of focusing on general regulations on climate change, planning and design documents target Europe and North America, including property rights, disclosure and financial safeguards for carbon storage. We conclude that action should now be taken to develop a set of practical rules that will pave the way for the effective implementation of CCS as soon as climate policy is moving forward.

Keywords: CCS, EOR, storage, regulatory, climate

1. Introduction

Given the magnitude of energy-related CO_2 emissions as global energy systems are in line with rising energy demand, the role of carbon capture and storage technologies will be critical. To achieve a significant impact on mitigating climate change and significantly reducing carbon dioxide emissions, one billion tons per year will be needed. This means that SS will need to be demonstrated and widely implemented in future decades in fossil power plants and industrial facilities [2]. Today, it is fair to say that CES is still at an early stage of development, with a number of pilot stations and demonstration in operation, but not yet mature enough to be considered as a technology to mitigate competition at present. Several reasons have been put forward to explain the current status of the classification of chemicals [1]. Insufficient policies supporting climate service costs and a lack of a business model that encourages private investment are key reasons. While other low-carbon technologies such as renewable energy have received sufficient attention to allow for their development and dissemination, the promotion of such programs is based on policy programs that have failed to provide effective financial mechanisms to ensure delivery.

Over the last decade, progress has been made in establishing the legal and regulatory framework necessary to implement CCS. Nevertheless, it was a slow and not always satisfying process for the industry. It is particularly important to define the regulation so rigorously that it takes due account of health, safety and the environment, but it has not been so stringent as to inhibit the growth of CCS [2].

There are two categories of legal and regulatory problems related to CCS. First of all, there are general regulations on climate change that include emission reduction targets and incentives to credit for avoided emissions. Having the right regulations on climate change is essential to create the necessary market for implementing CCS. Examples of this type of legislation can be found in Europe, where CCS has been included in the scope of the revised EU Emissions Trading Directive to provide complementary funding [2]. Financial support for the CCS demonstration through the EEPR1 and NER3002 programs and the existence of an EU carbon allowance market have given rise to the construction and operation of CCS in 12 power plants and

industrial plants in Europe by 2015 [1]. Despite efforts, the EU will not achieve this goal. The main reason is the reduction of the price of carbon dioxide under the EU Emissions Trading System, as a result of which prices of CO_2 allowances are an order of magnitude lower than the climate and energy package from 2008, which predicted prices in the range of 30 EUR / tCO_2 by 2020 [2].

The US introduced the main climate laws, including the 2003 Climate Change Act, the 2007 Environmental Mitigation Act, and the US Clean Energy and Security Act 2009. While the United States Congress did not pass any of these bills and opportunities for climate legislation before the next 2016 presidential election are essentially nil, administrative action has taken place. In 2010, the US Environmental Protection Agency introduced a mandatory requirement for reporting greenhouse gases, including CO_2 injections and emissions. In September 2013, the EPA published draft legislation limiting CO_2 emissions from new power plants. The draft regulations for the reduction of CO_2 emissions from existing power plants were published in June 2014. None of these activities will, however, create significant markets for CCS [2].

The second category of regulations, and focus of this paper, is the set of regulations applied to CCS facilities to ensure that operations are safe and effective in transporting, injecting and retaining the captured CO_2. If these legal and regulatory issues are not addressed well, they could present a significant hurdle for CCS projects. In addition, the regulatory framework influences stakeholder engagement towards CCS, recognized as a significant component of the CCS system [2].

2. The Storage of CO_2 permitting process

There are several critical regulatory challenges facing CCS projects that are common to all regions. These are discussed below;

The European CCS Directive states that storage sites should not be operated without a storage permit that ensures that the requirements of the Directive are met and that the storage takes place in an environmentally safe way. The ROAD project in the Netherlands filed the storage permit application in 2010 [2]. The EU Directive was implemented in the Dutch legislation in its original format without any amendment adding national provisions. After two years of a difficult process, especially because of the permitting obligations and lack of sufficient clarity in the Guidance Documents for the implementation of the Directive, the EC concluded that the application confirms the suitability of the CO_2 storage location chosen [2].

However, the project still does not have the final storage permit. The ROAD project could not submit all the required plans fully developed at the moment of the permit application. The Directive requires all the final plans to be submitted with the application, but the normal practice is that this type of information would only be completed after a final investment decision on the project is taken, which requires a granted storage permit. The Dutch Government committed then to ensure that the remarks made by the European Commission are further elaborated in due course [2]. It was agreed that the final plans will be submitted one year before the injection of CO_2 starts by 2015 [1]. No other storage permit has been submitted for review to the European Commission, showing the difficulties that project developers are facing.

Norway, which has gained experience since 1996 in the storage of carbon dioxide in geological formations, has taken independent action to address the organizational challenges facing the Commission. Norway had no ad hoc legislation in the area of the ship security control system for the authorization of the Slipner and Snowhift projects [2]. The regulations were based on the Petroleum Act of 29 November 1996 No. 72, which is very different from the regulations set by the EU Directive. Norway demonstrates successful carbon dioxide storage experiences that the authorization process depends to a large extent on close cooperation between project developers and competent national authorities [2]. In the United States, any SES project requires a Class VI design to inject carbon dioxide into the Earth's surface. EPA is the sixth grade executive from September 2011. At the time of publication there are only two projects that have pending applications for a sixth class permit good permit from 2011 and 2013. These are the industrial sources Archer Daniels Midland (Decatur Project) and Photo Regine 2.0 projects respectively. Tenaska Taylorville had applied for a residence permit. However, during the long grace process, Tenasca announced that it was cancelling the project because it was no longer economically viable [2].

2.1 CCS legislation

At present, the US Federal Government has addressed the permitting of underground injection of CO_2 through the Environmental Protection Agency. The EPA's Underground Injection Control is primarily concerned with the protection of Underground Sources of Drinking Water and has designated all subsurface injection to be permitted through one of the six categories or "classes"[2].

In September 2011, the EPA established the most recent well class, the UIC Class VI well, which is specifically for the underground injection of CO_2 [1]. CO_2-EOR projects will still be permitted through a UIC Class II well that is designed for oil and gas injection activities. However, if they want to claim CO_2 storage, they will need to convert to a Class VI permit. Class VI well permits have a much more stringent requirements than Class II wells, including a contentious 50-year long-term post closure liability period. Since the establishment of Class VI well permits, the EPA is firm that all large-scale non-EOR CCS injection projects need to obtain a Class VI well permit [2].

Complementary to the UIC are Subpart RR and Subpart UU of the EPA's Greenhouse Gas Reporting Program. These subparts require the annual reporting of all CO_2 volumes from sequestration sites, including received, injected and emitted CO_2. Subpart RR is only for reporting CO_2 volumes from geologic sequestration sites and Class VI wells. Subpart UU is for all other facilities that inject CO_2 underground including EOR projects [2]. These Subparts came into law in September 2012 and they provide the EPA with necessary data on current CO_2 volumes that are sequestered in the US.

On 4 March 2014, an amendment to the Conservation and Recovery Act was amended to exclude CO_2 streams as hazardous wastes, if captured and injected into the ground under Category 6 of the International Standard Classification of Geological Storage [4]. Although this development reduces some regulatory uncertainty, it is a small step in an organizational environment where there is still a lot of unknown. Gaps in areas such as pore ownership and long-term liability remain precarious [2].

Some of these problems have been solved by individual countries. Nine countries have addressed some of the specific legal requirements necessary to implement the CCS project. North Dakota, Wyoming and Montana have adopted several bills and have provided potential CCS project operators with good guidance on how to run CCS projects in their country. Other countries have adopted the basic principles for only a few important topics that are needed [4]. Another important factor regarding legislation on CCS projects at state level is the existence of a CO_2 storage fund. Six countries have adopted legislation on the establishment of funds for the long-term management and monitoring of CCS facilities. Money can come from various fees: fees for submitting a project application, license fees, annual user charges, closing fees and, if allocated, amount per ton of CO_2 injected [1].

Like the United States, Canada has decades of experience in its oil and gas operations, which form a solid foundation for the organization of quality control system projects. Canada also announced the standard for the performance of carbon dioxide emissions at the federal level. This strict performance standard will enter into force on 1 July 2015 for new coal-fired units as well as units reaching the end of their economic life. Units should not emit more than 420t / g on average during the calendar year, which is similar to the cycle of a high-efficiency natural gas cycle. Units with a quality control system may receive a temporary exemption from the standard until 2025 [2].

The provinces of Alberta, Saskatchewan and British Columbia are at the forefront of developments in terms of the draft statement and the regulatory framework. Related legal issues such as ownership, administration and royalties of resources, land use, regulation of the exploitation, development, conservation and use of natural resources fall within the jurisdiction of the provinces, while the federal and provincial governments share environmental protection responsibilities [2]. Many carbon dioxide operations are active in Alberta and Saskatchewan. Saskatchewan activities began in the early 1980s with Shell's proposal to conduct a small pilot project KO-2. Current regulatory tools for oil and gas operations have been applied. This starting point has influenced Saskatchewan's approach to regulating underground injections of carbon dioxide since then. In addition, there are regulations for the disposal of gas in deep water reservoirs and depleted hydrocarbon tanks in Alberta and British Columbia [2]. There is extensive operational experience with regard to the separation,

acquisition, transfer and injection of these gases and, most importantly, the existence of a regulatory framework dealing with the permitting, operation and abandonment of these gases [3].

The amendment to the Climate Change Act and the Alberta emission management act came into force in 2007 and provides for a maximum trading system that applies to all emission emitters of over 100,000 tonnes of carbon dioxide per year. Alberta also introduced an amendment to the CCS Act (Bill 24) to address some of the main obstacles to the publication of the CES system, adopted in December 2010. In March 2011, recommendations for organizational improvements in response to 1.3 billion two commercial projects in the province [2]. The regional association submitted its recommendations by the end of 2012, pointing out gaps and issues related to the regulatory framework [3]. Other Canadian provinces that have introduced SES regulations are British Columbia and Saskatchewan. They are also based on existing legislation in the oil and gas sector [4].

3. CO_2-EOR Process

CO_2-EOR has been expanding continuously in North America since its first action in the 1970s. While operations in natural CO_2 sources have reached full capacity, interest in the use of anthropogenic carbon dioxide has increased. Currently CO_2 is estimated at about $ 20-30 / ton [5].

In the absence of strong national policy tools such as cap-and-trade system applied to GHG emissions, or other incentive mechanisms to encourage CCS investment, potential revenue derived from CO_2-EOR is being viewed as a possible pathway to maintain North America's progress and build a business case for demonstration projects. The three power demonstration projects which have taken final investment decision and commenced construction have contracts to sell the captured CO_2 for EOR purposes. These are the Kemper County IGCC project in Mississippi, NRG's Parish Plant in Texas, and Boundary Dam in Saskatchewan in Canada [2].

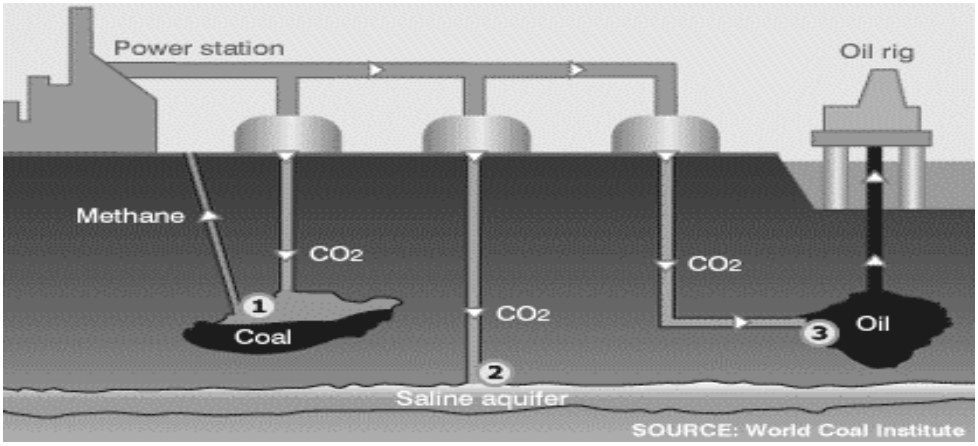

Fig.1 CO_2-EOR Process

The legal framework for CO_2-EOR has a long trajectory and is now well established. However, while CO_2-EOR and CCS might share common aspects, the legal and regulatory frameworks are in essence quite different. The CO_2-EOR operation aims to maximize the production of oil in a commercially - based premise and it is primarily regulated by oil and gas laws [2]. CO_2 is a commodity that may be injected, extracted and re-used multiple times. In contrast, the CCS operation presupposes the permanent storage of CO_2, with the aim at reducing the impact of CO_2 emissions on the environment [2].

In the United States, there are currently many states with oil and gas extraction operations that have EPA class II priority for handling CO_2-EOR. Only the state of North Dakota has applied for the assignment of a Class VI priority, which would allow geological storage of CO_2. A Class II well permit may be re-authorized for Class VI promise when the original purpose of CO_2 injection changes from EOR to long-term storage [4]. According to the EPA, class II aquifer can be extended to class VI drilling, but only if operators can prove that the aquifer does not serve as a source of drinking water or may in the future and / or that there is a high concentration of dissolved solids [3]. However, given the lack of political driver, EOR operators are currently not interested in

obtaining Class VI permits. In addition, EOR operators were very scared of Class VI permits because of their more stringent requirements compared to Class II and the long processing time of Class VI permits so far [1].

In Europe, the potential for carbon dioxide - the different uranium - is significantly different from that in North America. Oil fields in Europe are mainly located abroad adding technical complexity and expenses to the project. However, examples such as the North Sea suggest that CO_2 may be commercially viable. The Dunne project in the UK combines the geological storage of CO_2 for additional revenue in the North Sea. This project represents a somewhat different approach to ODS than has been observed in places such as the United States so far. Instead of maximizing the efficiency of oil production for each CO_2 tone, which would save as little carbon dioxide as possible, the primary objective of the project is to store a certain amount of carbon dioxide. However, the Wadi Valley project failed to secure both the British government and the European NER300 funds financing. The reliance on revenue from carbon dioxide was considered to increase project risk [5].

4. Conclusion

The deployment of South-South cooperation projects around the world faces many challenges, including financial issues, public acceptance and the establishment of a regulatory framework. In most countries, many legal approaches are developed with a significant potential for CO_2 storage and climate support activities. Despite the approach taken, care should be taken that its legal framework is consistent with the collection of new knowledge on the storage of chemicals. Although progress has been made, examples of projects being analysed in Europe, North America and Australia show that the legal framework is still immature and often insufficient to ensure the success of the declaration and the effectiveness process. Even for some SES regulatory frameworks, the process of mass storage licensing is long, over 2 years in cases that have been tested in Europe and North America [2].

Critical common challenges facing CCS projects include long-term responsibility and financial responsibility, resulting in delays and difficulties. Therefore, the first developers can play an important role in creating the right framework. Lessons learned can apply to the development of CCS rules in the relevant jurisdictions and, more broadly, in all jurisdictions.

The lack of a strong and comprehensive legal framework creates an environment of uncertainty that slows down the progress of the Commission's explanatory projects. Although the current economic and political situation is not conducive to the launch of a large number of quality control system projects, the delay in creating a healthy legal environment of the Convention on Combating Desertification is not an effective strategy. Priority should be given to the procedures for creating a set of realistic regulations that will pave the way for effective global implementation of the climate control system after the climate policy approaches.

References

[1] EL. Aldrich, C. Koerner. 2011. Assessment of Carbon Capture and Sequestration Liability Regimes, *The Electricity Journal*, 2011, 24 (7), pp. 35-48.

[2] Lubion, Monica, H. Javedan, H. Herzog. Challenges to Commercial Scale Carbon Capture and Storage: Regulatory Framework, *Massachusetts Institute of Technology Journal*, 2015, pp. 1-21.

[3] C.F.J. Feenstra, T. Mikunda, T., S. Brunsting. What happened in Barendrecht?! Case study on the planned onshore carbon dioxide storage in Barendrecht, the Netherlands. *ECN Policy Studies ECN*, 2010, 10, pp. 057.

[4] V.R. Clark, H.J. Herzog. Assessment of the US EPA's Determination of the Role for CO_2 Capture and Storage in New Fossil Fuel-Fired Power Plants. *Environmental Science & Technology,* 2014, 48 (14), pp 7723–9.

[5] H.H. Herzog. Scaling up carbon dioxide capture and storage: From megatons to gigatons, *Energy* Economics, 2011, 33, pp. 597–604.

Environmental Impact of a Palm Beach Renewable Energy Facility No. 2

Oleksandr Cahplygin[1], *Martyna Badera*[1]

[1]*Energy and Environmental Engineering, Silesian University of Technology, e-mail: kern.klassman@gmail.com*

Abstract

Nowadays society of developed countries is concerned with questions of nature protection. Therefore, all construction projects should use all available technological systems and engineering decisions to provide a minimal environmental footprint (human impact on Earth's ecosystem) during future operations. Moreover, such project should also be planned in the way of the least usage of raw materials, soil exploitation, water usage or need in transportation. The current article provides an overlook of environmental impact and life cycle assessment for Palm Beach renewable energy facility, with the aim to conclude whether or not this power plant meets a requirement for environmental protection.

Keywords: Environment Impact, Life Cycle Assessment, Palm Beach renewable energy facility, waste, emission

1. Introduction

Almost every single waste management facility by default considered as friendly to the environment. However, management of solid waste requires lands for operation, consumes natural resources and leaves a series of emissions. On the one site, waste management facilities leave a burden on the natural environment. On the other side, there are a lot of useful products such as electricity and recycled materials which are being generated as a result of its operation. What is more, plant like this does not require fossil fuels for its operation.

Dealing with the situation which has different avenues in this article, two key questions will be analyzed 1) the character of the environmental effect of Palm Beach Renewable Energy Facility No. 2 (PBREF No. 2) and 2) environmental impact assessment and life cycle analysis. Impact assessment includes a summary of environmental impacts on water, air, soil, flora and fauna. Life cycle assessment will be applied to analyze each step of the operational cycle of the plant: from waste collection to electricity production. Moreover, the environmental footprint of the building of this power plant will be included.

2. Environmental Impact Assessment

2.1 Palm beach renewable energy facility No. 2

Palm Beach Renewable Energy Facility No. 2 (Fig. 1) began commercial operation following successful completion of the plant acceptance tests in 2015. Solid Waste Authority (SWA) of Palm Beach County possessed this plant and it was the first greenfield waste-to-energy (WTE) facility which started to operate in North America in 20 years. It has been made by the combination of U.S. and European WTE emissions control and metals recover technologies. PBREF No. 2 is one of the most efficient plants working today. The main features of REF 2 are as follows:

- Usage of carbon powder to remove mercury and another surplus and volatile organic compounds (VOCs) from ash.
- Utilization of lime which is in the form of slurry to control gases which are acidic in nature in the Spray Dryer Absorbers (SDA).
- Usage of Baghouses that filter not only fly ash but lime and, carbon powder too; moreover, they prevent the release of particulates.

- Usage of ammonia to crack nitrogen oxide into harmless nitrogen and water vapor in the Selective Catalytic Reduction System (SCR) [1].

Another feature of REF 2 is an exclusive rooftop rainwater collection system that includes a 2-million-gallon cistern. This system provides a portion of the water necessary to operate the facility, reducing REF 2's usage of treated water.

While reducing waste, the electricity of 100 MW is generated for Palm Beach County. This is enough electricity to deliver power for an assessed 44,000 homes and businesses in Boca Raton City. At capacity, REF 2 will process about 1 million tons of post-recycled municipal solid waste annually and 3,000 tons daily.

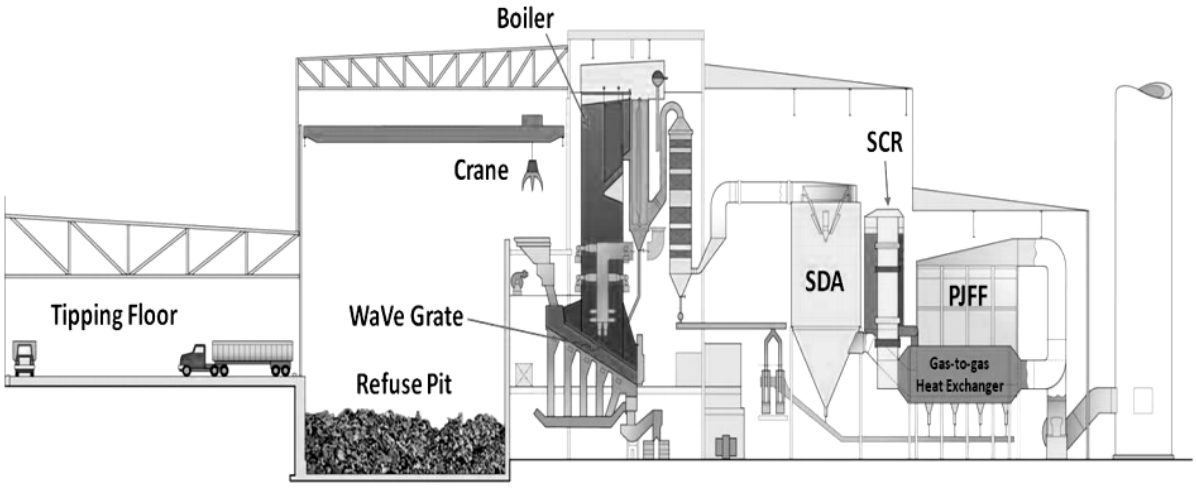

Fig. 1 Palm Beach renewable energy facility No. 2 [2]

2.2 Impact on air quality

The PBREF No. 2 post-combustion emissions control system provides control of primary and secondary pollutants which should be below permitted levels. Selective catalytic reduction (SCR) helps in NO_x control. Acid gases are removed via dryer absorber (SDA) in combination with the pulse jet fabric filter (PJFF). Particulate including metals and lead are carefully controlled by the PJFF. CO, volatile carbons (VOCs) and dioxins/furans are controlled through the combustion process and powdered activated carbon (PAC) injection in combination with the PJFF provides additional dioxin/furan control. Finally, mercury (Hg) is controlled by the PAC injection in combination with the fabric filter.

In the post-combustion emissions control system, PAC is injected into the flue gas. This process occurs before entering the vertical SDA for acid gas control and mixing of the flue gas with the PAC. The flue gases are ejected at the SDA with the desired relative humidity, which usually corresponds to outlet temperature range of 138 to 143^{o}C. Afterwards, gases passing through the PJFF for particulate elimination, including fly ash, unreacted lime reagent from the SDA, and reaction products from the SDA and PAC injection. Flue gases leaving the fabric filter then passing through a reheating heat transfer system to increase the flue gas temperature to 232^{o}C before passing vertically downward through the SCR reactor to further reduce NOx emissions. The flue gas passes back through the heat exchanger system to recover energy back into the power cycle before passing through the induced draft fans and eventually the stack. This system is designed to reduce capital costs and maintain the maximum energy recovery to keep the plant efficiency high enough.

Considering that exploitation of PBREF2 was started in 2015 it is impossible to evaluate air emissions through operational years. Because of that, to evaluate an impact on ambient air, Table 1 is provided, in which is presented the comparison of actual emissions from PBREF2 test, maximal allowed emissions according to US policy and analogical emissions from the gas turbine with the same capacity as analysed one.

Tab. 1 Comparable table of air emissions from PBREF2 to air [3]

Pollutant	**PBREF No.2 Emission Permit**	**PBREF No.2 Actual Emissions test**	**Natural Gas turbine**
Nitric Oxide	< 50 ppm	30-31 ppm	20-220 ppm
Carbon Monoxide	< 100 ppm	15-24 ppm	5-330 ppm
Sulfur Dioxide	< 24 ppm	10-21 ppm	Trace-100 ppm
Sulfur Trioxide	Not required	Not detectable	Trace-4 ppm
Unburned Hydrocarbons	< 7 ppm	0.2-2.7 ppm	5-300 ppm
Particulate Matter	12 mg/dscm	0.6-2.5 mg/dscm	Trace-25 ppm

It can be seen from the Table 1 that air emissions and therefore an environmental impact is not exceeding the acceptable limit given for this plant, and is lower than emission of other type of construction (hear gas turbine).

2.3 Impact on soil

Due to waste incineration process, great amount of municipal solid wastes (MSW) is being utilized. PBREF2 minimizes the volume of material which will require landfills by almost 90%. Also plant effectively eliminates the residual organic compounds. The WTE process effectively removes new MSW landfill gaseous emissions of a variety of dangerous volatile and chlorinated hydrocarbons including ammonia, mercaptans/ sulfides, toluene, dichloromethane, and acetone among others. So, comparing these positive effects it can be concluded that all negative impact on soil due to the building has been compensated.

2.4 Impact on water quality

The main design objective, concerning water supply for PBREF2 is to reach better than zero discharge principle and minimum water usage. Figure 2 provides information about PBREF2 water supply, which includes:

- Harvested rainwater from all main roofs of buildings at the plant and the PBREF No. 1 tipping floor roof which is stored in 7.6 million liters' storage tank. This source covers from 5% to 15% of all water needs, depending on the season.
- Off-site industrial water. Up to 35% of water is supplied to PBREF2 from that source.
- Cooling tower blowdown from PBREF No. 1. This source supplies about 60% of the plant water needs - minimizing the deep well injection from the total PBREF site below the PBREF No. 1 rate, so providing better than net-zero discharge for the PBREF No. 2.

In summary, no de-chlorinated or portable water is needed for plant operation, so water impact is minimal. No nature water sources are used.

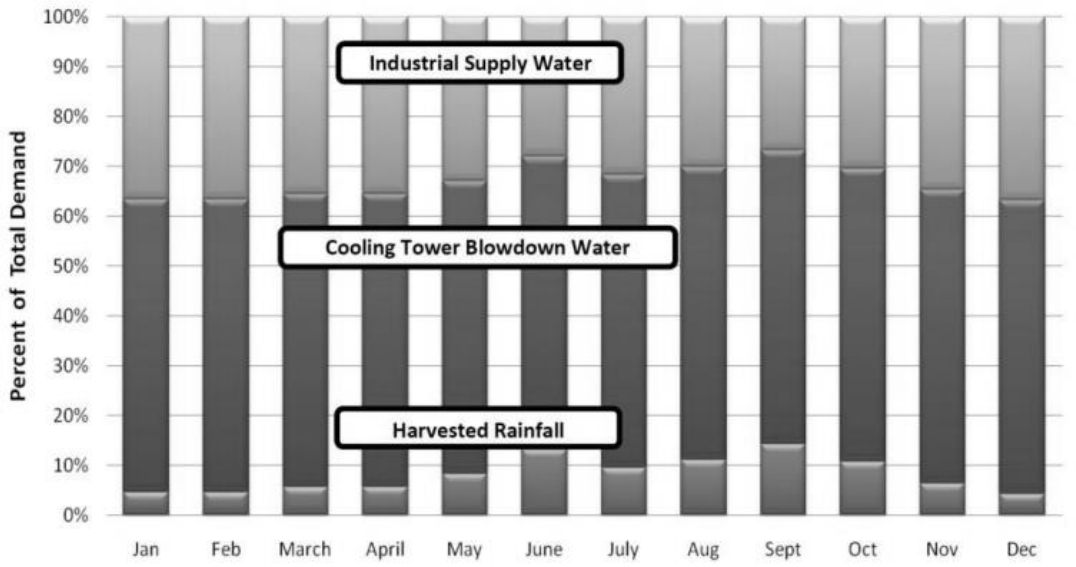

Fig. 2 Nominal water supply sources for PBREF No. 2. [3]

2.5 Impact on flora and fauna

During construction process around 2000 trees were cut or moved to the different place. Moreover, a lot of large local animals, including 10 big alligators were relocated from building site to special animal area – Grassy Waters Everglades Preserve. Considering that construction took place near already existing PBREF1, it was much easier to maintain building site as small as possible. Because, no additional place for workers living or materials storage were needed. Combining this factor with a good treatment of animals and plants it can be concluded that impact on flora and fauna is also minimal.

3. Life Cycle Assessment

The following parameters should be defined to perform the life cycle assessment;

- Functional Unit – ton, input (amount of waste entering a treatment facility)
- Type of LCA study – Observation
- Time horizon – 1 year
- Geographical Scope - Palm Beach County, Florida

The next step is to create a plan of LCA, to evaluate what parameters should be inspected and discussed. First of all, Life Cycle Inventory should be created to gain an understanding of what kind of processes and connection between them are going through PBREF2 operation. Below is description of all energy and feed inputs to the plant and all energy and pollution outputs from the plant as a result of its working cycle. Also treatment process for all negative outputs should be mentioned.

Next stage is to overlook building and construction process of an actual power plant with its environmental impacts and emissions. And the last part of LCA is an evaluation of obtained results and its discussion.

3.1 Inventory

Mixed waste collected from rounding cities are the main fuel inputs to analyzed power plant. Waste type is mixed municipal solid waste, which are stored in plastic bags or containers.

For technological part of LCI, the type of waste treatment is given as a mass burn. Total capacity of plant is 3000 tons of MSW per day. Type of reactor is B&W Stirling mass burn power boiler. Dust removing performed by fabric filter, acid gases are treated with Spray Dryer Absorber (with fabric filter). For De-NOx system a selective non-catalytic reduction is used.

The input of energy includes water resources (described in section 2.4), the energy needed for the pump and auxiliary input of gas for igniting. Two diesel fire pumps are installed. These fire pumps are standby units and will serve to provide power to pump water for fire suppression purposes in the event of an emergency situation. Each fire water pumps is expected to be powered by a nominal 186 kW diesel-fired engine.

3.2 Operational process inspection

The operational process of PBREF2 is considered as a typical waste-to-energy power plant cycle, it can be seen in Figure 3. It starts with MSW generation, then comes collection and transportation of that waste. The reclamation process comes next, and after that thermal treatment with all its inputs and outputs flows. And, finally, landfilling of the rest wastes occurs.

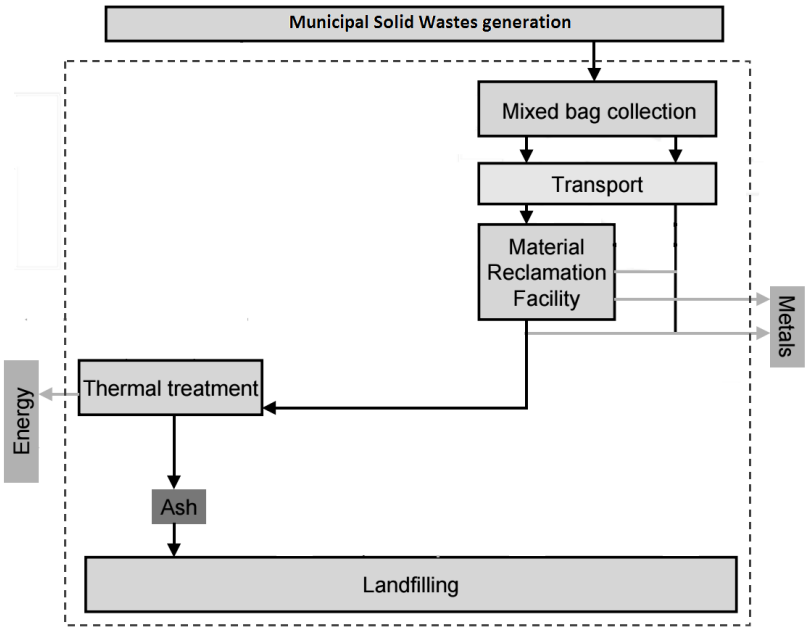

Fig. 3 Operational cycle of PBREF No. 2 [3]

3.2.1 Collection and transportation

The area where all activities take place, is around 50 miles in diameter with the average hauling distance of 25 miles. Approximately, about two-thirds of the waste stream is delivered by transfer trailer and the remaining one by roll-off containers and packer trucks. They return empty from the facility. Residential MSW is generally collected with a 20-to 30-cubic yard truck. Since, packer truck utilization is normally about 80 percent with a packing density of 750 pounds per cubic yard, one truck collects about 7.5 tons of MSW per load. The average consumption of diesel oil per load is 39 l/load which suggests a fuel consumption of 5,4l diesel per ton of MSW [4].

Fig. 4 Collection and transportation process

3.2.2 Waste burning process

Combustion reaction generates heat which is used to boil water in order to produce steam. Steam is delivered to the turbine generator where the energy is converted to up to 95 gross MW of electricity and afterward it is sold to Florida Power & Light. Flue gases generated by the combustion reaction are then processed by the emissions control system to remove air pollutants.

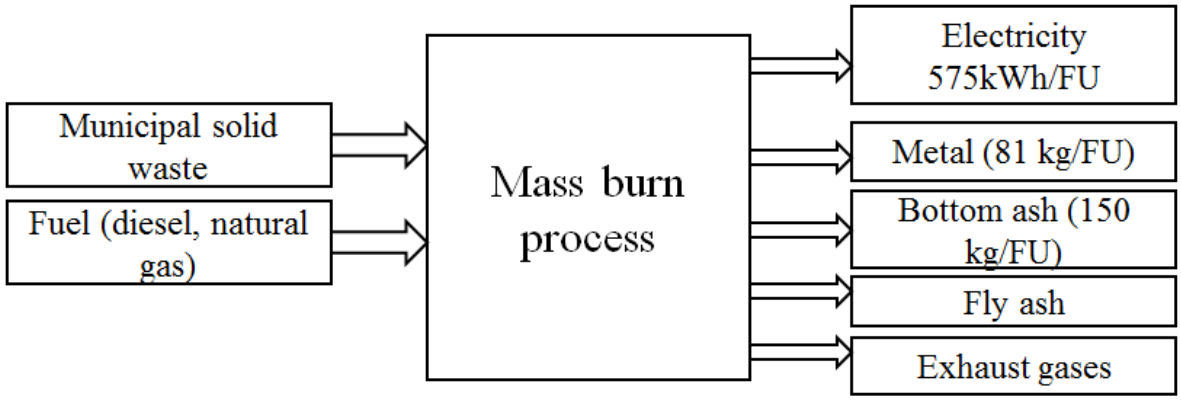

Fig. 5 Waste mass burn process

Input for this process is described as Municipal Solid Waste (MSW) (approx. 3000 ton/day), diesel for power plant pumps and auxiliary gas for ignition. All emissions from those actions will be evaluated in final emission table. Also as a harmful output can be considered 9 kg per ton of MSW of un-recycled metal, which should be landfilled

The useful output from mass burn process is 625kWh of electricity per one ton of MSW. That amount of electricity is enough to power 50,000 houses in Palm Beach area, Another useful output is an 81 kg of useful metal per one ton of burned MSW.

In addition, the amount of combined fly ash residue and bottom ash, which is generated at the facility, is assumed to be 150 kg/ton of MSW. Ash is transported to a local landfill in 20 miles by the typical tandem truck, filled based on weight of the material. Diesel needed for transportation is equal to 0,61 liter per ton of MSW.

Combined table of harmful emissions during operational process of power plant is shown in Table 2.

Tab. 2 Harmful emissions during operational process of PBREF2 [2, 4]

	Boilers (tons/year)	**Diesel Fire Pumps (tons/year)**	**Total annual emissions of Plant (ton/year)**	**Total annual emissions of Plant (ton/tonMSW)**	**Total annual emissions of Plant (Ton/MWh)**
Nitrogen Oxides (NOx)	759,06	0,14	759,4	6,94E-04	1,16E-03
Carbon Monoxide (CO)	434,86	0,066	435	3,97E-04	6,62E-04
Sulfur Dioxide (SO2)	298,66	0,00275	298,7	2,73E-04	4,55E-04
Hydrogen Chloride (HCl)	141,72	-	141,7	1,29E-04	2,16E-04
VOCs	59,79	3,42E-03	59,8	5,46E-05	9,10E-05
Particulate Matter (PM10, PM2.5)	56,08	0,00612	56,1	5,12E-05	8,54E-05
Lead (Pb)	0,65	-	0,65	5,94E-07	9,89E-07
Fluorides (as HF)	13,59	-	13,6	1,24E-05	2,07E-05

Sulfuric Acid Mist (SAM)	95,22	-	95,2	8,69E-05	1,45E-04
MWC Organics (as Dioxins/Furans)	6,08E-05	-	0,0000608	5,55E-11	9,25E-11
Mercury (Hg)	0,07	-	0,07	6,39E-08	1,07E-07
Cadmium (Cd)	0,047	-	0,047	4,29E-08	7,15E-08
Ammonia Slip	49,5	-	49,5	4,52E-05	7,53E-05

3.3 Building process inspection

3.3.1 Steel

In order to build PBREF2 steel need to be produced and delivered to the building site. For logistic reasons, the best possible steel source is a Florida Pipe and Steel company, which already exists and sells metal in Palm Beach. The distance between the steel factory and the power plant is 11 km, and assumingly shipment is performed by trucks. The truck produces 80 grams of CO_2 per tonne transported per kilometer. Shipment of steel also causes emissions, but in comparison with emissions from steel production they are very small. However, shipment emissions also is provided in Table 3. Total emissions due to simplified calculations are 1.84 ton of CO_2 per ton of steel. For other kind of emission from trucks, values are presented in Table 4.

Tab. 3 Emission associated with steel production process [5]

	Steel production	**Shipment**	**Total**
CO2 [ton/ton of steel]	1,84	1.13E-4	1,84

Tab. 4 Truck emission [6]

CO	**HC**	**NOx**	**PM**
g/kWh			
1.5	0.13	0.40	0.01

3.3.2 Cement

For logistic reasons the best possible steel source is a CEMEX company placed in Palm Beach, Florida. The distance between the steel factory and the power plant is 10 km, and transportation is performed by trucks. The truck produces 80 grams of CO_2 per tonne transported per kilometer. Additionally, taking into account production of cement, about 40% of CO_2 is produced by burning fossil fuels. Rest of the production is produced with production of electricity to power plant machinery. Total emissions due to simplified calculations are 774 ton of CO_2 per ton of cement (Table 5). The other kinds of pollutions produced by trucks are provided in the Table 4.

Tab. 5 Cement Emissions [7]

	Cement production	**Transport**	**Total**
CO2 [ton/ton of cement]	1	8	9

4. Overall influence evaluation and discussion

Summarising all outputs and inputs during the operational process of Palm Beach Renewable Energy Facility #2, all environmental influences can be evaluated and divided it into positive and negative factors. Negative influence in numbers is shown in Table 6.

All values are presented in relation to chosen functional unit per ton of MSW. So, analyzing provided information we can conclude that from one ton of MSW on PBREF2 could be obtained 625kWh of electricity, 81 kg of recycled metal. In addition, the great positive effect of landfill reduction appears from plant operation. Up to 90% of waste in Palm Beach since 2015 is being burned on PBREF2, and this fact can prolong life cycle of available landfills there up to 70 years.

Tab. 6 Negative environmental influences evaluation

NEGATIVE INFLUENCE (/tonMSW)	
Diesel consumption of trucks	6,1 l
Metal to landfill	9 kg
Ash to landfill	150 kg
Ammonia Slip	0,045206 kg
Nitrogen Oxides (NOx)	0,693000 kg
Carbon Monoxide (CO)	0,397260 kg
Sulfur Dioxide (SO2)	0,272785 kg
Hydrogen Chloride (HCl)	0,129406 kg
VOCs	0,054612 kg
Particulate Matter (PM10, PM2.5)	0,051233 kg
Lead (Pb)	0,000594 kg
Fluorides (as HF)	0,012420 kg
Sulfuric Acid Mist (SAM)	0,086941 kg
MWC Organics (as Dioxins/Furans)	5,55251E-08 kg
Mercury (Hg)	6,39269E-05 kg
Cadmium (Cd)	4,29224E-05 kg
CO_2 for building (per ton of material)	2614 kg

Positive environmental influences evaluation:

- Reduce of volume of material which need to be landfilled daily by up to 90%
- Production of 96 MW Renewable Energy
- Recycling of 81 kg of metal for every ton of MSW burned
- 625 kWh of c electricity. Enough for maintain 50 000 houses
- Cancelled emission from the land field
- Reduced water and soil contamination.

Additionally, a lot of harmful emissions is being emitted to the atmosphere. However, comparing to conventional power plants provided numbers is quite small. One of the biggest problems concerning operation is an ash landfilling; 150 kg of ash for every ton of MSW should be treated. Nowadays, this problem is being solved through usage of ash in road construction. In that way, ash does not need a landfilling which is a positive trend. In addition, 1,567.89 kg of CO_2 is emitted to the atmosphere due to transportation and production of cement and steel needed for building of PBREF2. However, these numbers are also comparably low, considering that all required factories located very close to an actual facility.

5. Summary

Summarizing all provided information, it can be claimed that Palm Beach renewable energy facility is one of the most advanced waste-to-energy power plant with a really small. According to environmental impact assessment, emissions to ambient air are fulfilling all requirements of US government.

Impact on soil is visible, but it can be compensated with the positive effect from landfill reduction. Water impact is minimal, cause PBREF2 using advanced water economy technology. No natural source of water needed for operation. Flora and fauna are also preserved due to its unique treatment.

As for life cycle assessment, current power plant in Palm Beach is technologically advanced. This fact correlates with obtained results of LCA. In this article the whole operational process of power plant was inspected. All results were evaluated and overlooked. Based on that, we can conclude that PBREF2 is a 'clean' power plant because negative effects from emissions are being strongly countered with all positive effects from waste utilization and electricity production. Moreover, building process was examined with regards to CO_2 emissions which are also not critical due to good logistics and the fact that building site already existed since PBREF1.

Considering all present information, we can safely conclude that PBREF2 is one of the most cutting-edge technology power plant with little environmental footprint. Investments similar to this presented in this paper can be very helpful in solving a problem of waste management and treatment.

Acknowledgment

This paper has been written as a part of KIC Inno energy activity in Clean Fossil and Alternative Fuels Energy MSc program within project "Environmental Impact and Thermoeconomic Evaluation in Energy Sector". Work was conducted under the direction of Lucyna Czarnowska, PhD.

References

[1] SWANA, https://swana.org/Portals/0/Awards/2017/Winners/Excellence2017-WtE-gold.pdf, (05/12/217).
[2] Ray Schauer, https://www.google.pl/url?sa=t&rct=j&q=&esrc=s&source=web&cd=2&cad=rja&uact=8&ved=0ahUKEwiXnfyxgf_XAhXGAsAKHfhXBPIQFgg5MAE&url=http%3A%2F%2Fwww.iswa.org%2Findex.php%3FeID%3Dtx_bee4mecalendar_download%26eventUid%3D447%26filetype%3Dpublic%26filenum%3D3&usg=AOvVaw29xblizt3_FntPMCSWj11_, (20/11/2017).
[3] J.B. Kitto, *World-Class Technology for the Newest Waste-to-Energy Plant in the United States — Palm Beach Renewable Energy Facility No. 2*, Orlando, Florida, 2016.
[4] Splid Waste Authority of PBC/NCRRF, http://arm-permit2k.dep.state.fl.us/psd/0990234/0000513A.pdf, (01/12/2017).
[5] METSEC, "Encironmental Impacts of Steel", http://www.metsec.com/sustainability/environmental-impacts-of-steel/, (10/03/2017).
[6] Dieselnet, https://www.dieselnet.com/standards/eu/hd.php, (05/12/2017).
[7] J. Merle, "*CEMEX and EU ETS*", CEMEX, Ecoperation Building Solutions.
[8] J. Stubenvoll, S. Bohmer, I. Szendyj *State of the Art for Waste Incineration Plants, Federal Ministry of Agriculture and Forestry*, Vienna, November 2002.

Cellular mechanisms of heavy metals accumulation, detoxification and tolerance in hyperaccumulating plants

Marta Jaskulak[1], Anna Grobelak[1]

[1]Faculty of Infrastructure and Environment, Czestochowa University of Technology, e-mail: martajaskulak@gmail.com,agrobelak@is.pcz.pl

Abstract

Pollution on soils with heavy metals is a consistently rising problem worldwide. The major contribution to this problem are industrial activities such as mining and manufacturing. Industrial waste can make soil unsuitable for use for a long time by lingering at the surface of soil. Second biggest contribution includes agricultural activities. Most pesticides and other chemicals used in agriculture degrade slowly and cannot be decomposed naturally, resulting in their long-lasting presence in environment. As a result they can seep into the deeper layers of the soil and pose threat to groundwater reservoirs. Paper summarizes present knowledge about plants responses to contamination with heavy metals and their ability to accumulate metals that can be used in phytoextraction process for extraction of pollutants from contaminated soil. The principal mechanisms reviewed are: stress proteins including peroxidases, superoxide dismutase and content of proline, phytochelatin based sequestrations, metallothioneins, production of ethylene, mechanisms for cell wall immobilization etc.

Keywords: Phytoremediation, heavy metals, soil pollution, toxicity, plant stress

1. Introduction

Soil contamination with heavy metals is a continuously increasing problem worldwide that creates numerous threats to human health by its influence on crop production, and quality of groundwater and crops (Table 1.) [1]. Heavy metals are the most spread group of inorganic pollutants mostly due to anthropogenic activities such as manufacturing, use of synthetic fertilizers in agriculture and car emissions. Metal concentrations in soil range from even less than one to as high as 100000 mg kg-1 [2,3]. Accumulation of metals such as Lead (Pb), Chromium (Cr), Nickel (Ni) can seep through food chain and cause DNA damage due to their mutagenic abilities which can lead to carcinogenic changes in bodies of animals and humans. Since long-term persistence of heavy metals in the environment causes a threat to human health and crop production, technologies involved in remediation of contaminated areas gained an importance [4,5].

Phytoremediation, is wildly accepted technology used in remediation of contaminants from soil by use of hyperaccumulating plants. Proper identification of suitable plant species for this process is one of the most important step influencing efficiency of the process. Such plants are characterized by their remarkable biochemical mechanisms like an ability to accumulate and translocate metals in their cells [6].

As most other stress factors, heavy metals induce oxidative stress by disrupting metabolic chains. This leads to the imbalance in reactive oxygen species (ROS) generation and neutralization [6]. In normal conditions ROS such as superoxide radicals, singlet oxygen, hydrogen peroxide and hydroxyl radicals are removed by antioxidants (ascorbate, glutathione, α-Tocopherol, carotenoids) or enzymes such as superoxide dismutase (SOD), catalase (CAT) and peroxidases (POD, GPX, APX) [7]. Overflow of ROS, that cannot be properly neutralized by antioxidative system, cause damage in proteins and DNA. Toxic effects of that imbalance accumulates in cells and leads to plants death [5,8]. Activity of those enzymes can be used to determine stress levels and also to determine environment toxicity long before any visible impact on growth appears. Such assay may be an useful tool in the environmental engineering, for example as an indicator in phytoremediation efficiency or in order to determinate severity of soil pollution. Artificial increase in the rate of ROS

neutralization may lead to an increase in yield quality and enable some species to be cultivated outside their native climates [9].

Tab. 1 Toxic effects induced by metals [6,7,8]

Metal	Effects
Uranium, cadmium, zinc, copper	Decrease in photosynthesis efficiency, decrease in chlorophyll content, chlorosis, changed ration of *a* and *b* chlorophyll
Aluminum, cadmium, copper	Decrease and even total inhibition of roots elongation, increase in volume of cortex
Cadmium, lead, aluminum	Peroxidation of membranes that leads to change in lipids composition and membrane leakage
Cadmium, uranium lead	Decrease in presence of essential micronutrients like iron, calcium or magnesium

2. Hyperaccumulation of heavy metals

Hyperaccumulation of heavy metals in plants occurs when concentration of a metals reaches to >0.1-1% of dry weight. Plant species known as hyperaccumulators. Can survive relatively contamination with metals and store metal ions in their cells and are characterized by their extraordinary abilities to absorb and accumulate metals [7]. Almost all species possess some abilities for metal tolerance based on 3 main processes: exclusion, chelation and sequestration. In current years nearly 400 of plant species have been reported as a hyperaccumulators for heavy metals [7,8].

Mechanisms of metals hyperaccumulation in plants is a complex phenomenon which involves many steps, starting with transport of metals from soil to root cells, translocation in xylem and finally sequestration and detoxification of metals in plans cells [9,10].

High efficiency in processes like sequestration and detoxification are a key property that allows hyperaccumulators to concentrate heavy metals in cells without phytotoxic effects. These elements are highly involved in homeostasis of essential metal micronutrients. Mechanisms of detoxification and sequestration in aerial organs consist mostly in complexation of heavy metals with ligands and transport to vacuoles and cell walls [11,12].

3. Influence of heavy metals on plants cells

When heavy metals enter cells cytoplasm, they are immediately bound with appropriate cellular compound which allows avoidance of toxic metal ions [13]. An example of metal chelators are organic acids such as citrate and nicotianamine (NA) which exhibits high stability for both binding and translocation of metals. In hyper-accumulating plants, concentration of NA is much higher than even in highly related species of non-accumulators [14]. Histidine has a major role in chelation of nickel and another amino acid – proline is probably involved in heavy metal chelation although the mechanisms of that role are still unknown [15].

Glutathione (GSH) is a low molecular weight chelator that can create complex formations with heavy metals which are necessary for induction of phytochelatin. Previous studies showed a direct link between overexpression of GSh and an increase in heavy metals tolerance in Arabidopsis thaliana which suggest lowering of oxidative stress caused by toxic concentrations of heavy metals by GSH [16].

Overexpression and overproduction of chelators like citrate, phytochelatins, metallothioneins, phytosiderophores or an overexpression of metal transporters leads to an increase in both tolerance and accumulation of metals in plants. Among all chelators, Metallothioneins (MT) and Phytochelatins (PCS) are widely studied in recent years [16,17].

Metallothioneins (Mts) are proteins containing sulfur with highly flexible structure. Flexibility allows for different coordination geometers to bind with different metals. MTs are divided into three main classes: first one – MT1 consist of polypeptides closely related to mammals and is characterized by the lack of aromatic amino acids and histidine's. Type 2 of metallothioneins was firstly discovered in yeasts and cyanobacterias. Saccharomyces cerevisiae Mt2, contributes to plant's tolerance of copper. Phytochelatins belong to the thing

class of MT and were identified in a vast number of plant species including dicots, monocots, gymnosperms and algae. Heavy metals such as Pb, Cd, Hg, Zn can induce synthesis of metalotionein genes in plants and animals. Cadmium is the most powerful activator of MT genes in plants. Mt1 genes are expressed mostly in the roots and Mt2 in shoots of plants [18].

As mentioned before, overexpression of chelators can lead to an increase in tolerance and accumulation of heavy metals. One study showed that, accumulation of cadmium in tobacco can be increased when plants have the transgenes coding chelator – polyhistidine. Introducing metalotionein gene in tobacco also improved the tolerance of plant to Ni, Cd and Zn contamination. An increase in metal uptake, mostly for Fe, Cd, Mn and Zn was also observed in plants characterized with overproduction of ferritin through genetic modification. In transgenic *Brassica juncea* L., overexpression of ferratin, gamma-glitamylcsteine synthetase and glutathione synthetase caused higher accumulation of various metals – Cd, Cr and even Pb, in mixes or alone (Table 2)[19,20].

Defense mechanisms based on antioxidant response to heavy metals keep formation of ROS at a low level. Still, contamination disrupts the balance between creation and detoxification of free radicals. Plant cells possess a wide range of antioxidant network based on non-enzymatic antioxidant's such as glutathione, ascorbate as well as enzymatic antioxidants like catalase (CAT), superoxide dismutase (SOD), peroxidase (POD) or glutathione reductase (GR). Accumulation of heavy metals can change the activity of those enzymes in a species-specific way. One example is cadmium accumulator – *Targets erecta* which exhibits an decrease in activity of SOD and CAT when exposed to cadmium but another Cd accumulator: *Avena strigose* showed an increase in activity of those enzymes when exposed to cadmium. Similar results occur in other plant species therefore patterns between enzyme activity are strictly specific for each species and should be taken into consideration when testing imbalance in oxidative stress induced by heavy metals [21].

Tab. 2 Some examples of hyperaccumulators [21,22,23]

Plant species	Metal	Bioaccumulation
Berkheya coddii	Ni	5500
Eichronia crassipes	Cr	6000
Sesbania drummondii	Cd	1700
Thlaspi caerulescens	Zn	20000
Thlaspi caerulescens	Cd	80
Brassica juncea	Ni	4000
Sorghum sudanense	Cu	5330

3.1 Targets of metal toxicity in plants

All metal binding molecules including metalloproteins are direct targets of heavy metals. Metalloproteins contain metals in their molecular structure which can be substituted by toxic metal. One example of such phenomenon is replacement of magnesium by zinc, cobalt or nickel in RuBisCO (ribulose-1,5-bisphosphate-carboxylase/oxygenase that is a key protein for photosynthesis. Ions of cadmium can interfere with the homeostasis of zinc and calcium which are essential macronutrients. Iron molecules present in ferritin can be replaced even by uranium (Table 3) [23].

Tab. 3 Examples of metal substitution in metalloproteins [24,25]

Toxic metal	Native metal	Protein
Cd, Mn, Pb, Zn	Mg	RuBisCO
U, Al, Pb	Fe	Ferritin
Zn	Ca	Endonuclease
Pb, Cd	Ca	Calmodulin
Cd	Mn	Oxygen evolving complex in photosystem II

3.2 Transport

When heavy metals enter plants cells a wide range of coping strategies occurs. One of them, is transporting metal ions out of the cell or to sequestrate it into vacuole in order to remove the contaminant form places with sensitive metabolic activi-ties. Vacuoles are suitable reservoir for excessive accumulation of heavy metals. Metal transporters play crucial role in protection of plant cells from phytotoxic effects induced by metals and in maintenance of the homeostasis. There are several classes of metal transporters in plants. Main ones include ATPases, Nramps, ZIP family, CDF's and finally ABC transporters. Overexpression of genes coding different types of transporters is often observed in hyperaccumulators [26,27].

4. Conclusions

Soil degradation becomes a rising threat to world agriculture. First global scale assessment in 1999 indicated that about 15% of global land area is affected by human induced degradation [1]. More recent studies revealed growth of that percentage to about 24% and about 19% of that area is used to produce food [2]. One of most notable soil contaminants around the world are heavy metals that not only decrease yield of crops but also can accumulate in biomass and pose a threat to humans and livestock [3–5]. Like many other abiotic stress factors, heavy metals induce oxidative stress by interrupting cell metabolism. Improper flow of ions leads to excess of reactive oxygen species (ROS) [6]. With no stress factors present ROS (superoxide and hydroxyl radicals, singlet oxygen and hydrogen peroxide) are also produced, but in amounts low enough to be quickly neutralized by antioxidants (glutathione, ascorbate, αTocopherol, carotenoids) or enzymes - superoxide dismutase (SOD), catalase (CAT) and peroxidases (POD, GPX, APX) [7]. ROS that are not removed in time may cause oxidative damage to nucleic acids and proteins, ultimately leading to cell death [8, 9]. Assesment of activity of enzymes such as GPX or SOD may be viable way to determine stress levels and in consequence to assay environment toxicity. As phytotoxicity is traditionally evaluated in tests involving seed germination, result accuracy is limited due to many factors that are hard to control and foresee without extensive pretesting, such as seed genetic variability and natural tendency to sprouting [10,11].

Due to a rising problem of soil pollution with heavy metals in recent years special focus is putted on further development of quick but highly sensitive, plant stress detection methods that will allow to both: determinate the severity of contamination and possible options of phytoremediation as well as a indicator of efficiency of this phytoremediation processes. Further knowledge about plants ability to tolerate, ac-cumulate and detoxification metal irons is necessary for several purposes: (i) enhancing accumulation of metals that are microelements for nutritional purposes, (ii) for cleaning up contaminated soils, (iii) to mine rare metals which can be accumulated in plants, (iv) to predict health risk induced by metal accumulation in crops [28,29].

Areas with heavy metal-polluted soils are increasing significantly throughout the world, as a result of industrialization, mining operations, improper waste and water treatment [18,10,19]. It is widely known that heavy metals cause abiotic stress that results in plants improper development, lower yield and in high concentrations cause plant death. It was found that soon after exposure to heavy metals, metabolism of ROS gets altered and oxidative stress is induced [8,3].

Further knowledge on biochemical and physiological responses of plants to stress helps develop new strategies for purification of contaminated areas and overall improvement of the environment. In transgenic plants, capacity of metal uptake, transport and detoxification can be altered therefore, finding a suitable species with extraordinary antioxidant mechanisms is a key point in success of process. Overexpression of specific genes such as phytochelatin and metallothioneins is directly connected to heavy metal stress. Moreover, the role of miRNA and HSPs in plants stress tolerance induced by heavy metals is still unknown [30,31].

Acknowledgment

Research funded from internal grant BS PB 401/304/11.

References

[1] E. Agostini, M.S. Coniglio, S.R. Milrad, H.A. Tigier, A.M. Giulietti. Phytoremediation of 2,4-dichlorophenol by Brassica napus hairy root cultures. *Biotechnol Appl Biochem*, 2003, pp. 252-271.

[2] E.L. Arthur, P.J. Rice, T.A. Anderson, S.M. Baladi, K.L. Henderson, J.R. Coats. Phytoremediation—An overview. *Crit Rev Plant Sci*, 2005, 24, pp. 109–122.

[3] R. Boominathan, P.M. Doran. Ni-induced oxidative stress in roots of the Ni hyperaccumulator, Alyssum bertolonii. *New Phytol*, 2002, 156, pp. 205–215.

[4] H.H. Harms. In-vitro systems for studying phytotoxicity and metabolic fate of pesticides and xenobiotics in plants. *Pestic Sci*, 1992, 35, pp. 277–281.

[5] T. Lebeau, A. Braud, K. Jezequel. Performance of bioaugmentationassisted phytoextraction applied to metal contaminated soils. *Environ Pollut*, 2008, 153, pp. 497–522.

[6] T.V. Nedelkoska, P.M. Doran. Characteristics of heavy metal uptake by plant species with potential for phytoremediation and phytomining. *Minerals Eng*, 2000, 13, 549–561.

[7] C. Lodewyckx, S. Taghavi, M. Mergeay, J. Vangronsveld, H. Clijsters, D. Van der Lelie. The effect of recombinant heavy metal-resistant endophytic bacteria on heavy metal uptake by their host plant. *Int J Phytoremed*, 2001, 3, pp. 173–187.

[8] L. Van Nevel, J. Mertens, K. Oorts, K. Verheyen. Phytoextraction of metals from soils: How far from practice? *Environ Pollut*, 2007, 150, pp. 34– 40.

[9] J.O. Coleman, M.M. Blake-Kalff, T.G. Davies. Detoxification of xenobiotics by plants: Chemical modification and vacuolar compartmentation. *Trends Plant Sci*, 1997, 2, pp. 144–151.

[10] P. Schroder, C.E. Scheer, F. Diekmann, A. Stampfl. How plants cope with foreign compounds: Translocation of xenobiotic glutathione conjugates in roots of barley (Hordeum vulgare). *Environ Sci Pollut Res*, 2007, 14, pp. 114–122.

[11] M. Alexander. Aging, bioavailability, and overestimation of risk from environmental pollutants. *Environ Sci Technol*, 2000, 34, pp. 4259–4265.

[12] J.G. Burken, J.L. Schnoor. Predictive relationships for uptake of organic contaminants by hybrid poplar trees. *Environ Sci Technol*, 1998, 32, pp. 3379– 3385.

[13] A.G. Groeger, J.S. Fletcher. The influence of increasing chlorine content on the accumulation and metabolism of polychlorinated biphenyls (PCBs) by Paul's Scarlet rose cells. *Plant Cell Rep*, 1998, 7, pp. 329–332.

[14] R. Nakazawa, Y. Kameda, T. Ito, Y. Ogita, R. Michihata, H. Takenaga. Selection and characterization of nickel-tolerant tobacco cells. *Biol Plant*, 2004, 48, pp. 497–502.

[15] T. Yoshihara, K. Tsunokawa, Y. Miyano, Y. Arashima, H. Hodoshima, K. Shoji, H. Shimada, F. Goto. Induction of callus from a metal hypertolerant fern, Athyrium yokoscense, and evaluation of its cadmium tolerance and accumulation capacity. *Plant Cell Rep*, 2005, 23, pp. 579–585.

[16] L. Chroma, M. Mackova, P. Kucerova, C. In der Wiesche, J. Burkhard, T. Macek. Enzymes in plant metabolism of PCBs and PAHs. *Acta Biotechnol*, 2002, 22, pp. 35–41.

[17] S. Khaitan, S. Kalainesan, L.E. Erickson, P. Kulakow, S. Martin, R. Karthikeyan, S.L. Hutchinson, L.C. Davis, T.H. Illangasekare, C. Ngoma. Remediation of sites contaminated by oil refinery operations. *Environ Prog*, 2006, 25, pp. 20–31.

[18] R. Boominathan, P.M. Doran. Cadmium tolerance and antioxidative defenses in hairy roots of the cadmium hyperaccumulator, Thlaspi caerulescens. *Biotechnol Bioeng*, 2003, 83, pp. 158–167.

[19] S. Eapen, K.N. Suseelan, S. Tivarekar, S.A. Kotwal, R. Mitra. Potential for rhizofiltration of uranium using hairy root cultures of Brassica juncea and Chenopodium amaranticolor. *Environ Res*, 2003, 91, 127–133.

[20] L. Garnier, F. Simon-Plas, P. Thuleau, J.P. Agnel, J.P. Blein, R. Ranjeva, J.L. Montillet. Cadmium affects tobacco cells by a series of three waves of reactive oxygen species that contribute to cytotoxicity. *Plant Cell Environ*, 2006, 29, pp. 1956–1969.

[21] T.V. Nedelkoska, P.M. Doran. Hyperaccumulation of cadmium by hairy roots of Thlaspi caerulescens. *Biotechnol Bioeng*, 2000, 67, pp. 607–615.

[22] T.V. Nedelkoska, P.M. Doran. Hyperaccumulation of nickel by hairy roots of Alyssum species: Comparison with whole regenerated plants. *Biotechnol Prog*, 2001, 17, pp, 752–759.

[23] H. Azevedo, C.G.G. Pinto, C. Santos. Cadmium effects in sunflower: Membrane permeability and changes in catalase and peroxidase activity in leaves and calluses. *J Plant Nutr*, 2005, 28, pp. 2233–2241.

[24] V. Van Sint Jan, C. Costa de Macedo, J.M. Kinet, J. Bouharmont. Selection of Al-resistant plants from a sensitive rice cultivar, using somaclonal variation, in vitro and hydroponic cultures. *Euphytica*, 1997, 97, pp. 303–310.

[25] L.A. Schaider, D.R. Parker, D.L. Sedlak. Uptake of EDTA-complexed Pb, Cd and Fe by solution- and sand-cultured Brassica juncea. *Plant Soil*, 2006, 286, pp. 377–391.

[26] T.V. Nedelkoska, P.M. Doran. Hyperaccumulation of nickel by hairy roots of Alyssum species: Comparison with whole regenerated plants. *Biotechnol Prog*, 2001, 17, pp. 752–759.
[27] E. Olmos, J.A. Hernandez, F. Sevilla, E. Hellin. Induction of several antioxidant enzymes in the selection of a salt-tolerant cell line of Pisum sativum. *J. Plant Physiol*, 1994, 144, pp. 594–598.
[28] H. Kupper, E. Lombi, F.J. Zhao, S.P. McGrath. Cellular compartmentation of cadmium and zinc in relation to other elements in the hyperaccumulator Arabidopsis halleri. *Planta*, 2000, 212, pp. 75–84.
[29] M. Mackova, T. Macek, P. Kucerova, J. Burkhard, J. Pazlarova, K. Demnerova. Degradation of polychlorinated biphenyls by hairy root culture of Solanum nigrum. *Biotechnol Lett*, 1997, 19, pp.787–790.
[30] D.G. Davis, R.H. Hodgson, K.E. Dusbabek, B.L. Hoffer. The metabolism of the herbicide diphenamid (N-N-dimethyl-2,2-diphenyl-acetamide) in cell suspensions of soybean (Glycine max). *Physiol Plant*, 1978, 44, pp. 87–91.
[31] S. Eapen, KN Suseelan, S Tivarekar, SA Kotwal, R Mitra. Potential for rhizofiltration of uranium using hairy root cultures of Brassica juncea and Chenopodium amaranticolor. Environ Res 91:127–133, 2003.

Biosorption of Crystal Violet - A review

Naureen Khanam [1], Onyebuchi Ofili [1]

[1]Faculty of Energy and Fuels, AGH University of Science and Technology, email: naureen.khanam@gmail.com, onyebuchiofili@gmail.com

Abstract

The present article presents review of use of low cost boisorbents for the removal of Crystal Violet (CV) dye from waste water. Adsorption technique is the most attractive separation technique among all the physio-chemical processes. Activated carbons used for the dye removal commercially are meant to be replaced by biosorbents because of its low cost and availability. Extensive researches are going on for the removal of dye from textile, printing, pharmaceutical and other industries waste water. Crystal violet removal has been indicated in many researcher's report. This article is based on some literature that focuses on agricultural waste, biomass and carbon formation from biomass for the removal of CV from waste water.

Keywords: Crystal Violet (CV), biosorbent, adsorption capacity, waste water, dye removal

1. Introduction

Water is one of the main three constituents of earth and it is vital for all known forms of life. Water covers 71% of the earth's surface and about 65% of human body contains water. Only 0.25% of the freshwater on Earth is contained in river systems, lakes and reservoirs, which are the water we are most familiar with and the most accessible water source to satisfy human needs in our daily lives. But fresh water has already become a limiting resource in many parts of the world. [1] Rapid industrialization, population explosion, climate change will cause this limitation unbearable in future. In this context, protection of natural water resources and development of new technologies for water and wastewater treatment have become key environmental issues of the 21st century.

Dye pollutants are a major source of environmental contamination and color is the first contaminant to be recognized in waste water [2]. Dyes may be defined as substances that, when applied to a substrate provide color by a process that alters, at least temporarily, any crystal structure of the colored substances [3] [4] The presence of very small amounts of dyes in water (less than 1 mg/L for some dyes) is highly visible and undesirable [2]. Colored dyes are not only aesthetic, carcinogenic but also hinder light penetration and disturb life processes of living organisms in water [5].

Crystal violet or gentian violet (also known as methyl violet 10B or hexamethyl pararosaniline chloride) is a triarylmethane dye. The chemical formula is $C_{25}N_3H_{30}Cl$. This is a well-known cationic dye.

Crystal violet itself was first synthesized in 1883 by Alfred Kern (1850–1893) working in Basel at the firm of Bindschedler and Busch [6]. Crystal violet also shows photo-degradation characteristics in presence of UV light [7] Crystal violet is used for various purposes: a biological stain, a dermatological agent, a veterinary medicine, an additive to poultry feed to inhibit propagation of mold, intestinal parasites and fungus etc. It is also extensively used in textile dying [8], paint and printing inks [9]. Crystal violet has antibacterial, antifungal, and anthelmintic properties and was formerly important as a topical antiseptic. The medical use of the dye has been largely superseded by more modern drugs, although it is still listed by the World Health Organization.

The dye has been found to have cytotoxic and carcinogenic effects on mammalian cells and can also cause severe damage to the cornea and conjunctiva[9].Some triphenylmethane dyes, including CV, are potent clastogens, possibly responsible for promoting tumor growth in some species of fish[10].

Among all the physio-chemical treatment methods, adsorption has been recognized as an attractive separation technique for the removal of dyes from wastewater because of its low cost, simple design and high

efficiency. One of the most widely used adsorbents is activated carbon because of its large surface area and high adsorption capacity. However, the relatively high cost and difficult regeneration of activated carbon restrict its use in industrial wastewater treatment. This limitation has encouraged the search for inexpensive and readily available adsorbents for the removal of dyes, such as natural materials, biosorbents, and waste materials from industrial and agricultural process [8, 11]

This article represents technical feasibility of some low cost biosorbents that is used for CV dye removal from waste water and water. The main theme of this article is to present summary about the use of biosorbents for waste water treatment. An extensive list of adsorbents literature has been compiled. No information about experimental conditions has been included here. Readers are highly suggested to do extensive search in the literature section for any experimental conditions information.

2. Removal of Crystal Violet by Low cost Biosorbent

2.1 Agricultural Solid Waste

The sorption of dye onto agricultural by-products is becoming a potential alternative for inorganic/organic removal from aqueous solution. It is economical, environment friendly, efficient for dye removal and can replace the most widely used commercial activated carbon. Waste materials and raw agricultural solid wastes from forest industries such as leaves, bark and sawdust have been applied as adsorbents for dye removal. Agricultural by-products are available in large quantities around the world, as wastes. These materials may have potential as sorbents due to their physio-chemical characteristics. Recently, many researchers have indicated the effective removal capabilities of various agricultural solid wastes as adsorbents to remove inorganic/organic pollutants including dyes. Table 1 shows the absorption capacities of different agricultural by-products:

Tab.1 Adsorption capacities q_m (mg/g) of raw and waste agricultural by-products

Adsorbents	**Adsorption capacity, q_m (mg/g)**	**References**
Sunflower (*Helianthus annuus* L.) seed hull (SSH)	92.59	[12]
Formosa papaya (*Carica papaya* L.) seed powder (FPSP)	85.99	[13]
Pineapple leaf powder	78.22	[14]
Rice bran	42.25	[15]
Wheat bran	80.37	[15]
Palm kernel fiber	78.9	[16]
Cucumis sativa fruit peel	34.24	[17]
Raw tendu leaves	42.29	[18]
Mangrove plant (*Sonneratia Apetala*) leaf powder (MPLP)	200	[19]
Mangrove plant (*Sonneratia Apetala*) fruit powder (MPFP)	250	[19]
Mango (*Mangifera Indica*) leaf powder (MLP)	200	[19]
Tamarind (*Tamarindus indica*) fruit shell	142.857	[19]

Orange Peel	14.3	[20]
Calotropis procera	4.14	[21]
Cyperus rotundus	54.24	[22]
Citrullus lanatus rind	46.68	[22]
Citrullus lanatus rind	11.9	[23]
Syzygium cumini leaves	38.75	[24]
Treated *Artocarpus odoratissimus* Skin	118	[25]
NaOH- Treated *Artocarpus odoratissimus* Skin	195	[25]
Cocoa (Theobroma cacao) Shell (CSTC)	43.50	[26]
Coir Pith	2.56	[27]
Coir Pith	65.53	[28]
Sawdust	37.83	[28]
Sugarcane Fiber	10.44	[28]
Sugarcane dust	3.8	[29]
Peanut Shell	245.63	[30]
Romanian conifer sawdust (particle size 1 – 2 mm)	12.594	[31]
Romanian conifer sawdust (particle size < 0.1 mm	20.877	[31]
Sagaun sawdust	4.259	[32]
Mansonia wood saw dust	17.7	[33]
Coffee waste	125	[34]
polyphenol-extracted coffee grounds	36.82	[35]
carboxylate-functionalized sugarcane bagasse (SMA)	692.1	[36]

Different agricultural wastes have been used as adsorbent to remove crystal violet such as Palm kernel fiber [16] , Rice bran [15], Pineapple leaf powder [14] , Raw tendu leaves [18], Peanut Shell [30], Orange Peel [20], Coffee waste [34], Sugarcane dust [29], Tamarind (*Tamarindus indica*) fruit shell powder (TFSP) [19], Cocoa (Theobroma cacao) Shell(CSTC) [26], Teak tree (*Tectona Grandis*) bark powder (TTBP) [19]. Table 1 presented the compilation results of various agricultural raw and waste by-products in the removal of crystal violet dye and their adsorption capacity. Among the biosorbents, peanut shell [30] shows 245.63mg/g adsorption capacity which is much higher as an bio adsorbent. Other agricultural products such as Mango leaf powder, Almond tree (*Terminialia cattapa*) bark powder (ATBP), Mangrove plant (*Sonneratia Apetala*) leaf powder (MPLP), Teak tree (*Tectona Grandis*) bark powder (TTBP) shows considerably better adsorption quality.

2.2 Biomass

Removal of CV dye by biomass (dead or living), fungi, algae was the also a concern of recent researches. The use of biomass for wastewater treatment is increasing because of its availability in large quantities at low cost. Due to its physico-chemical characteristics, biomass has a high potential as an adsorbent. Some biomass adsorbent shows higher adsorption density than the commercially available adsorbents. Table. 2 presents the compilation results of various biomass and their maximum adsorption capacities toward CV removal.

Tab. 2 Adsorption capacities q_m (mg/g) of different Biomass

Adsorbents	Adsorption capacity, q_m (mg/g)	References
Powdered mycelial biomass of *Ceriporia lacerata* P2	239.25	[37]
HDTMA-modified *Spirulina sp.*	101.87	[38]
Bacillus amyloliquefaciens biofilm	582.41	[39]
Lentinus edodes CCB-42 immobilized in loofa sponges	381.679	[40]

2.3 Biomass/Solid waste based activated carbon adsorbent

Activated carbon from biomass can be a good replacement for the expensive coal based Activated carbons. The abundance and relatively cheap price of biomass may cause this to be a reliable alternative. The different activation methods, porosity, surface chemistry and pyrolysis temperature may also cause these different biomass based activated carbons to show different adsorption capability. A suitable carbon should possess physical characteristics such as texture, porosity, high surface area. The acid and base character of a carbon also influences the nature of the dye isotherms. The adsorption capacity depends also on the accessibility of the pollutants to the inner surface of the adsorbent, which depends on their sizes[41]. Tab. 3 displays the compilation of various activated carbon from biomass/agricultural solid waste and their maximum adsorption capacity towards CV removal.

Tab. 3 Adsorption capacities q_m (mg/g) of activated carbons from biomass/agricultural solid waste by product

Adsorbents	Adsorption capacity, q_m (mg/g)	References
Phosphoric acid activated carbons(PAAC) from male flowers of coconut tree	60.42	[42]
Sulfuric acid activated Carbon(SAAC) from male flowers of coconut tree	85.8	[42]
Nanoporous carbon from tomato paste waste (TWNC)	68.97	[43]
Ricinus Communis Pericarp Carbon	48.0	[44]
Jute fiber carbon	27.99	[45]
sulfuric acid activated Rice husk	64.875	[46]
Zinc chloride activated Rice husk	61.575	[46]

Nanoporous carbon from tomato paste waste (TWNC) [43], Sulfuric acid activated Rice husk [46], Sulfuric acid activated Carbon (SAAC) from male flowers of coconut tree [42], Phosphoric acid activated carbons (PAAC) from male flowers of coconut tree [42] shows good adsorption capacity among all the mentioned adsorbents. The activated carbon from male flower of coconut tree shows higher adsorption capacity for activation with sulfuric acid than phosphoric acid. So different activation method affects the adsorbent capacity.

3. Conclusions and discussions

The review has attempted to cover some low cost biosorbents that can be used to remove CV from waste water so that readers can get an idea of vast research of low cost biosorbents that can be used for waste water treatment. Adsorption capacity for some biosorbents are much higher. Most of the biosorbents are locally

available, cost efficient. So, these biosorbents proposes benefit for commercially replacement of the coal based activated carbon in future for waste water treatment.

Acknowledgment

One of the authors (Naureen Khanam) is thankful to Md. Akhtarul Islam, Professor, Shahjalal University of Science & Technology, Sylhet, Bangladesh for his cordial support and supervision.

References

[1] N. Ahalya, R. Kanamadi, T. Ramachandra, Biosorption of chromium (VI) from aqueous solutions by the husk of Bengal gram (Cicer arientinum), *Electronic Journal of Biotechnology*, 2005, 8(3), pp. 0-0.
[2] I. M. Banat, P. Nigam, D. Singh, R. Marchant, *Bioresource technology*, 1997, 61, pp. 103-103
[3] K. Othmer. *Encyclopedia of Chemical Technology*, v. 7, 5th Edition. Wiley-Interscience; 2004.
[4] A. Bafana, S. S. Devi, T. Chakrabarti, *Environmental Reviews*, 2011, 19, pp. 350-371.
[5] O'Neill, F. R. Hawkes, D. L. Hawkes, N. D. Lourenco, H. M. Pinheiro, W. Delee. *Journal of Chemical Technology and Biotechnology*, 1999, 74, pp. 1009-1018.
[6] A. Kern. Manufacture of purple dye-stuff, 1883.
[7] G. Favaro, D. Confortin, P. Pastore, M. Brustolon. *Journal of Mass Spectrometry*, 2012, 47, pp. 1660-1670.
[8] S. Chakraborty, S. Chowdhury, P. Das Saha, *Carbohydrate Polymers*, 2011, 86, pp. 1533-1541
[9] P. D. Saha, S. Chakraborty, S. Chowdhury. *Colloids and Surfaces B: Biointerfaces*, 2012, 92, pp. 262-270
[10] Cho BP, Yang T, Blankenship LR, Moody JD, Churchwell M, Bebland FA, Culp SC. Synthesis and characterization of N-demethylated metabolites of malachite green and leuco malachite green, *Chem Res Toxicol*, 2003, 16, pp. 285–294
[11] A. Mittal, J. Mittal, A. Malviya, D. Kaur, V. Gupta. *Journal of Colloid and Interface Science*, 2010, 343, pp. 463-473.
[12] B. H. Hameed. *Journal of Hazardous Materials*, 2008, 154, pp. 204-212.
[13] F. A. Pavan, E. S. Camacho, E. C. Lima, G. L. Dotto, V. T. A. Branco, S. L. P. Dias. *Journal of Environmental Chemical Engineering*, 2014, 2, pp. 230-238.
[14] S. Chakraborty, S. Chowdhury, P. D. Saha. *Applied Water Science*, 2012, 2, pp. 135-141.
[15] X. S. Wang, X. Liu, L. Wen, Y. Zhou, Y. Jiang, Z. Li. *Separation Science and Technology*, 2008, 43, pp. 3712-3731.
[16] G. O. El-Sayed. *Desalination*, 2011, 272, pp. 225-232.
[17] T. Smitha, S. Thirumalisamy, S. Manonmani. *Journal of Chemistry* 2012, 9, pp. 1091-1101.
[18] G. Nagda, V. Ghole. Glutaraldehyde Treated Tendu Waste from Bidi Industry as an Efficient Sorbent for Chromium from Aqueous Solutions, *Global Journal of Environmental Research*, 3(3), pp. 274-279.
[19] S. Patil, V. Deshmukh, S. Renukdas, N. Pate. *International Journal of Environmental Sciences*, 2011, 1, pp. 1116-1134.
[20] G. Annadurai, R.-S. Juang, D.-J. Lee. *Journal of Hazardous Materials*, 2002, 92, pp. 263-274.
[21] H. Ali, S. K. Muhammad. *Journal of Environmental Science and Technology*, 2008, 1, pp. 143-150.
[22] K. S. Bharathi, S. P. T. Ramesh, *Applied Water Science*, 2013, 3, pp. 673-687.
[23] B. K. Suyamboo, R. S. Perumal. *Iranica Journal of Energy & Environment*, 2012, 3, pp. 23-34.
[24] A. Mehmood, S. Bano, A. Fahim, R. Parveen, S. Khurshid, *Korean Journal of Chemical Engineering*, 2015, 32, pp. 882-895.
[25] L. B. Lim, N. Priyantha, T. Zehra, C. W. Then, C. M. Chan, *Desalination and Water Treatment*, 2015, pp. 1-15.
[26] T. Chinniagounder, M. Shanker, S. Nageswaran. *Research Journal of Chemical Sciences* 2011, 1, pp. 38-45.
[27] C. Namasivayam, M. D. Kumar, K. Selvi, R. A. Begum, T. Vanathi, R. Yamuna, *Biomass and Bioenergy* 2001, 21, pp. 477-483.
[28] H. Parab, M. Sudersanan, N. Shenoy, T. Pathare, B. Vaze, *CLEAN–Soil, Air, Water* 2009, 37, pp. 963-969.

[29] S. Khattri, M. Singh, *Adsorption science & technology* 1999, 17, pp. 269-282.
[30] H. A. Begum, M. A. Islam, T. Muslim. *Bangladesh Pharmaceutical Journal* 2015, 17, pp. 163-171.
[31] D. Suteu, D. Bilba, C. Zaharia, A. Popescu. *Scientific Study & Research. IX*, 2008, 3, pp. 293-302.
[32] S. Khattri, M. Singh. *Environmental Progress & Sustainable Energy*, 2012, 31, pp. 435-442
[33] A. E. Ofomaja, Y.-S. Ho. *Bioresource technology* 2008, 99, pp. 5411-5417.
[34] R. Lafi, A. ben Fradj, A. Hafiane, B. Hameed. *Korean Journal of Chemical Engineering* 2014, 31, pp. 2198-2206.
[35] M. D. Pavlovid, A. V. Buntid, K. R. Mihajlovski. S. S. Šiler-Marinkovid, D. G. Antonovid, Ž. Radovanovid, S. I. Dimitrijevid-Brankovid. *Journal of the Taiwan Institute of Chemical Engineers*, 2014, 45, pp. 1691-1699.
[36] B. C. S. Ferreira, F. S. Teodoro, A. B. Mageste, L. F. Gil, R. P. de Freitas, L. V. A. Gurgel. *Industrial Crops and Products*, 2015, 65, pp. 521-534.
[37] Y. Lin, X. He, G. Han, Q. Tian, W. Hu. *Journal of Environmental Sciences* 2011, 23, pp. 2055-2062.
[38] U. A. Guler, M. Ersan, E. Tuncel, F. Dügenci. *Process Safety and Environmental Protection* 2016, 99, pp. 194-206.
[39] P. Sun, C. Hui, S. Wang, L. Wan, X. Zhang, Y. Zhao. *Colloids and Surfaces B: Biointerfaces* 2016, 139, pp. 164-170.
[40] G. G. Gimenez, S. P. Ruiz, W. Caetano, R. M. Peralta, G. Matioli. *World Journal of Microbiology and Biotechnology* 2014, 30, pp. 3229-3244.
[41] G. Crini. *Bioresource technology* 2006, 97, pp. 1061-1085.
[42] S. Senthilkumaar, P. Kalaamani, C. Subburaam, *Journal of Hazardous Materials*, 2006, 136, pp. 800-808
[43] F. Güzel, H. Sayğılı, G. A. Sayğılı, F. Koyuncu. *Journal of Industrial and Engineering Chemistry*, 2014, 20, pp. 3375-3386.
[44] S. Madhavakrishnan, K. Manickavasagam, R. Vasanthakumar, K. Rasappan, R. Mohanraj, S. Pattabhi, Journal of Chemistry 2009, 6, pp. 1109-1116.
[45] K. Porkodi, K. V. Kumar, Journal of Hazardous Materials 2007, 143, pp. 311-327.
[46] K. Mohanty, J. T. Naidu, B. Meikap, M. Biswas, Industrial & engineering chemistry research 2006, 45, pp. 5165-5171.

Effects of Chlorine based refrigerants on atmosphere and search for alternative refrigerants - A review

Muhammad Ferdous Raiyan [1], Omais Abdur Rehman[1]

[1] Silesian University of Technology, e-mail: muhammadferdousraiyan@gmail.com, omais94@gmail.com

Abstract

This article discusses the detrimental effects of CFC (Chlorofluorocarbon) and HCFC (Hydro-Chlorofluorocarbon) based refrigerants on environment, their usage throughout the world and proposes some alternative environment friendly refrigerants. The effects were determined based on two indices known as Ozone Depletion Potential (ODP) and Global Warming Potential (GWP). Both indices were found to be higher for CFC and HCFC based refrigerants. This paper also discusses potentials of various refrigerants and their areas of application in refrigeration and air-conditioning systems. From the literature, it is finally proposed that Hydro-fluorocarbon (HFC) refrigerants are better from environmental perspective to replace CFC based refrigerants. The study describes the selection of refrigerants selected for each utilisation based on the thermodynamic, physical and environmental properties and explores the studies reported with new refrigerants in domestic refrigerators, commercial refrigeration systems and air-conditioners.

Keywords: Refrigerants, ozone layer depletion, chlorofluorocarbon, hydro-fluorocarbon, ODP, GWP

1. Introduction

Chlorine based refrigerants (CFCs and HCFCs) are used in most of air conditioning and refrigeration system for their suitable properties such as stability, non–flammable, good material compatibility and good thermodynamic properties. Refrigerants such as Ammonia, Carbon dioxide, Sulphur dioxide and methyl chloride were used in the late 1800s and early 1900s. All these refrigerants were found to be toxic or hazardous properties, so it is not popular as well as halocarbon. The use of CFCs have been increased rapidly since their selection in the 1930s for their availability and properties. Results from many researches show that ozone layer is being depleted due to the presence of chlorine in the stratosphere. The general consensus for the cause of this is that CFCs and HCFCs are large class of chlorine containing chemicals, which migrate to the stratosphere where they react with ozone. Later, chlorine atoms continue to convert more ozone to oxygen. The discovery of ozone layer's destruction which is a shield for earth against UV radiation, has created concerns all over the world. The CFCs have been banned in developed countries since 1996, and in 2030, producing and using of CFCs will be prohibited completely in the entire world. There is plan to ban partially halogenated HCFC refrigerant in future. Researches are trying for alternative refrigerants which are efficient as well as don't pose a threat to ozone layer. Research has shown that hydrocarbons are good alternative to existing refrigerants.

Technical advancement and economic growth throughout the world during have produced severed environmental problems, and researchers believe that these technological advances may contribute to human comfort but at the same time they also can threaten the environment through ozone depletion and global warming [1-2]. ODP is an index that characterizes the participation of the molecule to the depletion of the ozone layer and can be determined from the molecular structure of a given substance whereas GWP is an index characterizing the participation of the molecule to the greenhouse effect [3]. The ozone depletion potential (ODP) of a chemical compound is the ratio of amount of ozone layer depletion to the amount of depletion caused by trichlorofluoromethane (R-11 or CFC-11) being fixed at an ODP of 1.0. And GWP is a measure of how much energy the emissions of 1 ton of a gas will absorb over a given period of time, relative to the emissions of 1 ton of carbon dioxide (CO2). In 1984 a significant phenomenon was discovered by the British Antarctic Survey, which is called "ozone hole" [4]. During the Antarctic spring in October, when the sun first rises above the horizon, a major, although temporary, loss of stratospheric ozone was observed. Chlorine in the stratosphere by

the CFCs was considered to be the main reason. In 1987 governments negotiated the Montreal Protocol, the first international treaty to protect the global environment [5]. The countries responsible for approximately 95 percent of the world's production capacity for CFCs and halons have signed the Montreal Protocol. Every two years, the parties are required to assess the science, economics, and alternative technologies related to the protection of the ozone layer [6]. Johnson [7] reported that HFC refrigerants are considered as one among the six targeted greenhouse gas under Kyoto protocol of United Nations Framework Convention on Climate Change (UNFCCC) in 1997. Most of the developed countries reduced the production and consumption of halogenated refrigerants, which demands for suitable alternatives. HC and HFC based refrigerants with zero ODP and low GWP are being considered as long term refrigerants. But HC refrigerants have flammability issues, which restrict the usage in existing systems. However, flammability reduction can be done by blending HC refrigerants with HFC refrigerants Yang *et al.* [8]. Formeglia *et al.* [9] reported that, it is possible to mix HC refrigerants with other alternatives such as HFC refrigerants.

2. Destruction of ozone layer by chlorine based refrigerants

The earth's atmosphere is composed of the troposphere and the stratosphere. The troposphere, the lowest part of the atmosphere, extends from the earth's surface to approximately 10 km into space at the equator but less at the polar regions. The stratosphere, which is the layer above the troposphere, extends approximately 50 km into space. The stratospheric layer contains 90 percent ozone. The greatest concentration of ozone is found from 15- 40 km in the stratosphere. This gas layer, which forms a semi-permeable blanket, protects the earth by reducing the intensity of harmful ultra-violet (UV-A), (UV-B) & (UV-C) rays from the sun. UV-A, have the longest wavelengths (320nm-400nm), and are only slightly affected by ozone levels. UV-B (280-325nm), are strongly affected by ozone levels. Decreases in stratospheric ozone mean that more UV-B radiation can reach Earth's surface, causing sunburns, snow blindness, immune system suppression, and a variety of skin problems including skin cancer and premature aging. UV-C (180-280 nm) has the shortest wavelengths, and is very strongly affected by ozone levels. Virtually all UV-C radiation is absorbed by ozone, water vapor, oxygen and carbon dioxide before reaching Earth's surface. Atmospheric layer shown in Figure 1.

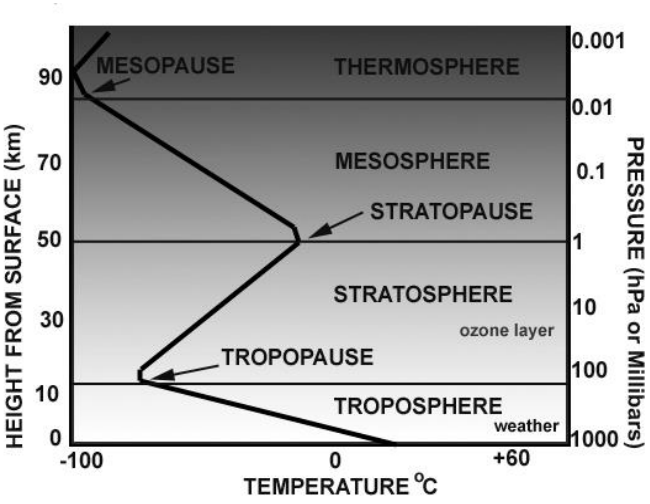

Fig. 1 Atmospheric layer [10]

Ozone is made up of three oxygen atoms. The instability of the molecule allows free oxygen atoms to react easily with nitrogen, hydrogen, chlorine, and bromine. Because CFCs contain a chlorine atom, when they enter the stratosphere, they start to deplete it.

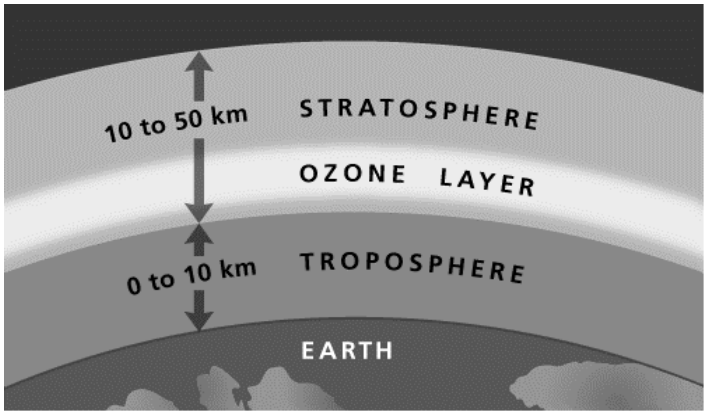

Fig. 2 Atmospheric layer [10]

According the Rowland-Molina theory, each chlorine atom in the stratosphere can destroy 100,000 ozone molecules. This decrease in the amount of ozone in the stratosphere allows more ultraviolet radiation to reach the earth's surface. Reaction in stratosphere can be written as following:

$$O_3 + hv = O_2 + O$$

$$O_2 = O + O$$

$$O_2 + O = O_3$$

Here it is observed that naturally ozone formation is done cyclically. But R22 (Difluoromonochloromethane, CHClF2) refrigerants leaked during the manufacturing and for normal operation or at the time of servicing or repair, mix with surrounding air and rise to troposphere and then into stratosphere due to normal wind or storm. The ultraviolet radiation strikes a HCFC molecule and causes a chlorine atom to break away. The chlorine atom collides with an ozone molecule and steals an oxygen atom to form chlorine monoxide and leave a molecule of ordinary oxygen.

$$\boldsymbol{CHClF_2 + hv = CHF_2 + Cl}$$

$$\boldsymbol{O_3 + Cl = ClO + O_2}$$

$$\boldsymbol{O + ClO = Cl + O_2}$$

There are many CFC and HCFC based refrigerants with high GWP and ODP and causing threat to the atmosphere. Approximate atmospheric lifetime, GWP and ODP of some CFCs and HCFCs are tabulated in Table 1 and Table 2.

Tab. 1 Global warming potential for different CFC compounds [5]

ASHARE code	**Compound**	**Atmospheric lifetime (years)**	**GWP**	**ODP** [11]
CFC-11	CCl_3F	50±5	4000	1
CFC-12	CCl_2F_2	102	8500	1
CFC-113	$CClF_2CCl_2F$	85	5000	0.8
CFC-114	$CClF_2CClF_2$	300	9300	0.1
CFC-115	CF_3CF_2Cl	1700	9300	0.6

Tab. 2 Global warming potential for different HCFC compounds [5]

ASHARE code	**Compound**	**Atmospheric lifetime (years)**	**GWP**	**ODP** [11]
HCFC-22	$CHClF_2$	13.3	1500	0.05
HCFC-123	CF_3CHCl_2	1.4	93	0.012
HCFC-124	CF_3CHClF	5.9	480	0.02-0.04 [12]
HCFC-141b	CH_3CCl_2F	9.4	630	0.11 [12]
HCFC-142b	CH_3CClF_2	19.5	2000	0.065a

3. Prospect of HFC based refrigerant as an alternative for CFC and HCFC

Hydro-Chlorofluorocarbon (HFC) based refrigerants are frontrunners for replacing the CFC and HCFC based refrigerants because of the absence of chlorine content. HFCs are also being used to make blends with HCFC refrigerants. HFCs are non-ozone depleting and the preferred refrigerant in a wide range new refrigeration and air conditioning installations. These refrigerants are non-flammable, safe, easy to use, and energy efficient in the correct application. The choice of refrigerant is usually made by the equipment manufacturer and will be dependent on the application and required operating conditions.

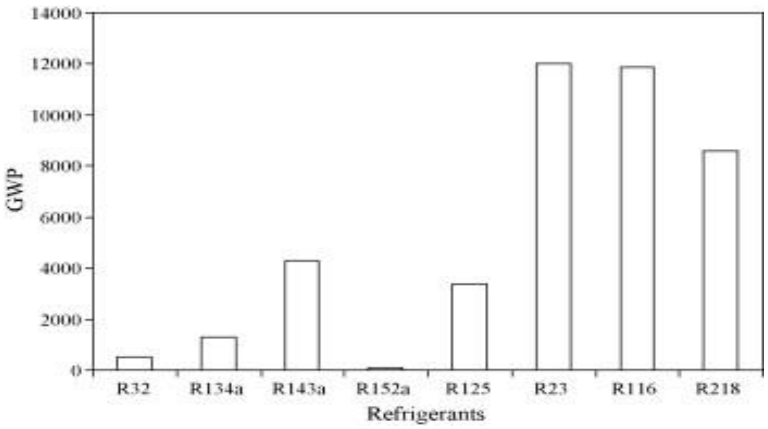

Fig. 3 GWP of some HFC based refrigerants [15]

From Fig.3, GWP of different HFC based refrigerants can be observed. It is found that R-23 and R-116 have a higher GWP which almost reaches upto 12000. Octafluropropane (R-218) has a slightly lower value than the previous ones whereas for other refrigerants the values vary between 500 and 4000.

He *et al.* [13] performed theoretical and experimental investigation with HFC mixture composed of R152a and R125 at different weight ratios with R12 in refrigerator. It has been found that the discharge temperature of the mixture was found to be slightly higher than that of R12. The energy consumption of the domestic refrigerator with optimum proportion 85:15 by weight percentage at 97 gm is 1.156 kWh per day with 2.8–3.2% higher COP than that of R12. The mixed refrigerant R152a/R125 seems to be the long-term alternative to replace R12 as a new generation refrigerant of domestic refrigerators, due to its better environmentally acceptable properties and its favourable refrigeration performance. Hydrocarbon based refrigerants are now also considered. Though they are flammable but non-toxic. The flammability of HC refrigerants can be reduced by blending them with HFC refrigerants Yang *et al.* [14]. The main advantage of HC refrigerants is their solubility with mineral oil, which is traditionally used as a lubricant for chlorine based refrigeration systems. HFCs are composed of substances containing hydrogen, fluorine and carbon chemicals. The HFC gases are used extensively in every

day RAC (Refrigeration and Air Conditioning) systems. There is no current ban upon these gases but responsible use and equipment inspections is mandatory under the "F gas" regulations. The HFC refrigerants have no ozone depletion potential, but do act as a greenhouse gas. Table 3 contains information regarding ODP and GWP for various HFC based refrigerants.

Tab. 3 GWP and ODP for different HFC compounds [16]

ASHARE code	Atmospheric lifetime (years)	GWP	ODP
R23	24.3	14800	0
R32	6-7.3	580	0
R125	32.6	3200	0
R134a	14-15.6	1600	0
R143a	55-64.2	3900	0
R152a	1.5-8	140	0

Thermal and mechanical performance of HFC refrigerants and their blends have also been investigated. HFC and their blends not only gave satisfactory result for environment but also in the vapour compression refrigeration or air conditioning system. Table 4 provides information regarding different performance parameters while using HFC refrigerant in the system.

Tab. 4 Performance result by using R407C as sole substitute for R22 by Devotta *et al.* [17]

Refrigerant	Alternative	System	Findings
R22	R407C	Window A/C	Cooling capacity was lowered from 2.1 to7.9%
			High power consumption (6–7%)
			Low COP by 8.2% to 13.6%
			Evaporator capacity was decreased by 3.3–6%

Using hydrocarbons (HC) along with HFCs has come out as a prospective alternative refrigerant. Different research works have been performed so far to check the feasibility of these blends. Jabraj et al. [18] performed experiment on window air conditioning system by using blends of R407C and HC. It gave much better result than only R407C and it's tabulated in Table 5 and 6.

Tab. 5 Performance result by using the blend of R407C and HC refrigerant.

Refrigerant	Alternative	System	Findings
R22	R407C/20% HC	Window type A/C	5–10.5% lower energy consumption with 8–11% higher COP
			9.5–12.5% higher refrigeration capacity

Tab. 6 Performance result by using the blend of R407C and HC refrigerant.

Refrigerant	Alternative	System	Findings
R22	R407C/20% HC	Window type A/C	Pull-down time was lower than that of R22 by about 32.51%
			3.7–11.46% higher discharge pressure

The coefficient of performance (COP) of a refrigeration cycle reflects the cycle performance and is the major parameter while selecting a new refrigerant. Fig. 4 shows the variation of COP with varying ambient air temperature for the investigated refrigerants. COP obtained using R507 in the system was higher than those of R22 and R404A at all ambient air temperatures. The lowest COP was obtained using R404A. Compared with R22, the average COP of R507 increased by 10.6%, while that of R404A reduced by 16.0% [19].

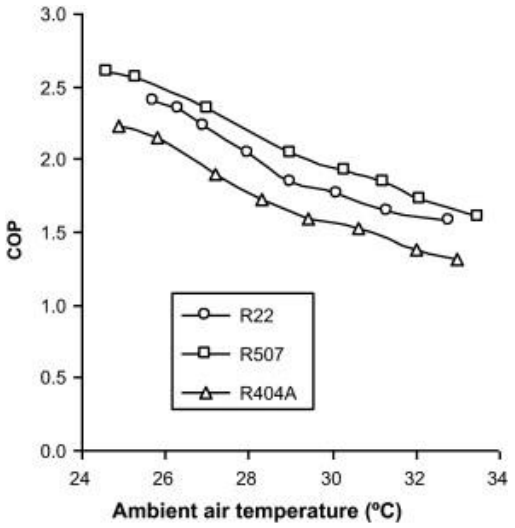

Fig. 4 Variation of COP with ambient temperature for different refrigerants [19].

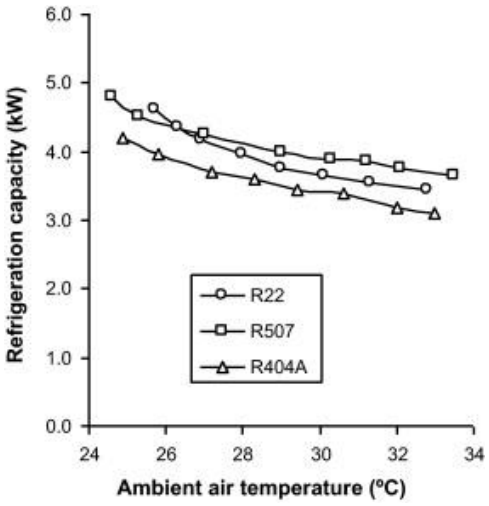

Fig. 5 Refrigeration capacity vs. ambient air temperature [19]

Among the refrigerants, R507 exhibited the maximum refrigeration capacity. Behaviour of R 507 was found to be close to that of R22 and had an average refrigeration capacity of 4.7% higher than that of R22. But refrigeration capacity for R404A was 8.4% lower than that of R22. Besides, energy consumption varied depending on the type of refrigerant. Among the refrigerants, R404A has the highest energy consumption. The results showed that, comparing to R22, energy consumed by R404A was increased by 13.8% and for R507 it was reduced by 2.0%. Figure 5 and Figure 6 represent the change in cooling capacity and energy consumption respectively.

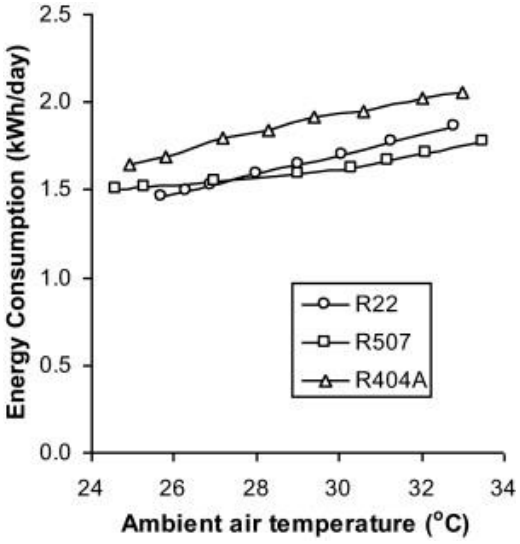

Fig. 6 Change in energy consumption for different refrigerants [19]

4. Conclusions

Due to global warming and other atmospheric problems, it is now extremely important to minimize the detrimental effects by adopting new, alternative, suitable and eco-friendly refrigerants. As discussed in the article, finding new refrigerants sometimes becomes quite challenging due to different things such as proper thermophysical properties, flammability issue and solubility with the lubricant oil. The article discussed how ozone layer is depleted and presented two measuring indices (GWP and ODP) to address this problem. GWP was found to be higher for all CFC based refrigerants whereas significantly lower for HCFC refrigerants. On the other hand, moderate rise has been experienced for HFC refrigerants compared to the HCFCs. HFC has zero ODP thus making it a suitable refrigerant for protecting ozone layer. While suggesting alternative refrigerants, results from the literature show that HFC (R 407C) and HC mixture exhibited a better performance in terms of COP and refrigeration capacity. R 507 (HFC) also showed better result than R22 and R404A as it consumed less electric power and at the same time refrigeration capacity and COP were also increased.

References

[1] Y. Hwang, M. Ohadi, R. Radermacher. Natural Refrigerants, Mechanical Engineering, *American Society of Mechanical Engineers*, 1998, 120, pp. 96-99.

[2] BO. Bolaji. Selection of environment-friendly refrigerants and the current alternatives in vapour compression refrigeration systems, *TRGJSM Journal of Science and Management*, 2011, 1, pp. 22-26.

[3] S. Benhadid-Dib, A. Benzaoui. Refrigerants and their environmental impact Substitution of hydro chlorofluorocarbon HCFC and HFC hydro fluorocarbon. Search for an adequate refrigerant, *Energy Procedia*, 2012, 18, pp. 807-816.

[4] JC. Farman, BG. Gardiner, JD. Shanklin. Large Losses of Total Ozone in Antarctica Reveal Seasonal ClOx/NOx Interaction, *Nature*, 1985, 315, pp. 207-210.

[5] RL. Powell, CFC phase-out: have we met the challenge?, *Journal of Fluorine Chemistry*, 2002, 114(2), pp. 237-250.
[6] L. Mattarolo. Refrigerants and environment protection, *I. Ulusal Sogutma ve Iklimlendirme Sempozyumu*, Istanbul, Turkey, 1990, pp. 51-70.
[7] E. Johnson. Global warming from hfc, *Environmental Impact Assessment Review*, 1998, 18(6), pp. 485-492.
[8] Z. Yang, B. Liu, H. Zhao. Experimental study of the inert effect of R134a and R227ea on explosion limits of the flammable refrigerants, *Experimental Thermal and Fluid Science*, 2004, 28, pp. 557-563.
[9] M. Formeglia, A. Bertucco, S. Brunis. Perturbed hard sphere chain equation of state for applications to hydroflurocarbons, hydrocarbons and their mixtures, *Chemical Engineering Science*, 1998, 53, pp. 3117-3128.
[10] https://www.google.com/search?q=atmospheric+layers&tbm, (15/11/2017).
[11] https://www.epa.gov/ozone-layer-protection/ozone-depleting-substances, (15/11/2017).
[12] http://web2.unep.fr/hcfc/about/default.aspx?type=list, (15/11/2017).
[13] M.-G. He, T.C. Li, Z.-G. Liu, Y. Zhang. Testing of the mixing refrigerant HFC152a/HFC125 in domestic refrigerator, *Applied Thermal Engineering*, 2005, 25, pp. 1169-1181.
[14] M.Mohanraj, S .Jayaraj, C.Muraleedharan. Environment friendly alternatives to halogenated refrigerants—A review, *International Journal of Greenhouse Gas Control*, 2009, 3(1), pp. 108-119.
[15] M. Calm, G.C. Hourahan. Refrigerant data summery, *Engineering Systems*, 2001, 18, pp. 74-88.
[16] I. Sarbu. A review on substitution strategy of non-ecological refrigerants from vapour compression-based refrigeration, air-conditioning and heat pump systems, *International Journal of Refrigeration*, 2014, 46, pp. 123-141.
[17] S. Devotta, A.S. Padalkar, N.K. Sane. Performance assessment of HCFC-22 window air conditioner retrofitted with R-407C, *Applied Thermal Engineering*, 2005, 25, pp. 2937-2949.
[18] D.B. Jabaraj, P. Avinash, D. Mohanlal, S. Renganarayanan. Experimental investigation of HFC407C/HC290/HC600a mixture in window air conditioner, *Energy conservation and Management*, 2006, 48, pp. 3084-3089.
[19] BO. Bolaji. Performance investigation of ozone-friendly R404A and R507 refrigerants as alternatives to R22 in a window air-conditioner, *Energy and Buildings*, 2011, 43(11), pp. 3139-3143.

Bioaugmentation of degraded soils

Aneta Murtaś [1], Joanna Hiller[1], Anna Grobelak[1]

[1]Department of Environmental Engineering, Czestochowa University of Technology, e-mail: anetamurtas@gmail.com

Abstract

Progressive development of variety branches of industry causes increase degradation of soils. The quality of soil is getting worse due to the deposition of pollutants. Moreover, deteriorating soil's quality causes disturbance of ecosystem's harmony and its natural attenuation is significantly longer. There are many ways to improve soil quality. Among them we can mention: cleaning, extraction, thermal treating, chemical oxidation, composting and bioremediation. The most important of them is use of living organisms to accumulate and convert contaminants. This kind of remediation is called bioremediation. Biological processes of soil remediation have many advantages but also some limitations. A lot more opportunities in this field gives bioaugmentation. This process refers to enriching soil with microorganisms which have specific ability to remove pollutants. This technique of pollutants removal from contaminated side allows to use native microflora, microorganisms from site contaminated with the same chemicals and also engineered microorganisms with changed genetic information. Furthermore, because of physiological biodiversity of microbial consortia it is possible to spread out any pollution. This work summarizes the possibility of to using specific species of microorganisms in bioaugmentation process and possibly ways of entering microorganisms to degraded soils.

Keywords: Bioaugmentation, quality of soil, degradation, microorganisms, consortium

1. Bioaugmentation as a kind of soil's bioremediation

Biological process of pollution's decay in soil could be intensified by enriching soil's environment by microorganisms which is called bioaugmentation. In this process inoculum of microorganisms is introduced to the soil. This inoculum contains specific, selected microbes [1]. The characteristic feature of introduced microbe's population is: high resistance to toxic actions of pollution, ability to quick adaptation as well as to contamination degradation [2,3,4,5]. Microbes introduced to a contaminated soil may constitute biomass of microorganism, firstly been isolated from contaminated ground. After isolation from the polluted soil, microorganisms are adapted to the some concentration of pollution [1]. Application of bioaugmentation is specially recommended, where limited or reduced autochthonic population is, which leads to contamination decay. Also, bioaugmentation may be indispensable in the case of contaminated ground with mix of different compounds. In this situation inoculum acclimation and adaptation to decay of toxic substances are significantly more difficult [6].

Bioaugmentation is innovative method of cleaning environment. In some cases, using forest and even sludge to purify agricultural environment in this method are noticed. For example, *Azotobacter* and *Azospirillum* spp. are used in order to intensify growth of yields [6].

Bioaugmentation of contaminated soils could be conducted two ways: firstly, on a contaminated side– *in situ* or secondly, after having transported contaminated ground to controlled conditions- *ex situ. In situ* methods are particularly important when it is not possible to transport contaminated matters. *In situ* bioaugmentation is primarily used on extended surface contaminated ground [7], nevertheless, this strategy is not possible to applicate for each kind of pollutions [3]. On the other hand, *ex situ* bioaugmentation requires placement where polluted ground is put in designed place specially prepare for it. Transport of this material to a controlled conditions place allows to increase bioaugmentation effectiveness. It leads to accelerate soil recultivation process [8]. The choice of bioaugmentation method depends on some factors as pollutant's toxicity and its migration in

environment. For example, *in situ* bioaugmentation is preferred when contaminant does not show high toxicity level and the danger of contaminant migration does not occur.

2. Microorganisms used in bioaugmentation

Living microorganisms plays key role in a bioremediation process. Bacteria, archaea and fungi belonging to the heterotrophic microorganisms are generally used in this method. It is possible to degrade practically each pollution due to the huge biodiversity of physiology, metabolism of microflora living in soil. Microbes show huge ability to the adaptation as well as to use the pollution as an energy source and building substrates [6]. The effectiveness of bioaugmentation depends on the choice of appropriate microorganisms [6,9]. High efficiency of this process can be achieved by using microbes characterized by: short period of generation, high speed of action, high mobility, ability to adhesion and positive chemotaxis to attractant and economic [2,3].

There are several methods of bioaugmentation because of using selected group of microorganisms. We can mention autochthonic, allochthonic and genetic type of bioaugmentation [6]. First of them, autochthonic bioaugmentation (also called as a reinoculation with autochthonic microorganisms) refers to using microorganisms with specific characteristic isolated from contaminated environment and then proliferated under laboratory conditions. Thus, these microbes as an inoculum are introduced to a contaminated soil again [6]. Allochthonic bioaugmentation refers to using microorganisms dwelling in the environment contaminated with similar compound in chemical point view. Allochthonic bioaugmentation is usually called as a bioenriching via participants of science environment [6,10]. Genetic bioaugmentation is the last kind of bioaugmentation and it relies on applicating genetically modified microorganisms. These microorganisms are constructed with genetic engineering methods or by spontaneous and inducted mutagenizes. Genetically modified microorganisms have ability to biodegrade pollutions more efficiently. Furthermore, genetic bioaugmentation might lead to vector's introduction bringing specific genes (usually related with metabolic enzymes production) [6,11,].

2.1 Microorganisms used in purifying soils contaminated with heavy metals

Heavy metals present in the ground inhibit autochthonic microorganisms development and as a result their basic physiological functions are disturbed [3]. Organic compounds decay and transformation are unsettled in special. Thus, matter microflora's activity moreover theirs population are limited as a result of death of sensitive and weak species of microorganisms. However, it also causes resistant to this changes microorganisms proliferation which leads to limit biovariety and enhance these microorganisms resistant to heavy metal. These bacterial strains, which characterized high resistant, are especially using in a process of bioremediation in an environment contaminated with heavy metals [2,3].

Most bacteria such as *Actinomycetes*, yeast and fungi are used in biological recultivation process of green lands polluted with heavy metals [12]. Among them bacteria are the most common used in biosorption processes. Biosorption process refers to removing metals with using microorganisms. It can be leaded by binding metal's ions via polimer's reactive groups (located in cell's guard of microbes). Another way of leading heavy metal's biosorption is immobilizing them on surface of salts, metal complexes or hydroxide characterized by insolubility. The next way is metabolic reactions where final product is secrete.

Therefore, it is shown that heavy metals degradation effectiveness is 10 times longer by Gram (+) bacteria in compare to Gram (-) bacteria [13].

2.2. Microorganisms used in purifying soils contaminated with petroleum

Commonness of petroleum causes more and more environment contamination with petroleum derivates. Getting this substances into the ground could be caused by accident or leak of petrol station's installation located underground. Ground is also contaminated by surface runoff polluted with petroleum substances and melt water from places located near petroleum stations. Polluted soil with this substances can also be caused by targeted introduction to the ground- for example through introduction of petroleum wastewater purified by filter fields [7,14,15].

Mainly, biological decomposition of petroleum substances is led by oxygen bacteria, which use these substances as a source of energy and carbon source. Petroleum carbohydrates decay could be also leading by

fungi. Majority of them decay carbohydrates at co-metabolism pathways, so they need additional basic growth substrate such as glucose or cellulose. Moreover, petroleum contamination decay runs significantly longer in compare to bacteria and what is more, whole mineralization process requires present of some kind of bacteria [9,22]. Anaerobic microorganism could be used for degradation of hydrocarbons like: benzene (*Dechloromonas* RCB and JJ) or toluene (*Geobacter metallidurans, G. grbicium, Thauera aromatica* K172 and I1, *Azoarcus sp.* T, *Dechloromonas* RCB and JJ, *Desulfobacterium cetonicum, D. toluolica*) [16,17,18,19,20]. In additional, it is possible to degrade xylene, hexadecane or naphthalene [13].

There are many petroleum carbohydrates degraded by microorganisms: mainly bacteria and fungi but also some *Cyjanobacteria* and green alga. Among which can be mentioned: *Acetobacter pasterianus, Achromobacter sp., Comamonas sp., Delftia acidovoran, Ochrobactrum anthropic, Sphingobium abikonense, Stenotrophomonas rhizophila, Pseudomonas sp., Micrococcus sp., Chryseomonas luteola, Bacillus sp., Alcaligenes sp., Rhodococcus erythropolis* [21,22,23,24,25]. The most problematic issue is removal PAH and long chain carbohydrates from a soil. To degrade PAH ligninlitic fungi like *Phanaerochaete chrysosporium, Trametes versicolor, Bjerkandera sp., Pleurotus ostreatus* are the most commonly used [26] Long chain carbohydrates degradation is led by *Pseudomonas, Acinetobacter, Arthrobacter, Fusarium Corynebacterium* (also aromatic carbohydrates), *Nocardia, Mycobacterium, Geobacillus* and majority of *Candida* [23,27].

2.3. Microorganisms promoting plant growth

Microorganisms promoting plant growth are commonly used in bioaugmentation. Soil's microorganisms often live in symbiosis with plants causes plant growth promoting. Usually, they live in roots zone called rhizosphere [18]. Rhizosphere-associated microorganisms use plant's exogenous substances as a source of carbon and energy. On the other hand, plant are provided with the products of microorganism's metabolism [28,29]. Among plant growth promoting bacteria (PGPB) we can mention: *Achromobacter, Azospirillum, Enterobacter, Serratia, Streptomyces* spp. and other microbes with high activity in soil contaminated with heavy metals. These bacteria are also called as a rhizobacteria [30,31,32]. Importantly, PGPB group are endophytic bacteria which promote plant growth in adverse environment, in burdensome conditions for plant. These kind of bacteria may penetrate plants' tissue and cells and as a result they lead metabolic processes there. The other group are PGPR (plant growth promoting rhizobacteria) which are able to synthese phytohormones and binding nitrogen from atmosphere, providing these substances to a plant. Some of the PGPR are able to produce siderophores improving contamination substances bioavailability (like polycyclic aromatic hydrocarbons, PAH) [33,34].

Plant's inoculation with PGPR bacteria (especially with Pseudomonas) makes possible of limiting stressors effect for example high concentration of toxins in environment. They are also able to improve of yields growth up to 144% [33]. PGPR bacteria may intensify phytoremediation of soil's environment by limiting plant's stress, improving photosynthesis and achieve more plants biomass for phytoremediation [34].

PGPB bacteria can be divided into three groups: plant growth promoting bacteria PGPB, biocontrol-PGPB and plant stress homeoregulating bacteria PSHB). First of them, PGPB influence on plant growth, second control pathogens; growth and development. In turn, plant stress homeoregulating bacteria influence on decreasing stress factors on plant which result their unimpeded growth and development [14].

PGPR bacteria can affect to plant growth two ways: indirect and direct. Bacteria can limit susceptibility diseases and stimulate plants; phytopatogene's defence- that is indirect way of growth promoting. When it comes direct way of plant growth promoting, bacteria may provide essential mineral substances and plant hormones [35].

Bioaugmentation of soils in the mentioned before cases can be used an assisted process to phytoremediation.

3. Biopreparations inoculated into a soil

Microorganisms inoculation can be done using either only one strain of microbe or consortium of selected microorganisms [6,36]. For example, single strain – *Pseudomonas sp*. WBC-3 may be used in decontamination process of soil polluted with parathion [37], while *Sphingomonas* sp. TrD23 can be used for degradation of antibacterial and antifungal agent called triclosan [38].

Scientists proved that it is more effective to use consortium of microorganisms for biodegradation processes due to the fact that more metabolic characters of microorganisms can fill each other. It shows that indirect products of the biological decay of contamination may be substrate for other microorganisms where is created following sequence of reactions. Specific strains of bacteria play their role in the specific step of this sequence of reactions [6,36].

In bioaugmentation processes we can use genetically modified organisms –GMO. For example there is possible to use Zhang et al. experiment, in which they have been used plasmid pDOC (*B. laterosporus*) caring some genes responsible for degradation insecticide chlorpyrifos. The plasmid was introduced to the soil contaminated with chlorpyrifos (insecticide concentration 200 mg/kg dry wt soil). which lead to transfer of plasmid to bacteria strains live in this soil (*Pseudomonas* and *Staphylococcus*). These bacteria gained ability to chlorpyrifos decomposition within 5 days since the moment of its application to the soil [39]. However, using GMO in bioaugmentation is not widely accepted in society and it meets with ecologists and other environment disapprobation [14].

Enhancement of effectiveness of soil's bioaugmentation might be achieved via using microbes able to synthase siderophores (surface active agents) which improve pollutants bioavailability [4,38]. Bacteria like *B. megaterium* or *P. aureginosa* present this kind of ability for producing siderophores. Using these microbes it is possible to decay wide range of carbohydrates contaminating soil [25].

Introduction of biopreparations usually is achieved 2 ways: by surface spray or by direct injection. Since biological preparate has high cell's density, it is not problematic to introduce it to soil [40]. Biopreparations introducing to the soil's environment require a revival to get high degradation activity. Using prepared biopreparations leads to the lack of knowledge about their negative affect to autochthonic flora. The most profitable way is to use preparations with autochthonic microorganisms suitably selected for specific contamination. High concentration of toxins may cause some limits for possibility of forming each metabolic pathway of pollution degradation. In this case it is justified to use biopreparations with enzymes produced by microorganisms. Those preparations contain simple enzymes or whole complexes of microorganisms biocatalysts [4].

Acknowledgment

The work was conducted within the framework of the project TANGO1/266740/NCBR/2015.

References

[1] Ł. Podsiadło, T. Krzyśko-Łupicka, Techniki bioremediacji substancji ropopochodnych i metody oceny ich efektywności, *Inżynieria i Ochrona Środowiska*, 2013, 16, 4, 459-479.
[2] V. Andreoni, L. Cavalca, M.A. Rao, G. Nocerino, S. Bernasconi, E. Dell'Amico, L. Gianfreda, Bacterial communities and enzyme activities of PAHs polluted soils, *Chemosphere*, 2004, 57(5), 401–412.
[3] R. Boopathy, Factors limiting bioremediation technologies, *Bioresouce Technology*, 2000, 74, 63-67.
[4] O. Marchut-Mikołajczyk, E. Kwapisz, T. Antczak, Enzymatyczna bioremediacja ksenobiotyków, *Wydawnictwo Politechniki Częstochowskiej*, 2013, 1, 39-55.
[5] R. U. Meckenstock, M. Elsner, C. Griebler, T. Lueders, C. Stumpp, J. Aamand, B. M. Van Breukelen, Biodegradation: Updating the Concepts of Control for Microbial Cleanup in Contaminated Aquifers, *Environmental Science and Technology*, 2015, 49(12), 7073–7081.
[6] M. Kacprzak, Wspomaganie procesów remediacji gleb zdegradowanych, *Wydawnictwo Politechniki Częstochowskiej*, Częstochowa 2007.
[7] P. Sarkar, A. Roy, S. Pal, B. Mohapatra, S.K. Kazy, M.K. Maiti, P. Sar, Enrichment and Characterization of Hydrocarbon-Degrading Bacteria from Petroleum Refinery Waste as Potent Bioaugmentation Agent for In Situ Bioremediation. *Bioresource Technology*, 2017.

[8] J. Nowak, Bioremediacja gleb z ropy i jej produktów, *Biotechnologia*, 2008, 1(80), 97-108.
[9] M. Tyagi, M.M.R da Fonseca, C.C.C.R de Carvalho, Bioaugmentation and biostimulation strategies to improve the effectiveness of bioremediation processes, *Biodegradation*, 2011, *22*(2), 231–241.
[10] B. Kołwzan, Usuwanie zanieczyszczeń naftowych z gruntu metodą pryzmowania, *Ochrona Środowiska*, 2009, 2, 3-10.
[11] A. Shukla, S. Srivastava, Emerging Aspects of Bioremediation of Arsenic. In R. Singh & S. Kumar (Eds.), *Green Technologies and Environmental Sustainability*, 2017, 395–407.
[12] S. El Baz, M. Baz, M. Barakate, L. Hassani, A. El Gharmali, B. Imziln, Resistance to and accumulation of heavy metals by actinobacteria isolated from abandoned mining areas, *Scientific World Journal*, 2015.
[13] T.J. Gentry, C. Rensing, I.L. Pepper, New approaches for bioaugmentation as a remediation technology. Crit. Rev., *Environ. Sci. Technol*, 2004, 34, 447–494.
[14] M. Kacprzak, Fitoremediacja gleb skażonych metalami ciężkimi, *Wydawnictwo Politechniki Częstochowskiej*, Częstochowa 2013, 96-98.
[15] S.K. Samanta, O.V. Singh, R.K. Jain, Polycyclic aromatic hydrocarbons: environmental pollution and bioremediation, *Trends Biotechnol*. 2002, 20, 243-248.
[16] R. Chakraborty, S.M.O. Connor, E. Chan, J.D. Coates, Anaerobic Degradation of Benzene, Toluene, Ethylbenzene, and Xylene Compounds by Dechloromonas Strain RCB, *Applied and Environmental Microbiology*, 2005, 71(12), 8649–8655.
[17] Ł. Drewniak, M. Ciezkowska, M. Radlinska, A. Skłodowska, *Construction of the recombinant broad-host-range plasmids providing their bacterial hosts arsenic resistance and arsenite oxidation ability*, *J. Biotechnol* 2015, 196–197, 42–51.
[18] S. Liu, G. Zeng, Q. Niu, Y. Liu, L. Zhou, L. Jiang, M. Cheng, Bioresource Technology Bioremediation mechanisms of combined pollution of PAHs and heavy metals by bacteria and fungi: A mini review, *Bioresource Technology*, 2017, 224, 25–33.
[19] C. Marchand, M. St-Arnaud, W. Hogland, T.H. Bell, M. Hijri, Petroleum biodegradation capacity of bacteria and fungi isolated from petroleum-contaminated soil, *International Biodeterioration and Biodegradation*, 2017, 116, 48–57.
[20] R. Rabus, R. Nordhaus, W. Ludwig, F. Widdel, Complete oxidation of toluene under strictly anoxic conditions by a new sulfate-reducing bacterium, *Applied and Environmental Microbiology*, 1993, 59(5), 1444–1451.
[21] V.M. Alvarez, J.M. Marques, E. Korenblum, L. Seldin, Comparative bioremediation of crude oil-amended tropical soil microcosms by natural attenuation, bioaugmentation, or bioenrichment, *Appl. Environ. Soil Sci*, 2011, 1–10.
[22] H. Dudasova, L. Lukacova, S. Murinova, A. Puskarova, D. Pangallo, K. Dercova, Bacterial strains isolated from PCB-contaminated sediments and their use for bioaugmentation strategy in microcosms, *J Basic Microbiol* 2014, 54, 253–260.
[23] C. Guarino, V. Spada, R. Sciarrillo, Assessment of three approaches of bioremediation (Natural Attenuation, Landfarming and Bioaugmentation Assisted Landfarming) for a petroleum hydrocarbons contaminated soil, *Chemosphere*, 2017, 170, 10–16.
[24] F.S. Lang, J. Destain, F. Delvigne, P. Druart, M. Ongena, P. Thonart, Characterization and Evaluation of the Potential of a Diesel-Degrading Bacterial Consortium Isolated from Fresh Mangrove Sediment, *Water, Air, and Soil Pollution*, 2016, 227(2).
[25] O. Marchut-Mikołajczyk, E. Kwapisz, T. Antczak, Enzymatyczna bioremediacja ksenobiotyków, *Wydawnictwo Politechniki Częstochowskiej*, 2013, 1, 39-55.
[26] Y. Zhang, J.-F Wu, J. Zeyer, B. Meng, L. Liu, C.-Y. Jiang, S-Q. Liu, S-J. Liu, *Proteomic and molecular investigation on the physiological adaptation of Comamonas sp. strain CNB-1 growing on 4-chloronitrobenzene*, Biodegradation, 2009, 20, 55–66.
[27] C. Thion, A. Cèbron, T. Beguiristain, C. Leyval, PAH biotransformation and sorption by Fusarium solani and Arthrobacter oxydans isolated from a polluted soil in axenic cultures and mixed co-cultures, *International Biodeterioration and Biodegradation*, 68(September 2014), 28–35.
[28] L. Wang, X.-Q . Chi, J.-J. Zhang, D.-L. Sun, N.-Y. Zhou, Bioaugmentation of a methyl parathion contaminated soil with Pseudomonas sp. strain WBC-3., *Int. Biodeterior. Biodegr.*, 2014, 87, 116–121.
[29] N.A. Zhou, A.C. Lutovsky, G.L. Andaker, J.F. Ferguson, H.L. Gough, *Kinetics modeling predicts bioaugmentation with Sphingomonas cultures as a viable technology for enhanced pharmaceutical and personal care products removal during wastewater treatment*, Bioresour. Technol., 2014, 166, 158–167.
[30] P. Kämpfer, S. Ruppel, R. Remus, Enterobacter radicincitans sp. nov., a plant growth promoting species of the family Enterobacteriaceae, *Syst Appl Microbiol*, 2005, 28, 213–221.
[31] Y. Ma, R.S. Oliveir, H. Freitas, C. Zhang, Biochemical and Molecular Mechanisms of Plant-Microbe-Metal Interactions: Relevance for Phytoremediation, *Frontiers in Plant Science*, 2016, *7*, 1–19.

[32] G. Selvakumar, M. Mohan, S. Kundu, A.D. Gupta, P. Joshi, S. Nazim, H.S. Gupta, Cold tolerance and plant growth promotion potential of Serratia marcescens strain SRM (MTCC 8708) isolated from flowers of summer squash (Cucurbita pepo), *Letters in Applied Microbiology*, 2008, 46(2), 171–175.
[33] B.R. Glick, Plant Growth-Promoting Bacteria: Mechanisms and Applications, *Scientifica*, 2012, 1–15.
[34] J. Rakowska, K. Radwan, Z. Ślosorz, E. Pietraszek, M. Łudzik, P. Suchorab, Usuwanie substancji ropopochodnych z dróg i gruntów, *CNBOP-PIB* 2012, ISBN: 978-83-61520-53-5.
[35] G. Brader, S. Compant, B. Mitter, F. Trognitz, A. Sessitsch, Metabolic potential of endophytic bacteria, *Current Opinion in Biotechnology*, 2014, 27(100), 30-37.
[36] J. Richard, T. Vogel, Characterization of a soil bacterial consortium capable of degrading diesel fuel, *International Biodeterioration & Biodegradation*, 1995,44(2), 93–100.
[37] P. Vejan, R. Abdullah, T. Khadiran, S. Ismail, N. Boyce, Role of plant growth promoting rhizobacteria in agricultural sustainability-A review, *Molecules*, 2006, 21(5), 1–17.
[38] A. Napora, A. Grobelak, A. Placek, K. Nowak, M. Kacprzak, Wpływ bakterii PGPR i dodatków glebowych na promowanie wzrostu roślin.
[39] Q. Zhang, B. Wang, Z. Cao, Y. Yu, Plasmid-mediated bioaugmentation for the degradation of chlorpyrifos in soil, *Journal of Hazardous Materials*, 2012, Volumes 221–222, Pages 178-184.
[40] I. Rabęda, Bakterie i grzyby mikoryzowe zwiększają wydajność roślin w fitoremediacji metali śladowych, *Kosmos. Problemy nauk przyrodniczych*, 2011, 60, 3-4 (292-293), 423-433.

Oil spills - dangers and clean-up by GEnIuS

Sebastian Zborowski [1], Katerina Ilijovska [1]

[1]Faculty of Energy and Fuels, AGH University of Science and Technology, email: szboro@interia.pl katerina.ilijovska@gmail.com

Abstract

The main objective of this study is to examine case of oil spills and their threat to the environment, but also a closer look to a new absorbent being developed by Directa Plus – Grafysorber. The new project is said to be more effective in both technical way and economical. Furthermore, this work shows current detection methods of oil leakages and their clean-up methods. The study is focused on GEnIuS project that claims to be even 10 times better than actual absorbents available on the market. Not only it is better, but it also doesn't require any extra additives like dispersants or sinking agents that may cause additional environmental problems due to their toxicity. The study also includes an economical aspect of adapting the Grafysorber for cleaning oil spills, as the producers declare that it will be 50-60 % cheaper than other absorbents. Our calculations showed that by introducing this product to small leakages we may get a considerable amount of money saved.

Keywords: Oil, spill, absorbent, graphite, clean-up

1. Introduction

Recently the world has experienced many oil spills, for example Deepwater Horizon in the Gulf of Mexico, or Exxon Mobile in Nigeria in 2010 and smaller ones in close past, like leakage from Trans-Israel pipeline in 2014 or recent Agia Zoni II ship sinking. Each of those spills cause environmental damage to both animals and flora.

Nowadays we have several ways to detect oil spills and leakages on sea and land, but in many cases reaction time is very long. It requires time to gather proper equipment and team to start cleaning, but also on many occasions the location is also a problem, for example in deep sea stations.

Uncontrolled oil spills may lead to many environmental disasters. They are harmful for the marine life and also pose a threat to the habitat of land animals and humans. The animals that are especially affected by oil leakages are the fishes and birds, because oil sticks to their husks or feathers making them unable to survive.

2. Detection

Detection and monitoring of oil spills is a crucial step before the clean-up process. The purpose of the detection is to identify the spill location, the size and extent of the spill, direction and magnitude of oil movement as well as the wind, current and wave information for predicting future oil movement. Knowing this information, it is easier to proceed with further steps and choose the right method for sanation.

There are various methods for detection of oil spills, but the most used ones are belong to the category of remote sensing techniques. The main strengths of remote sensing lay in the wide, synoptic coverage that provides consistent results over large and often inaccessible areas. Repeatability of results also plays a role in ensuring the usefulness of the image data.

There are three main activities related to management of oil spills in the marine environment in which satellite remote sensing has a role: contingency planning, emergency response and monitoring. Contingency planning for oil spills involves gathering baseline data, identifying economically and environmentally sensitive areas and assessing the availability of facilities and equipment to be used in clean-up efforts should an oil spill occur. Disaster response to a specific oil spill incident involves identification of the location and extent of a spill

short-term monitoring of spill. Monitoring program involve frequent imaging of areas where spills or illegal dumping are likely to occur.

The remote sensing devices include the use of infrared video and photography from airborne platforms, thermal infrared imaging, airborne laser fluourosensors, airborne and space-borne optical sensors, as well as airborne and spaceborne SAR. All these devices have their own advantages and disadvantages [1, 2].

3. Clean-up methods

There are many responses to oil spills, to name a few:

- Mechanical recovery
- Dispersion
- In Situ Burning
- Sand screening
- Bioremediation

Mechanical methods are the most common tools for absorption of spilled oil. They allow the further recovery of liquid, thus reducing economic impact for companies. Also there are many different products on the market related to this method. They are made mostly from polypropylene and unfortunately do not have great reuse factor, thus they have to be utilized after usage.

Dispersion uses mixtures of emulsifiers and solvents to break long oil structures into small ones, like droplets. Next, the newly formed oils may easily disperse through a water volume and small droplets biodegraded with the presence of microbes. The disadvantage of this method is that it provides only a partial solution, because it exposes water life to further oil contact [3].

In Situ Burning is, as the name shows, burning oil on site of spillage. Thanks to taking such action, the amount of unwanted liquid on the water surface may be decreased. However, there are many concerns connected with this method such as: smoke and pm-10 impact on humans, burning is not complete or total [4].

Sand screening is done after oil is deposited on shores and can be easily separated from sand. It is obvious that this method is not good for on-site and immediate action, but only after a longer period. It helps with cleaning already stained environment and is very effective.

Bioremediation is considered a green technology compared to others. It requires specific parameters of oil and environmental (density, concentration, temperature, oxygen etc.). Its purpose is to ease the biodegradation of oil by usage of microorganisms. Thanks to many different organisms – algae, bacteria it is possible to breakdown toxic waste products into safes constituents [5].

4. GEnIuS project

GEnIuS stands for: Graphene Eco Innovatice Sorbent. The purpose of the project is to find and introduce a new solution for oil spill removal that is more efficient and less toxic. Laboratory tests were made by C. E. A. R. LABORATORI RIUNITI s. r. l. in Merone, Italy for both parameters. There were not toxic chemicals after 24 hours during water wash and the adsorption equal to even 94 grams of oil in 1 gram of the sorbent [8]. Below we compared fraction of oil absorbed per 1 gram of different materials. For Grafysorber we used 54.59 g/g, because this is the result for low viscosity oil, which other materials are shown in.

Tab. 1 Comparison between different absorbent's properties. [6, 7, 8]

Product	Company	Weight [kg]	Adsorption [l]	Fraction [g/g]
Eco-Sop	Chemtex	5.9	105	16.37
SMOG 4050	HRT POLSKA	7.6	143	17.31
Absorbent boom	DEYUAN MARINE	8	192	22.08
GRAFYSORBER	**Directa Plus**	n/a	n/a	**54.59**

Grafysorber is made out of super-expanded graphite, which is obtained by plasma heating intercalated graphite. Thanks to this process the sorbent gain very high surface area and low density, by drastically increased volume. Below in the picture we showed 5 grams of Grafysorber before and after the process.

A B

Fig. 1. 5 grams of Grafysorber A: before, B: after, plasma heating [9].

5. Economic review

The cost of removal oil from water and shore is defined by many factors, like:

- Location
- Oil type
- Clean-up strategy
- Spill amount

Due to this fact reduction of material cost and method used may not be that significant as from [10] we may find that it is only around 10% of the total cost. Still looking at numbers and total cost of 3,8 billion $ from Exxon Valdez oil spill reduction in any factor saves millions of money.

We compared costs of materials in two cases:

- Small leakage of oil in local scale – 500 tonnes, comparing Polish product with Grafysorber.
- Deepwater Horizon oil spill as an example of huge spill – 492 000 tonnes, comparing Chinese product with Grafysorber.

Unfortunately we didn't get access to actual data concerning Grafysorber's costs of preparation nor foreseen market price, so we agreed to make it the price of Polish company as an example of a medium cost product.

The same comes with Chinese product, even though they have a complete product they don't put the costs on their website nor answer to e-mails with questions. We estimated the cost to be 11 $/kg, because the adsorption is greater and company is present on global markets.

Also for calculations we have used only one type of method, when in reality there are several used simultaneously, like mechanical, dispersant.

Results of calculations were shown in Tables 2 and 3.

Tab. 2 Economic comparison between Polish product and Grafysorber on a small scale spill.

	SMOG 4050	**Grafysorber**
Price [$/kg]	9,6	9,6
Adsorption [g/g]	17	55
Oil spill [t]	500	
Used material [kg]	29 411,8	9 090,9
Cost of material [$]	282 353,28	87 272,64

Tab. 3 Economic comparison between Chinese product and Grafysorber on a large scale spill.

	Absorbent Boom	**Grafysorber**
Price [$/kg]	11	9,6
Adsorption [g/g]	22	55
Oil spill [t]	492 000	
Used material [kg]	22 363 636	8 945 454
Cost of material [$]	245 999 996	85 876 358

6. Conclusions and discussions

The use of the new absorber will have a great impact on the market, since its efficiency is much greater than the other currently available products. Additional properties that make this product favourable are its high oil recovery rate, recyclability and non-toxicity.

As shown in the tables 2 and 3 in both cases we get 65-70% of savings on cost material only. Because the fraction of material costs in total price of removal is 10% we get around 5-7% of cost decrease. Given the real numbers of spilled oil of billions of $ we get savings of millions of $.

In small scale case we may decrease also location factor, since often it is only leakage in harbours, industry or local pipeline leakage. This may increase the material cost share in total cost and thus increase savings up to even 60%.

Considering all the information and analysis provided in this paper, we can conclude that Grafysorber is an innovative product that has the potential to become the number one solution in the oil spills clean-up sector.

References

[1] Natural Resource Canada, http://www.nrcan.gc.ca/node/9323, (03.12.2017).
[2] D. Gionet, K. Bannerman, L. Gamble, G. Staples, Emerging Practices in Oil Spill Preparedness and Response Using Space-Based Radar, *Interspill Conference*, 2015.
[3] J. Frometa, M. DeLorenzo, E. Pisarski, P. Etnoyer. Toxicity of oil and dispersant on the deep water gorgonian octocoral Swiftia exserta, with implications for the effects of the Deepwater Horizon oil spill, *Marine Pollution Bulletin*, September 2017, 122, pp. 91-99.
[4] Office of Response and Restoration, https://response.restoration.noaa.gov/insituburning, (03.12.2017).
[5] R. Jezequel, Bioremediation of oil contaminated environment, *Interspill Conference*, 2015.
[6] Chemtex, http://www.chemtexinc.com/eco-sop-oil-only-cotton-pads-126.html, (03.12.2017).
[7] HRT-POLSKA, http://sorbenty.hrt.pl/opis/3794436/smog4050100-sorbent-tylko-do-oleju-mata-gruba-premium-040m-x-050m-100-szt.html, (03.12.2017).
[8] DEYUAN MARINE, https://www.deyuanmarine.com/Oil-Only-Absorbent-Booms-pd010603.html, (03.12.2017).
[9] GEnIuS Project, http://genius-project.com, (03.12.2017).
[10] Melt Blown Technologies, http://blog.meltblowntechnologies.com/how-much-it-costs-to-clean-up-an-oil-spill, (03.12.2017).

Oxygen sensitivity of hydrogenesis' and methanogenesis'

Gaweł Sołowski[1], Bartosz Hrycak[1], Dariusz Czylkowski[1], Izabela Konkol[1], Adam Cenian[1], Krzysztof Pastuszak[2]

[1] Instytut Maszyn Przepływowych im R. Szewalskiego, Polskiej Akademii Nauk; e-mail:gsolowski@imp.gda.pl, cenian@imp.gda.pl, dariusz.czylkowski@imp.gda.pl, bartosz.hrycak@)imp.gda.pl

[2]Katedra Algorytmów i Modelowania; Wydział Informatyki, Telekomunikacji i Informatyki Politechniki Gdańskiej, e-mail: krzpastu@pg.edu.pl

Abstract

In the chapter, results of dark fermentation of sour cabbage in presence of oxygen with concentrations 2-9% are presented. The presence of oxygen in such concentration inhibits methanogesis (and methane production more than 2 times) and increases hydrogen production 6 times. It also shortens the fermentation process above 40%.

Keywords: Dark fermentation, anaerobic digestion, sour cabbage, oxygen, hydrogen

1. Introduction

Hydrogen is a good energy carrier and raw substrate for chemistry. However, the search for efficient way of its production is still continued. As the fossil fuels become more rare, the need for sustainable ways of production like dark fermentation become more clear. Dark fermentation is anaerobic digestion of sugars or glycerol into hydrogen, carbon dioxide and low organic acids. The method is still just lab-scale process and needs improvements, especially its efficiency[1]. One of the known problem is related to inhibition of methanogenesis; competing for substrates process, which also uses hydrogen produced during hydrogenesis. Therefore, strong emphasis is put for such pretreatment method of inoculum that inhibit methanogenic activities. These methods includes heat shock freezing, chemical agents (bases, acids, chloroform), microwave interactions, shaking, etc [2–4].

The experiments presented in the chapter show results related to oxygen sensitivity of both processes: hydrogenesis and methanogenesis. As they are anaerobic only small amount of oxygen was allowed to reactor.

2. Materials and Methods

The fermentation process of sour cabbage was performed in bottles of volume 2 dm^3. As inoculum sludge from biogas plant in Lubań (Pomerania Region) was used. The sour cabbage load of dry organic mass content equal 10 g/dm^3 was applied for the process. The load was prepared by milling and mixing of sour cabbage. The fermentation process was continued up to 16 days in temperature 38°C and initial pH ~7.9 in presence of oxygen: under concentration 2%-9.2% and no oxygen. The oxygen flow rate was about 4.5 cm^3/h. The biogas produced was measured by Owen method and analyzed with Gas Chromatography.

3. Results and discussion.

GC analysis allowed determination of methane, hydrogen, hydrogen sulfide, carbon dioxide and nitrogen concentration. The biogas volume obtained during 16 days was 21.36 dm^3 in bottle with oxygen addition and 9.59 dm^3 under strictly anaerobic conditions. The total biogas production is shown in Figure 1.

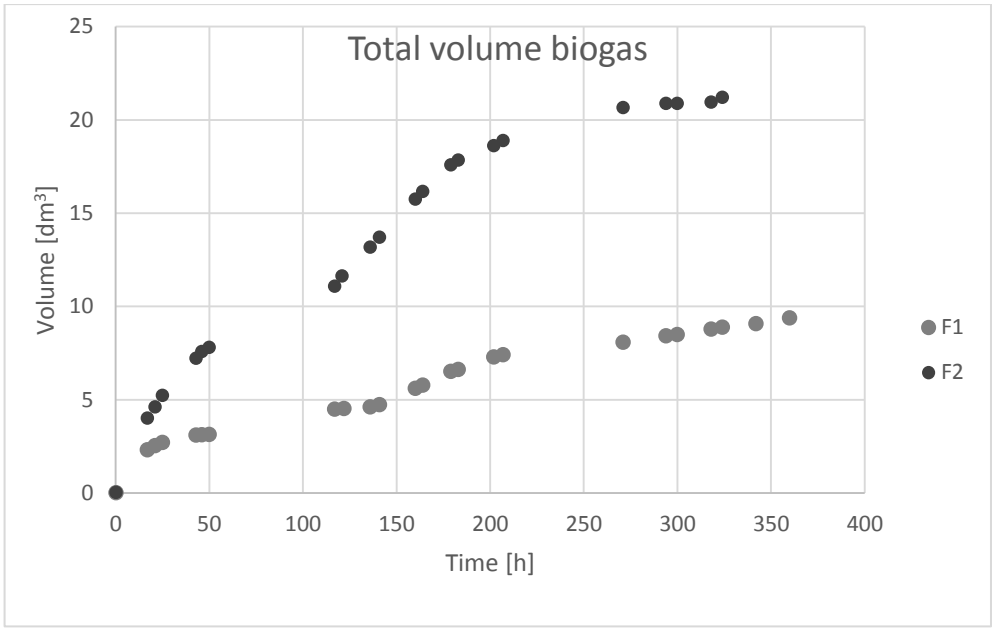

Fig. 1 Total biogas production under strict anaerobic conditions (black dots) and with small addition of oxygen (gray dots).

Under low oxygen condition, methane and hydrogen production during 207 hours amounted 2.86 dm^3 and 0.48 dm^3, respectively (see gray dots and squares in Figure 2 and 3. Under strict anaerobic conditions, the volume of methane and hydrogen produced during 360h amounted 6.60 dm^3 and 0.08 dm^3, respectively; after 207 the respective volume were 5.69 dm^3 of methane and 0.07 dm^3 of hydrogen - see blue dots and diamonds in Figure 2 and 3.

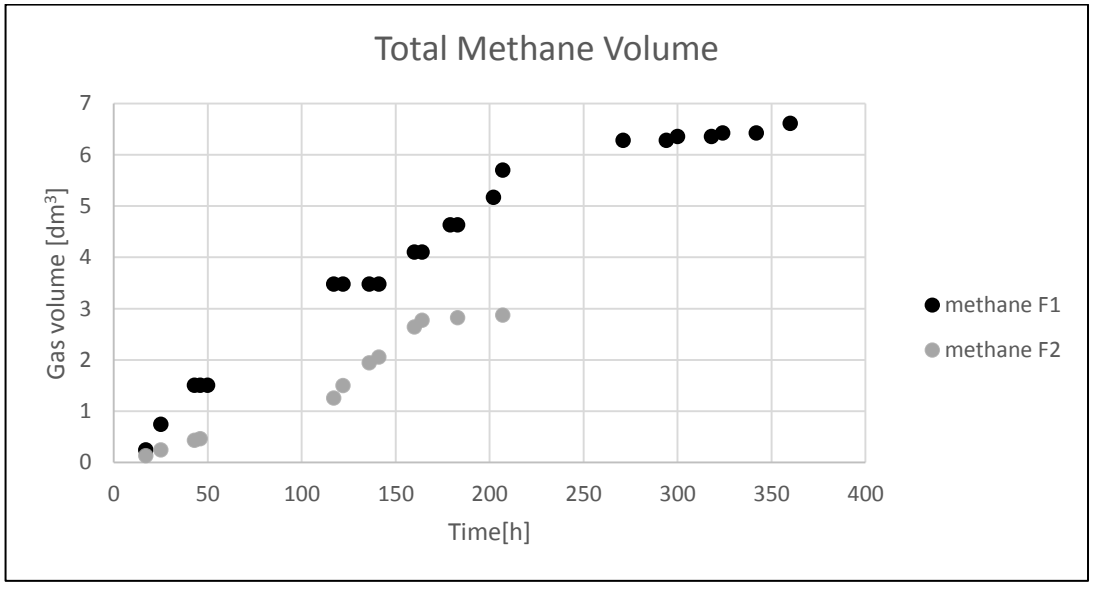

Fig. 2 Total methane production under strict anaerobic conditions (black dots) and with small addition of oxygen (gray dots).

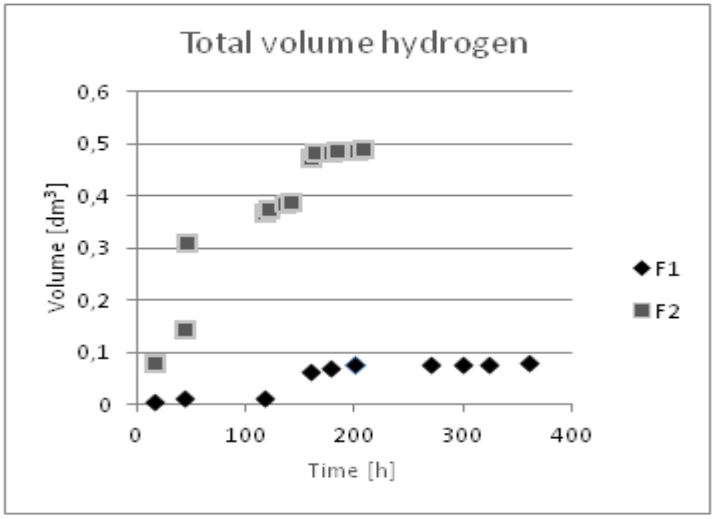

Fig. 3 Total hydrogen production under strict anaerobic conditions (black diamonds) and with small addition of oxygen (gray-black squares).

The presence of oxygen significantly inhibits methane production but net hydrogen production increases. The concentration of methane under strict anaerobic conditions reached even 70%; hydrogen concentration was 4.6%. After oxygen addition the hydrogen and biogas production increases, leading to concentrations of hydrogen and methane 2.6% and 15 %, respectively.

The hydrogen production is less sensitive to presence of oxygen than methane. Recently oxygen is commonly used for removing hydrogen sulfide production from anaerobic digestion and sewage plants[5,6].

4. Conclusions

Hydrogen can be produced using dark fermentation process under strictly anaerobic conditions or after small addition of oxygen. During 16 days (207 hours) 2.86 dm^3 of methane and 0.48 dm^3 of hydrogen were produced under small oxygen participation. Under strict anaerobic conditions more methane is produced and much less of hydrogen, i.e. 5.69 dm^3 of methane and 0.07 dm^3 of hydrogen were produced during 207 h and 6.60 dm^3 and 0.08 dm^3, respectively after 360 h. The presence of oxygen in considered concentrations shortened the fermentation process about 40% in compare to completely anaerobic process.

The oxygen seems to be another stress agent inhibiting methanogenesis that could be used during fermentation process not only for pretreating of inoculum. The phenomenon needs further research.

References

[1] K. Willquist, V.N. Nkemka, H. Svensson, S. Pawar, M. Ljunggren, H. Karlsson. Design of a novel biohythane process with high H2 and CH4 production rates. *International Journal of Hydrogen Energy* 2012;37:17749–62. doi:10.1016/j.ijhydene.2012.08.092.

[2] S.R. Chaganti, D.H. Kim, J.A. Lalman. Dark fermentative hydrogen production by mixed anaerobic cultures: Effect of inoculum treatment methods on hydrogen yield. *Renewable Energy* 2012;48:117–21. doi:10.1016/j.renene.2012.04.015.

[3] J.L. Wang, W. Wan. Comparison of different pretreatment methods for enriching hydrogen-producing bacteria from digested sludge. *International Journal of Hydrogen Energy* 2008;33:2934–41. doi:10.1016/j.ijhydene.2008.03.048.

[4] G. Sołowski, M.S. Shalaby, H. Abdallah, A.M. Shaban, A. Cenian. Work in progress: Production of hydrogen from biomass and its separation using membrane technology. *Renewable and Sustainable Energy Reviews* 2017. doi:10.1016/j.rser.2017.10.027.

[5] P.A. Terry. Application of Ozone and Oxygen to Reduce Chemical Oxygen Processing Plant. *International Journal of Chemical Engineering* 2010;2010:1–6. doi:10.1155/2010/250235.

[6] T. Duangmanee. *Micro-aeration for hydrogen sulfide removal from biogas*. Iowa State University, 2009. http://lib.dr.iastate.edu/etd/10748, (17/11/2017).

Preliminary study on computational modelling of slow solar pyrolysis of biomass

Zuzanna Kaczor [1], Zbigniew Buliński [1], Sebastian Werle[1]

[1]Institute of Thermal Technology, Silesian University of Technology, e-mail: zuzanna.kaczor@polsl.pl, zbigniew.bulinski@polsl.pl, sebastian.werle@polsl.pl

Abstract

The paper collects and briefly describes the current literature state regarding the numerical analysis of the pyrolysis process and its accompanying phenomena. The paper presents preliminary computations of heat and fluid flow during the solar pyrolysis. The main model assumptions of the performed analyses are pointed out together with their justification. The literature review concentrates on the pyrolysis of the substance, generally understood as biomass. The work also includes notices about interesting, though possibly out of the mainstream, works that might inspire other researchers. The authors aimed to prepare a comprehensive literature review covering the problem of numerical modelling of biomass pyrolysis. This work is intended to be a kind of guide connecting the studied problem with its simulation method. The review shows that the fast pyrolysis process in fluidised bed reactors is currently of greatest interest. The second part of the work describes the preliminary mathematical model of a solar pyrolysis process of waste biomass. In this model, a single pellet heating process is investigated, and the impact of the two main factors influencing this process is tested, namely an inert gas stream and a power of a light source.

Keywords: Literature review, CFD, pyrolysis, numerical model, porous media

1. Introduction

Global trends in climate policy lead to increased use of renewable energy sources and motivate the development of new technologies of its production. At present, biomass is indicated as a source of renewable energy with high potential, because its resources in the world are significant and at the same time they are not used as they could be. The process of pyrolysis and gasification is a well-known way to adopt biomass to a wider range of uses. Pyrolysis as a thermal decomposition process, carrying out in the absence of oxygen, is a strongly endothermic phenomenon. Therefore, it requires large amounts of energy input. Hence, the idea of combining two renewable energy sources, sun and biomass - although biomass energy also comes from the sun - is not new. Many researchers have carried out investigations of the pyrolysis process of solar biomass, both slow and fast, by building different types of reactors [1]. Currently, investigation of the pyrolysis process and solar pyrolysis process is a very popular among scientists, as it is evidenced by numerous scientific works.

Besides the construction of an experimental stand a numerical analysis, it is part of a project focusing on the in-depth examination of solar pyrolysis phenomenon and determining the influence of selected parameters on the process products.

The purpose of this paper is to collect information on the CFD analyses carried out so far in the field of biomass pyrolysis, including software, methodology, simplifications, examined parameters. Furthermore, in this study will be presented a numerical model preliminary to the process of numerical analysis of slow solar pyrolysis of waste biomass.

2. Literature review

The literature provides many examples of attempts to model the pyrolysis or phenomena that are part of this process, e.g. flow, circulation, fluidization, heat transfer, chemical reactions. Below a summary of the works that relate to these issues is presented, categorized into several groups of the most common problems.

2.1 Fast pyrolysis and Catalytic fast pyrolysis

Catalytic fast pyrolysis (CFP) is a process in which the biomass in the inert environment of nitrogen is heated up to a temperature of 400 to 600 °C very rapidly with heating speed even up to 500°C/s. The process takes place in the presence of a catalyst, which function is to partially deoxygenate products which makes the produced bio-oil more stable [2,3]. It is very popular to conduct CFP process or just fast pyrolysis without the catalyst in fluidized bed reactors.

To build a complete, accurate model of CFP pyrolysis in a fluidized bed reactor, one must first model the flow; this problem was described by Adkins et al.[2]. Researchers prepared a numerical model of fluidization and circulation of the catalyst. 3D model was developed in BarracudaVirtual Reactor commercial Computational Fluid Dynamics software. To validate the model a series of cold flow experiments were performed under laboratory conditions. The aim of the work was to determine the drag model, which would give the best correlation with experimental data. All developed models used Large Eddy Simulation approach to describe turbulence.

Xue et al. [3] prepared 2D and 3D numerical models of the fast pyrolysis process in the fluidal reactor. The developed model considered multiphase flow (gas with particles of biomass) as well as chemical reactions composing the pyrolysis process. Authors built a lab-scale reactor to carry out validation of the developed model. They used Euler-Euler multiphase model to describe two-phase flow inside the reactor. The biomass was defined as a mixture of cellulose, hemicellulose, and lignin. All walls of the domain were defined as adiabatic accept one section with temperature 800 K which was simulating the external heating. Nominal biomass flow was equal to 100 g/h with a temperature of 300 K. Within the work an influence of a few parameters on product yield was investigated, e.g. model parameters: 2D and 3D geometry; operating conditions: temperature of the process, velocity of fluidizing gas; biomass characteristic: composition and particle diameter.

In [4] and [5] Yu et al. described comprehensively hydrodynamic and chemistry in a downer fast pyrolysis biomass reactor created in Ansys Fluent Software. The object of the first work was to investigate the efficiency of gas-solid separator placed in outlet pipe of pyrolysis gas to clean it. Schematic diagram of the reactor system is shown in Fig.1.

In the second study biomass pyrolysis process was simulated to determine its susceptibility to varying operating conditions. Chemical reactions were assumed to be one step and global. Drying process was also taken into consideration. The heat needed to carry out the pyrolysis process is introduced into the reactor by heated-up sand, which was working as an inert solid.

Xiong et al. [6] presented a numerical model of pyrolysis in bubbling fluidized bed, which also included chemical reactions. For this purpose, a distributed activation energy model (DAEM) describing the kinetics of chemical reactions was coupled with simulations of a multi-phase turbulent flow. The geometry of the model was created based on the real laboratory experimental stand. The authors indicated that taking into account both flow simulations and process kinetics in one model does not necessarily result in a rapid increase of the simulation time. The results showed that the yield of pyrolysis products is strongly dependent on the process kinetics and flow conditions, but within the work author mainly focused on the process kinetics, explaining the reasons for selecting the DAEM model. Moreover, they described the impact of the adopted parameters and the complexity level of this model on the simulation results - yield of pyrolysis products. One of the main conclusions is that the tar yield is the most sensitive quantity for the complexity of the DAEM model.

Liu et al. [7] presented a mathematical model of fast biomass pyrolysis in the lab-scale fluidized bed reactor. Their model used Eulerian-Eulerian multi-phase granular flow model and multi-step kinetic model.

In their work, authors concentrated on the investigation of particle shrinkage process. To simulate this phenomenon, they applied 3-parameter shrinkage model where different values of parameter were tried. The simulation software was Ansys Fluent. The work showed how particle shrinkage impacts pyrolysis product yields and heating and motion conditions.

2.2 Pyrolysis in another type of reactors

Wu et al. [11] modeled pyrolisis process in Shenwu rotating bed reactor, where the deposit stated municipal solid waste. The process was investigated to determine the most favorable conditions from the point of view of the best possible recycling of biomass. A model including heat and mass transfer phenomena was validated experimentally.

Hooshdaran et al. [9] also focused on the influence of the boundary conditions on heat transfer, bed hydrodynamic and pressure drop in a conical spouted fluidal bed pyrolysis reactor.

2.3 Pyrolysis in bed of particles

Borello et al. [10] studied the pyrolysis process in a packed bed, which was treated as a porous medium. The model stated a tool to evaluate the yields of the process products and to determine the effect of the inert gas and the reactor walls temperature on product yield. The model was validated experimentally.

German researchers in 2001 carried out extensive experimental and numerical studies of wood bed pyrolysis which consists of many large, diverse particles. Peters et al. in [11] and [12] investigated the pyrolysis process and preceded by heating and drying process. The simulations also took into account the presence of void spaces between the particles, approximating the flow through these spaces with a model of a porous medium taking part in heat and mass exchange inside the bed.

Mahmoudi et al. [13] tested numerically influence of particle size and packing on the char production during biomass pyrolysis in stationary rectangle reactor. Authors took into account processes of heating-up, drying and pyrolysis, including flow through the void space, and found that preparing the bed as layers of small and big particles significantly increases char yield up to 46 %.

2.4 Another type of pyrolysis and gasification

Guizani et al. [14] investigated an interesting solution, namely the possibility of gasification of wood biomass with CO_2. The process was carried out at a high temperature equal to 850°C at high heating speed. Studies showed that comparing with nitrogen, use of CO_2 does not affect the speed of reaction or the yield of char. The process was called pyro-gasification, as the first part of the process was actually pyrolysis, and during later stages gasification took place. Carried research showed that 95% of whole process time was occupated by char gasification. The numerical model was built in COMSOL software.

Sagehashi et al. [15], examined experimentally and numerically superheated steam pyrolysis process of the biomass type that is most common in Japan, namely Japanese cedar (*Sugi*). The process was assumed to be carried out without any catalyst and to be portable. The model was used to calculate product yield of elementary biomass components pyrolysis and elaborate it as a function of temperature.

Eri et al. [16] studied biomass steam gasification in fluidized bed reactor, including model of the flow and chemistry of the process.

Motasemi et al. [17] created a microwave pyrolysis model of biomass pellets in the nitrogen environment. The model was built in Ansys CFX. The model included heat and mass transfer, chemical reactions and phase change phenomena. The model has been validated based on experimental data. The authors stated that components and formed volatiles influence microwave power absorbed by biomass which finally determined its temperature. Another important conclusion is that in higher temperature biomass absorb less power.

2.5 Solar pyrolysis

Commonly applied way to focus solar radiation is a linear concentrator system which is actually parabolic reflector concentrating sunbeams on a central pipe [1]. As it was mentioned at the beginning, solar pyrolysis is an ecologically very attractive idea. Some researchers have tried to use popular and proven solar concentrating technology for the pyrolysis process.

Work of Bashir et al. [1] gave an idea of a system of biomass conversion by fast solar pyrolysis. The numerically modeled part was the solar reactor, on which solar radiation was concentrated with the use of the parabolic reflector. The model was built using ANSYS Fluent commercial software. Authors used Euler−Euler approach to model the granular flow. Solar radiation expressed as a constant heat flux was defined on the outer wall of the reactor. The model was used to predict the reactor performance analysis.

Except works covering problems of research in the field of CFD modeling of the pyrolysis process there are also available works which concentrated on the modeling of the parabolic receiver, e.g. work of Wattana et al. [18].

Work of Soria et al. [19] presents a 2D numerical model of solar pyrolysis of a single beech pellet (diameter equals 10 mm, length equals 5 mm) built in Ansys Fluent software. The model took into account both the heat transfer process and the chemical reactions taking place in the sample. The tests were carried out for process temperatures from 600 to 2000°C, at heating speeds from 10 to 50°C/s. Experiments were carried out in the argon environment. Product yield results were compared with experimental data from the actual reactor. The reactor was transparent buble made of Pyrex glass (boron-silicon glass). The power of the solar radiation collected and transfered to the sample was 1.5 kW. The model shows the process of forming gas fraction components and enables the study of thermal decomposition of biomass of different origin.

2.6 Pyrolysis modeling in general, interesting cases

Romagnosi et al.[20] presented an in-depth, multi-parameter analysis of phenomena occurring in pyrolytic conditions in a porous medium. The work was carried out for the purpose of better understanding phenomena in the situation of fuel cooling of combustion chambers. When combustion chambers are lined with some porous material and as a coolant serves fuel, in this porous material occurs pyrolysis process of this fuel. The analysis concerned the flow, the diffusion of various fuel components, the consequences of using the real and ideal fluid model. Simulations involved processes in parameters up to 1200 K and 6 MPa.

Bret et al. in [21] performed interesting research about evaporation of a single droplet of bio-oil to investigate how diffusion rate influences the process. The complexity of the problem arises from the rich composition of bio-oil. Droplet diameter size taken into simulation was 1.7 mm and 1.6 mm in temperatures equal to 300°C and 500°C. The work revealed very interesting conclusion for bio-oil combustion in engines: better mixing reduces explosive boiling.

Feng et al. [22] when studying the process of cooling jet engines with fuel, specifically hydrocarbons, tried to explore the process of pyrolysis of this fuel, which takes place in thin cooling channels. They presented a 2D model of pyrolysis in a tube which allowed them to state the differentiation of phenomena caused by the distance from the channel wall. It appeared that changing the heat and mass transfer conditions affects the pyrolysis process. The authors concluded their work stating that the occurrence of pyrolysis aggravates the conditions of radiative heat transfer, hence increasing the heat flow directed to the channel intensifies the fuel pyrolysis process at the channel walls while simultaneously inhibiting fuel pyrolysis in the channel axis.

Cai et al. [23] in 2011 described in detail model of chemical reactions occurring during pyrolysis of solid fuels. Researchers have created a process model based on distributed activation energy model which should faithfully map process kinetics. Different sets of model parameters were checked to investigate their influence on calculation results. In 2014 Cai et al. [24] presented a review of the use of the DAEM (distributed activation energy model), which is being commonly applied to represent kinetics of lignocellulosic biomass pyrolysis. Within the work, the DAEM model is widely described. The DAEM model parameters most often adapted by scientists are reviewed, and recent publications about lignocellulosic biomass pyrolysis simulation with this model are analyzed.

3. Methodology and experimental setup

The paper presents a preliminary model of solar pyrolysis of waste biomass. Within this work, we aim to investigate phenomena that occur in one single pellet of biomass during solar pyrolysis. Especially, we concentrate on the influence of the mass flow rate of nitrogen and radiation heat flux on the heating-up process of a biomass pellet.

3.1 Research station and model assumptions

To build an experimental stand that would simulate solar pyrolysis process a xenon lamp was used to simulate radiation heat flux from the Sun. Moreover, it is assumed that the radiation will be focused on a surface of the insulated copper tube. Copper was chosen because of its large heat conductivity up to 400 W/mK.

Radiation heat flux is directed onto the central part of a tube; the rest is insulated. As an insulator Pyrogel® XT-E was chosen, which is a commercially available material. The thickness of insulation assumed in the model is equal to 15 mm. Scheme of the reactor is presented in Figure 1

The gap in insulation is actually one hole. But because of axisymmetry simplification of the numerical model, the gap forms a ring at the pipe surface, see Figure 2.

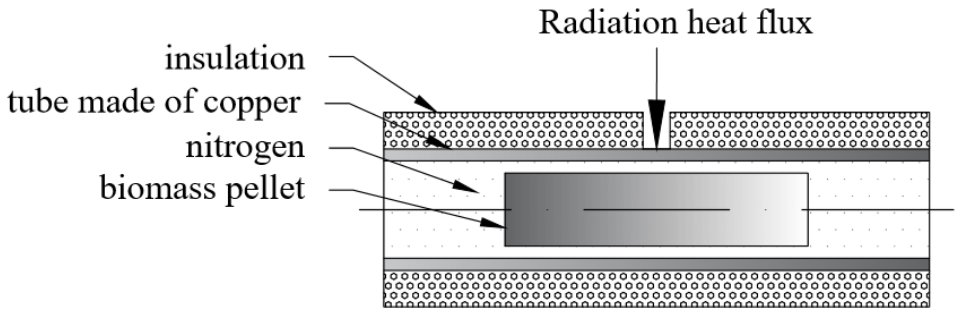

Fig. 1 Schematic of solar pyrolysis reactor

3.1.1 Model geometry

Typical wood biomass pellets are mainly a cylinder of dimensions, approximately, diameter 6 mm and length 25 mm. Dimensions of the whole reactor adopted in this work are shown in Figure 2. Insulation was introduced into the model by defining the thickness of external wall of copper tube and by determining its material.

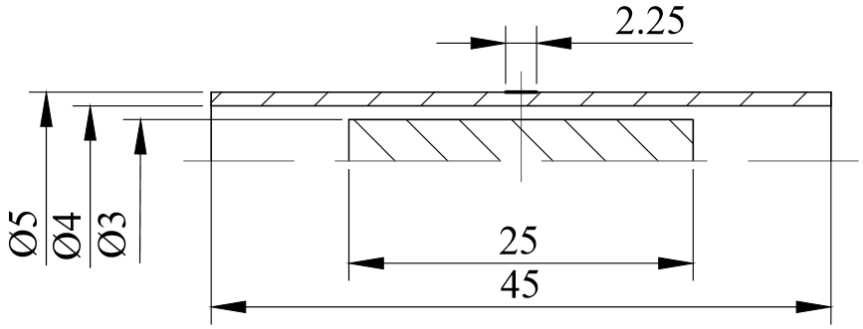

Fig. 2 Model geometrical dimensions

3.1.2 Continuum zones and boundary conditions

The most important geometry elements of the model are presented in Figure 3.

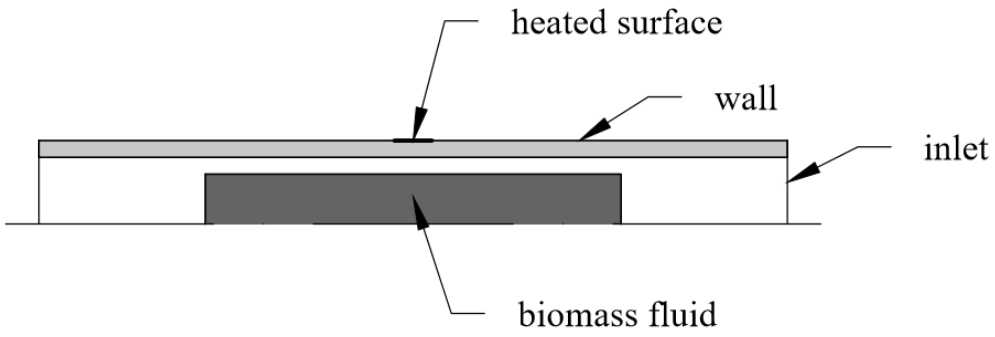

Fig. 3 Selected model elements

As was mentioned before within this work calculation will be carried out for 4 combinations of the maximum and minimum value of nitrogen volume flow rate and maximum and minimum value of lamp power. Values of these quantities are collected in Table 1. Values for lamp power output results from regulation range (60-100%) of the chosen lamp (18.5 W) and from estimated loses of this power (10%).

Tab. 1 Main inputs value

Nitrogen flow rate	
Minimum	$\dot{V}_{N2,min} = 0.05\ \ l/min$
Maximum	$\dot{V}_{N2,max} = 1\ \ l/min$
Lamp power	
Minimum	$P_{min} = 18{,}5\ W \cdot 90\% \cdot 60\% = 9.99\ \approx 10W$
Maximum	$P_{max} = 18.5\ W \cdot 90\% = 16.65\ W$

Inlet represents velocity inlet boundary condition at which nitrogen velocity is assumed. Value of the velocity was calculated as a function of adopted nitrogen volume flow rate and a cross-section of the *inlet.*

Heated surface indicates the spot on which radiation heat flux is focused. Value of heat flux is counted as the quotient of lamp power and area of the radiation surface ring according to defined dimensions.

Summarization of two above boundary condition is collected in Table 2.

Tab. 2 Main boundary condition

	$\dot{V}_{N2,min} = 0.05\ \ l/min$	$\dot{V}_{N2,max} = 1\ \ l/min$
$P_{min} \approx 10W$	$\dot{q}$=141468 W/m^2 w=0.03789 m/s	$\dot{q}$=141468 W/ m^2 w =0.7579 m/s
$P_{max} = 16.65\ W$	$\dot{q}$=235545 W/ m^2 w =0.03789 m/s	$\dot{q}$=235545 W/ m^2 w =0.7579 m/s

Wall represents the external surface of the tube covered with the insulation having thickness equal to 15 mm. Properties of the insulation material are based on the data provided by the producer on the official website.

Insulation heat capacity was calculated for volume composition of air (90%) and silica (SiO_2, 10%); glass fiber was skipped. Below, in Table 3 the most important properties of insulation material are shown.

Tab. 3 Insulation material properties

Material:	Pyrogel® XT-E
Composition:	
silica skeleton with porosity:	99.8%
reinforced with glass fiber	
air:	90%
Density:	0.20 g/cm^3
Thermal Conductivity in process average temperature 200 °C :	0.028 W/mK
Heat capacity:	993.2 J/kgK

Biomass fluid was defined as porous medium consisting of nitrogen (fluid) and wood (solid). The parameters of the model of interactions between porous matrix and gas: C (viscous resistance) and D (inertial resistance), were calculated according to the equations (1) to (3):

Momentum equation for porous media [27]:

$$S = -D\nu \cdot v - C\frac{1}{2}\rho_f \cdot v^2 \tag{1}$$

Ergun's equation [25]:

$$\frac{dP}{dx} = -\frac{\beta\mu(1-\varphi)^2}{{d_p}^2\varphi^3} \cdot v - \frac{\alpha\rho_f(1-\varphi)}{d_p\varphi^3} \cdot v^2 \tag{2}$$

Where,

S source term for the momentum equation
ν dynamic viscosity of nitrogen, (kg/ms)
ρ_f density of nitrogen, (kg/m^3)
v velocity of the fluid through porous medium, (m/s)
K permeability of pellet, (m^2), $K = 1 \cdot 10^{-14}\ m^2$ (for spruce biomass pellets [26])
d_p mean particie diameter, (m), $d_{por,SD} = 5 \cdot 10^{-5}\ m$ (for spruce biomass pellets [26])
α,β shape coefficients, (-), α= 1.75, β=150 [25]
φ porosity, (-), calculated by equation (3) [25]:

$$\frac{1}{K} = \frac{\beta(1-\varphi)^2}{{d_p}^2\varphi^2} \tag{3}$$

Results for porosity and drag coefficients are as follows:

$$\varphi = 0.07979$$
$$C = 1.268e + 08$$
$$D = 5.691e + 18$$

4. Results

Effect of nitrogen mass flow rate and lamp power on pellet heating process was assessed based on the temperature of the biomass pellet as a function of time. The values of average, maximum and minimum temperatures are presented in the graphs, Figure 4-6. In Figure 7 are collected contours of temperature distribution after 10 min of the heating process for different values of boundary conditions.

The graphs clearly show that at the maximum value of the nitrogen mass flow rate, the pellet is not able to reach the assumed temperature of the process 400°C even after 2 times longer than was predicted (5 min) duration of the heating process.

The change of nitrogen flow rate has a much greater effect on the analysis results than the change of heat flux. That is because the ratio of the maximum to the minimum nitrogen flow is 20 and the ratio of the maximum to the minimum lamp power is equal to 1.665 only.

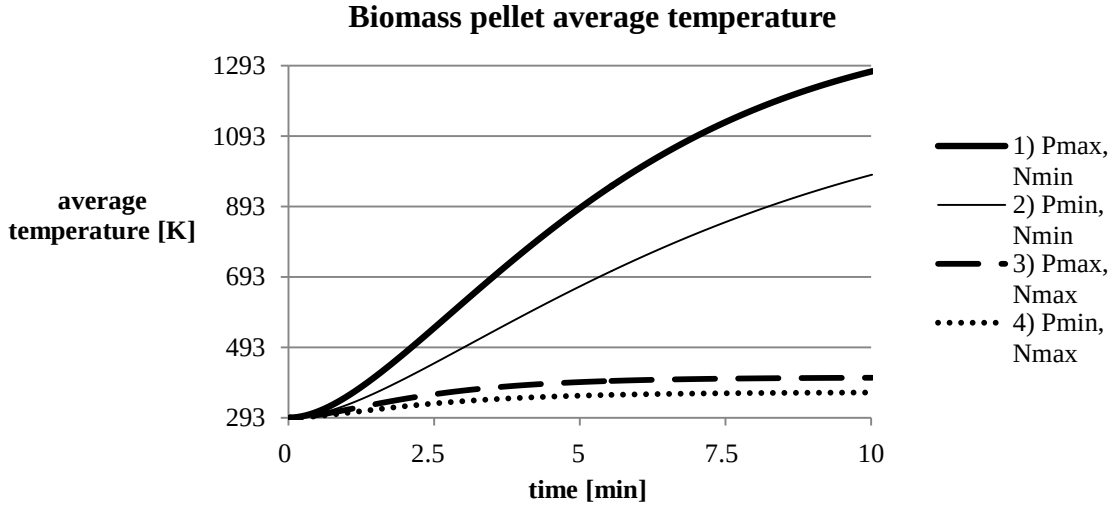

Fig. 4 Average pellet temperature for different sets of boundary conditions

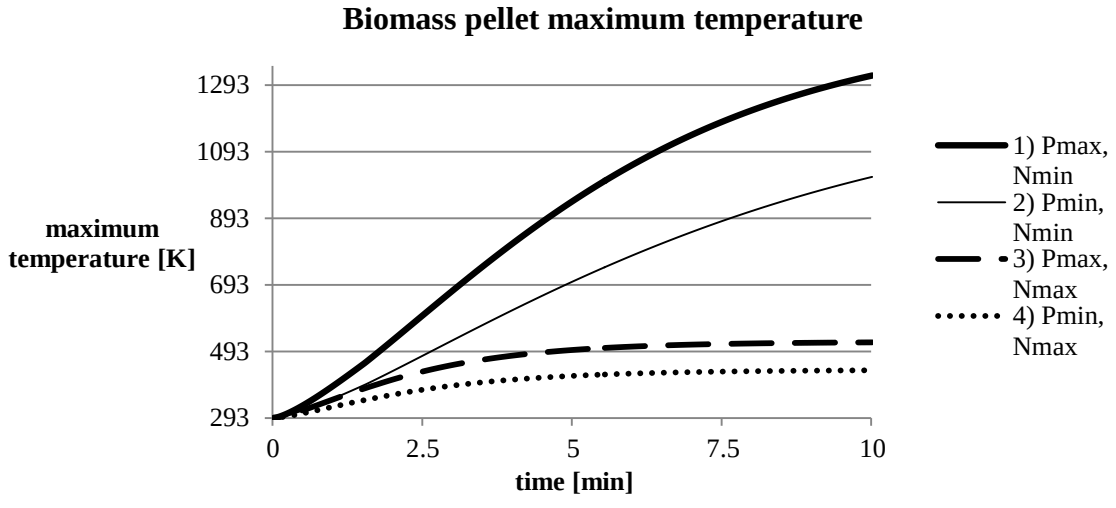

Fig. 5 Maximum pellet temperature for different sets of boundary conditions

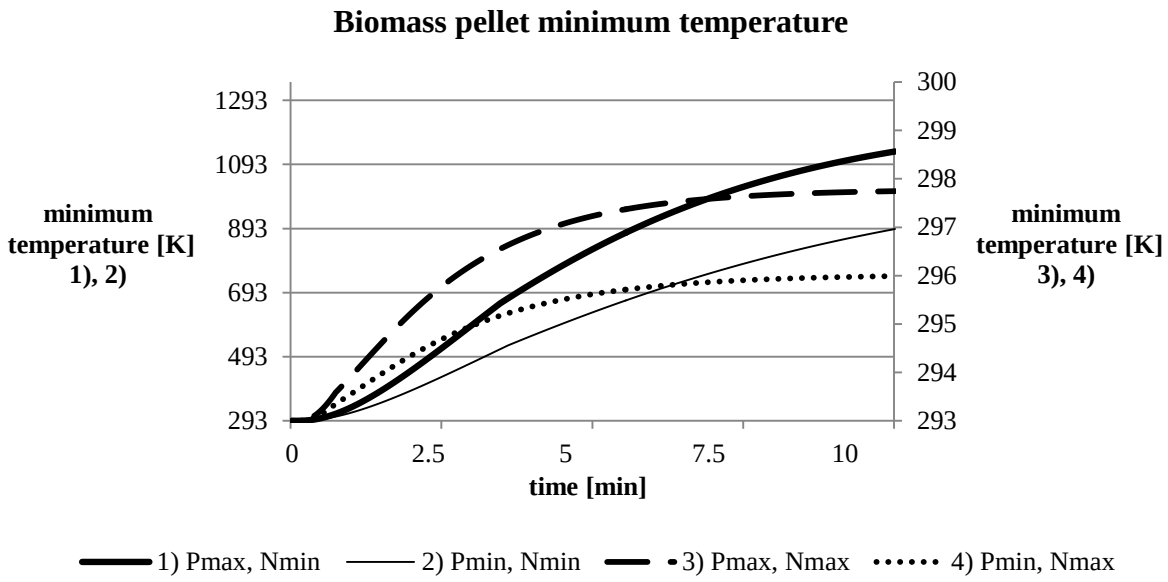

Fig. 6 Minimum pellet temperature for different sets of boundary conditions

Temperature distributions in the reactor (Figure 7) indicate that copper fulfills very well the function of equalizing and uniforming distribution of heat in the reactor. Even for the maximum nitrogen flow the tube temperature is almost uniform.

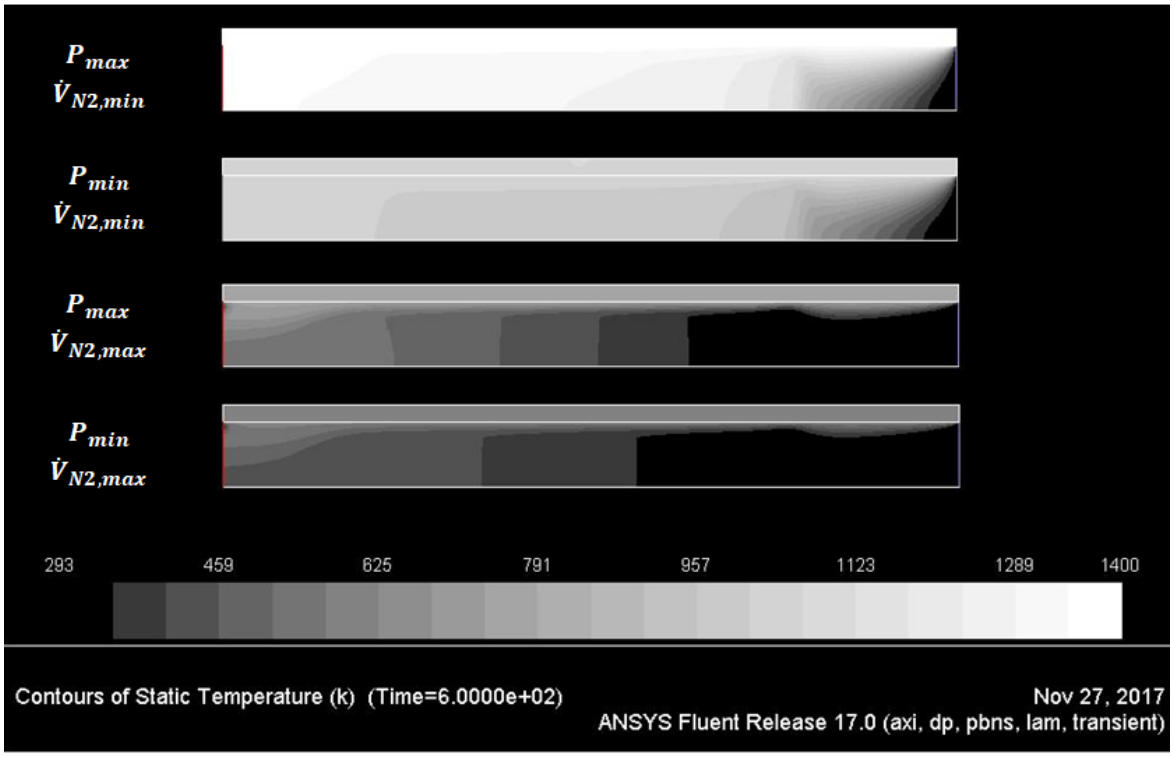

Fig. 7 Temperature distribution in the system after 10 minutes of heating

5. Summary

The paper reviews information about numerical analyzes of the pyrolysis process available in scientific literature. It can be stated, that researchers use similar methods to similar problems. Also in the case of this work solar reactor was adopted as a method investigated in earlier works and commonly operating on an industrial scale (parabolic mirror). The first simulation verified the initial assumptions of the nitrogen volume flow rate and the lamp power. They have shown that nitrogen stream ~1 l/min effectively suppresses the operation of the lamp. On the other hand, the power of the lamp in the regulation range of 60-100% ensures the pellet warming up to the assumed temperature of a process for both extreme adopted value, the difference is visible in the rate of heating. The research will allow selecting more appropriate parameter of gasifier operation for further research.

Acknowledgment

The paper has been prepared within the frame of the project *Study on the solar pyrolysis process of the waste biomass* financed by National Science Centre, Poland (registration number 2016/23/B/ST8/02101).

References

[1] M. Bashir, X. Yu, M. Hassan, Y. Makkawi, Modeling and Performance Analysis of Biomass Fast Pyrolysis in a Solar-Thermal Reactor, (2017). doi:10.1021/acssuschemeng.6b02806.

[2] B.D. Adkins, N. Kapur, T. Dudley, S. Webb, P. Blaser, Experimental validation of CFD hydrodynamic models for catalytic fast pyrolysis, Powder Technol. 316 (2017) 725–739. doi:10.1016/j.powtec.2016.11.060.

[3] Q. Xue, D. Dalluge, T.J. Heindel, R.O. Fox, R.C. Brown, Experimental validation and CFD modeling study of biomass fast pyrolysis in fluidized-bed reactors, Fuel. 97 (2012) 757–769. doi:10.1016/j.fuel.2012.02.065.

[4] X. Yu, Y. Makkawi, R. Ocone, M. Huard, C. Briens, F. Berruti, A CFD study of biomass pyrolysis in a downer reactor equipped with a novel gas – solid separator — I : Hydrodynamic performance, 126 (2014) 366–382. doi:10.1016/j.fuproc.2014.05.020.

[5] X. Yu, M. Hassan, R. Ocone, Y. Makkawi, A CFD study of biomass pyrolysis in a downer reactor equipped with a novel gas – solid separator-II thermochemical performance and products, 133 (2015) 51–63. doi:10.1016/j.fuproc.2015.01.002.

[6] Q. Xiong, J. Zhang, F. Xu, G. Wiggins, C.S. Daw, Journal of Analytical and Applied Pyrolysis Coupling DAEM and CFD for simulating biomass fast pyrolysis in fluidized beds ☪, 117 (2016) 176–181.

[7] B. Liu, K. Papadikis, S. Gu, B. Fidalgo, P. Longhurst, Z. Li, A. Kolios, CFD modelling of particle shrinkage in a fl uidized bed for biomass fast pyrolysis with quadrature method of moment, Fuel Process. Technol. 164 (2017) 51–68. doi:10.1016/j.fuproc.2017.04.012.

[8] D. Wu, A. Zhang, L. Xiao, Y. Ba, H. Ren, L. Liu, Pyrolysis characteristics of municipal solid waste in oxygen-free circumstance, 105 (2017) 1255–1262. doi:10.1016/j.egypro.2017.03.442.

[9] B. Hooshdaran, S.H. Hosseini, M. Haghshenasfard, M.N. Esfahany, M. Olazar, CFD modeling of heat transfer and hydrodynamics in a draft tube conical spouted bed reactor under pyrolysis conditions : Impact of wall boundary condition, Appl. Therm. Eng. 127 (2017) 224–232. doi:10.1016/j.applthermaleng.2017.08.044.

[10] D. Borello, L. Cedola, G. V Frangioni, R. Meloni, P. Venturini, P. De Filippis, B. De Caprariis, Development of a numerical model for biomass packed bed pyrolysis based on experimental validation q, Appl. Energy. 164 (2016) 956–962. doi:10.1016/j.apenergy.2015.08.007.

[11] B. Peters, E. Schro, C. Bruch, Measurements and particle resol v ed modelling of the thermo- and fluid dynamics of a packed bed, 70 (2003) 211–231.

[12] B. Peters, C. Bruch, Drying and pyrolysis of wood particles : experiments and simulation, 70 (2003).

[13] A. Houshang, F. Hoffmann, B. Peters, X. Besseron, Numerical study of the influence of particle size and packing on pyrolysis products using XDEM, Int. Commun. Heat Mass Transf. 71 (2016) 20–34. doi:10.1016/j.icheatmasstransfer.2015.12.011.

[14] C. Guizani, O. Louisnard, F.J.E. Sanz, S. Salvador, Biomass and Bioenergy Gasi fi cation of woody biomass under high heating rate conditions in pure CO 2 : Experiments and modelling, Biomass and Bioenergy. 83 (2015) 169–182. doi:10.1016/j.biombioe.2015.09.017.

[15] M. Sagehashi, Superheated steam pyrolysis of biomass elemental components and Sugi (Japanese cedar) for fuels and chemicals, 97 (2006) 1272–1283. doi:10.1016/j.biortech.2005.06.002.

[16] Q. Eri, J. Peng, X. Zhao, CFD simulation of biomass steam gasification in a fluidized bed based on a

multi-composition multi-step kinetic model, Appl. Therm. Eng. (2017). doi:10.1016/j.applthermaleng.2017.10.122.

[17] F. Motasemi, A.G. Gerber, Multicomponent conjugate heat and mass transfer in biomass materials during microwave pyrolysis for biofuel production, Fuel. 211 (2018) 649–660. doi:10.1016/j.fuel.2017.09.082.

[18] A. Wattana, W. Rakwichian, W. Ekasilp, A. Tusnapucki, Velocity and Temperature Distribution of Flowing Water in a Solar Parabolic Trough Receiver, 6 (2011).

[19] J. Soria, K. Zeng, D. Asensio, D. Gauthier, G. Flamant, G. Mazza, Comprehensive CFD modelling of solar fast pyrolysis of beech wood pellets, 158 (2017) 226–237. doi:10.1016/j.fuproc.2017.01.006.

[20] L. Romagnosi, N. Gascoin, E. El-tabach, I. Fedioun, M. Bouchez, J. Steelant, Pyrolysis in porous media : Part 1 . Numerical model and parametric study, Energy Convers. Manag. 68 (2013) 63–73. doi:10.1016/j.enconman.2012.12.023.

[21] J. Brett, A. Ooi, J. Soria, The effect of internal diffusion on an evaporating bio-oil droplet e The chemistry free case, Biomass and Bioenergy. 34 (2010) 1134–1140. doi:10.1016/j.biombioe.2010.03.006.

[22] Y. Feng, Y. Jiang, X. Li, S. Zhang, J. Qin, Y. Cao, H. Huang, Numerical study on the influences of heat and mass transfers on the pyrolysis of hydrocarbon fuel in mini-channel, Appl. Therm. Eng. 119 (2017) 650–658. doi:10.1016/j.applthermaleng.2017.03.010.

[23] J. Cai, C. Jin, S. Yang, Y. Chen, Bioresource Technology Logistic distributed activation energy model – Part 1 : Derivation and numerical parametric study, Bioresour. Technol. 102 (2011) 1556–1561. doi:10.1016/j.biortech.2010.08.079.

[24] J. Cai, W. Wu, R. Liu, An overview of distributed activation energy model and its application in the pyrolysis of lignocellulosic biomass, Renew. Sustain. Energy Rev. 36 (2014) 236–246. doi:10.1016/j.rser.2014.04.052.

[25] D. A.Nield, A. Bejan, Convection in Porous Media Third Edition, page 12.

[26] Morten G. Grønli, Morten C. Melaaen, Mathematical Model for Wood PyrolysisComparison of Experimental Measurements with Model Predictions, Energy& Fuels, 2000, 14, 791-800.

[27] Fluent 6.3 User's Guide: https://www.sharcnet.ca/Software/Fluent6/html/ug/node272.htm (27/11/2017).

Selective Catalytic Reduction of NO with Ammonia over Functionalized Activated Carbon Promoted with Cu

Marwa Saad[1], Anna Białas[1], Cezary Czosnek[1], Bogdan Samojeden[1], Monika Motak[1]

[1]Faculty of Energy and Fuels, AGH University of Science and Technology, e-mail:anbialas@agh.edu.pl

Abstract

Catalysts for low temperature Selective Catalytic Reduction (SCR) of NO_x with ammonia were obtained from activated carbon (AC). To functionalise AC, the samples were treated with HNO_3 with various concentrations. The materials were additionally modified with urea to form basic sites. So-obtained catalysts were tested in SCR-NH_3 and their thermal stability and selectivity to undesired N_2O was examined as well. The most active sample was promoted with various loadings of copper. The structural, chemical and textural properties of the obtained catalysts were examined with X-ray diffraction, IR spectroscopy and low temperature sorption of nitrogen. The catalytic efficiency of AC systems increased with the acid concentration and 1% of copper was sufficient to attain almost complete NO conversion at low temperatures. The high catalytic activity of the 1Cu/AC sample was ascribed to its hydrophobicity and the presence of carboxylic and N-containing groups. This catalyst also exhibited high specific surface area and contained copper in an amorphous form or high dispersion.

Keywords: Activated carbon, O-, N-containing groups**,** copper, catalyst, NO_x removal

1. Introduction

Nitrogen oxides are mainly formed during fuel combustion. Their main components are NO and NO_2 designated NOx. NOx cause acid rains and take part in the formation of photochemical smog, which influence human health and the environment [1-3].

Selective Catalytic Reduction (SCR) of NOx with ammonia is the most efficient method of the reduction of NOx emissions from stationary sources and is widely used in EU, USA and Japan. SCR-NH_3 catalysts must fulfil many requirements e.g.: to be active in the reduction of NOx under oxidizing atmosphere and not sensitive to the changes in oxygen content, to be selective to N_2 and not form N_2O, a greenhouse gas, more harmful than CO_2. Moreover, they must exhibit good stability and not undergo structural or chemical changes under operation conditions [2].

Nowadays, the most frequently applied catalysts in the SCR process are made in the form of a monolith with vanadium as an active component and titania as a support with the addition of tungsten oxide or molybdenum oxide promotors to increase the catalyst lifetime. On the other hand, it was found that the same active component showed higher NO conversion supported on activated carbon than on Al_2O_3, TiO_2, zeolite or metal-organic framework [4-6]. An alternative technology uses activated carbons for simultaneous removal of SOx and NOx.

Carbons containing oxygen and/or nitrogen surface functionalities, used as catalysts or as supports for active components, have been widely investigated because the carbon surface is relatively inert, which prevents side reactions and the cost of conventional carbon materials is lower than other supports. What is more, carbon materials can be produced in various forms (granules, fibers, foams, homogeneous stones, fabrics, blankets, etc.) and an active phase deposited on activated carbon can be easily recovered by the combustion of the support. Treatment of carbonaceous materials with acids or N-containing molecules results in the increase of their acidic or basic properties which are crucial for the adsorption of NH_3 and NO, respectively [7-13].

Strong or weak oxygen functional groups can be introduced on the surface of carbon by the treatment with an acid [14]. The acidic character of the surface depends on the type of an oxidant [15-17] and the number of the groups depends additionally on the concentration of the oxidant, the temperature of treatment and its duration.

HNO_3 was most often used to change the type and number of oxygen-containing surface groups because it causes the higher increase in acidity than other oxidants, gaseous or in solution, which leads to the higher increase in activity.

N-modification is also beneficial for activated carbon stability, AC samples treated with urea undergo oxidation to CO_2 at higher temperatures [18].

The impact of transition metal deposition on the activated carbon has been investigated as well [19,20] e.g. activated carbon supported Cu was more active than alumina one this effect was ascribed to the better distribution of Cu. N- functionalized AC promoted with Mn or Fe oxides/hydroxides were also investigated [21,22]. However, triple functionalization by acidic treatment, N-groups introduction and promotion with copper was not yet investigated.

The aim of the presented work was the synthesis of Cu/doubly functionalized AC catalysts for the Selective Catalytic Reduction of NOx with ammonia as well as the examination of their activity, selectivity and thermal stability taking into consideration the preparation variables such as pre-oxidization degree (HNO_3 concentration), modification with urea (as the precursor of N-groups) and Cu loading (wt.%). The physicochemical properties of the obtained samples were determined as well, using X-ray diffraction, FT-IR spectroscopy and low temperature N_2 sorption.

2. Experimental

2.1 Catalysts preparation

2.1.1 Acidic treatment of activated carbon

Activated carbon (designated AC) was of the N/M type, produced by Gryfskand, Hajnówka, Poland. The first step in its treatment was the oxidation with nitric acid - concentration 10M or 14M, at 90^{o}C for 2 hours. The amounts used were 30 cm^3 of the HNO_3 solution per 1 g AC. Then the sample was washed to ca. neutral pH with distilled water and filtered. Finally, the preparations were dried at 110^{o}C for 24 hours (designated 10 or 14).

2.1.2 Introduction of N-groups

The introduction of N groups was carried out by incipient wetness impregnation with the urea solution (5 wt. %). Then the sample was dried at 110^{o}C for 24 hours. After that thermal decomposition was conducted in the flow of O_2/He (2.25%), at a rate of 100 cm^3/min, at 350^{o}C, for 2 hours. The obtained samples (designated 10U or 14U) were ground and sieved to obtain 0.25 - 1 mm fraction. At the end of this step, functionalized activated carbon was ready for the deposition of an active phase.

2.1.3 Active phase deposition

Copper was deposited on functionalized carbon - 14U, by incipient wetness impregnation with a solution of $Cu(NO_3)_2$, using various concentrations of the salt to obtain 1%, 5% or 10% Cu loading. The samples were dried at 110^{o}C for 48 hours and after that the precursor decomposition was carried out in the flow of O_2/He (2.25%), at a rate of 100 cm^3/min, at 250^{o}C for 1 hour. The samples were designated 14U1Cu, 14U5Cu or 14U10Cu.

2.2 Catalyst characterization

2.2.1 Catalytic tests

The activity tests in the Selective Catalytic Reduction of nitrogen oxide by ammonia were performed at atmospheric pressure in a fixed-bed flow reactor containing 0.2 g of a catalyst (0.25 - 1 mm fraction). The temperature inside the reactor was measured by a thermocouple, near the center of the catalyst, with an electronic temperature controller (Lumel RE19). The reaction mixture contained 800 ppm NO, 800 ppm NH_3, 3.5 vol. % O_2 and He balance. The total flow was 100 cm^3/min. The concentrations of NO and N_2O and CO_2 were analyzed by a FT–IR detector (ABB 2000 AO series). The catalytic tests were performed at temperatures ranging from 140 to 400 or to 450°C in the case of functionalized carbonaceous and 14U1Cu samples, for 1 h at each temperature. NO conversion was calculated according to the equation (1):

$$NO\ conversion = \frac{NO\ in - NO\ out}{NO\ in} * 100\% \quad (1)$$

Where,

NOin is the inlet NO concentration
NOout is the outlet NO concentration

2.2.2 Physicochemical characterization

The catalysts were characterized by X-ray diffraction, infrared spectroscopy and low-temperature nitrogen sorption.

The XRD measurements were carried out using a PANalytical–Empyrean diffractometer, equipped with Cu Ka (λ = 1.5406Å) radiation source, within the 2θ range from 5 to 90° and with a step of 0.02°/min. XRD measurements were performed for all samples at room temperature.

Fourier-transform–infrared (FT–IR) spectra were obtained for fresh activated carbon, functionalized AC and Cu containing carbonaceous materials with a Perkin Elmer Frontier FT–IR spectrometer. Sixty scans were taken for each spectrum for wavenumbers from 400 to 4000 cm^{-1} registered with a resolution of 4 cm^{-1}. The catalyst samples were mixed with KBr at a 1:300 ratio and pressed into pellets.

Specific surface area, pore volume and size were determined from nitrogen sorption at –196°C. The measurements were performed with a GeminiV2.00 model 2380 apparatus (Micromeritics). Before the measurements, the catalysts were outgassed at 150°C for 2h. The isotherms were used to determine the surface area using the BET method and the micropore volume was assessed by the single point method at p/p_0=0.3.

3. Results and discussion

3.1 Functionalised activated carbon

3.1.1 NO SCR over oxidised N-containing AC

Fig.1 shows the effect of the concentration of nitric acid used for AC oxidation (at the pre-oxidation step followed by urea impregnation) on the sample activity in Selective Catalytic Reduction of NO with ammonia. For the 10U sample, the conversion of nitrogen oxide increased from 28% at 140°C to 86% at 450°C, whereas over the 14U sample this conversion increased from 76% at 140°C to 96% at 450°C. The sample treated with the more concentrated acid turned out to be the better catalyst in SCR which can be explained by forming a higher number of acidic sites which may have additionally influenced the distribution of urea and thus formation of basic groups. The difference in samples activity was more pronounced in the low temperature SCR range.

To check the selectivity of these catalysts, the N_2O formation was analyzed and is presented in Figure 2. The similar amount of N_2O was formed over both samples at 140°C – ca. 70 ppm. The significant difference was observed at 350°C – 90ppm over 10U and 180 ppm over 14U, and at the end of SCR tests at 450° C these concentrations were equal to 175 ppm for 10U and 195 ppm for 14 U. Although, the 14U catalyst was more active - the measured NO conversion was close to 100% as seen in Fig. 1, it caused the formation of higher amounts of N_2O. This could result from an excess of labile surface oxygen formed during AC acid treatment with more concentrated HNO_3 [16].

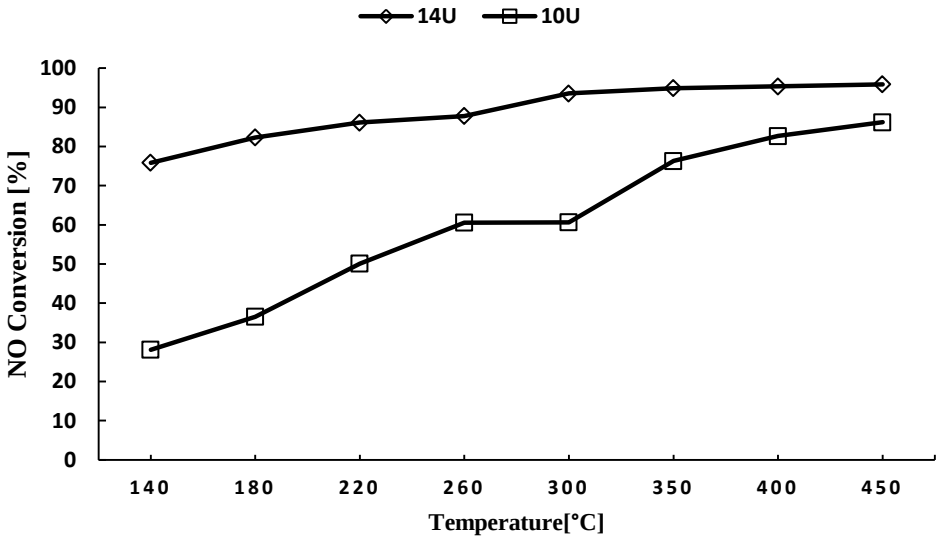

Fig.1 NO conversion over activated carbon oxidized with 10 or 14 M HNO_3 and N-doped.

Since a carbon catalytic material can be burnt under oxygen containing atmosphere, to examine the stability of our functionalized carbon samples the CO_2 formation was observed as presented in Figure 3. For the 10U sample the CO_2 concentration increased slowly from 60 ppm at 140°C to 90 ppm at 260°C and then a rise in the CO_2 formation to 3860 ppm at 450°C was observed. In the case of the sample treated with 14M HNO_3 the concentration of CO_2 increased from 140 ppm at 140°C to 710 ppm at 260°C until it reached 11420 ppm at 450°C.

It is additional negative influence of oxygen-containing surface species, 14M HNO_3 caused the formation of more oxidizing sites on AC than those formed during treatment with 10M HNO_3 and as a result faster burning of AC occurred over the 14U sample.

To explain the reasons of different catalysts activity, their structure, the presence of chemical groups and textural properties were determined.

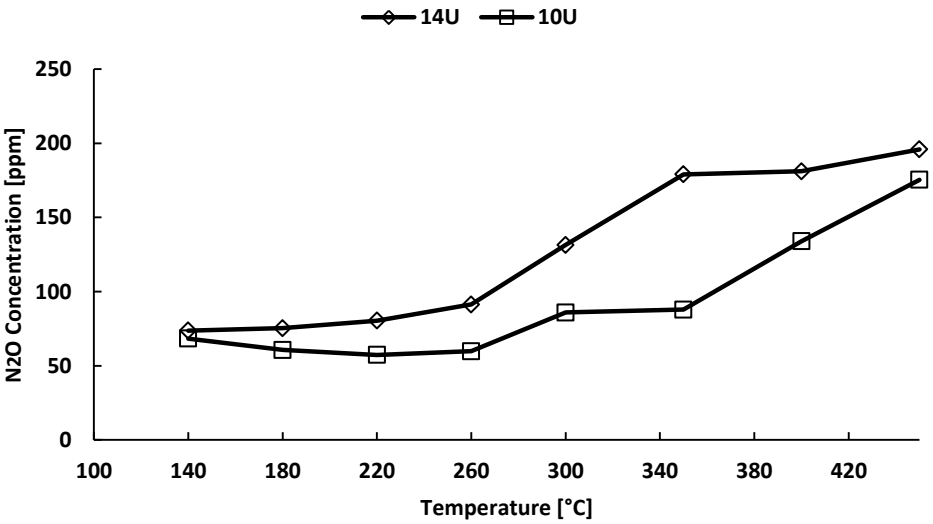

Fig. 2 N_2O formation over activated carbon oxidized with 10 or 14MHNO_3 and N-doped.

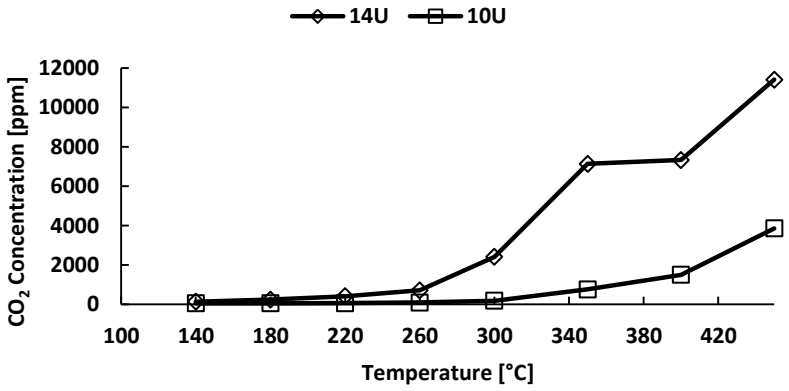

Fig. 3 CO_2 formation over activated carbon oxidized with 10 or 14M HNO_3 and N-doped.

3.1.2 Structural, chemical and textural properties of oxidised, N-containing AC

The structure of carbon materials was examined with powder X-ray diffraction, its results are shown in Figure 4. For all samples wide bands are observed which suggest the presence of small crystallites. Three diffraction bands at ca 2θ = 25 and 43 and 77° can be attributed to (002), (101) and (110) planes, respectively, of the graphite phase of carbon [01-075-1621]. No major differences for 10U sample treated with 10M nitric acid were observed as compared to 14U

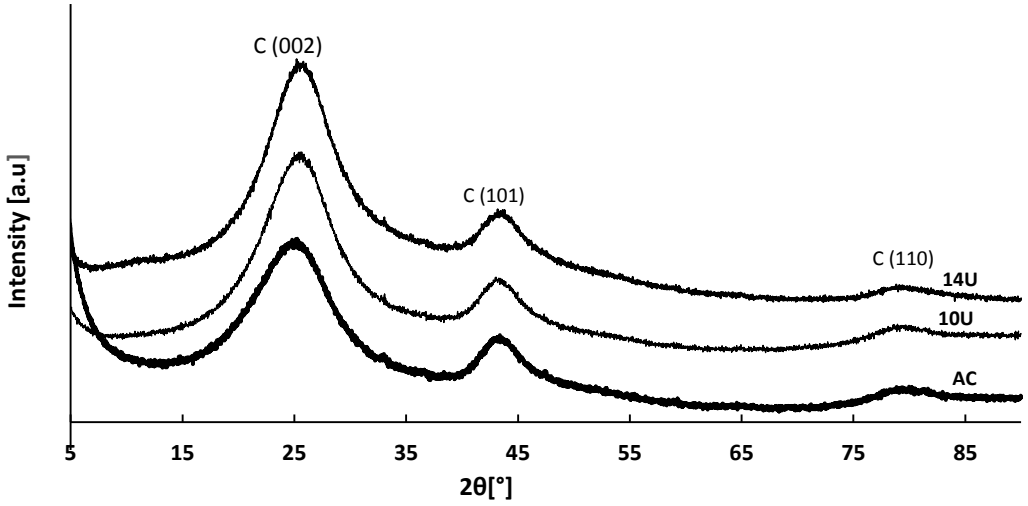

Fig. 4 XRD pattern of activated carbon and AC after treatment with HNO_3 and urea.

The presence of functional groups in the obtained carbon materials was examined with IR spectroscopy. As seen in Figure 5 for activated carbon peaks at ca. 1120, 1560, 1715 and 3430 cm^{-1} can be distinguished. They can be ascribed to N-containing, non-aromatic carboxylic groups and water, respectively. Peak at 1120 cm^{-1} can origin from C-N (aliphatic) or N-H groups, the band at 1715 cm^{-1} is typical of carbonyl stretching of carboxylic group, the peak at 1560 cm^{-1} is ascribed to the stretching mode of carboxylic anions, whereas peak at 3430 cm^{-1} can be attributed to absorbed water [23,24]. After acid treatment and nitrogen deposition the peaks coming from carboxylic group became more intensive for the sample which was pretreated with nitric acid of higher concentration.

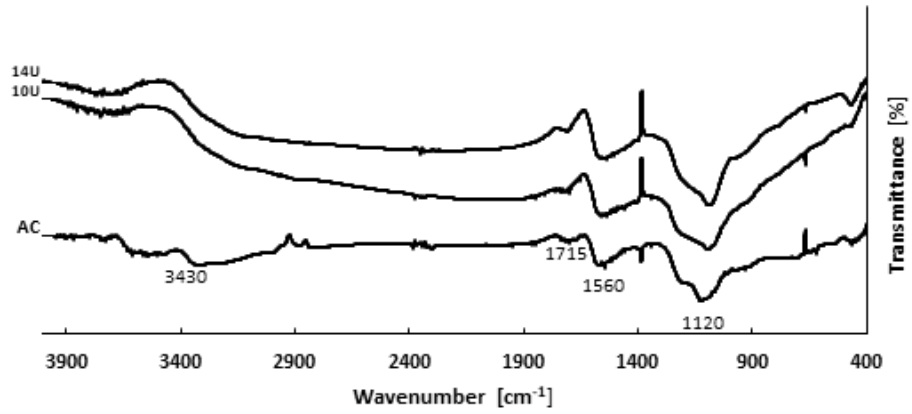

Fig.5 Fourier transform infrared spectra of activated carbon and its samples oxidized with 10 or 14M nitric acid and N-doped.

The amount of nitrogen containing groups grew as well. After acid treatment followed by urea impregnation and decomposition, the samples 10U and 14U became hydrophobic, which is confirmed by the disappearance of the band at 3430 cm^{-1}.

The textural parameters of carbonaceous materials which can influence catalytic activity are summarized in Table 1. Activated carbon exhibited the BET specific surface area over 700m^2/g, its micropore volume was equal to 0.36cm^3/g. After mild oxidation with 10M HNO_3 followed by urea deposition and decomposition the SSA_{BET} increased by ca 100m^2/g and micropore volume was above 10% higher as well. The oxidation with the more concentrated acid resulted in the decrease of surface area and micropore volume by ca 10%, maybe a part of micropores in AC was destroyed under these more severe conditions. On the other hand, this more developed surface did not result in higher catalytic efficiency (cp, Figure 1). The average pore width was for the all carbonaceous materials close to 2nm, confirming their microporosity.

Tab. 1 Specific surface area and pore volume and size of carbonaceous samples

Sample	Specific surface area [m^2/g]	Micropore volume [cm^3/g]	Pore width [nm]
AC	722	0.36	2.00
10U	829	0.41	1.96
14U	643	0.32	1.97
14U1Cu	623	0.31	1.97
14U5Cu	348	0.17	1.97
14U10Cu	372	0.19	1.98

3.2 Cu doped functionalized activated carbon

3.2.1 NO SCR over copper/carbonaceous material

The treatment of AC with the more concentrated acid resulted in the more efficient catalyst in SCR. Although its selectivity to N_2O was higher and thermal stability lower, the differences between 10U and 14U samples were small in the low temperature range and the 14U catalyst was chosen for promoting it with copper to improve its activity. Carbonaceous materials were doped with small amounts of copper – 1, 5 or 10%, and tested in SCR of NO (Figure 6). Copper increased the conversion of NO over functionalized AC to above 90% at 140^{o}C for 14U10Cu and 14U1Cu samples and to about 95% at 220^{o}C for all copper promoted samples. This efficiency was retained for the 14U1Cu catalyst to 450^{o}C.

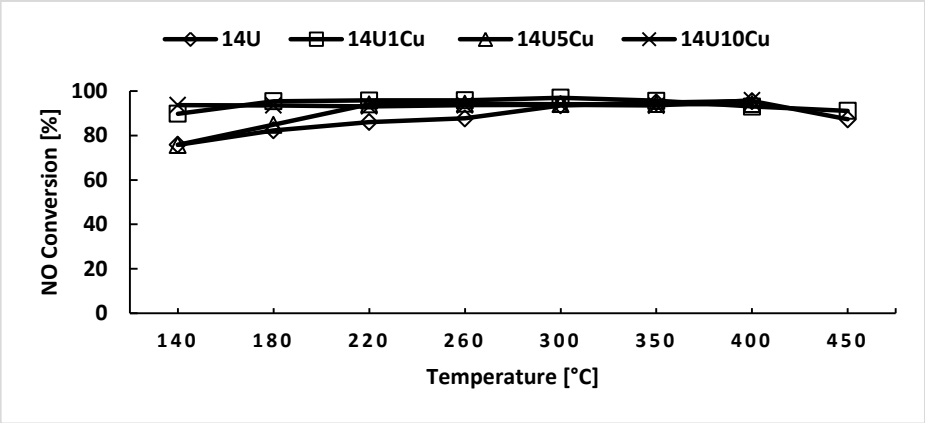

Fig. 6 NO conversion over Cu promoted activated carbon oxidized with 14M HNO_3 and N-doped.

As one can predict the addition of an oxidative metal to the functionalized AC caused the increase in N_2O formation (Figure 7). In the case of the 14U1Cu sample N_2O concentration grew by ca 25 and 50% at 180 and 220°C, respectively, in comparison to the 14U sample. The maximum N_2O formation over this sample was achieved at 350°C. The preparations with higher copper concentrations caused about twice increase in N_2O formation compared to the 14U catalyst, with the maximum at 300°C. The decrease in N_2O formation for higher temperatures arose most probably from the loss of catalyst due to combustion of the support. It should be mentioned, however, that at the most interesting lower temperature region (at 140°C), this negative effect connected with the increased formation of N_2O was not observed for the catalysts with low Cu content (1%).

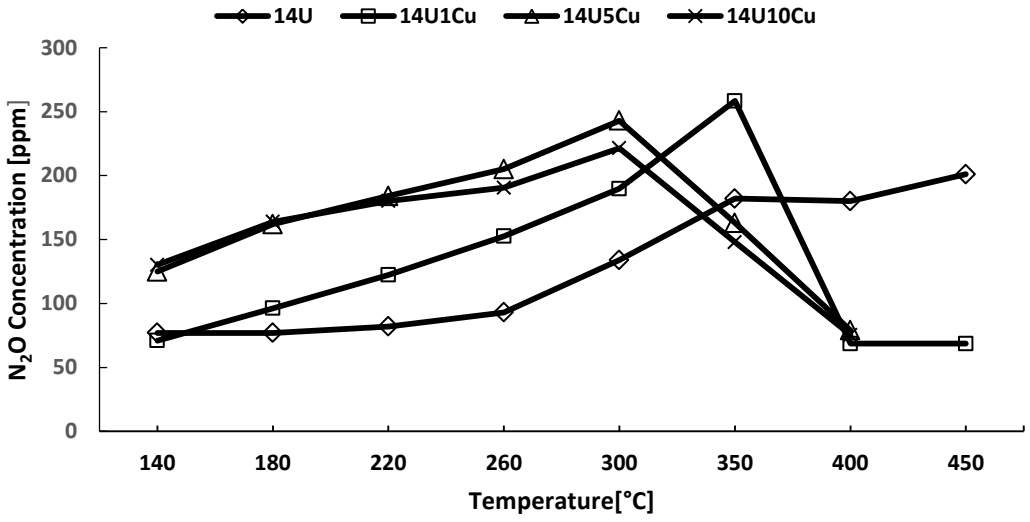

Fig. 7 N_2O formation over Cu promoted activated carbon oxidized with 14M HNO_3 and N-doped.

Copper addition should also lower the thermal stability of carbonaceous materials. As seen in Figure 8, 1% Cu content had almost no influence on the catalyst stability to 300°C in comparison to HNO_3 and urea functionalized AC. And in the 14U1Cu sample the carbonaceous component was still present at 450°C. For the catalysts with higher copper concentration fast combustion of functionalized AC material began at 260°C and at 450°C the carbonaceous part of the catalysts was burnt out. Thus it may be concluded that the amount of promoting copper may be tailored so as to keep high stability of the carbonaceous support. Additionally, as the most interesting temperature region for AC-based catalysts is under 250°C, it may be concluded is the stability of triply functionalized materials studied here is satisfactory.

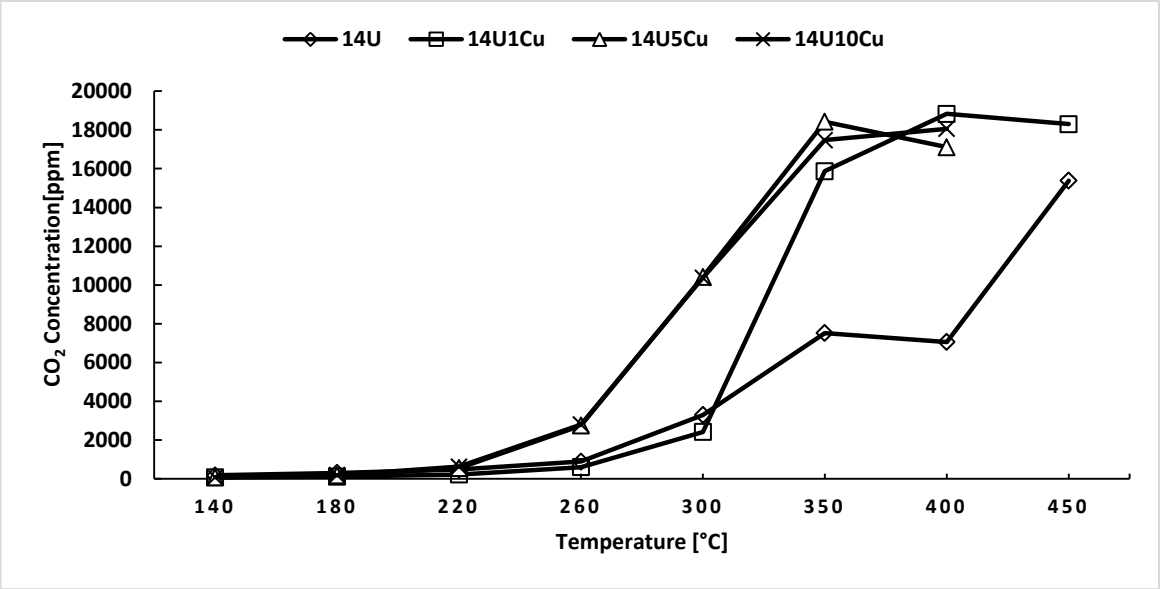

Fig. 8 CO_2 formation over Cu promoted activated carbon oxidized with 14M HNO_3 and N-doped.

3.2.2 Structural, chemical and textural properties of copper/carbonaceous catalysts

To examine the structure of copper present in carbonaceous materials XRD patterns were recorded (Figure 9). For the sample with 1% of copper only the graphite phase is visible as in activated carbon and functionalized AC. Thus it may be concluded that Cu oxide or hydroxide is most probably either very well dispersed over the surface or is present in the amorphous form. The 5% addition of copper caused the appearance of the reflections at 2θ ca 35.5 and 36.5°. They can be ascribed, respectively, to the most intensive (002) plane of CuO [00-045-0937] and (111) plane of Cu_2O [01-078-2076]. This reduced copper oxide was the more abundant crystalline phase in the 14U5Cu sample. Further increasing in copper content to 10% resulted in turning up a more crystalline copper containing phases. The reflections at 2θ ca 29.4, 42.2, 61.2, 73.5° can be attributed to the (110), (200), (220) and (311) planes of Cu_2O, respectively, whereas, the reflections at 2θ ca 38.5 and 48.7 arise from the (111) and (-202) planes of CuO, respectively. Also pure copper is present in the 14U10Cu sample with the reflections at 2θ ca 43.2 and 50.4° corresponding to the (111) and (200) planes, respectively, of Cu [01-070-3039]. The presence of copper(I) oxide and copper resulted from the reductive properties of carbonaceous materials.

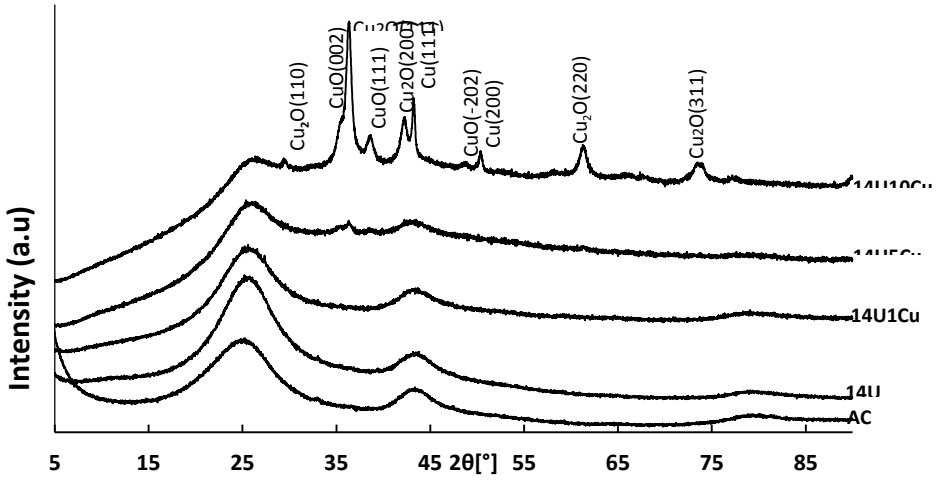

Fig. 9 XRD pattern of activated carbon and Cu promoted AC oxidized with 14M HNO_3 and N-doped.

The changes in the presence of chemical groups after introducing copper species were observed by means of FT IR spectroscopy (Figure 10). The deposition of 1% of Cu did not change significantly the intensity of peaks coming from carboxylic groups and the sample was hydrophobic – the absence of the band from adsorbed water at ca 3430 cm^{-1}. For the samples with a larger content of copper the decrease in bands from carboxylic and nitrogen containing groups is observed, which could be caused by their reaction with copper or oxidation. These samples lost their hydrophobicity, because the peak typical of adsorbed water appears.

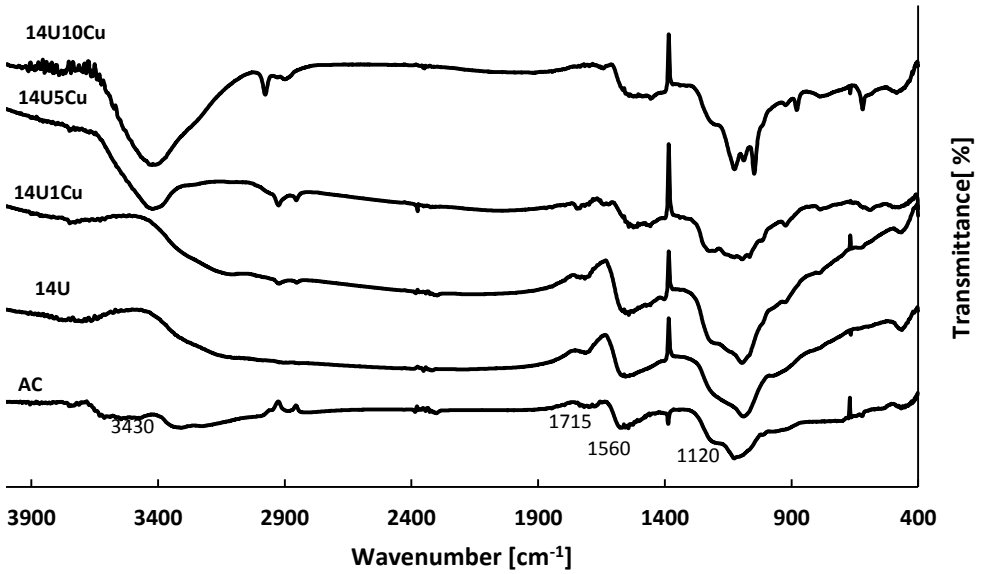

Fig. 10 FT IR spectra of activated carbon and Cu promoted AC oxidized with 14M HNO_3 and N-doped.

The deposition of 1% of copper on functionalized carbonaceous material caused an insignificant specific surface area decrease, the micropore volume remained stable as well (Table 1). The increase in the Cu content resulted in almost 50% lowering of SSA_{BET} and pore volume. As discussed earlier (Figure 9) higher copper concentration brought about the appearance of crystalline phase, with small crystallites in the case of the 14U5Cu sample. They may have been formed either on the outer sides of AC particles or at the inlet to the pores, thus blocking the narrow pores.

4. Summary

The carbonaceous catalysts for low temperature NO SCR with ammonia were obtained from activated carbon. To functionalize it, AC was first treated with nitric acid with the concentration of 10 or 14M, and subsequently impregnated with 5% of urea. As a result, carboxylic and N-containing groups were formed on AC. Mild oxidation with acid caused the development of additional specific surface area of carbonaceous material, but did not result in its better catalytic activity in NO SCR. Better catalytic efficiency resulted from the higher concentration of carboxylic and N-containing groups, formed on the sample oxidised with more concentrated HNO_3. This sample was chosen for promoting with various amounts of copper to improve its catalytic activity at low temperatures. 1% of copper improved catalytic activity without worsening the thermal stability of the functionalised AC sample or significant increase in undesired N_2O formation. This lowest copper content, in contrast to higher 2 or 5% copper concentrations, allowed to retain the advantages of functionalised carbonaceous materials – hydrophobicity, high concentration of carboxylic and N-containing groups and well developed specific surface area and additionally to obtain well dispersed amorphous copper sites.

Further investigation should focus on the synthesis of a more selective and thermally stable catalyst. The first step could deal with copper and urea concentration optimisation, and the next with promoting with an additional metal.

Acknowledgment

Marwa Saad is grateful to the Ministry of Foreign Affairs and the Ministry of Science and Higher Education of the Republic of Poland for the Ignacy Łukasiewicz Scholarship. The investigation was carried out due to the statutory work funds of the Energy and Fuels Faculty, AGH UST (11.11.210.373).

References

[1] L. Glassman, *Combustion,* 2nd Ed., Academic Press, New York, pp. 142-159, 1987.
[2] S. Hjalmar, *NOx Control Technologies for Coal Combustion*, IEA Coal Research, London, 1990.
[3] S. Wood. Select the right NOx control technology, *Chemical Engineering Progress*, 1994, pp. 32.
[4] J. A. Loiland, R. F. Lobo. Low temperature catalytic NO oxidation over microporous materials, *Journal of Catalysis*, 2014, 311, pp. 412-423.
[5] I. Mochida, M. Ogaki, H. Fujitsu, Y. Komatsubara and S. Ida. Catalytic activity of coke activated with sulphur acid for the reduction of nitric oxide, *Fuel*, 1983, 62, pp.753- 867.
[6] Y. Komatsubara, S. Ida, H. Fujitsu, I. Mochida. Catalytic activity of PAN-based active carbon fiber (PAN-ACF) activated with sulphuric acid for reduction of nitric oxide with ammonia, *Fuel*, 1984, 63, pp 1738-1742.
[7] K. Kusakabe, H. Kawamura, H. J. Kim and Sh. Moroka. Effect of SO_2 on coke catalyzed reduction of NO by ammonia, *Fuel*, 1990, 69, pp.571- 604.
[8] E. Richter, H. J. Schmidt and H. G. Schecker. Adsorption and Catalytic Reactions of NO and NH_3 on Activated Carbon, *Chemical Engineering Technology*, 1990, 13, pp. 332-340.
[9] L. Singoredjo, F. Kapteijn, J. A. Moulijn and H. P. Boehm. Modified activated carbons for the Selective Catalytic Reduction of NO with NH_3, *Carbon*, 1993, 31, pp. 213-222.
[10] S. N. Ahmed, R. Baldwin, F. Derbyshire, B. McEnaneyj and J. Stencel. Catalytic reduction of nitric oxide over activated carbons, *Fuel*, 1993, 72, pp 146–154.
[11] S. Biniak, G. S. Szymanski, J. Siedlewski, A. Swiatkowski. Catalytic reduction of nitric oxide over activated carbons, *Carbon*, 1997, 35, pp. 1689-1849.
[12] C.L. Mangun, K.R. Benak, J. Economy, K.L. Foster. The influence of surface modification of activated carbon with gaseous ammonia on adsorption properties, *Carbon*, 2001, 39, pp. 1809-1820.
[13] J. Lee, D. J Suh, S. Park and D. Park. Effects of pyrolysis conditions on the reactivity of char for the reduction of nitric oxide with ammonia, *Fuel*, 1993, 72, pp. 935-939.
[14] J. K. Lee, T. J. Park, and D. Park. Catalytic activity of chars prepared by fluidized bed pyrolysis for the reduction of nitric oxide with ammonia, *Ind. Eng. Chem. Res.*, 1993, 32, pp. 1882-1887.
[15] L. Singoredjo, F. Kapteijn, J. A. Moulijn and H. P. Boehm. Modified activated carbons for the selective catalytic reduction of NO with NH_3, *Carbon*, 1993, 31, pp. 213-222.
[16] L. Ewbank. Stability of functionalized activated carbon in hot liquid water, *Carbon,* 2014, 77, pp. 143-154.
[17] M. Wang, J. Zhu, Y. Yan and Q. Xu. Novel N-doped porous carbon microspheres containing oxygen and phosphorus for CO_2 absorbent and metal-free electrocatalysts, *RSC Adv.*, 2015, 5, pp. 28080-28084.
[18] M. Koebel, M. Elsener, and G. Madia. Reaction Pathways in the Selective Catalytic Reduction Process with NO and NO_2 at Low Temperatures, *Journal of Industrial and Engineering Chemistry Research, American Chemical Society*, 2001, 40, pp. 52-59.
[19] K. H. Chuang, Ch. Yuan, L, M. Y. Wey. Y. N. Huang. NO removal by activated carbon-supported copper catalysts prepared by impregnation, polyol, and microwave heated polyol processes, *Applied Catalysis A: General*, 2011, *397*, pp. 234-240.
[20] M. E. Gálvez, A. Boyano, R. Moliner, M. J. Lázaro. Low-cost carbon-based briquettes for the reduction of NO emissions: Optimal preparation procedure and influence in operating conditions, *Journal of Analytical and Applied Pyrolysis*, 2010, 88, pp. 80-90.
[21] T. Grzybek, J. Klinik, M. Motak, H. Papp. Nitrogen-promoted active carbons as catalytic supports: 2. The influence of Mn promotion on the structure and catalytic properties in SCR, *Catal Today*, 2008, 137, pp. 235-241.
[22] B. Samojeden, T. Grzybek. The influence of the promotion of N-modified activated carbon with iron on NO removal by NH_3-SCR (Selective catalytic reduction), *Energy*, 2016, 116, pp. 1484-1491.
[23] R. Bansal, M. Goyal. *Activated Carbon Adsorption*, Taylor&Francis Group, 2005.
[24] T. J. Bandosz, C. O. Ania. Activated carbon surface in environmental remediation, *Surface Chemistry of Activated Carbon and its Characterization*, Elsevier, 2006.

Prospects for development of conventional combined heat and power plants in Poland - a case study

Czekaj Anna [1], Marciniec Jakub [1], Michałkiewicz Martyna [1]

[1]Power Engineering (2nd sem. MSc), Silesian University of Technology, e-mail: czekaj.an@gmail.com, kuba.mar@interia.pl, me.michalkiewicz@gmail.com

Abstract

This paper presents a small-scale feasibility study, investigating the financial profitability of setting a new coal-fired heat & power plant in Poland. The domestic energy market was analyzed in terms of political, economic, social, technological, legal and environmental aspects. Thermodynamic cycle of the plant was simulated with the use of EES software. This was followed by discounted cash flow analysis, resulting in calculation of basic profitability indicators. The investment turned out to be unprofitable. Also, major risk factors were taken into account in a sensitivity analysis, which considered fluctuations of energy prices on the market and possible legal constraints in the future. Presentation of the outcome is followed by final conclusion about the analyzed solution.

Keywords: Conventional power plant, energy policy in Poland, profitability of energy system, mercury removal, energy market conditions

1. Introduction

The aim of this paper is to examine the profitability of construction of a new Combined Heat & Power (CHP) plant in Jaworzno city (Silesian Voivodeship, Poland).

1.1 Market Identification

Over the past several years, about 30 000 new inhabitants have come to the Silesian Province every year as a part of the internal migration. Twenty thousand people, in turn, move to other regions of Poland, which gives about 10 000 new inhabitants every year in this area [1]. Due to attractive living and working conditions in the central part of the Silesian Voivodeship, this trend is likely to increase, especially in urban areas.

The primary assumption for this study is a rapid increase of Jaworzno city population and construction of several new large housing estates. As a consequence, a new market for heat delivery is identified. It is assumed that a dedicated research has indicated the need for new 115 megawatts of thermal power, which exceeds the already installed capacity.

1.2 Analyzed Solution

A new heat & power plant construction is analyzed. The chosen technology is similar to already existing units. An extraction steam turbine is used, powered by a Circulating Fluidized Bed (CFB) hard-coal-fired boiler. Hot water is produced in a steam-condensing shell & tube heat exchanger. The installation is not a Centrally Dispatched Unit governed by Electric System Operator. A detailed process description is given in Section 3.

1.3 Criteria for Solution Assessment

The project appraisal is based on the economic analysis. The most important results of the study are the profitability indicators: Net Present Value (NPV), Internal Rate of Return (IRR) and Discounted Payback Time (DPB).

2. Market Analysis

For the purpose of this study a market analysis was performed, according to the PESTEL methodology (regarding **P**olitical, **E**conomic, **S**ocial, **T**echnological, **E**nvironmental and **L**egal aspects) [2].

2.1 Political Factors

The European Union's policy on energy development envisages combating the global warming, increasing renewable energy sources share in the system, and promoting high-efficiency technologies. In addition, the Council of the European Union has been involved in the matter of low emissions in large agglomerations in the last couple of years.

From the purposes mentioned above, the construction of a coal-fired unit in the current situation is not an advisable solution for the EU, but it may be argued that the proposed CHP would be highly efficient and would reduce households with individual heating systems - this could minimize the problem of low emissions in the area.

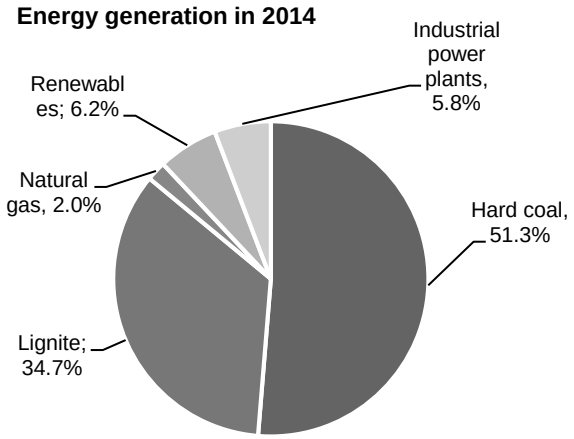

Fig. 1 Electric energy production structure for Poland.

The Polish electricity system is based on fossil fuels, with a small share of renewables (Figure 1) [3]. This is caused by the high availability of coal in the country. The country's balance sheet assets are estimated at 56 220 million tons in 2015, of which more than 70% is energy of coal [4].

A new coal-fired facility will have a positive impact on the economy of the country for several reasons:

- New market for coal in Poland;
- A modern facility located in the agglomeration will reduce the problem of low emissions in the area;
- Heat sales will increase the comfort and prosperity of local residents;
- Due to growing smog problems in the agglomeration, CHP may reduce the level of harmful air pollution in the area.

A new CHP plant on the Polish market in the current energy policy situation may be met with the disapproval of the European Council, but when the smog problem develops in the area, a new unit, easily controlled in terms of emissions, might become an argument for construction.

2.2 Economic Factors

The economic factors taken into consideration were: coal, heat and electricity prices and inflation rate. Coal prices trend for Poland (2011-2017) is presented in Figure 2. Transportation cost is estimated as 15% of base price. Electricity prices (inflation-updated to 2017) are shown in Figure 3. Inflation rate and its assumed future

values are depicted in Figure 4. Recent values and trends were essential for the choice of reliable economic assumptions.

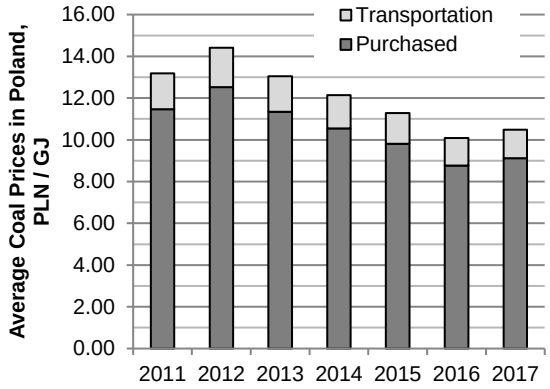

Fig. 2 Coal prices at Polish market [5].

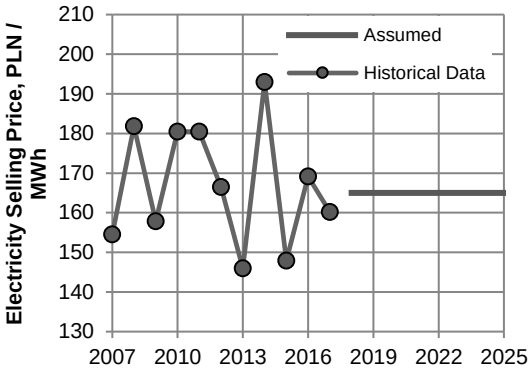

Fig. 3 Electricity prices at Polish balance market [6].

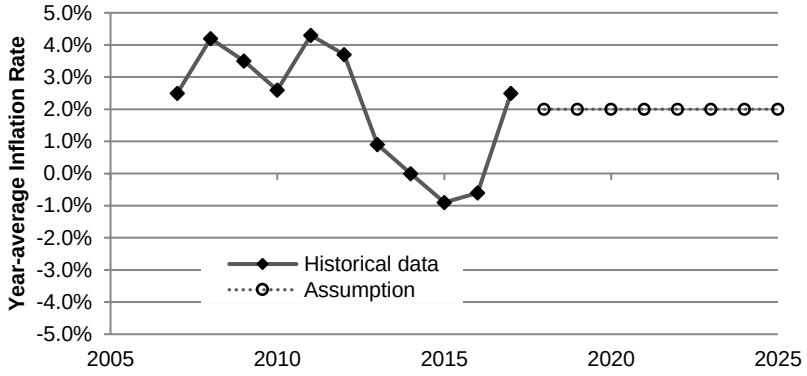

Fig. 4 Inflation rate in Poland in recent years [7].

2.3 Social Factors

Recent surveys of Polish public opinion about preferred future energy sources placed coal at 5th place, after wind, solar, water and nuclear energy [8]. This shows that accepting coal investments is becoming increasingly difficult for the society. Another survey shows that most Poles are indifferent to decisions about energy, if they do not directly threaten their pockets or safety [8].

For a few years in the autumn-winter season in Silesia the acceptable concentration of dust has been exceeded [9]. Increasing smog problem requires an action aimed at minimizing the danger for the society health . An effective campaign encouraging people to switch to district heating can improve air quality and advertise the idea of a new power unit.

In the case of Jaworzno city, the NIMB ('Not In My Backyard') syndrome should not occur, since by 2018 the city will have three power plants in operation. However, it is recommended that a series of meetings with the inhabitants be carried out prior to the official construction in order to increase the support for the project. This is important because NIMBY causes a protest against almost 90% energy investments, which is associated with delays in construction [8].

2.4 Technological Factors

A new CHP plant would be located in the vicinity of already operating CHP units in Jaworzno. There are several advantages of this idea:

- There is enough space for the object to be created in the neighbourhood of existing units;
- Instead of building a new transport infrastructure, the existing facilities can be used, which may significantly reduce the cost of construction;
- Combined heat and power plants with CFB boilers are a proven solution commonly used in Poland.
- Through a proven solution, employees will be deployed faster on site.

2.5 Environmental & Legal Factors

The analyzed CHP plant has to respect all emission limits (Table 1). As a consequence, appropriate flue gas treatment systems have to be applied.

Tab. 1 Future emission limits (according to BAT) [10].

Boiler Thermal Power, MWt	**50-100**	**100-300**	**>300**
SO_x concentration mg/m^3_n	400	200	150 (200)
NO_x concentration mg/m^3_n	300	200	150
Dust concentration mg/m^3_n	20	20	20
Hg concentration mg/m^3_n	1-3	1-3	1-2

SULFUR OXIDES Chemical absorption can be used. This process would be carried out through a wet limestone method: The acid flue gas passes through an absorption zone in which SO_2 is bound to lime water by absorption into $CaSO_3$ and oxidation to $CaSO_4$ (gypsum). In comparison to other methods, it is inexpensive in construction and operation. It has simple construction, however, it causes the necessity to heat the flue gas before entering the chimney, and consumes a lot of water and energy [10][11].

NITRIC OXIDES Two methods will be used to prevent/remove nitrogen oxides: a primary method (Flue Gas Recirculation) and secondary (Selective Catalytic Reduction). The process is based on a reaction of nitric oxides NO and NO_2 (NOx) with a reagent sprayed into the flue gas. This reaction takes place on the surface of the catalysts at a temperature of about 300 - 400 ºC and provides over 90%-efficient reduction of nitric oxides. The problem in this case is the threat of ammonia emission (ammonia slip) and the high operating cost because of the reagents used[10][11].

ASH For the removal of ash the most expensive, but also the most effective method is the electrostatic precipitator (EPS). Particles of dust, electrically inert are electrified by electric charge. The dust that holds the charge naturally attracts the opposite charge and settles on it. On the electrode, the dust is discharged and cyclically removed by physical means such as precipitation or flushing [10][11].

MERCURY New documents [10] foresee a mercury emission limit, stating that a typical power plant is allowed to emit up to 52-57 kg Hg per year. After combustion, mercury is released in two forms: solid form (with ash) approx. 10% and gas (remaining part). There are several types of mercury released during the combustion process:

- Elemental Mercury Hg^0 - **gaseous form**
- Divalent mercury Hg^{2+} - **gaseous form**
- Mercury adsorbed on emitted dust - **solid form**

Solid mercury can be effectively removed by methods already used, such as wet flue gas desulphurization or bag filters. Owing to this, the solid mercury is not so dangerous.

Mercury released in gaseous form is the most dangerous (especially elemental mercury), due to its residence time in the atmosphere (from 6 months to even 2 years). In addition, its durability allows it to travel long

distances and it is insoluble in water. This last property does not allow mercury to be removed by means of commonly used methods.

In order to remove elemental mercury in CHP, the method of secondary mercury removed using activated carbon will be applied. Active carbon is often impregnated with other elements that are readily associated with mercury, such as sulphur, chlorine, iodine. The addition of these elements to activated carbon allows an intensification of mercury removal.

The active carbon method involves the injection of suitably prepared sorbent (with activated carbon) after the combustion chamber and activated carbon particles together with mercury removal in the electrostatic precipitator. In addition, if TOXECON II technology is used, which can be installed in the penultimate section of the electrostatic precipitator and is designed to catch active carbon particles together with mercury, ash can be used as a raw material for sale. In future this will not be permitted if the ash is not purified.

3. Technical & Thermodynamic Analysis

3.1 Plant Structure

The analyzed CHP unit structure (Figure 5) is inspired by Units 2 and 3 already existing at the 'Jaworzno II' CHP plant. The parameters taken for analysis (Table 2) are not the exact parameters of existing installations [12].

Tab. 2 Plant basic nominal parameters.

Name	Unit	Value
Available Heat Power	MWt	115.0
Net Electric Power	MW	160.4
Boiler heat duty	MWt	370.8

The unit is equipped with a hard-coal-fired Circulating Fluidized Bed boiler of nominal capacity 540 t/hour. Live steam (13.5 MPa, 535°C) runs the steam turbine. Steam from first four extractions is supplied to two LP and two HP heat exchangers for heat regeneration, and to the deaerator. Steam from 5th extraction is used to produce hot water in Water Heater (WH). Remaining steam flows into the condenser (CND). Condensate is then heated up in LP part, deaerated and collected in feedwater tank (FWT). The feedwater pressure is elevated by feedwater pumps. After heating up in HP part, feedwater is supplied to the boiler. Water absorbs heat and evaporates. The final product of boiler is superheated high-pressure live steam. The plant produces both electric power and heat.

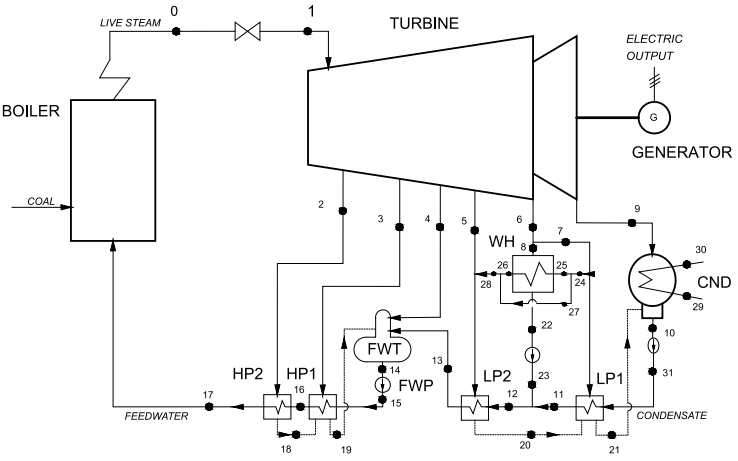

Fig. 5 Process Flow Diagram of the plant.

3.2 Plant Specification Data

The key operating parameters of the unit are presented in Table 3.

Tab. 3 Selected parameters of the plant.

Parameter	Value
Live steam parameters	13.5 MPa / 535°C
Live steam mass flow	150 kg/s
Extraction steam pressures	2.55 / 1.46 / 0.8 / 0.5 / 0.32 MPa
Condenser pressure	6 kPa
Feedwater Pump discharge pressure	15 MPa
Feedwater temperature at boiler inlet	225°C
District Heating water return / forward	70°C / 130°C
Cooling water	2700 kg/s; inlet 17°C
Own Needs Power (% of Gross Power)	10%
Gross Power @ Min./Max heat production	179.1 / 151.6 MW_{el}
Net Power @ Min/Max heat production	160.4 / 135.7 MW_{el}
Boiler Duty	370.8 MWt
Boiler Average Energy Efficiency	92.5%

3.3 Fuel Specification Data

Hard coal can be delivered from 3 coal mines owned by TAURON Wydobycie: "Sobieski", "Janina" and "Brzeszcze"[13]. The assumed coal lower heating value (LHV), coal elemental composition and resulting raw flue gas composition (for air excess ratio $\lambda = 1.2$) are demonstrated in Table 4. Ash and slag production is set as 12.2% of the fuel stream.

Tab. 4 Coal and flue gas details.

Quantity	Symbol	Value
carbon mass fraction	c	60.00%
sulfur mass fraction	s	0.50%
nitrogen mass fraction	n	5.50%
oxygen mass fraction	o	5.00%
hydrogen mass fraction	h	3.00%
moisture mass fraction	w	15.00%
mineral matter fraction	p	11.00%
LHV (lower heating value)	W_d	22.0 MJ/kg
flue gas CO_2 molar dry	$[CO_2]$	15.80%
flue gas N_2 molar dry	$[N_2]$	80.65%
flue gas O_2 molar dry	$[O_2]$	3.55%
flue gas SO_x molar dry	$[SO_x]$	494 ppm

3.4 Plant Operation Regime

Operation of the plant is strongly dependent on the outdoor conditions (e.g. temperature, wind speed, insolation) influencing the current heat demand in district heating system. A duration graph of heat demand is depicted in Fig. 6. Plant operating parameters are adjusted to water heater duty currently required, thus affect the electricity production. Live steam mass flow is maintained constant.

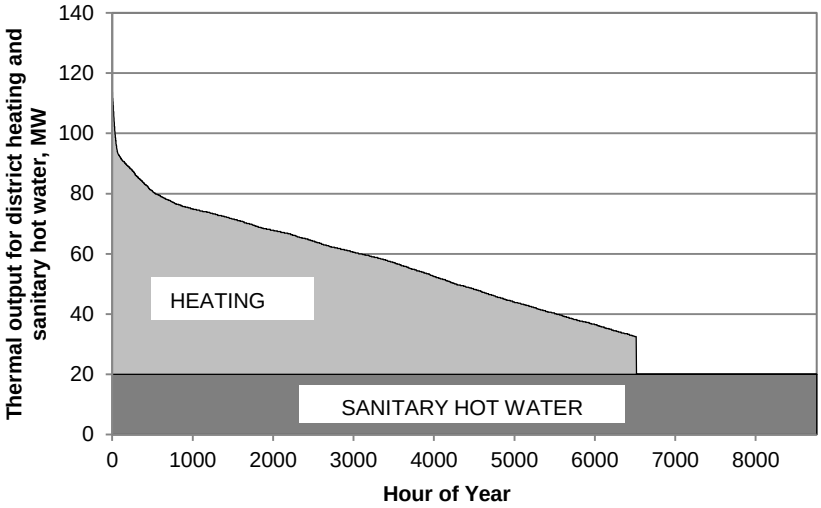

Fig. 6 Heat load duration graph for identified market.

The heat demand profile was based on a typical year meteorological database [14] for Katowice city (16 km from plant location), providing data on probable temperature waveform throughout a year. Momentary heating demand was computed proportionally to difference between indoor (20°C) and outdoor temperature. Sanitary hot water consumption is estimated at the level of 20 MW. These two sums up to total heat load of the plant. Calculations were performed for every hour of a year. The heating season duration was evaluated as 6517 hours per year.

3.5 Calculation Results

The water & steam cycle calculation was based on mass and energy balances. Computations were performed with the use of EES software (Engineering Equation Solver). Table 5 includes selected results for 2 extreme states (min. and maximum heat load).

Tab. 5 Plant operating parameters for minimum and maximum heat load.

Parameter	**Unit**	**State 1**	**State 2**
State description	-	*SHW* only*	*Full load*
Thermal power	MW_{th}	20.0	115.0
Electric power (gross)	MW_{el}	179.1	151.6
FW pump power	kW_{el}	3063	3158
Heat regeneration (total)	MW_{th}	94.26	77.12
Unit transformer efficiency	%	99.5	99.5
Chemical Energy Consumption	MW_{chem}	400.86	400.86
Net Exergy Efficiency	%	39.4	38.1

** SHW = Sanitary Hot Water*

3.6 Production & Utilities Consumption

The total annual production and utilities consumption of the plant are summarized in Table 6. The Energy Utilization Factor (EUF) for the plant is quite low. This is caused by high power/heat ratio. This means that it should not be compared with typical EUF of heat-oriented CHP plants.

Tab. 6 Annual Production/Consumption Table.

Quantity	Value	Unit
Heat Production	1 536 175	GJ
Gross Electricity Production	1 366 074	MWh
Net Electricity Production	1 223 319	MWh
Primary Energy Consumption	11 544 908	GJ
Coal Consumption	524 769	t
Flue gas emission	3 721	mln m^3_n
CO_2 emission	1 154 491	t
Ash & Slag production	64 022	t
DEMI water consumption	2 160	t
EUF, gross	55.9	%
EUF, net	50.3	%
Power/Heat Ratio	3.20	-
Average Exergy Efficiency	39.3	%

4. Economic Analysis

4.1 Methodology

For the purpose of this study, a cash flow analysis was carried out.

Discounted cash flow was calculated as:

$$CF_t = -J_{0,t} + S_{n,t} - K_{e,t} - K_{op,t} - P_{d,t} + L_t \tag{1}$$

Where:

$J_{0,t}$ ('0' year only) - total capital expenditures for building the plant, updated to the startup year.

$S_{n,t}$, $K_{e,t}$, $K_{op,t}$, $P_{d,t}$, L_t – respectively: Net Revenue, Plant Operational Costs, Other Costs, Income Tax, Liquidation Revenue [15].

Discount Rate is based on Real Discount Rate weighted-average evaluation:

$$r = \sum_j u_j \frac{r_{CoC,j} - i}{1 + i} \tag{2}$$

Where: u_j - capital share from j-th source, $r_{CoC,j}$ – cost of capital for j-th source [15].

Net Present Value (NPV) was computed as:

$$NPV = \sum_{t=o}^{N} \frac{CF_t}{(1+r)^t} \tag{3}$$

Where N means plant operation period (in years) assumed for the analysis [15].

Internal Rate of Return (IRR) is a number, which yields:

$$\sum_{t=0}^{N} \frac{CF_t}{(1+IRR)^t} = 0 \tag{4}$$

Also, the **Discounted Payback Time** (DPB) is defined by relation:

$$\sum_{t=0}^{DPB} \frac{CF_t}{(1+r)^t} = 0 \tag{5}$$

Investment is profitable if: $NPV > 0$, $IRR > r$ and $DPB < N$. The financial analysis takes into account also business liquidity of the project. The beginning of the construction phase is 2020. Plant startup is in 2025.

4.2 Capital Expenditures Estimation

The capital expenditures (CAPEX) were estimated as follows:

- Installed cost of CFB boiler and heat exchangers (including equipment) were calculated with correlations given in literature [16];
- Total Installed Cost of steam turbine (including condenser and equipment), as well as the feedwater pump (FWP) was evaluated based on U.S. Dept. of Energy report [17] and methodology presented therein. Cost of steam turbine was multiplied by pressure correction factor of 2.21 [16];
- Remaining capital costs were approximated according to distributive factors given in literature [15].
- Values were converted from U.S. dollars ($) to Polish złoty (PLN) by exchange rate: 3.67 PLN / $.
- The installed costs of particular elements were updated using Cost Index Method [17]:

$$CAPEX_{(2019)} = CAPEX_{(y)} \frac{CEPCI_{(2019)}}{CEPCI_{(y)}} \tag{6}$$

The CEPCI (Chemical Engineering Plant Cost Index) for the year before planned investment beginning was predicted as an extrapolation of CEPCI historical values trend (see Figure 7) [18].

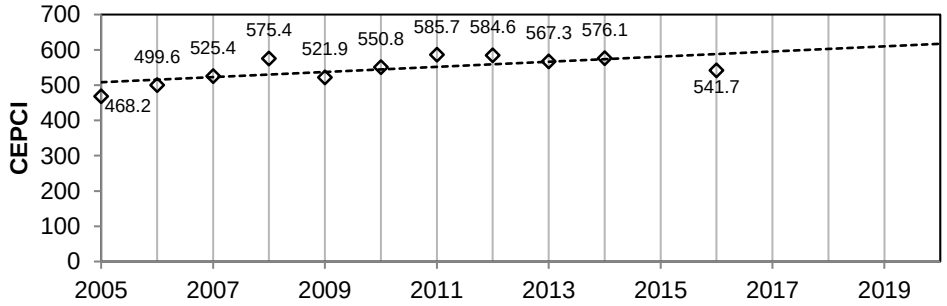

Fig. 7 CEPCI values in recent years and its linear-regression-based forecast.

Table 7 presents the results of CAPEX estimation.

Construction of the CHP plant is expected to last 5 years, which is why investment cost had to be updated for the '0'-year of project. The following cost distribution in time was assumed: 2020: 10%, 2021: 20%, 2022: 40%, 2023: 20%, 2024: 10%. The result of this operation is final CAPEX value: **1 292 862 521 PLN** in 2025.

Capital cost obtained with presented method should only be treated as a rough estimate. Actual expense may differ by +/- 30% from values presented above. In fact, more rigorous cost prediction is not obtainable at this level of analysis. Moreover, the installed cost of process equipment may be strongly affected by fluctuations of energy and steel prices in time, as well as by the outcome of business negotiations.

Tab. 7 Plant Capital Cost Breakdown.

No	Element / Subsystem	% of total CAPEX	Total Installed Cost, PLN
1	Studies & Project Documentation	1.75%	19 966 732
2	Land Reclaim & Preparation	0.60%	6 845 737
3	Fuel Supply Department	2.70%	30 805 815
4	Turbine & Steam Cycle Equipment	22.4%	255 894 781
5	Steam Boiler & Auxiliary Devices	45.0%	513 337 826
6	Industrial Water Systems	7.93%	90 477 819
7	Power Output	2.50%	28 523 903
8	Combustion products removal systems (ash, slag, SOx, NOx, mercury)	5.31%	60 584 769
9	Auxiliary and service objects	3.38%	38 564 316
10	Startup System, Compressed Air Station, Acetylene Station, Hydrogen Station		
11	Transport Management Objects		
12	External Networks & Objects		
13	Land Arrangement		
14	Maintenance Facilities	1.92%	21 906 357
15	Investment services	4.02%	45 866 435
16	Margin	2.02%	23 047 313
17	By-the-way Investments	0.45%	5 134 302
TOTAL		**100.00%**	**1 140 956 107**

4.3 Financial Assumptions

The economic environment assumptions were made according to recent and present market conditions in Poland and Europe. The most important values are listed in Table 8.

Tab. 8 Conditions used for financial calculations (base scenario).

Quantity	Value	Unit
Equity capital share	56%	
Foreign capital share	44%	
Bank profit margin	3.50%	
WIBOR12M index	1.85%	
Debt interest rate	5.35%	
Assets share	65%	
Equity capital interest rate	11.0%	
Inflation Rate	2.00%	
Debt Repayment Period	15	years
Real Discount Rate	6.39%	
Reinvestment Rate	10.0%	
Grace period for debt repayment	1	year(s)

The own (equity) capital share and grace period were adjusted to satisfy the cash liquidity condition. It is, however, quite high compared to typical 20÷35%. This requires company's own contribution of 700÷800 mln PLN. Problems with financing are likely to occur. Table 9 shows the market prices of energy media, environmental costs and some key plant performance indicators.

In calculations, the actual heat load of the plant is 100% equal to the design heat load. Also, the whole net electric energy production is sold at the market.

Tab. 9. Market conditions used for the analysis (base scenario).

Quantity	Value	Unit
Electricity price (2025)	165.00	PLN/MWh
Heat price (2025)	38.00	PLN/GJ
Ash and slag selling price (2025)	50.00	PLN/t
Hard coal price (2025) (LHV=22 MJ/kg)	265.00	PLN/t
CO2 allowances price	35.00	PLN/t CO2
Supplementary water cost	1.00	PLN/t
SO_2 emission cost	530.00	PLN/t
NO_X emission cost	530.00	PLN/t
CO_2 emission cost	0.29	PLN/t
Ash emission cost	350.00	PLN/t
Average salary	5000.00	PLN/month
O&M annual cost	1.5%	of CAPEX
Number of employed Staff	10	per Shift
Annual Operation Time	8000	h / year

4.4 Liquidity Conditions

Project liquidity condition is crucial for the safety of investment. Therefore, the minimum cash balance has to be greater than 0. Liquidity is affected by:

- Bank loan parameters (magnitude, repayment period, interest rate, grace period);
- Annual net income;
- Nominal costs;
- Depreciation & Amortization method applied;

The magnitude of bank loan depends on the total CAPEX and share of equity capital in the investment. The greater the own capital share, the safer the project's liquidity is.

Calculations revealed very weak liquidity of the investment. As stated before, the own capital share had to be increased in order to fulfill the liquidity condition. Project cost projection is presented in Figure 8.

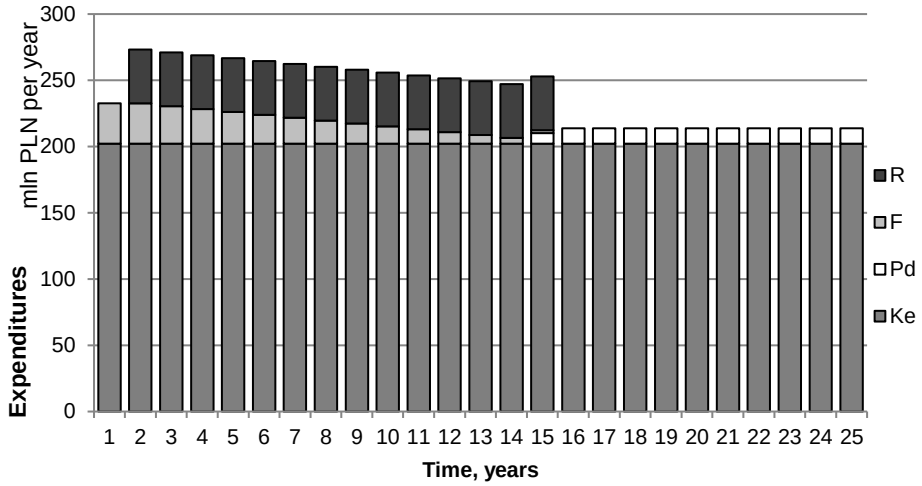

Fig. 8 Project cost projection.
(R - Credit Installment, F - Interest, P - Income Tax, Ke - Operating Cost).

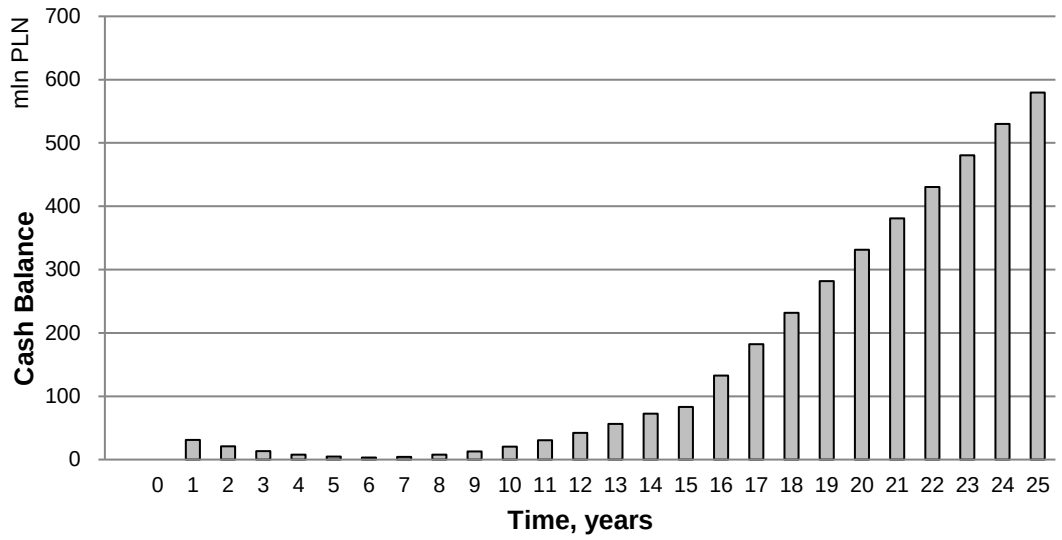

Fig. 9 Nominal cash balance of the project (equity point of view).

Due to the grace period, loan repayment is delayed, which provides financial liquidity but increases the total credit nominal cost by 6.25%. The nominal cash balance of the project (equity point of view) is depicted in Figure 9.

During the credit repayment period the cash balance is very low, yet positive. As soon as the credit is repaid, it becomes an ascending function of time.

4.5 Profitability Indicators

Main profitability indicators were evaluated based on formulae given in Section 4.1 and CF projection tables created in MS Excel worksheet. Their values are listed in Table 10.

Tab. 10 Profitability indicators (base scenario).

Net Present Value	$\boldsymbol{NPV}$	**- 575 050 458 PLN**
Net Present Value Ratio*	$NPVR$	-0.444
Internal Rate of Return	IRR	0.69%
Discounted Payback Time	DPB	(no payback)

* $NPVR = NPV/CAPEX$

In this case the investment is **unprofitable**. NPV is deeply negative and IRR falls below the discount rate. The project is expected to bring losses, if base scenario is considered.

4.6 Sensitivity Analysis

Since many factors in this analysis are not certain, a sensitivity analysis of the solution was carried out. The variables were examined within the range +/- 30% of base values. Net Present Value (NPV) was chosen as the output. The results of the analysis are visible in a graph (Figure 10).

Results indicate that the most influential factors are: electricity price, hard coal price and total investment cost. Figures 11÷14 show the relations between selected parameters and the economic effect of investment.

According to presented results, current energy market situation is highly unfavorable for analyzed investment. Not only is the hard coal very expensive, but also the electricity prices at the market are not high enough to attract the investors. If the electric energy price rises and coal price falls, a CHP plant investment

might become profitable. Table 11 illustrates the Break-Even Points (BEP) of key variables in the economic model. NPV was treated as a linear function. BEP is then its intersection point with $NPV = 0$ axis.

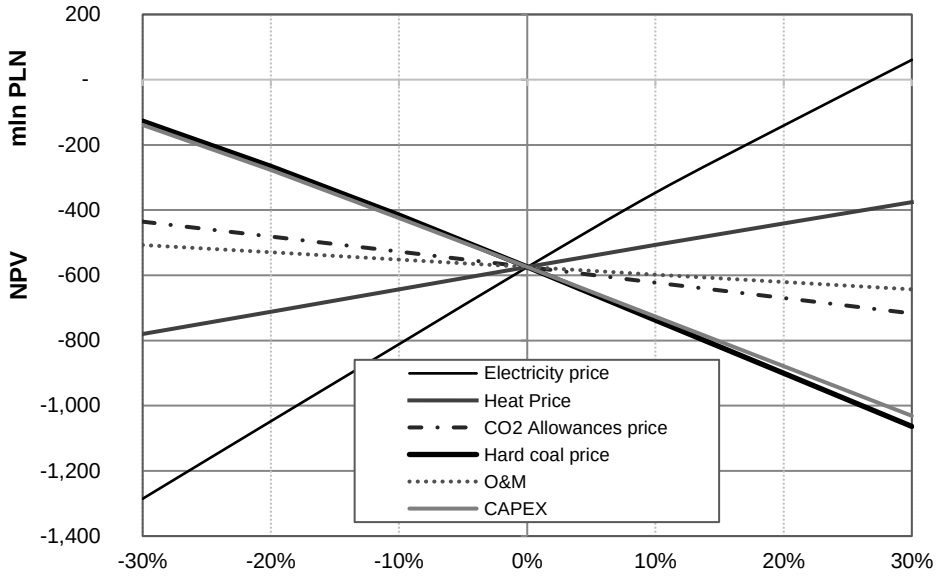

Fig. 10 NPV sensitivity graph.

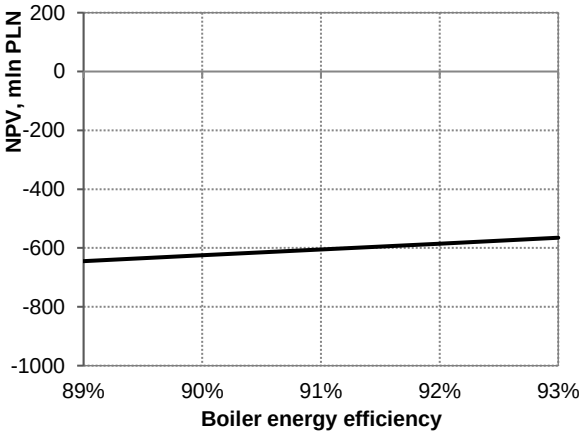

Fig. 11 NPV vs boiler efficiency.

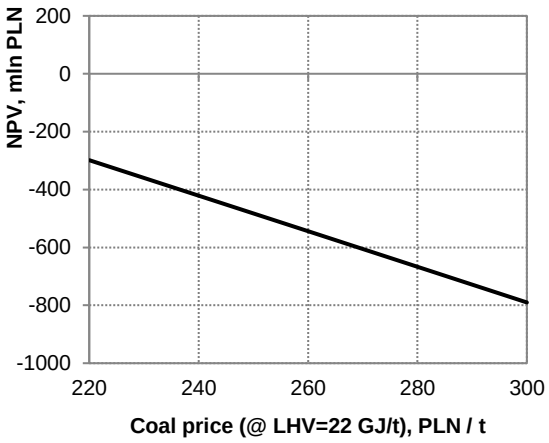

Fig. 12 NPV vs coal price.

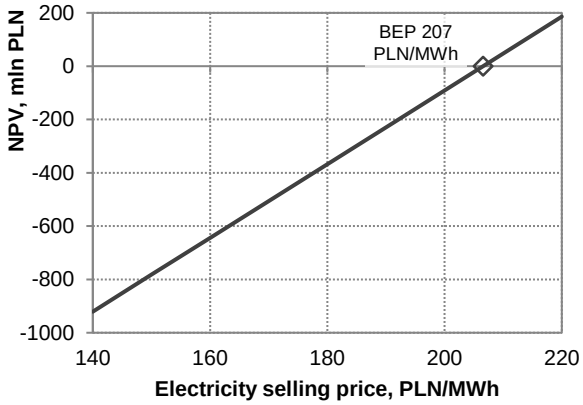

Fig. 13 NPV vs electricity price.

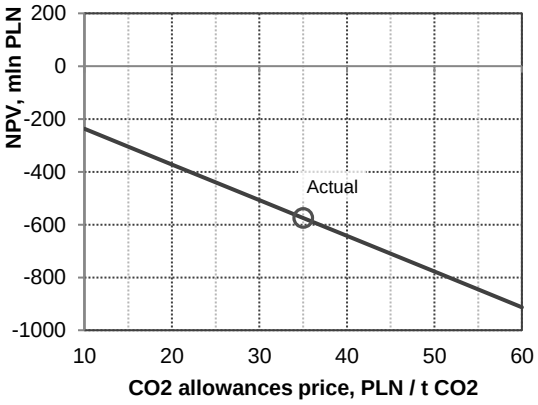

Fig. 14 NPV vs CO_2 allowances price.

Tab. 11 The Break-Even Points for analyzed solution.

Quantity	Base Values	Break-Even Points	Unit
Electricity price	165.00	206.56	PLN / MWh
Heat price	35.00	70.18	PLN / GJ
Hard coal price	265	171.42	PLN / t
CO2 allowances price	35.00	-7.54	PLN / t CO2
Total CAPEX	1 292 862 521	804 715 703	PLN
NPV	**- 575 050 458**	**0**	**PLN**

The influence of particular factors can be expressed by means of sensitivity index (SI) :

$$SI_i = \left| \frac{\Delta(NPV)/NPV_0}{\Delta X_i / X_{i_0}} \right| \tag{7}$$

where: X_i - i-th examined variable,
$\Delta(NPV)/NPV_0$ - relative change in NPV due to modification of X by ΔX.

Computed SI values are presented on a chart (Fig. 15).

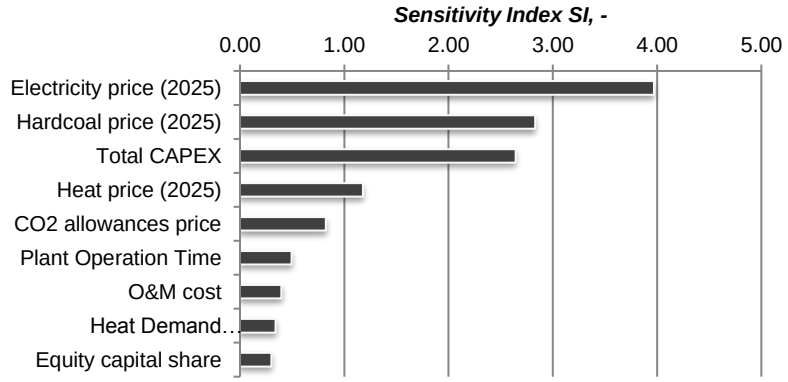

Fig. 15 Sensitivity of NPV for various factors.

Again, the most important factors are clearly the electricity price, coal price and CAPEX. Heat price is much less affecting the economics, as the considered CHP plant is power-oriented and heat is not its dominant product.

The EU ETS (European CO_2 Emission Trade System) plays a noticeable role in plant profitability. The carbon dioxide emission allowances price has even stronger impact on NPV than annual Plant Operation Time, Operation & Maintenance cost or actual heat demand.

5. Summary

5.1 Investment Assessment

The technology applied for this study proved unprofitable. Although the local market seems to be promising, the economic and legal considerations of Polish and European energy market are very unfavorable. The analyzed investment is not expected to pay back, unless the electricity and heat prices rise high enough, or additional subsidies are offered for electricity and/or heat produced in this kind of plant.

5.2 Risk Factors

The European Union has been forcing European governments to promote renewable energy sources rather than conventional technologies. Public opinion is critical to coal-related activities. Prices of electricity and heat are expected to increase, but not enough to meet CHP plant's economic requirements. If coal price rises, the economic environment may become even less business-friendly. The investment will be profitable only in case large subsidies for cogeneration are provided by the state.

5.3 Optimization Opportunities

The analyzed plant is relatively simple in terms of technological structure. Compared to modern solutions, the considered technology is out-of-date. Also, many parameters can yet be optimized. The available technologies allow for higher steam parameters, better turbine performance and very good control system. With modern cooling systems, the condenser pressure is often much lower than assumed in this study. The power/heat ratio and heat exchangers sizes can also be optimized. Improved plant structure and parameters should have significant positive effect on plant economy.

5.4 Final Conclusions

The study demonstrated unfavorable market conditions for conventional CHP plants. In analyzed case, a CHP plant investment would bring a severe financial loss. Potential investors are advised against such solutions. There is, however, a small chance for this business if future economic and legal situation changes significantly.

Acknowledgment

This article was prepared within the projects Innovative Systems for Fossil Fuels Conversion and Thermoeconomic Analysis in Power Engineering carried out at Faculty of Energy and Environmental Engineering, Institute of Thermal Technology, the field of study Power Engineering - Thermal Energy Systems. Work was conducted under the direction of Lucyna Czarnowska, PhD.

References

[1] Baza Demografia GUS (Central Statistical Office of Poland), http://demografia.stat.gov.pl/bazademografia/Tables.aspx, (16/11/17).
[2] Professional Academy Webpage, https://www.professionalacademy.com/blogs-and-advice/marketing-theories---pestel-analysis, (10/11/17).
[3] A. Szurlej et al.: Zapotrzebowanie krajowego sektora energetycznego na surowce energetyczne – stan obecny i perspektywy do 2050r.
[4] Bilans zasobów złóż kopalin w Polsce wg. stanu na 31.12.2015, Państwowy Instytut Geologiczny – Warszawa 2016.
[5] Indeks PSCMI 1 (Polish Steam Coal Market Index), http://www.polskirynekwegla.pl/indeks-pscmi-1, (12/11/17).
[6] PSE Webpage, https://www.pse.pl/web/pse-eng/areas-of-activity/electricity-market/electricity-prices-and-volumes, (02/11/2017).
[7] GUS (Central Statistical Office of Poland),http://stat.gov.pl/obszary-tematyczne/ceny-handel/wskazniki-cen/wskazniki-cen-towarow-i-uslug-konsumpcyjnych-pot-inflacja-/roczne-wskazniki-cen-towarow-i-uslug-konsumpcyjnych-w-latach-1950-2014/ , (02/11/17).
[8] Z. Łucki: Energetyka a społeczeństwo – aspekty socjologiczne, Wyd. Naukowe PWN, Warszawa 2011.
[9] System monitoringu jakości powietrza (Air Quality Control System), http://powietrze.katowice.wios.gov.pl/, (10/11/17).
[10] The European IPPC Bureau, http://eippcb.jrc.ec.europa.eu/reference/, (10/11/17).
[11] Z. Gnutek, W. Kordylewski: Maszynoznawstwo energetyczne, Oficyna Wydawnicza PWr, Wrocław 2003.
[12] A. Czekaj: Bilansowanie i ocena energetyczna bloku ciepłowniczego z turbiną upustowo-kondensacyjną, Politechnika Śląska, Gliwice 2016.
[13] TAURON Wydobycie Website, http://www.tauron-wydobycie.pl/oferta-handlowa/wegiel, (15/11/17).
[14] Ministerstwo Infrastruktury i Budownictwa (Polish Dept. of Infrastructure & Building), http://mib.gov.pl/2-Wskazniki_emisji_wartosci_opalowe_paliwa.htm, (25/10/17).

[15] D. Laudyn: Rachunek ekonomiczny w elektroenergetyce, Oficyna Wyd. Politechniki Warszawskiej, Warszawa 1999.
[16] J. Kalina: Analiza i optymalizacja układów technologicznych energetyki rozproszonej zintegrowanych z termicznym zgazowaniem biomasy, Wyd. Politechniki Śląskiej, Gliwice 2013.
[17] H.P. Loh et al.: Process Equipment Cost Estimation Final Report, U.S. Dept. of Energy, National Energy Technology Laboratory, 2002.
[18] Chemical Engineering Online, http://www.chemengonline.com/pci-home, (02/11/17).

Passive House Building Analysis: Challenges, technologies and trends to improve energy efficiency in buildings - A review

Abhijit Mohod[1], Eric Pla Erra[1]

[1]Faculty of Power and Environmental Engineering, Silesian University of Technology, email: abhijit.mohod@gmail.com, ericpla.e13@gmail.com

Abstract

The following review article provides an overview of the actual situation and challenges in the sector of energy efficiency in buildings. The article identifies a house as the smallest unit in the electric grid and presents innovative solutions to lessen the energy consumption, which only help the end consumer economically, but it also addresses the challenges identified in the article. The building efficiency sector has improved a lot during recent years, but it still has issues to solve and a lot of margin to grow, especially with the new technologies and trends that are being globalized at the moment.

Keywords: Energy efficiency, VLC, IoT, batteries, greenhouse effect

1. Introduction

To conform to the Paris Accord to reduce the global emission of CO2 and green house gases, efficient utilization of energy plays an important role. Efficient use of energy by deploying intelligent systems not only reduces the pressure from the electric grids but it also offers substantial savings to the end user over time. It is thus imperative that capital should be invested in technologies that offer smart solutions to decrease the overall energy consumption in residential and industrial spaces.

2. Challenges to improve energy efficiency in buildings

A grid provides energy to towns and communities and a house can be viewed as the smallest unit of the electric grid. The incremental savings in energy in this small unit can lead to significant overall savings. However, there are challenges in achieving the stated goal.

The major challenges that we identify are as follows:

- Efficiency in utilization of energy must increase
- Measuring energy utilization and subsequent savings
- Diversification of efficient energy sources

These three challenges can be addressed by employing smart devices operating with innovative technologies to monitor and control the amount of energy used by appliances in a given household. These smart devices can be great tool to reduce the overall utility costs and in turn reduction in the energy bill for the end customers.

Building new power plants and associated grid network to meet increasing demand costs capital based on the size of the plant, type of fuel, location among several other factors. Recovering the capital cost of infrastructure and return on the investments to the financial stakeholders makes the cost per unit energy higher. Thus, installation of smart devices for monitoring and control of energy becomes an attractive choice. It must be noted that the increase in efficiency does not make new plants being unnecessary or irrelevant but it defers the investment decision. In the wake of rapid decentralization of energy and swift development of smart technologies, deferring a large-scale investment option is plausible approach, which potentially saves money. It can be also safe to assume that since the price of technology reduces over time, deferring an investment to future may save additional monies.

For a consumer the savings obtained from the usage of smart devices is more attractive than the idea of contributing to the goals of low carbon emissions. A visual indicator to demonstrate the savings, which is tied to consuming less energy, encourages consumers to think about various ways in which energy can be saved.

This in turn paves way to the diversification of efficient energy sources from the perspective of the consumer. Installing various devices in a single household that can - keep a check on the total power consumed, optimize the power consumption and indicate the most power consuming appliances to eliminate the waste energy, becomes a desired "low-hanging" choice for the consumer when it comes to overall savings. These savings are realized to a greater degree especially in the cities with higher cost of living.

Using innovative devices equipped with cutting edge sensors for measurements and advanced data analytical tools, aggregate usage of energy by buildings and communities can be realized and the areas of concern can be identified and the successes can be replicated. It must be noted that the appliances, conditions or user behavior can generate waste energy and thus, appropriate approach and mitigation strategies must be developed to discern the true nature of waste.

3. New trends and technologies

Energy efficiency in buildings started centuries ago. Our ancestors already used their available resources in order to keep as much heat as possible inside their homes, or the other way around, they tried to keep it as fresh as possible. In recent times, this market has seen a huge improvement, as most countries already have regulations for new buildings regarding energy consumption. New trends have appeared, like the Passive House Standard, in order to establish some rules and criteria to achieve excellent results. But the world is changing, new technologies are discovered and developed, and energy efficiency is in the path to benefit from them.

3.1 Internet of Things (IoT)

IoT is way of connecting smart devices in such a way that they exchange data to create intelligent systems. It is an upcoming trend that will have an impact in almost every sector in the near future. Energy efficiency in buildings is not an exception as it is already implementing IoT to reduce energy consumption through collection, storage and management of data.

There are four main groups of devices in a smart building: lighting, appliances, home automation, and grid devices:

3.1.1 Lighting

Smart lighting is based on the usage of LED lightbulbs which can sense light and/or motion and are controlled remotely.

3.1.2 Smart Appliances

Consumer electrical and electronics equipment like heating and refrigeration systems, washers and dryers, include intelligent sensors and actuators, which can monitor and hence optimise the usage of energy as well as maintenance cycle.

3.1.3 Home Automation

These groups are mainly formed by gateways, actuators and sensors, which will manage energy use but also comfort and home security.

- A gateway is a hardware device that can be interfaced with smart devices within a house in order to control them. A Gateway can also be connected to cloud network.
- Home energy management system (HEMS) controls and records energy use through the gateway with user input via an app.
- Sensors can monitor light, motion, temperature, pollution, humidity, etc. in order to optimize the correct usage of its corresponding regulatory systems.

3.1.4 Example of Grid – Smart Devices

- Smart meters: Utility companies install electronic measuring devices to monitor customer's energy usage via a smart meter. Smart meters prove useful in management of the grid. Anything that can be measured can be improved. Installation of smart meters do not translate to saving of energy however, it informs the user of high energy consuming devices. With smart meter, the household consumption is measured in real time at suitable intervals, which can range from 15 to 60 minutes. Smart meter data can also be used to validate efficiency project savings. As seen in Figure 1, the installation of smart meters in on the rise.
- Time-variant pricing: This results in additional savings in the energy cost to the consumer due to network of intelligent systems. Time-variant pricing evaluations show peak electricity demand savings due to load shifting. They are not useful in gathering data about the efficiency of the system.
- Load disaggregation technology: This technology uses data from the smart meter to perform analysis on the utilization of energy by individual home device installed. Utilities may market specific appliances, for example a low power consuming cooling and refrigeration device, or houses with high peak demand, also this data can be used to develop reports that can compare the energy usage of a home with prior history and also with a peer's home connected to the network.

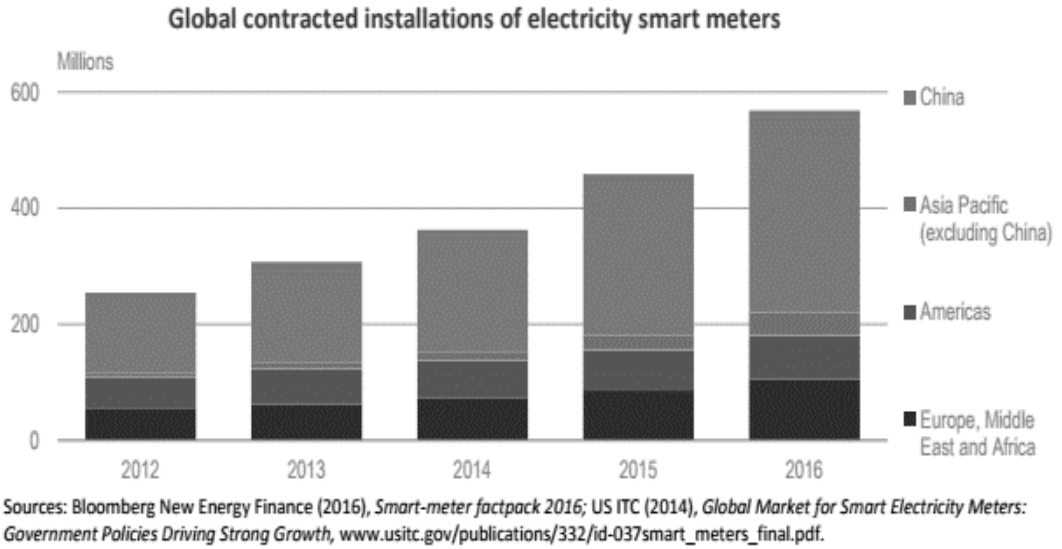

Fig. 1 Global contracted installations of electricity smart meters

3.2 Visible Light Communication

Visible light communication, or VLC, is an optical wireless communication technology which uses visible light between 400 and 800 THz. The technology uses LEDs for high data communication (up to 500 Mbit/s) or ordinary fluorescent lamps for low data communication (to the order of 10 kbit/s). In order to receive the signals from the light sources we have two different options at the moment:

- Cell phone camera or even a simple digital camera (in both cases an array of pixels).
- Specially designed electronic devices, which will usually contain also a photodiode.

In order to use this breakthrough technology in buildings to reduce its energy consumption, LED lightning will be the only possible choice, as they consume much less energy than conventional lights. LEDs will then provide efficient lighting and pulses to transmit data, that will be order of magnitudes faster than the current Wi-Fi set ups. This will be crucial in the upcoming years, as mentioned in the previous point, IoT manages a huge information of data that need better infrastructures to be assessed.

The two main contributions of Visible Light Communication to energy efficiency in buildings are:

- Lighting and IT installations can be united into a single system, reducing energy consumption and construction materials, making the system more efficient overall.
- Energy management systems can be built on a solid VLC network platform. VLC capabilities need to be exploited while undertaking new building projects.

3.3 Smart Batteries

Lithium-ion batteries are the key element of the new generation of batteries. They offer an excellent overall efficiency and a much longer service life than lead-acid traditional batteries. Its main drawback is that the initial investment is much higher and sometimes it makes them unviable. However, the technology has reached a point where it is cost-effective in power grid applications. This trend is expected to continue in the residential and commercial sectors, where batteries can provide some interesting benefits:

- Households subject to hourly electricity rates may charge their batteries when prices are at their lowest point, in order to consume the energy when the price is at regular or even high price.
- Households can accumulate surplus generation from a renewable energy system.
- Possible interaction with smart grids in a near future: Houses have a chance to collaborate with utility companies during peak demand. The peak demand can be met from energy generation from solar and wind farms.
- Backup power during electric service interruptions.

The following table shows a comparison between three main types of batteries:

Table. 1 Comparison between three main types of batteries

	Flooded Lead Acid	**VRLA AGM**	**Lithium-Ion (NMC)**
Initial cost per capacity ($/kWh)	131	221	530
Cost per life cycle ($/kWh)	$0.17	$0.71	$0.19
Specific energy (Wh/kg)	30	40	150
Regular Maintenance	Yes	No	No
Number of cycles to 80% SOH	200-1000	200-650	1000-4000
Typical state of charge window	50%	50%	80%
High temperature sensitivity	Degrades above 25°C	Degrades above 25°C	Degrades above 45°C
Available power constant current	0.2C	0.3C	1C
Fast charging time (hrs)	8-16	4-8	2-4

3.4 Energy Management Services

The Software as a Service (SaaS) business model follows a very simple principle: the client pays a monthly fee to use the selected service instead of buying an initial costly investment in order to install or use the same service. This is a great plus for smaller companies or individuals, because they usually do not have the required capital to purchase the whole package.

This business model has been a huge success in the IT industry, but the increasingly connected electrical and mechanical installations in buildings are making this business model an improvement for the energy sector. The control system can monitor indoor and outdoor conditions in real time in order to manage all the preventive and corrective actions so the maximum energy efficiency is achieved in the building.

Remote monitoring of home system is possible in which the client can hire a service provider that has expertise in managing the energy consumption of the client's house. This will save the client's money and time to research and employ specialized solutions.

4. Conclusions

It is clear that the efficiency in buildings is a potential market that has been exploited during recent years but that still has a lot of growth margin, especially with the new trends and technologies mentioned in this article.

This market is governed by two main actors: cost-benefit and government regulations. Most of the households will not improve their energy efficiency if they do not see a clear benefit in the electricity bill, for example. On the other hand, laws and regulations are forcing new buildings to follow some standards, and in a near future, all buildings will need an energetic certificate.

The appearance of new technologies will create a huge economic and environmental opportunity to change how we understand energy efficiency in buildings.

References

[1] D. M. Grueneich. The Next Level of Energy Efficiency: The Five Challenges Ahead, *The Electricity Journal*, Stanford University, 2015.

[2] F. Jammes. *Internet of things in energy efficiency*. The internet of things (Ubiquity Symposium), Ubiquity Volume 2016, Number February, 2016.

[3] International Energy Agency, *Market report series: energy efficiency 2017*, Typeset in France, October 2017.

[4] Top 10 Inventive Green Building Trends for 2017, http://www.ny-engineers.com/blog/top-10-inventive-green-building-trends-for-2017, (04/12/2017).

Technical and Economic Analysis of Infusion of Renewable Energy to Power Coal Mines

Olapade Olushola Tomilayo [1], Okoro Faith Eferemo[1]

[1]Energy and Fuels, AGH University of Science and Technology, email: olusolatomy@yahoo.com, okorofaitheferemo@gmail.com

Abstract

Over the years, Renewable energy infusion or substitution has become a focal point of the environmental movement, taking perspective both from the angle of the reserves to production ratio and from the angle of Costs incurred in form of positive and negative externalities. Energy obtained from renewable resources puts much less strain on the limited supply of fossil fuels, which are non-renewable resources. A coal mine is usually powered by various sizes of diesel generating during exploration process which leads to high CO_2 emission. This paper shows the possibility of substituting the environmental unfriendly, unstable and expensive diesel fuels with clean, cheaper and environmentally friendly renewable energy substitute, leading to a reduction in cost, carbon foot print, improving the energy efficiency of the exploration process. Simulation was done with excel that shows the distinction in a case study in Africa where the coal mine runs entirely on diesel fuel and a scenario where there is a substitution by renewable energy (Solar PV) which led to about 68.5% reduction in CO_2 emission.

Keywords: Renewable energy infusion, coal mines, carbon footprint, economic analysis, power

1. Introduction

1.1 Status of coal energy sector

Energy is necessary for survival. Without it, many billions of people would be left cold and hungry. The major source of energy comes from fossil fuels, and the dominant fossil fuel are oil, coal, and natural gas. Coal has actively affected the way humans live, work and relate to one another since the Industrial Revolution [1]. It has been referred to as the greatest resource that has been able to transform the world from fuelling steam engines, powering industry and generating electricity coal still plays a significant role in today development (Figure 1)

The growing public concern over climate change has compounded aversion to coal, further undermining an industry already opposed for its adverse effects on health, wellbeing, and local ecologies [3]. As the most carbon intensive fossil fuel, a phase-out of coal has been advocated as one of the simplest and most effective means of reducing carbon emissions. Thus, the world is currently undergoing a transition from fossil fuel to renewable energy edging closer towards a low carbon energy system [4]. However, while renewable energy appears set to eclipse coal in the coming decades, the International Energy Agency's World Energy Outlook forecasts that coal production will continue to rise, increasing 10% by 2040 [5].Coal mining accounted for 8% of total global anthropogenic methane emissions in 2010, and these emissions are projected to increase by 33% to 784 million metric tons of carbon dioxide equivalent (MtCO2e) by 2030 [6].To bridge the gap Coal mining industries, are searching for ways to make the extraction of this resource as green as possible, this is where renewable energy infusion comes into play.

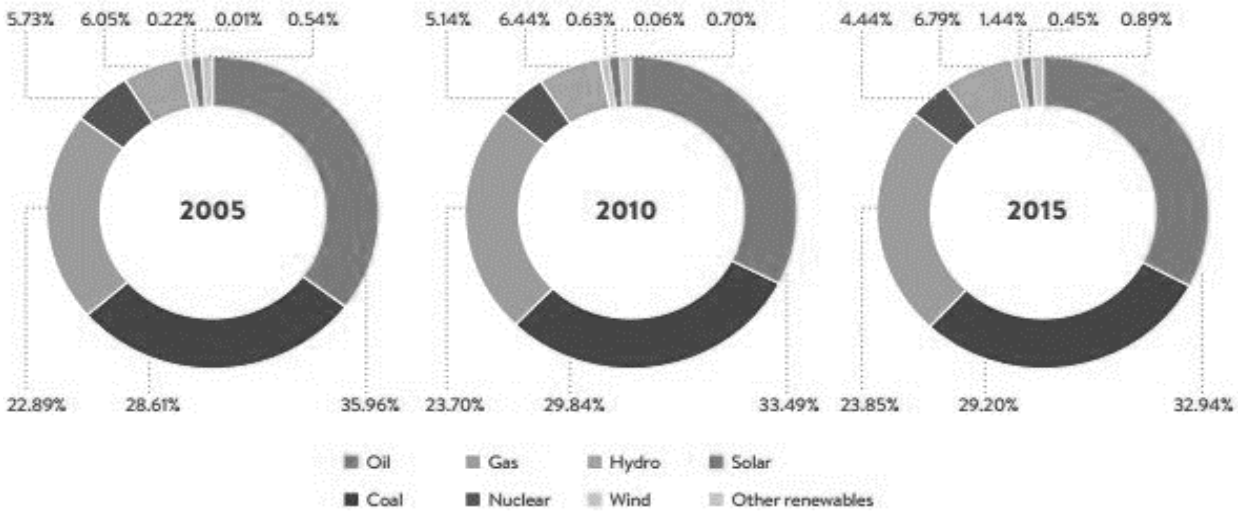

Fig. 1 Comparative Primary Energy consumption over the past 15years [2]

1.2 Sources of power in coal mining

Internal combustion engines are devices that generate work. To produce work, the combustion is carried out in a manner that produces high-pressure combustion products that can be expanded through a turbine or piston. There are three major types of internal combustion engines in use today: (1) the spark ignition engine, which is in automobiles; (2) the diesel engine, and (3) the gas turbine. A spark-ignition engine is an internal combustion engine, where the combustion process of the air-fuel mixture is ignited by a spark from a spark plug. They are normally used for automobiles. In diesel engines, air is drawn into the cylinder through the intake valve. Fuel is injected directly into the cylinder of the diesel engine, beginning toward the end of the compression stroke. As the compressed heated air mixes with the fuel spray, the fuel evaporates and ignites. Turbulent mixing profoundly influences the combustion process and pollutant formation in the steady-flow combustor, which increases GHG in the environment.

Sulphur dioxide, nitrogen oxides and particulate emissions from power stations can be substantially reduced through the application of flue gas de-sulphurisation, selective catalytic reduction (SCR), and low NO_x burner and precipitator technologies. The economic cost of addressing the environmental sustainability issue has reduced over time for these technologies. The challenge to reduce CO_2 emissions from fossil fuel-based power generation is also capable of being addressed through these various technology options. Clean coal technology encompasses both the goal of removing most CO_2 emissions associated with using fossil fuels and the progressive reduction of emissions through improved combustion efficiency. The former will involve increasing costs to meet tighter environmental requirements. The latter will improve the economics of power generation and help to preserve scarce fossil fuel resources. Both will be needed to improve the environmental performance of coal to the necessary extent over an acceptable timeframe. This research project explored the technical and economic analysis of infusing renewable energy to power coal mines.

2. Methodology

2.1 Case study description

South Africa's coal resources are in the Ecca deposits (Figure 2), a stratum of the Karoo Supergroup, and date from the Permian period between 280 and 250 Ma. The coal measures are generally shallow, thus making their exploitation suitable for open-cast and mechanized mining. South African coal has a comparatively medium ash content which can be reduced by washing before sale. Higher grades of final product are delivered to export markets, with the lower grade product burned by specially designed power station boiler hearths. Coal mining in South Africa started around late 19th century in Witwatersrand. The first coal was mined in appreciable quantity in Highveld coal field close to the nascent Witwatersrand gold mines. Demand grew slowly, but exponentially as

the country entered a period of industrialization during and following the second world war. Power stations were built particularly on the coal fields of Witbank and Delmas, as well as Sasol's major coal-based synfuels and organic chemicals complex at Secunda. As we approach the century's second decade, the power stations that were built over 30 years ago will remain operational at least until the mid-century. New and modern thermal power stations are being built and the coal sector employs in the region of 87,500 people, the third largest group in the mining sector after gold and platinum group metals. Their annual earnings are in the region of R20 billion [7]. The major coal mining companies account for around 85% of all production. They are Anglo American plc, South32's South Africa Energy Coal [8], Sasol Mining, Glencore Xstrata, and Exxaro [9]. Due to confidentiality clause, the exact mining company used in this research, cannot be disclosed.

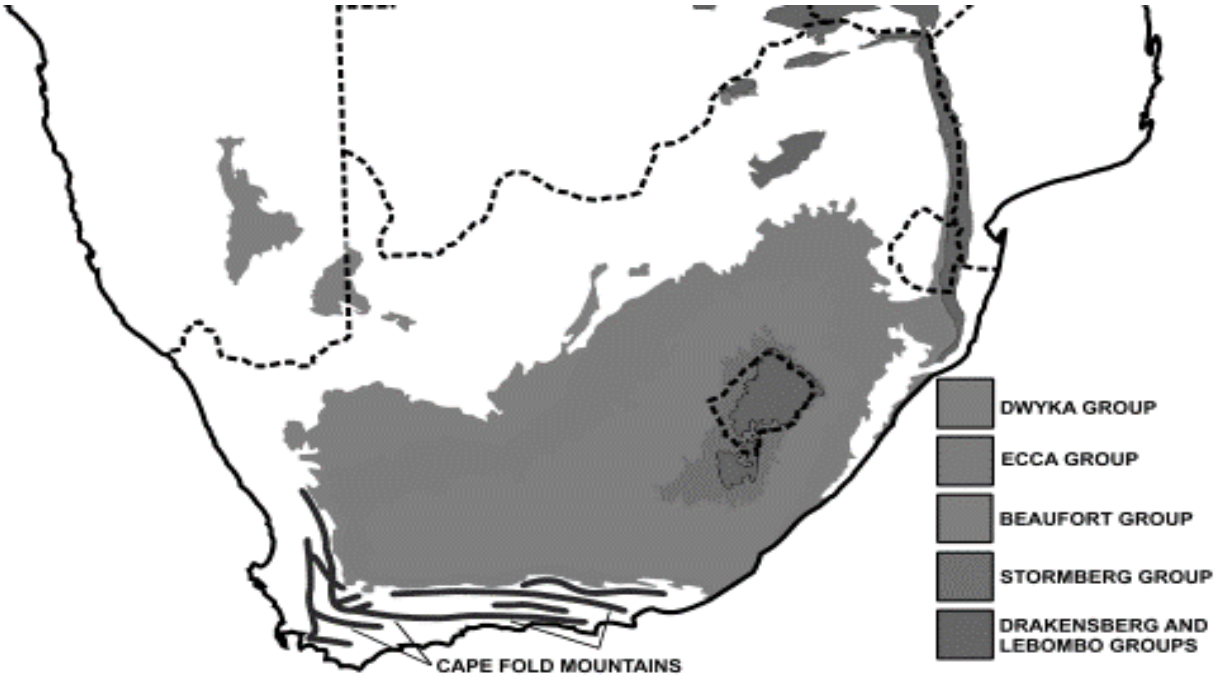

Fig. 2 Geographical locations of coalmines deposit in South Africa [10]

2.2 Plant Energy Analysis

A Hybrid power generation solution for a mine with a peak load of 5.5 M, and 2 sets 3.7 MW with available capacity of Generating Sets (GE) 40% efficiency of GE installed capacity. The electric charge of the day is different to that of the night due to public lighting, return of the workers to the house and supply of power to the surrounding village. The critical load requires a continuous supply (only from 19h to 23h which is 5.5 MW as current peak) (Figure 3). The energy produced in a year is 29 228 300KWh, and the fuel consumption is 6,682,527 litres for 2015.The storage tank on site included 4 tanks of 50,000 litres. The transportation of fuel is done by train once a week.

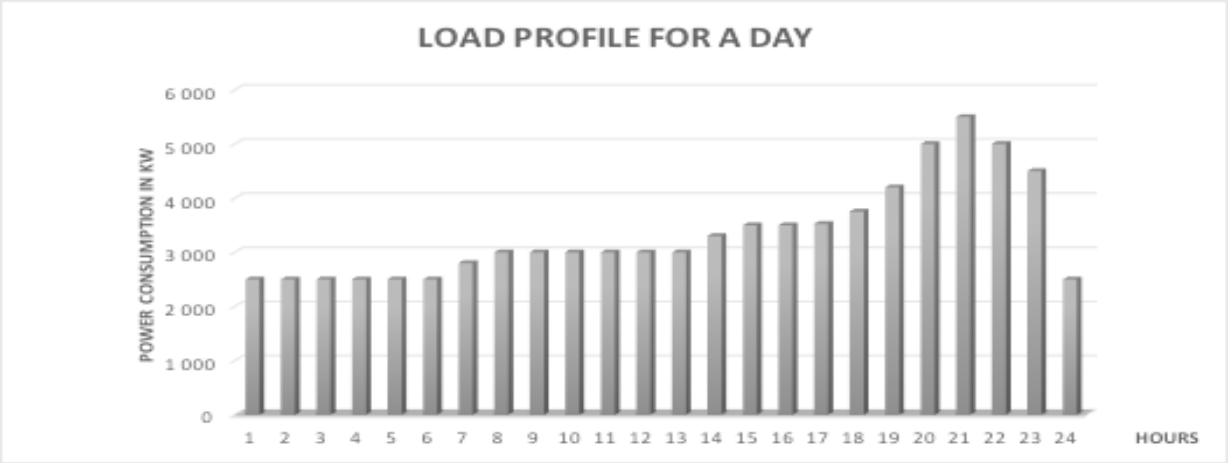

Fig. 3 Daily Load Profile

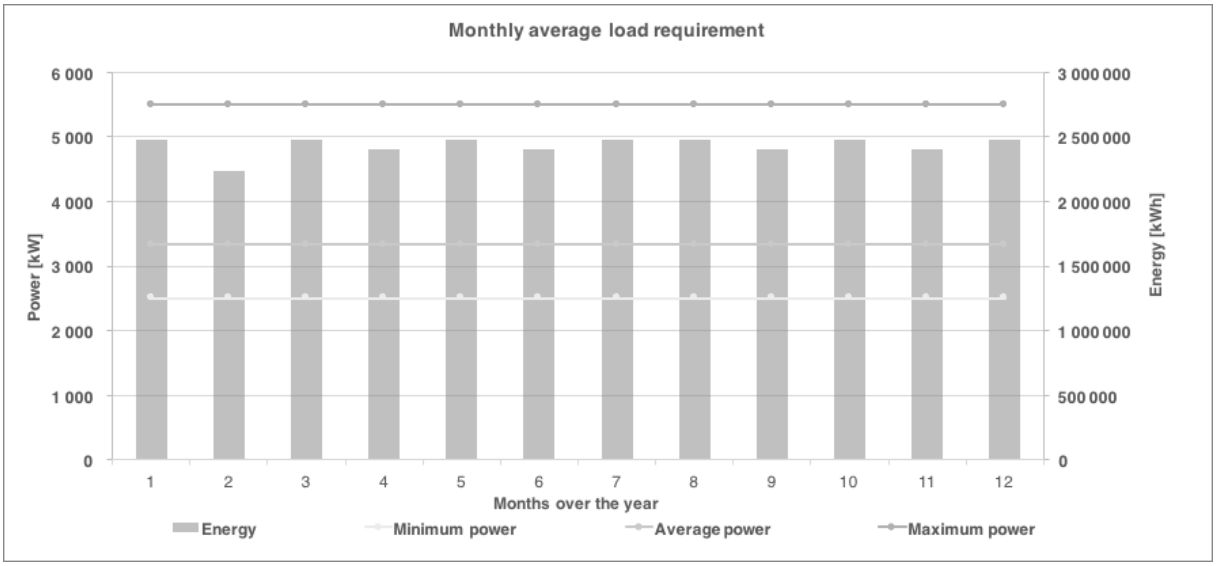

Fig. 4 Monthly Load Profile

2.3 Procedure

In the attempt to carefully analyse, and predict the best configuration in terms of cost and technical feasibility, a spreadsheet simulator called "XXX" was used to simulate for different scenarios by adjusting the battery size and Photovoltaic size and the corresponding result was obtained. The simulator works based on the sizing logic of reducing the percentage of power from the diesel generator set and infusing renewable energy (Solar PV) to the best possible configuration optimizing cost and technicalities.

3. Mathematical modelling and result analysis

Table 1 shows the existing mine with 100% reliance on heavy powered diesel generating sets for the day to day running of the whole operation of the mine, and supply to a nearby village the calculated LCOE is 272$/MWh.

Tab. 1 Business as usual scenario

CURRENT GENERATION SYSTEM		
Peak Power	MW	5,500
Total energy requirements	MWh	29 227
DIESEL		
Total diesel production	MWh	29 227
Diesel consumption	L	7 302 987
Diesel consumption including diesel loss	L	7 302 987
Diesel production to the load	MWh	29 227
CO2 emissions	Tons	4 382
Capex	$	2 745 400
Fuel cost	$ / L	1,00
O&M	% capex	10,00%
NPV Capex	$	5 900 772
NPV Opex	$	118 376 725
NPV MWh	MWh	456 581
Diesel LCOE	$ / MWh	272

$$\phi = HHv \times \rho \times \zeta \tag{1}$$

Where,

ϕ Power Input, (KWh/l),
HHv Higher heating value, (MJ/Kg),
ρ Density, (Kg/l),
ζ 0.278Kwh/MJ.

$$\eta = \vartheta/\phi \tag{2}$$

Where,

η Efficiency of the Generator, (%),
ϑ Power output, (KWh/l).

$$LCOE = \sum_{t=1}^{n} \alpha \div \sum_{t=1}^{n} \aleph \tag{3}$$

Where,

α Discounted capex and opex , ($),
$\aleph$ Discounted power generated, (Mwh)

Numerous simulations were made by changing the battery rating and the size of the expected PV farm for diesel price at 0,70 ,1 and 1,30 $/L and the results for each scenario is displayed in turns in the Tables below.

Tab. 2 Simulation results for scenario of infusing 4500KWp of PV plant

Price of Diesel		0,70 €/L	1,00 €/L	1,30 €/L
Peak load	kW	5500	5500	5500
Diesel genset	kW	7 400,00	7 400,00	7 400,00
PV plant	kWp	4 500,00	4 500,00	4 500,00
BESS Nominal capacity	kWh	2 760,00	2 760,00	2 760,00
Grid maximum power	kW	0,00	0,00	0,00
PCS power	kW	6 300,00	6 300,00	6 300,00
RES production to the load	%	100,0%	100,0%	100,0%
RES production to the HESS	%	0,0%	0,0%	0,0%
RES production to the BESS	%	0,0%	0,0%	0,0%
RES production curtailed	%	0,0%	0,0%	0,0%
Load covered by RES	%	23,1%	23,1%	23,1%
Load covered by Battery storage	%	0,0%	0,0%	0,0%
Load covered by Diesel	%	76,8%	76,8%	76,8%
Load covered by Grid	%	0,0%	0,0%	0,0%
Liters of diesel saved	L	1 956 982	1 956 982	1 956 982
Capex	$	7 562 464	7 562 464	7 562 464
IRR	%	20,38%	29,95%	40,09%
Pay back	Y	5,76	4,03	3,08
Status quo blended LCOE	$ / MWh	197,23	272,19	347,15
Blended Total LCOE	$ / MWh	171,95	226,83	281,70

Tab. 3 Simulation results for scenario of infusing 6200KWp of PV plant

Price of Diesel		0,70 €/L	1,00 €/L	1,30 €/L
Peak load	kW	5500	5500	5500
Diesel genset	kW	7 400,00	7 400,00	7 400,00
PV plant	kWp	5 400,00	5 400,00	5 400,00
BESS Nominal capacity	kWh	2 760,00	2 760,00	2 760,00
Grid maximum power	kW	0,00	0,00	0,00
PCS power	kW	6 300,00	6 300,00	6 300,00
RES production to the load	%	98,7%	98,7%	98,7%
RES production to the HESS	%	0,0%	0,0%	0,0%
RES production to the BESS	%	1,3%	1,3%	1,3%
RES production curtailed	%	0,0%	0,0%	0,0%
Load covered by RES	%	27,4%	27,4%	27,4%
Load covered by Battery storage	%	0,3%	0,3%	0,3%
Load covered by Diesel	%	72,3%	72,3%	72,3%
Load covered by Grid	%	0,0%	0,0%	0,0%
Liters of diesel saved	L	2 275 711	2 275 711	2 275 711
Capex	$	8 690 516	8 690 516	8 690 516
IRR	%	20,93%	30,61%	40,90%
Pay back	Y	5,39	3,98	3,04
Status quo blended LCOE	$ / MWh	197,23	272,19	347,15
Blended Total LCOE	$ / MWh	165,77	217,38	268,98

Tab. 4 Simulation results for scenario of infusing 6200KWp of PV plant

Price of Diesel		0,70 €/L	1,00 €/L	1,30 €/L
Peak load	kW	5500	5500	5500
Diesel genset	kW	7 400,00	7 400,00	7 400,00
PV plant	kWp	6 200,00	6 200,00	6 200,00
BESS Nominal capacity	kWh	2 760,00	2 760,00	2 760,00
Grid maximum power	kW	0,00	0,00	0,00
PCS power	kW	6 300,00	6 300,00	6 300,00
RES production to the load	%	94,7%	94,7%	94,7%
RES production to the HESS	%	0,0%	0,0%	0,0%
RES production to the BESS	%	5,0%	5,0%	5,0%
RES production curtailed	%	0,3%	0,3%	0,3%
Load covered by RES	%	30,2%	30,2%	30,2%
Load covered by Battery storage	%	1,4%	1,4%	1,4%
Load covered by Diesel	%	68,4%	68,4%	68,4%
Load covered by Grid	%	0,0%	0,0%	0,0%
Liters of diesel saved	L	2 544 816	2 544 816	2 544 816
Capex	$	9 573 496	9 573 496	9 573 496
IRR	%	21,12%	30,99%	41,49%
Pay back	Y	5,37	3,93	3,00
Status quo blended LCOE	$ / MWh	197,23	272,19	347,15
Blended Total LCOE	$ / MWh	161,92	210,76	259,60

Tab. 5 Simulation results for scenario of infusing 6300KWp of PV plant

Price of Diesel		0,70 €/L	1,00 €/L	1,30 €/L
Peak load	kW	5500	5500	5500
Diesel genset	kW	7 400,00	7 400,00	7 400,00
PV plant	kWp	6 300,00	6 300,00	6 300,00
BESS Nominal capacity	kWh	2 749,60	2 760,00	2 749,60
Grid maximum power	kW	0,00	0,00	0,00
PCS power	kW	6 300,00	6 300,00	6 300,00
RES production to the load	%	94,1%	94,1%	94,1%
RES production to the HESS	%	0,0%	0,0%	0,0%
RES production to the BESS	%	5,4%	5,4%	5,4%
RES production curtailed	%	0,5%	0,5%	0,5%
Load covered by RES	%	30,5%	30,5%	30,5%
Load covered by Battery storage	%	1,5%	1,5%	1,5%
Load covered by Diesel	%	68,0%	68,0%	68,0%
Load covered by Grid	%	0,0%	0,0%	0,0%
Liters of diesel saved	L	2 573 486	2 573 675	2 573 486
Capex	$	9 939 069	9 675 256	9 939 069
IRR	%	20,80%	30,88%	41,50%
Pay back	Y	5,37	3,92	3,00
Status quo blended LCOE	$ / MWh	197,23	272,19	347,15
Blended Total LCOE	$ / MWh	161,14	209,68	258,22

Tab. 6 Simulation results for scenario of infusing 7200KWp of PV plant

Price of Diesel		0,70 €/L	1,00 €/L	1,30 €/L
Peak load	kW	5500	5500	5500
Diesel genset	kW	7 400,00	7 400,00	7 400,00
PV plant	kWp	7 200,00	7 200,00	7 200,00
BESS Nominal capacity	kWh	2 760,00	2 760,00	2 760,00
Grid maximum power	kW	0,00	0,00	0,00
PCS power	kW	6 300,00	6 300,00	6 300,00
RES production to the load	%	88,2%	88,2%	88,2%
RES production to the HESS	%	0,0%	0,0%	0,0%
RES production to the BESS	%	6,6%	6,6%	6,6%
RES production curtailed	%	5,2%	5,2%	5,2%
Load covered by RES	%	32,7%	32,7%	32,7%
Load covered by Battery storage	%	2,1%	2,1%	2,1%
Load covered by Diesel	%	65,2%	65,2%	65,2%
Load covered by Grid	%	0,0%	0,0%	0,0%
Liters of diesel saved	L	2 766 854	2 766 854	2 766 854
Capex	$	10 659 996	10 659 996	10 659 996
IRR	%	20,05%	29,86%	40,18%
Pay back	Y	5,47	4,03	3,07
Status quo blended LCOE	$ / MWh	197,23	272,19	347,15
Blended Total LCOE	$ / MWh	159,55	206,12	252,68

4. Summary

From all the analysis based the economics and technical sizing method, the scenario with Solar PV plant at 6300Kwp is the best to be infused into the existing genset, this will account for a saving of 2544 816 litres of Diesel per annum and reduction of CO_2 by almost 3000 tons (68.5%). On the side of economics for the three scenarios of price at 0.7,1 and 1.3$/l, the payback time is 5.37,3.93 and 3 years respectively from saving from diesel leading to 30% coverage of the total energy be renewables. From this paper, the following inference can be drawn; for constant power generation, storage device is required by renewable energy. In addition to that, different climate conditions, not cost is a hinderance to the growth of renewable energy in the energy sector. Thus, the Energy sector should work to ease their environmental impact on the world by reducing carbon emissions, a goal that is achievable through adaptation and integration of renewables at a reasonable cost.

Acknowledgment

We would like to express thanks to the peer reviewers as well as everyone who participated in this research. We also gratefully acknowledge support from the KIC InnoEnergy, Clean Fossil and Alternative Fuels Energy for this opportunity and support.

References

[1] S .Strauss, S. Rupp, T. Love (eds.), Cultures of Energy: *Power, Practices, Technologies*, Left Coast Press Inc, Walnut Creek, California, USA, pp. 267-283, ISBN 9781611321654.

[2] World Energy Council, www.worldenergy.org, (27/11/17).

[3] M. Arsel, B. Akbulut, F. Adaman. Environmentalism of the Malcontent: *Anatomy of an Anti-coal Power Plant Struggle in Turkey*, *The Journal of Peasant Studies*, 2015, 42(2), pp. 371-395.

[4] G. Bridge, S. Bouzarovski, M. Bradshaw, N. Eyre. Geographies of energy transition: *space, place and the low-carbon economy*, Energy Policy, 2013, 53, pp. 331–340.
[5] World Energy Needs and Nuclear Power, http://www.world-nuclear.org/information-library/current-and-future-generation/world-energy-needs-and-nuclear-power.aspx, (27/11/17).
[6] United States Environmental Protection Agency, https://www.epa.gov/global-mitigation-non-co2-greenhouse-gases/global-mitigation-non-co2-greenhouse-gases-coal-mining, (30/11/17).
[7] Chamber of Mines, http://chamberofmines.org.za/industry-news/11-mining-in-sa/major-sectors, (30/11/17).
[8] South Africa Energy Coal, https://www.south32.net/what-we-do/places-we-work/south-africa-energy-coal (30/11/17).
[9] Department of Energy (South Africa), https://en.wikipedia.org/wiki/Department_of_Energy_(South_Africa), (30/11/17).
[10] Coal in South Africa, https://en.wikipedia.org/wiki/Coal_in_South_Africa, (30/11/17).

The current and future trends in chemical CO_2 utilization

Bogdan Samojeden[1]

[1]*Faculty of Energy and Fuels, Akademia Górniczo-Hutnicza im. Stanisława Staszica w Krakowie, bogdan.Samojeden@agh.edu.pl*

Abstract

According to the Inter-governmental Panel on Climate Change (IPCC) in 2014 carbon dioxide concentration in the atmosphere approached 400 ppm, against the pre-industrial value of 280 ppm. A safe value of 450 ppm has been set for the year 2050 to protect Earth from climatic disasters. With the growing threat of the climate change resulting from increasing concentration of CO_2, technologies of carbon dioxide storage and utilization are considered an assurance for continuation of fossil fuel use. In order to fulfil this goal, new technologies of utilization of CO_2 are developed. In this paper different methods of chemical utilization of carbon dioxide, both selected emerging technologies and those under research are shortly discussed.

Keywords: CCS, chemical utilization of CO_2, carbon dioxide, dry refoming of methane, tri-reforming, metahation, CO_2-derived methanol

1. Introduction

Carbon dioxide and other greenhouse gases are potential global warming threats [1], [2]. It was estimated that burning 1 ton of carbon in fossil fuels results in more than 3.5 tons of carbon dioxide. Currently concentration of CO_2 in the atmosphere is approaching 1 tera ton [3]. Fossil fuels which were meeting 81% of world energy needs in 1990 are expected to provide 60% share in the primary energy by 2040 [4]. Globally, coal will continue as the most important fuel in the nearest future. The CO_2 concentration in atmosphere have increased from 280 ppmv in preindustrial times to 374 ppmv in 2005, and to 336 ppmv in 2013 while average temperature increased by 0.84 ^oC. Evidence from Intergovernmental Panel of Climate Change (IPCC) indicates that to limit global temperature rise to 2 ^oC above the average, the concentration of CO_2 equivalent greenhouse gases should not increase beyond 450 ppmv in 2050 [5]. In order to limit climate changes, CO_2 emissions must be controlled. Two ways of dealing with CO_2 problem are proposed: carbon capture and storage technologies (CCS) and carbon capture and utilization (CCU) [6]. The former are passive technologies which aim at separation of CO_2 from industrial outgases, including power plants, and subsequent storage in geological formations, depleted oil or gas fields, or unminable coal seams [1], [7]–[9] .Storage in depleted oil or gas fields or unminable coal seams may be combined with the production of fuels that are not produced via primary or secondary techniques and are, therefore, sometimes classified as CCSU (carbon capture, storage and utilization) methods. On the other hand, the goal of CCU technologies is to use CO_2 as a solvent or substrate for industrial processes, thus either substituting currently used raw materials or introducing new processes consuming CO_2. In this approach CO_2 is not a harmful pollutant anymore but a valuable low-cost resource [10]. Thus in this way CCU methods may lead to added-value products – chemicals (e.g. polycarbonates, renewable methanol, urea etc), fuels or their precursors (syngas) or such as shown in Figure1. One of the fields that is especially interesting is the production of gas or liquid fuels [6], [10]–[13].

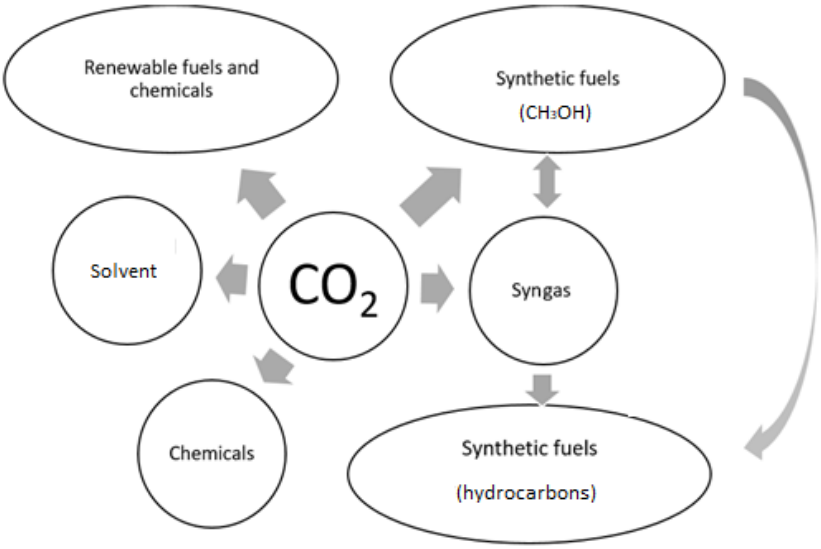

Fig. 1 Catalytic routes for CO_2 transformation into fuels and chemicals

2. The role of CCS and CCU in production of fuels

Technologies that utilize (or may in future utilize) CO_2 to obtain fuels may be divided into two categories, as illustrated by Table 1. The first category includes methods that allow to increase fuel production from either partly depleted natural reservoirs (oil or gas fields) or unconventional ones (methane-containing coal mines). Chemical reprocessing of CO_2 forms a second category. The processes listed in Table 1 have different technological status. Some of them belong to the category of mature or emerging technologies, some are under demonstration status, while others are still under research. When developed on industrial scale in the coming decades, the latter, together with the former, may create a new carbon dioxide based economy [14].

Tab. 1 Methods to increase fuels

Origin of fuels					
Conventional sources			**Chemical processes**		
Method	**Fuel**	**Technological maturity**	**Method**	**Fuel**	**Technological maturity**
Enhanced gas recovery EGR	Natural gas	economically feasible	Conversion CO_2 to CH_3OH	Methanol from CO_2	Emerging and research
Enhanced oil recovery EOR	oil	mature	CO_2 methanation	CH_4	Emerging and research
Enhanced coal bed methane recovery ECBM	methane	demonstration phase	DRM	Syngas → *	Research (R) or emerging (E) or mature (M)
Enhanced geothermal storage EGS	Natural resources	research phase/pilot plants	**Diesel oil plus gasoline via (F–T) Fischer-Tropsch Synthesis (M); gasoline via MTG (M); methane via CO (M) / CO_2 (E,R) methanation ; H_2 via (WGS) water gas shift reaction (M)*		

The role of CO_2 in the increased production of fuels is shortly described in the following chapters.

3. Fuels from natural reservoirs

Among the current technologies, only enhanced oil recovery (EOR) may be treated as fully mature. However, some other, such as Enhanced Gas Recovery (EGR) have been recognized as economically feasible. On the other hand, Enhanced Coal Bed Methane recovery ECBM is currently only at the demonstration stage. All mentioned processes may be treated as CCSU methods, as, apart from fuel production, they also store some CO_2 in depleted oil or gas fields, or mines. The storage may be treated as permanent or a mixture of permanent and non-permanent [15] . On the other hand, chemical processes lead to fuels that will be used in the nearest future, thus such methods must be treated as non-permanent CO_2 storage.

3.1 Enhanced oil recovery (EOR)

Various techniques for increasing the amount of crude oil (extracted from an oil field) are used for the enhanced oil recovery (EOR), which is also called tertiary recovery (as opposed to primary and secondary recovery). The US Department of Energy defined three primary techniques for EOR: thermal recovery, gas injection, and chemical injection [16]. Sometimes the term quaternary recovery is used to refer to more advanced, speculative, EOR techniques [17]–[19]. Using EOR, 30 to 60 percent, or more, of the reservoir's original oil can be extracted [16] compared with 20 to 40 percent when using primary and secondary recovery [20]. The method is, however, limited and not all reservoirs are amenable, because of miscibility of CO_2 and different type of oil. Thus only certain reservoirs, which fulfil criteria, such as: the previous application of primary and secondary methods of oil production, appropriate amount of oil still in place, appropriate depth and appropriate type of oil [15], [21], are amenable for EOR [15], [22] and simultaneous storage of CO_2 [15], [23].

3.2 Enhanced Gas Recovery EGR

The concept for enhanced gas recovery (EGR) is an area that had not been studied as comprehensively as EOR, although there is some experience on a large scale, such as e.g. the Salah project [24]. CO_2 is injected into natural gas reservoirs to artificially increase pressure, which results in increased yield from the well [25]–[29] . The concept did not find as broad application as EOR, although it was classified as economically feasible. Some older publications [30] indicated possible disadvantages, connected with the accessibility and price of CO_2 or the fact that there was a concern that injected CO_2 would mix rapidly with the existing methane gas and so degrade the resource.

3.3 Enhanced Gas Recovery ECBM

Enhanced coal bed methane recovery is a method of producing additional coalbed methane from a source rock, similar to enhanced oil recovery applied to oil fields. Carbon dioxide (CO_2) injected into a coal bed would occupy pore space and also adsorb onto the coal at approximately twice the rate of methane (CH_4), allowing for potential enhanced gas recovery [30]. This technique may be used in conjunction with carbon capture and storage in mitigation of global warming where the carbon dioxide that is sequestered is captured from the output of fossil fuel power plants. However, there are some restrictions on the method, concerning, among others, the maximum depth of the mine. Additionally, the mine in question cannot be exploited any more. The technological status of the method is demonstration stage.

3.4 Chemical processing of CO_2 as a source of fuels

A range of methods fall under the category of CO_2-to-fuels technologies, and these are at varying stages of development. Centi and Perathoner [31] suggest that the application of such processes could increase the industrial re-use of CO_2 10-fold in comparison to a relatively low current one, which was estimated by Peres-Fortes as ca 0.4 % of emitted carbon [32]. It should be mentioned, however, that chemical CO_2 reprocessing to added-value products (including fuels) is limited by certain restrictions. First of all, CO_2 balance must be taken into account. This means that the energy use for the new process cannot be higher than for the older (replaced) one. In general the primary energy input for these conversion technologies should be renewable energy, with the

current proponents focused on solar, wind or geothermal energy. The off-peak electricity also be taken into account. This is an important requirement for these technologies, as generally they have relatively low thermal efficiency (e.g. relatively small fraction of the energy input is converted to useful fuel). Consequently, the primary energy input needs to have a low CO_2 emissions intensity. If fossil-fuel based energy were used as the primary input into CO_2-based liquid fuel production, more CO_2 would be released than in case when the fossil fuel were used directly [33]. The second important issue is the amount of waste or by-products formed during these processes. The new processes utilizing carbon dioxide must not produce more waste than the traditional ones based on non-CO_2 technologies [34], [35].

Where the production of conventional fuels with CO_2 utilization is concerned, there are now either emerging processes or those still under research. One exception is the production of methanol, as in certain technologies CO_2 is used as an additive to syngas which is the main feedstock [36], [37]. The emerging technologies include the production of methanol directly from CO_2, and CO_2 methanation. Processes worth mentioning are alsodry reforming of methane, currently under extensive research, and tri-reforming of methane, currently at the conceptual stage and early research. Other possibilities are either the production of formic acid that is considered hydrogen carrier (with hydrogen as primary fuel) [15] or dimethyl ether (DME) [38], [39] which could replace conventional fuels due to its similar combustion properties [40].

3.5 CO_2-derived methanol

Classical methanol technologies are based on syngas (CO and H_2 mixture) and may be carried out in the presence of CO_2. Carbon dioxide is an additive which leads to the optimization of H_2 [36].

On the other hand, there is an emerging technology, in which methanol is obtained directly from CO2 as the main feedstock (CRI process [15], [41], [42]). The main reactions during hydrogenation of CO_2 are as follows:

$$CO_2 + 3H_2 = CH_3OH + H_2O \quad (1)$$

$$CO_2 + H_2 = CO + H_2O \quad (2)$$

The reaction (1) is a direct synthesis of methanol from carbon dioxide, while the (2) is reverse gas shift reaction. These two reversible reactions are both exothermic. It should be mentioned that from the economical point of view, cost of CO_2 hydrogenation reaction for methanol is higher than that of reaction based on CO/CO_2 mixture. On the other hand, reactions (1) and (2) can use CO_2 from flue gases in process industry. However, since CO_2 is not very reactive, considerably high reaction temperatures (typically, above 513 K) is necessary for acceptable CO_2 conversion. The accompanying reverse water-gas shift reaction is undesirable as it consumes hydrogen resulting indecreased yield of methanol. Meanwhile, the large amount of water produced by both reactions has certain inhibitory effect on ta catalyst [43]–[45], leading to its deactivation eventually. Other hydrogenated products, such as higher alcohols and hydrocarbons, are also produced in this process. Therefore, catalyst selectivity has critical importance.

Some demonstration-scale facilities have been developed in Europe in the last decade [46]. For example, Carbon Recycling International (CRI) in Iceland produces methanol by using geothermal energy and CO_2 from the same source. CRI has operated a commercial plant since 2011, with the capacity to produce 5 million liters of methanol per year [41], [42].

3.6 CO_2 reforming of methane

CO_2 reforming of methane, also called dry reforming of methane (DRM) is a highly endothermic reaction: (3).

$$CO_2+CH_4=2CO+2H_2 \qquad \Delta H=247 \text{ kJ/mol} \quad (3)$$

According to reaction (3), substrates are not expensive and result in added-value chemicals which are a feedstock in several important chemical processes.

Where fuels are concerned, reforming with CO_2 results in syngas production that can subsequently either be utilised in well-established Fischer-Tropsch process to produce different ranges of valuable liquid hydrocarbons,

or in the production of methanol. Methanol, on the other hand, is a feedstock for MTG process resulting in high-octane gasoline. Syngas is also the source of hydrogen. When water gas shift reaction is applied, the content of H_2 in syngas mixture can be increased at the cost of CO, according to the reaction (4):

$$CO + H_2O = CO_2 + H_2 \quad (4)$$

The DRM has as yet not been introduced on a large scale, although there are some commercial processes offered. The problems with DRM implementation are connected with (i) high endothermicity of the processs and (ii) the lack of appropriate catalysts [47]. The industrial applications of reforming process are so far limited to a combination of steam reforming and dry reforming reactions. The addition of CO_2 into a feed allows to control distribution of obtained products, i.e. H_2/CO molar ratio. Depending on the subsequent application of obtained synthesis gas, processes differ in operating parameters and feed composition. The main problem limiting the application of DRM reaction is the formation of carbon deposits on the catalyst surface. Therefore, the commercialization of DRM reaction on industrial scale depends on the offer of new stable and active catalyst and price of ton of CO_2 (7,5€ nowadays) [48], [49]. It should be mentioned that two commercial processes for DRM have been proposed, the Calcor process and the SPARG process, but it is still unclear if they can be used in the large scale technology [50], [51]. In Japan between 2002-2004 there was a pilot plant (JOGMEC GTL) where a mixture *H_2O:CO_2:natural gas* (with different ratio) with unrevealed catalysts were used. No deactivation during 6000 h was observed [52], [53]. The main difficulty in implementation of either of the mentioned technologies is to find a proper catalyst, which should be active, selective and stable i.e. should not undergo deactivation for longer periods of time [47]. The main problem with the catalysts is their deactivation, caused by the formation of filamentous-type carbon deposits via CH_4 decomposition or CO_x disproportionation. Among the catalysts, supported nickel was the most often studied, but interesting results have also been obtained with supported noble metals (Rh, Ru, and Pt) [45]. The noble metal-based catalysts show good activity and selectivity in DRM reaction [54]–[55]. From non-noble metals, only nickel-based catalysts showed similar activities and selectivities to those reported for noble metals.

A review of the studied catalysts was given in [47]. Lately interesting research on the application of hydrotalcites in DRM were published [56].

Tab. 2 Examples of materials studied as catalysts in dry reforming of methane (DRM)

Active material	**Support**	**Reaction conditions**	**Results**	**Ref.**
1 wt.% Pd, Rh, Ir, Ru, 2 wt.% Pt; IMP	Al_2O_3	500°C m_{cat} = 300mg; CH_4/CO_2 =1/1;	Ru > Pd > Rh > Pt > Ir	[54]
1wt.% Pd, Ru, Rh, Ir, Ni*; IMP	Al_2O_3	777°C;m_{cat}=50mg; CH_4/CO_2=1/1;	r > Rh > Ni > Pd > Ru	[57]
5 wt.% Fe, Co, Ni; IMP	CeO_2	700°C; CH_4/CO_2/Ar=1/1/3	Ni > Co >> Fe	[58]
3, 5 and 10 wt.% Ni, Rh, Pd, Ce; IMP	Al-pillared montmorillonites	650°C; CH_4/CO_2/He=1/1/8; m_{cat}=500mg;	3% Rh ≈ 10%Ni >>Pd >> 3%Ni >> Ce	[55]
10.3 wt % Ni, IMP	γ-Al_2O_3	800°C, CH_4/CO_2=1/1	x(CH_4)=92%, x(CO_2) = 94	[59]
10 wt % Ni, IMP	MgO	650°C, CH_4/CO_2=1/1	x(CH_4)=63%, x$(CO)_2$ = 75	[60]
63%wt Ni, 7%wt Al HT*		550°C, CH_4/CO_2=2/1	x(CH_4)=48%, x(CO_2) = 54, H_2/CO=2,4	[61]
0.78%wt. Ni, 21.66 %wt Mg, 8.35 %wt Al HT*		550°C, GHSV=20,000 h^{-1}, CH_4/CO_2/Ar = 2/1/7	x(CH_4)=28%, x(CO_2) = 24%, H_2/CO=1,6	[62]
43%wt Ni, Al HT*		700°C, ,CH_4/CO_2= 32/40	x(CH_4)=94%, x(CO_2) = 94%, H_2/CO=0.9	[63]

*HT – hydrotalcites (double-layer hydroxides)

3.7 Methanation

CO_2 methanation is an emerging technology using CO_2 as feedstock. It is represented by Sabatier reaction (5):

$$CO_2+4H_2=CH_4+2H_2O \qquad \Delta H = -165.0 \text{ kJ/mol} \tag{5}$$

The reaction is exothermic, but the CO_2 balance would be negative if hydrogen necessary for the process were to be obtained from fossil fuels. The solution to the problem is the application of renewable (solar, wind etc) or conventional off-peak energy excess (e.g. nuclear) for H_2O splitting into H_2 and O_2, as schematically illustrated by Figure 2.

If electrolysis hydrogen is supplied as an educt, as proposed in PtG – Power-to-Gas projects, CO_2 methanation allows for also the chemical storage of electricity [64], [65].

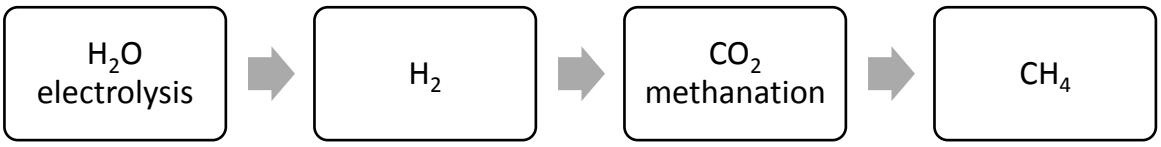

Fig. 2 CO_2 methanation process with unconventional H2 source

An overview of current CO_2 methanation projects at pilot and commercial scale was reported by Rönsch et al [66] and is given in Table 3. CO_2 methanation projects mostly take place in Europe. Hitachi Zosen INOVE (former Audi AG's ETOGAS) invested in a 6MW plant in Germany that uses renewable electricity from wind power and CO_2 from a biogas processing plant to produce methane [42], [67]. In Germany, the idea is the transformation of the energy system towards the one that is 100% based on renewable energies. This is associated with an increasing demand for chemical storage of electric energy and the compensation of fluctuating wind and solar energy production.

Tab. 3 Selected CO_2 methanation projects (adopted from [66])

Project name	**Location**	**Capacity power input [kW]**	**Name**	**Status**
Hashimoto CO_2 recycling plant	Sendai (JP)	n.d	IMR	Pilot plant 1996*
PtG Alpha Plant Bad Hersfeld	Bad Hersfeld (DE)	25	Etogas/ZSW	Pilot plant 2012
PtG Alpha Plant Morbach	Morbach (DE)	25	Etogas/ZSW	Pilot plant 2011
PtG Alpha Plant Stuttgart	Stuttgart (DE)	25	Etogas/ZSW	Pilot plant 2009
PtG Alpha Plant Stuttgart	Stuttgart (DE)	250	Etogas/ZSW	Pilot plant 2012
PtG Alpha Plant Rapperswil Erdgas Obersee	Rapperswil (CH)	25	Etogas/ZSW	Pilot plant 2014
E-Gas/PtG BETA plant	Werlte (DE)	6300	MAN	Commercial operation

* operation discontinued
n.d – no data given

CO_2 methanation requires a catalyst. There are numerical articles describing the possible materials. Mostly Ni-based catalysts are proposed. Examples of such materials are given in Table 4.

Tab. 1 Catalysts in CO_2 methanation (addopted from [68]

Catalysts	Content (%wt) of active metal	Reaction conditions	Results	Ref.
Ni-CeZrO	10	300°C, GHSV=30000 h^{-1}	x(CO_2) = 70%	[69]
Ni-TiO_2	15	218°C, GHSV=2400 h^{-1}	x(CO_2)=50%, x(CH_4)=99%	[70]
Co/KIT-6	20	260°C, GHSV= 22009 h^{-1}	x(CO_2)=45%, x(CH_4)=99%	[71]
Ru-TiO_2	0.8	180°C, GHSV=864 h^{-1}	x(CO_2)=100%, x(CH_4)=100%	[72]
Ni-CeO_2	10	300°C, GHSV= 10000h^{-1}	x(CO_2)=~90%, x(CH_4)=100%	[73]
Ni/H-Al_2O_3 (HT)	20	234°C, GHSV= 2400h^{-1}	x(CO_2)=50%	[74]
Ni/MCM-41	3	400°C, GHSV= 5760h^{-1}	x(CO_2)=56%, x(CH_4)=96%	[75]
$Ce_{0.95}Ru_{0.05}O_2$	-	400°C, GHSV= 45000h^{-1}	x(CO_2)=55%, x(CH_4)=99%	[76]
NiLa-HT	15	350°C, GHSV= 12000h^{-1}	x(CO_2)=76%, x(CH_4)=~100%	[77]

Methanation catalysts are typically composed of active metal particles dispersed on metal oxide supports. Up to now, a number of active metals including Ni, Fe, Co, Ru, Rh, Pt, Pd, W, Mo and various oxide supports (Al_2O_3, SiO_2, TiO_2, SiC, ZrO_2, CeO_2) were studied. A high methane selectivity of nearly 100% is the main aim, in accordance with the thermodynamic results [78]. However, high carbon dioxide conversion is difficult to reach at low temperatures because of the high kinetic barriers of the reaction processes [68].

3.8 Tri-reforming of methane (TMR)

The tri-reforming process is a very interesting concept in which CO_2 in flue gas could be used directly, without the energy-consuming stage of CO_2 separation. Because of H_2O and O_2 presence in flue gases, tri-reforming combines the three processes utilizing CH_4. In the tri-reforming of methane in a single reactor, the following reactions are coupled: methane steam reforming (5), methane partial oxidation (7) and carbon dioxide reforming of methane (8) [79]–[81]:

$$CH_4 + H_2O = CO + 3H_2 \qquad \Delta H = 207 \text{ kJ/mol} \tag{6}$$

$$CH_4 + \tfrac{1}{2} O_2 = CO + 2H_2 \qquad \Delta H = -36 \text{ kJ/mol} \tag{7}$$

$$CH_4 + CO_2 = 2CO + 2H_2 \qquad \Delta H = 298 \text{ kJ/mol} \tag{8}$$

The highly exothermic complete methane oxidation (9) influences positively the TRM process via improved energy balance:

$$CH_4 + 2O_2 = CO_2 + 2H_2O \qquad \Delta H = 880 \text{ kJ/mol} \tag{9}$$

Both reforming processes are endothermic reactions of steam (6) with CH_4 and CO_2 (8) with CH_4 with exothermic partial (7) and complete oxidation of methane (9) [79].

TRM is a new process designed for the direct production of synthesis gas with desirable H_2/CO ratios by reforming methane or natural gas. The concept of tri-reforming using power plant flue gas was first proposed by Song et al [82]. Before 1999, several papers were published on the study of combined CO_2 reforming and partial oxidation reaction [83]–[85] and simultaneous steam and CO_2 reforming of methane in the presence of oxygen [86]. The results in these papers indicated that combined tri-reforming is feasible. However, the new tri-reforming process still faces a number of challenges. They include, for example, effective conversion of CO_2 in the presence of O_2 and H_2O; the heat management; the minimization of the effect of SOx and NOx in flue gas on tri-reforming process; the management of inert gas N_2 in flue gas; and the integration of new process into power plants [87].

Tri reforming can also be used for converting and utilizing CO_2-rich natural gas [81], as some of them contain up to 50 vol% CO_2 and are not yet utilized commercially due to the high CO_2 concentration [87]–[91].

Tri-reforming process needs, however, efficient catalysts, which must be thermally stable, coke resistant and able to convert CO_2 efficiently in the presence of steam and O_2. Noble metals and Ni-based catalysts are established for all kinds of methane reforming reactions but Ni based catalysts are economically more preferable over noble metal based catalysts due to the high cost and low abundance of the noble metals. Tab. 5 shows the comparison of different catalysts studied in TRM and influence of active material on catalytic properties.

Tab. 5 The influence of active material on catalytic properties in TRM

Catalysts	Influence of active material on catalytic properties	Ref.
La/CeO_2	10 %at doping of La - CH_4 and CO_2 conversion increases from 93% and 83% to 96% and 86.5%, respectively	[92]
Ni–Mg/β-SiC (molar ratio Mg/Ni = 1/1; 1/10)	Catalysts (Ni–Mg/SiC 1/1) where Mg was firstly impregnated were less deactivated keeping a good catalytic behaviour. Impregnation of Ni and Mg yielded catalysts with the best catalytic performances	[93]
Ni/γ-alumina Ni/YZS (yttria-stabilized zirconia) Ni/β-silicon carbide Ni/CeO_2, Ni/β-SiC	Ni/Al_2O_3 - the lowest CH_4 and CO_2 reaction rates as a consequence of its low reducibility due to the formation of Ni aluminate. Ni/CeO_2 - the lowest H_2/CO molar ratio for the tri-reforming process. CeO_2 and β-SiC catalysts had the best characteristics as catalytic supports for TRM	[94]
Ni-CaO-ZrO_2	Promising catalytic activity and stability in methane tri-reforming and the methane conversion exceeds 70% under 973 K and atmospheric pressure	[95]
Ni@SiO_2 coreshell	11% Ni@SiO_2 stable activity at 750^{o}C (4 hours) without deactivation.	[79]
Ni–ZrO_2	4.8 wt% Ni loading for Ni–ZrO_2 catalyst was found to be the optimum Ni loading → stable for more than 100 h on time on stream with methane, carbon dioxide and steam conversion of ~95% at 800 °C	[96]

4. Conclusion

There are several processes considered, which may use CO_2 as feedstock for increased production of fuels. The methods may be divided into CCUS (CO_2 capture, utilization, and sequestration) and CCU (CO_2 capture and utilization). The technical maturnity of the method is quite varied. EOR is mature. Of the emerging methods and those under research, especially interesting are: CO_2-derived methanol, dry reforming of methane (DRM), CO_2 methanation, and tri-reforming. All these methods, however, require efficient catalysts. For DRM, CO_2 methanation and TRM the most promising are catalysts based on Ni as active component.

The development of CCUS and CCU methods will in future lead to carbon dioxide-based economy.

Acknowledgment

This work was supported by Grant AGH No. 11.11.210.373

References

[1] P. Baran, J. Cygankiewicz, and K. Zarębska, "Carbon dioxide sorption on polish ortholignite coal in low and elevated pressure," *J. CO2 Util.*, vol. 3–4, pp. 44–48, 2013.

[2] M. Motak, Ł. Kuterasiński, P. Da Costa, and B. Samojeden, "Catalytic activity of layered aluminosilicates for VOC oxidation in the presence of NOx," *Comptes Rendus Chim.*, vol. 18, no. 10, pp. 1106–1113, 2015.

[3] M. Mikkelsen, M. Jørgensen, and F. C. Krebs, "Synthesis and characterization of zwitterionic carbon dioxide fixing reagents," *Int. J. Greenh. Gas Control*, vol. 4, pp. 452–458, 2010.

[4] IEA, "CO2 Capture Facilities and Capacities," pp. 1–2, 2014.

[5] C. Ampelli, S. Perathoner, and G. Centi, "CO 2 utilization : an enabling element to move to a resource- and energy-efficient chemical and fuel production Subject Areas :," *Phil. Trans. R. Soc. A*, vol.

373:201401, 2015.
[6] R. M. Cuéllar-Franca and A. Azapagic, "Carbon capture, storage and utilisation technologies: A critical analysis and comparison of their life cycle environmental impacts," *J. CO2 Util.*, vol. 9, pp. 82–102, 2015.
[7] R. Safi, R. K. Agarwal, and S. Banerjee, "Numerical simulation and optimization of CO2 utilization for enhanced oil recovery from depleted reservoirs," *Chem. Eng. Sci.*, vol. 144, pp. 30–38, 2016.
[8] J. F. D. Tapia, J. Y. Lee, R. E. H. Ooi, D. C. Y. Foo, and R. R. Tan, "Optimal CO2 allocation and scheduling in enhanced oil recovery (EOR) operations," *Appl. Energy*, vol. 184, pp. 337–345, 2016.
[9] J. F. D. Tapia, J. Y. Lee, R. E. H. Ooi, D. C. Y. Foo, and R. R. Tan, "Planning and scheduling of CO2 capture, utilization and storage (CCUS) operations as a strip packing problem," *Process Saf. Environ. Prot.*, vol. 104, pp. 358–372, 2016.
[10] M. T. Ho, G. W. Allinson, and D. E. Wiley, "Comparison of MEA capture cost for low CO2 emissions sources in Australia," *Int. J. Greenh. Gas Control*, vol. 5, no. 1, pp. 49–60, 2011.
[11] J. F. D. Tapia, J.-Y. Lee, R. E. H. Ooi, D. C. Y. Foo, and R. R. Tan, "A Review of Optimization and Decision-Making Models for the Planning of CO2 Capture, Utilization and Storage (CCUS) Systems," *Sustain. Prod. Consum.*, 2017.
[12] M. M. F. Hasan, E. L. First, F. Boukouvala, and C. A. Floudas, "A multi-scale framework for CO2 capture, utilization, and sequestration: CCUS and CCU," *Comput. Chem. Eng.*, vol. 81, pp. 2–21, 2015.
[13] J. Patricio, A. Angelis-Dimakis, A. Castillo-Castillo, Y. Kalmykova, and L. Rosado, "Method to identify opportunities for CCU at regional level - Matching sources and receivers," *J. CO2 Util.*, vol. 22, no. October, pp. 330–345, 2017.
[14] S. L. Suib, A. Lawal, and R. J. Farrauto, "New and Future Developments in Catalysis," in *New and Future Developments in Catalysis*, 1st ed., S. Suib, Ed. Amsterdam, 2013, pp. 195–231.
[15] P. Brinckerhof, "Accelerating The Uptake Of CCS : Industrial Use Of Captured Carbon Dioxide (Report CCS)," 2011.
[16] U.S. Department of Energy, "Enhanced Oil Recovery." [Online]. Available: www.doe.gov. [Accessed: 29-Nov-2017].
[17] H. G. Douglas and E. N. Tiratsoo, *Introduction to petroleum geology*. Scientific Press, 1975.
[18] M. Walsh; and L. W. Lake, *A generalized approach to primary hydrocarbon recovery*, 1st ed. Elsevier Science, 2003.
[19] R. Miller, W. Michalski, and B. Stevens, *21st Century Technologies. Promises and Perils of a Dynamic Future*. OECD Publishing, 1998.
[20] A. Amarnath, "Enhanced Oil Recovery Scoping Study," Palo Alto, CA, 1999.
[21] N. Wildgust, "CO2 Storage in depleted oilfield: Global Application criteria for carbon dioxide enhanced oil recovery," 2009.
[22] L. P. He, P. P. Shen, X. W. Liao, Q. C. Gao, C. S. Wang, and F. Li, "Study on CO2 EOR and its geological sequestration potential in oil field around Yulin city," *J. Pet. Sci. Eng.*, vol. 134, pp. 199–204, 2015.
[23] International Energy Agency, "Carbon Capture and Storage Legal and Regulatory Review," 2011.
[24] P. S. Ringrose *et al.*, "The In Salah CO2 Storage Project: Lessons Learned and Knowledge Transfer," *Energy Procedia*, vol. 37, pp. 6226–6236, 2013.
[25] C. Khan, R. Amin, and G. Madden, "Carbon dioxide injection for enhanced gas recovery and storage (reservoir simulation)," *Egypt. J. Pet.*, vol. 22, no. 2, pp. 225–240, 2013.
[26] S. Jikich, D. Smith, W. Neal Sams, and G. Bromhal, "Enhanced Gas Recovery (EGR) with Carbon Dioxide Sequestration: A Simulation Study of Effects of Injection Strategy and Operational Parameters," *SPE East. Reg. Conf. Proc.*, pp. 31–39, 2003.
[27] M. Hasan, M. Eliebid, M. Mahmoud, S. Elkatatny, and R. Shawabkeh, "Enhanced Gas Recovery (EGR) Methods and Production Enhancement Techniques for Shale & Tight Gas Reservoirs," *SPE Kingdom Saudi Arab. Annu. Tech. Symp. Exhib.*, no. 2009, pp. 1–9, 2017.
[28] B. Kulga, R. Dilmore, C. Wyatt, and T. Ertekin, "Investigation of CO2 Storage and Enhanced Gas Recovery in Depleted Shale Gas Formations Using a Dual- Porosity/Dual-Permeability, Multiphase Reservoir Simulator," 2014.
[29] T. Dixon, "CCS Characterisation Criteria," 2009.
[30] L. H. Wickstrom, E. R. Slucher, M. T. Baranoski, and D. J. Mullett, *Geologic Assessment of the Burger Power Plant and Surrounding Vicinity for Potential Injection of Carbon Dioxide*, vol. 1. Columbus: Ohio Division of Geological Survey, 2008.
[31] G. Centi and S. Perathoner, "Opportunities and prospects in the chemical recycling of carbon dioxide to fuels," *Catal. Today*, vol. 148, no. 3–4, pp. 191–205, 2009.
[32] M. Pérez-Fortes, J. C. Schöneberger, A. Boulamanti, and E. Tzimas, "Methanol synthesis using captured CO 2 as raw material: Techno-economic and environmental assessment," *Appl. Energy*, vol. 161, pp.

718–732, 2016.
[33] Y. Wang, L. Yao, S. Wang, D. Mao, and C. Hu, "Low-temperature catalytic CO 2 dry reforming of methane on Ni-based catalysts: A review," *Fuel Process. Technol.*, vol. 169, no. June 2017, pp. 199–206, 2018.
[34] N. Seltenrich, "Emerging Waste-to -Energy Technologies," *Environ. Health Perspect.*, vol. 124, no. 6, pp. 106–111, 2016.
[35] World Nuclear Association, "'Clean Coal' Technologies, Carbon Capture & Sequestration," 2017. [Online]. Available: http://www.world-nuclear.org/information-library/energy-and-the-environment/clean-coal-technologies.aspx. [Accessed: 04-Dec-2017].
[36] R. Raudaskoski, E. Turpeinen, R. Lenkkeri, E. Pongrácz, and R. L. Keiski, "Catalytic activation of CO2: Use of secondary CO2 for the production of synthesis gas and for methanol synthesis over copper-based zirconia-containing catalysts," *Catal. Today*, vol. 144, no. 3–4, pp. 318–323, 2009.
[37] L. Bobrova, N. Vernikovskaya, and V. Sadykov, "Conversion of hydrocarbon fuels to syngas in a short contact time catalytic reactor," *Catal. Today*, vol. 144, no. 3–4, pp. 185–200, 2009.
[38] M. H. Huang, H. M. Lee, K. C. Liang, C. C. Tzeng, and W. H. Chen, "An experimental study on single-step dimethyl ether (DME) synthesis from hydrogen and carbon monoxide under various catalysts," *Int. J. Hydrogen Energy*, vol. 40, no. 39, pp. 13583–13593, 2015.
[39] Q. Zhang, Y. Z. Zuo, M. H. Han, J. F. Wang, Y. Jin, and F. Wei, "Long carbon nanotubes intercrossed Cu/Zn/Al/Zr catalyst for CO/CO2 hydrogenation to methanol/dimethyl ether," *Catal. Today*, vol. 150, no. 1–2, pp. 55–60, 2010.
[40] R. Dębek, M. F. G. Ribeiro, A. Fernandes, and M. Motak, "Dehydration of methanol to dimethyl ether over modified vermiculites," *Comptes Rendus Chim.*, vol. 18, no. 11, pp. 1211–1222, 2015.
[41] CRI, "The MefCO_2 project - Synthesis of Methanol from Captured Carbon Dioxide Using Surplus Electricity," *Carbon Recycling International (CRI)*, 2017. [Online]. Available: http://www.mefco2.eu/. [Accessed: 30-Nov-2017].
[42] S. Brynolf, M. Taljegard, M. Grahn, and J. Hansson, "Electrofuels for the transport sector: A review of production costs," *Renew. Sustain. Energy Rev.*, no. July 2016, pp. 1–19, 2017.
[43] T. Inui and T. Tatsuya, "Effective conversion of carbon dioxide and hydrogen to hydrocarbons," *Catal. Today*, vol. 10, pp. 95–106, 1991.
[44] K. Tomishige *et al.*, "Development of active and stable nickel-magnesia solid solution catalysts for CO 2 reforming of methane," vol. 114, pp. 375–378, 1998.
[45] E. Alper and O. Y. Orhan, "CO 2 utilization : Developments in conversion processes," *Petroleum*, vol. 3, no. 1, pp. 109–126, 2017.
[46] G. Gahleitner, "Hydrogen from renewable electricity: An international review of power-to-gas pilot plants for stationary applications," *Int. J. Hydrogen Energy*, vol. 38, no. 5, pp. 2039–2061, 2013.
[47] T. Grzybek, "Viable CO2 chemical sequestration applications," in *Development of coal, biomass and wastes gasification technologies with particular interest in chemical sequestration of CO2 : a monograph*, A. Strugała, Ed. Kraków: AKNET, 2012, pp. 99–150.
[48] R. Dębek, *Novel catalysts for chemical CO2 utilization (PhD Thesis)*. Kraków: Akademia Górniczo-Hutnicza im. Stanisława Staszica w Krakowie, 2016.
[49] "CO2 European Emission Allowances." [Online]. Available: http://markets.businessinsider.com/commodities/co2-emissionsrechte. [Accessed: 03-Dec-2017].
[50] S. C. Teuner, P. Neumann, and F. Von Linde, "The Calcor Standard and Calcor Economy Processes," *Oil Gas Eur. Mag.*, vol. 3, pp. 44–46, 2001.
[51] B. Elvers, *Ullmann's Energy: Resources, Processes, Products. Vol. 2*, XIX. Weinheim: Wiley-VCH Verlag GmbH & Co. KGaA, 2015.
[52] F. Yagi, R. Kanai, S. Wakamatsu, R. Kajiyama, Y. Suehiro, and M. Shimura, "Development of synthesis gas production catalyst and process," *Catal. Today*, vol. 104, no. 1, pp. 2–6, 2005.
[53] K. Katakura, M. Ihara, and Y. Suehiro, "The Challenge of Japan Oil , Gas and Metals National Corporation [JOGMEC] to develop the new GTL process - GTL process utilizing CO2 contained in the natural gas to explore stranded gas reserves -," in *GAS-TO-LIQUIDS 4th Annual World GTL Summit*, 2004, pp. 1–17.
[54] F. Solymosi, G. Kutsan, and E. A, "Catalytic Reaction of CH4 with CO2 over Alumina-Supported Pt Metals," *Catal Lett*, vol. 11, pp. 149–156, 1999.
[55] S. Barama, C. Dupeyrat-Batiot, M. Capron, E. Bordes-Richard, and O. Bakhti-Mohammedi, "Catalytic properties of Rh, Ni, Pd and Ce supported on Al-pillared montmorillonites in dry reforming of methane," *Catal. Today*, vol. 141, no. 3–4, pp. 385–392, 2009.
[56] R. Dębek, M. Motak, T. Grzybek, M. Galvez, and P. Da Costa, "A Short Review on the Catalytic Activity of Hydrotalcite-Derived Materials for Dry Reforming of Methane," *Catalysts*, vol. 7, no. 1, p. 32, 2017.

[57] A. T. Ashcroft *et al.*, "Selective oxidation of methane to synthesis gas using transition metal catalysts," *Nature*, vol. 344, pp. 319–321, 1990.
[58] K. Asami *et al.*, "CO2 reforming of CH4 over ceria-supported metal catalysts," *Catal Today*, vol. 84, pp. 27–31, 2003.
[59] A. Becerra, M. Dimitrijewits, C. Arciprete, and A. C. Luna, "Stable Ni/Al2O3 catalysts for methane dry reforming Effects of pretreatment," *Granul. Matter*, vol. 3, pp. 79–81, 2001.
[60] L. Li, L. Zhang, Y. Zhang, and J. Li, "Effect of Ni loadings on the catalytic properties of Ni/MgO(111) catalyst for the reforming of methane with carbon dioxide," *J. Fuel Chem. Technol.*, vol. 43, no. 3, pp. 315–322, 2015.
[61] R. Dębek, K. Zubek, M. Motak, M. E. Galvez, P. Da Costa, and T. Grzybek, "Ni-Al hydrotalcite-like material as the catalyst precursors for the dry reforming of methane at low temperature," *Comptes Rendus Chim.*, vol. 18, no. 11, pp. 1205–1210, 2015.
[62] R. Dębek, K. Zubek, M. Motak, P. Da Costa, and T. Grzybek, "Effect of nickel incorporation into hydrotalcite-based catalyst systems for dry reforming of methane," *Res. Chem. Intermed.*, vol. 41, no. 12, pp. 9485–9495, 2015.
[63] Z. Abdelsadek *et al.*, "In-situ hydrogasification/regeneration of NiAl-hydrotalcite derived catalyst in the reaction of CO2 reforming of methane: A versatile approach to catalyst recycling," *J. CO2 Util.*, vol. 14, pp. 98–105, 2016.
[64] K. Hashimoto, M. Yamasaki, K. Fujimura, T. Matsui, and K. Izumiya, "Global CO 2 recycling — novel materials and prospect for prevention of global warming and abundant energy supply," vol. 267, pp. 200–206, 1999.
[65] J. Lefebvre, M. Götz, S. Bajohr, R. Reimert, and T. Kolb, "Improvement of three-phase methanation reactor performance for steady-state and transient operation," *Fuel Process. Technol.*, vol. 132, pp. 83–90, 2015.
[66] S. Rönsch *et al.*, "Review on methanation – From fundamentals to current projects," *Fuel*, vol. 166, pp. 276–296, 2015.
[67] B. Bahor and van B. Michael, "Waste Management Sustainable Society," in *Renewable Energy Stystems*, New York: Springer New York, 2013, pp. 1475–1492.
[68] J. Gao, Q. Liu, F. Gu, B. Liu, Z. Zhong, and F. Su, "Recent advances in methanation catalysts for the production of synthetic natural gas," *RSC Adv.*, vol. 5, no. 29, pp. 22759–22776, 2015.
[69] Q. Pan, J. Peng, T. Sun, D. Gao, S. Wang, and S. Wang, "CO2 methanation on Ni/Ce0.5Zr0.5O2 catalysts for the production of synthetic natural gas," *Fuel Process. Technol.*, vol. 123, pp. 166–171, 2014.
[70] J. Liu *et al.*, "Enhanced low-temperature activity of CO2 methanation over highly-dispersed Ni/TiO2 catalyst," *Catal. Sci. Technol.*, vol. 3, no. 10, p. 2627, 2013.
[71] G. Zhou, T. Wu, H. Xie, and X. Zheng, "Effects of structure on the carbon dioxide methanation performance of Co-based catalysts," *Int. J. Hydrogen Energy*, vol. 38, no. 24, pp. 10012–10018, 2013.
[72] T. Abe, M. Tanizawa, K. Watanabe, and A. Taguchi, "CO2 methanation property of Ru nanoparticle-loaded TiO2 prepared by a polygonal barrel-sputtering method," *Energy Environ. Sci.*, vol. 2, no. 3, p. 315, 2009.
[73] S. Tada, T. Shimizu, H. Kameyama, T. Haneda, and R. Kikuchi, "Ni/CeO2 catalysts with high CO2 methanation activity and high CH4 selectivity at low temperatures," *Int. J. Hydrogen Energy*, vol. 37, no. 7, pp. 5527–5531, 2012.
[74] S. He *et al.*, "A surface defect-promoted Ni nanocatalyst with simultaneously enhanced activity and stability," *Chem. Mater.*, vol. 25, no. 7, pp. 1040–1046, 2013.
[75] G. Du, S. Lim, Y. Yang, C. Wang, L. Pfefferle, and G. L. Haller, "Methanation of carbon dioxide on Ni-incorporated MCM-41 catalysts: The influence of catalyst pretreatment and study of steady-state reaction," *J. Catal.*, vol. 249, no. 2, pp. 370–379, 2007.
[76] S. Sharma, Z. Hu, P. Zhang, E. W. McFarland, and H. Metiu, "CO2 methanation on Ru-doped ceria," *J. Catal.*, vol. 278, no. 2, pp. 297–309, 2011.
[77] D. Wierzbicki, R. Debek, M. Motak, T. Grzybek, M. E. Gálvez, and P. Da Costa, "Novel Ni-La-hydrotalcite derived catalysts for CO2 methanation," *Catal. Commun.*, vol. 83, pp. 5–8, 2016.
[78] Y. Zhu *et al.*, "Preparation of activated carbons for SO 2 adsorption by CO 2 and steam activation," *J. Taiwan Inst. Chem. Eng.*, vol. 43, no. 1, pp. 112–119, 2012.
[79] A. J. Majewski and J. Wood, "Tri-reforming of methane over Ni@SiO2 catalyst," *Int. J. Hydrogen Energy*, vol. 39, no. 24, pp. 12578–12585, 2014.
[80] K. Świrk, T. Grzybek, and M. Motak, "Tri-reforming as a process of CO 2 utilization and a novel concept of energy storage in chemical products," vol. 2038, pp. 1–10, 2017.
[81] C. Song and W. Pan, "Tri-reforming of methane: A novel concept for catalytic production of industrially useful synthesis gas with desired H2/CO ratios," *Catal. Today*, vol. 98, no. 4, pp. 463–484, 2004.

[82] C. Song, "Tri-Reforming: A New Process for Reducing CO2 Emission.," *Chem. Innov.*, vol. 31, pp. 21–26, 2001.
[83] A. T. Ashcroft, A. K. Cheetham, M. L. H. Green, and P. D. F. Vernon, "Partial oxidation of methane to synthesis gas using carbon dioxide," *Nature*, vol. 352, no. 6332. pp. 225–226, 1991.
[84] T. Inui, K. Saigo, Y. Fujii, and K. Fujioka, "Catalytic combustion of natural gas as the role of on-site heat supply in rapid catalytic CO2H2O reforming of methane," *Catal. Today*, vol. 26, no. 3–4, pp. 295–302, 1995.
[85] A. M. O'Connor and J. R. H. Ross, "The effect of O2 addition on the carbon dioxide reforming of methane over Pt/ZrO2 catalysts," *Catal. Today*, vol. 46, no. 2–3, pp. 203–210, 1998.
[86] V. R. Choudhary, A. M. Rajput, and B. Prabhakar, "NiO/CaO-Catalyzed Formation of Syngas by Coupled Exothermic Oxidative Conversion and Endothermic CO, and Steam Reforming of Methane," *Angew. Chemie Int. Ed. English*, vol. 33, pp. 2104–2106, 1994.
[87] S. A. Ghoneim, R. A. El-Salamony, and S. A. El-Temtamy, "Review on Innovative Catalytic Reforming of Natural Gas to Syngas," *World J. Eng. Technol.*, vol. 4, no. February, pp. 116–139, 2016.
[88] M. Halmann and A. Steinfeld, "Thermoneutral tri-reforming of flue gases from coal- and gas-fired power stations," *Catal. Today*, vol. 115, no. 1–4, pp. 170–178, 2006.
[89] H. Jiang, H. Li, H. Xu, and Y. Zhang, "Preparation of Ni/MgxTi1 - xO catalysts and investigation on their stability in tri-reforming of methane," *Fuel Process. Technol.*, vol. 88, no. 10, pp. 988–995, 2007.
[90] J. S. Kang, D. H. Kim, S. D. Lee, S. I. Hong, and D. J. Moon, "Nickel-based tri-reforming catalyst for the production of synthesis gas," *Appl. Catal. A Gen.*, vol. 332, no. 1, pp. 153–158, 2007.
[91] W. Cho *et al.*, "Optimal design and operation of a natural gas tri-reforming reactor for DME synthesis," *Catal. Today*, vol. 139, no. 4, pp. 261–267, 2009.
[92] L. Pino, A. Vita, F. Cipitì, M. Laganà, and V. Recupero, "Hydrogen production by methane tri-reforming process over Ni-ceria catalysts: Effect of La-doping," *Appl. Catal. B Environ.*, vol. 104, no. 1–2, pp. 64–73, 2011.
[93] J. M. García-Vargas, J. L. Valverde, J. Díez, P. Sánchez, and F. Dorado, "Preparation of Ni-Mg/β-SiC catalysts for the methane tri-reforming: Effect of the order of metal impregnation," *Appl. Catal. B Environ.*, vol. 164, pp. 316–323, 2015.
[94] J. M. García-Vargas, J. L. Valverde, F. Dorado, and P. Sánchez, "Influence of the support on the catalytic behaviour of Ni catalysts for the dry reforming reaction and the tri-reforming process," *J. Mol. Catal. A Chem.*, vol. 395, pp. 108–116, 2014.
[95] L. Si *et al.*, "Influence of preparation conditions on the performance of Ni-CaO-ZrO2 catalysts in the tri-reforming of methane," *J. Fuel Chem. Technol.*, vol. 40, no. 2, pp. 210–215, 2012.
[96] R. K. Singha *et al.*, "Energy efficient methane tri-reforming for synthesis gas production over highly coke resistant nanocrystalline Ni-ZrO2 catalyst," *Appl. Energy*, vol. 178, pp. 110–125, 2016.

Comparison of travelling - and standing-wave thermoacoustic engine on the basis of simple analytical approach

Krzysztof Grzywnowicz [1], Leszek Remiorz [1]

[1]Institute of Power Engineering and Turbomachinery, Silesian University of Technology, email: krzysztof.grzywnowicz@polsl.pl, leszek.remiorz@polsl.pl

Abstract

Due to profound understanding of thermoacoustic phenomenon derived in last decades of 20th century, thermoacoustic engines may become a valuable alternative classical solutions. Derivation of mathematical formulae, describing their functioning, allows to compare different designs and further optimize the setup. In this paper, a brief comparison of travelling- and standing-wave thermoacoustic engine concept was performed, basing on simplified analytical description. Analysis was focused on crucial operational parameters - acoustic power generated by the engine and its thermal efficiency. The results prove benefits from utilization of travelling-wave concept, coinciding with experimental data presented in references.

Keywords: Thermoacoustics, acoustics, thermoacoustic engine, travelling-wave TAE, standing-wave TAE

1. Introduction

Searching for environmentally-friendly power technologies forces engineers to find methods to exploit phenomena, stating mainly technical curiosities in the past. One among such fields of interest is the thermoacoustic phenomenon [8]. Major advantages of devices, basing this phenomenon during their functioning, is reduced number of mechanical parts - and therefore longer lifetime predicted - as well as possibility of application of environmentally-safe working fluids (i.e. noble gases) [7,8].

First scientific approach to observations of spontaneous induction of sound wave during heating a glass tube, derived by Rijke, Sondhauss and Rayleigh [7,8], derived basic understanding of this phenomenon. If considering an empty tube, made possibly of low-conducting material (i.e. glass), induction of acoustic wave will occur when heat transfer between solid and working fluid takes place - and only if heat is derived to the gas at the moment of its greatest compression or taken from at the moment of its greatest expansion [6,7]. Thus, the induction, called *thermoacoustic phenomenon*, connects rapid acoustic phenomena and relatively slow thermal interactions between working fluid and a solid [8]. Due to that fact, in order to improve heat transfer between gas and a solid, Carter et al. proposed introduction of the accumulative heat exchanger (called then *regenerator* or *stack*) inside the tube [7]. Further investigation of the phenomenon, performed by Swift, Wheatley and others, derived its explanation on the basis of principles of heat transfer and demonstrated the reversibility of the process, taking place during thermoacoustic sound wave induction [8].

The elementary thermoacoustic engine consists from: tube (*resonator*), either straight (in case of standing-wave engines) or looped (in case of travelling-wave), filled with working medium, where the sound may propagate, and three heat exchangers. First of them - hot heat exchanger - derives heat to the working medium, while cold heat exchanger takes the latent heat from the gas to ambient. Between those, third, accumulative heat exchanger is located. Its main role is partial accumulation of energy of working medium, transferred as heat either from medium to the stack (during and immediately after compression phase) or from the stack to the medium (during and immediately after expansion phase) [8]. Thermal phenomena, appearing in the regenerator, include also conduction of heat between subsequent gas particles, due to non-zero conductive heat transfer coefficient of the working medium. The scheme of thermal interaction between solid of regenerator and working gas (represented as series of infinitesmall gas volumes) is presented in Figure 1. As conduction of heat inside the

working medium domain and its high viscosity may cause significant losses, noble gases (i.e. helium, argon), nitrogen and ambient air are often used as working media in thermoacoustic engines [7].

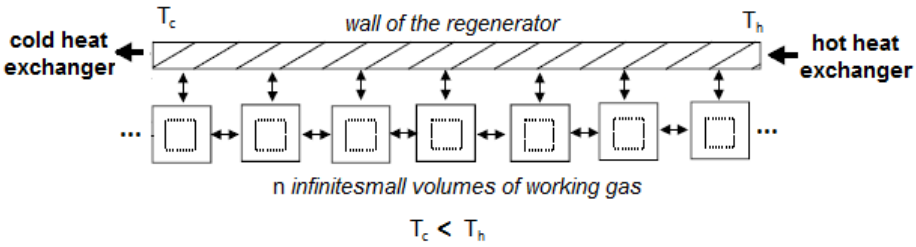

Fig. 1 Scheme of the heat transfer processes inside the regenerator (direction of heat flow depicted with arrows).

Further stages of thermal interaction between the stack and the working gas – and thus cyclic compression and expansion of working gas - lead to elementary oscillating flow inside the tube. If heat is continuously derived to the gas by hot heat exchanger, as well as latent heat taken out by cold heat exchanger, cyclic temperature and pressure variations occur, as stated by basic dependence (1):

$$T\mathrm{d}s = c_p \mathrm{d}T + \frac{T}{\rho^2}\left(\frac{\partial \rho}{\partial T}\right)_{\mathrm{p}} \mathrm{d}p = 0 \tag{1}$$

where: s – specific entropy, ρ - density, c_p – specific heat at constant pressure, p - pressure and T - temperature [8].

Assuming, that the working gas is an ideal gas and introducing changes in temperature and pressure (ΔT and Δp, respectively) instead of those quantities themselves, the dependence (2) is obtained [8]:

$$\frac{\Delta T}{T_{\mathrm{m}}} = \frac{\kappa - 1}{\kappa}\frac{\Delta p}{p_{\mathrm{m}}} \tag{2}$$

where: κ – adiabatic index.

The combination of oscillating flow inside the resonator, combined with positive acoustic impedance of the regenerator, as well as certain boundary conditions at edges of the resonator, forces the acoustic wave to form inside the tube [6,7,8].

Thermodynamic cycle, which is realized by working gas in a thermoacoustic engine, is similar to Brayton cycle in case of standing-wave devices [7] and to Stirling cycle in case of travelling-wave engines [7,8]. The p-V diagram of real Stirling cycle, appearing in a thermoacoustic engine, is presented in Figure 2.

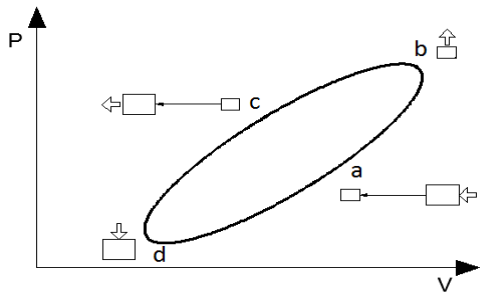

Fig. 2 The real Stirling cycle for thermoacoustic engine: a – compression phase; b – heat derived by gas, taken next by regenerator; c – expansion phase; d - heat derived by regenerator, taken next by working gas.

In case of the standing-wave device, there is single, straight tube present, and a standing wave is formed. Considering travelling-wave engine, presence of the feedback loop allows the sound wave to travel inside the resonator, while only part of the wave travels to the main tube of the resonator. As indicated, construction of standing-wave device is significantly simpler, comparing to the travelling-wave. Moreover, in those engines, number of additional phenomena (i.e. Gedeon streaming), affecting increase in thermal losses, may occur [6,7]. However, the thermodynamic Stirling cycle, present in the case of travelling-wave engines, is significantly more effective comparing to the Brayton cycle; thus, vital focus of scientific circles is put on devices using travelling acoustic wave [6,7].

The main aim of this paper is to perform simple analytical comparative analysis of standing- and travelling wave thermoacoustic engines of similar working parameters in order to determine potential differences in their working parameters. The functioning of those types of engines was compared on the basis of acoustic power, generated by the engine, and energy efficiency.

2. Basic analytical description of the thermoacoustic engine

Crucial parameters of any thermoacoustic device are actual temperature gradient across the regenerator ∇T_m and the critical temperature gradient ∇T_{crit}, [1] expressed by formula (3):

$$\nabla T_{crit} = \frac{T_m \beta p_1}{\rho_m c_p u_1} \tag{3}$$

where: T_m - cross-section averaged temperature of the fluid, β - thermal expansion coefficient, p_1 - acoustic pressure, ρ_m - mean density of working fluid, c_p - specific heat capacity at constant pressure, u_1 - working gas velocity.

As far as $\nabla T_m > \nabla T_{crit}$, power is produced within the regenerator and device performs as an engine [1], inducing pressure and velocity oscillations, presented using first order approximation on the x component of the momentum equation [1,2]:

$$-\rho_m \frac{\partial \mathrm{u}_1}{\partial \mathrm{t}} = \frac{\partial p_1}{\partial x} \tag{4}$$

where: t – time, x – position vector along x axis.

In ideal acoustic channel, the acoustic field may be described by expression of pressure distribution along given cross-section. Considering pure standing-wave thermoacoustic engine, pressure field may be described using following expression [1]:

$$p_1 = \frac{1}{2} p_a e^{i\omega t}\left[e^{-ikx} + e^{ikx}\right] \tag{5}$$

where: k - wave number, p_a - pressure amplitude, ω - angular frequency, x – position, t - time.

Substituting Eq. (5) into Eq. (4), the dependence of velocity distribution for standing-wave engine may be obtained [1]:

$$u_1 = \frac{1}{2} \frac{p_a e^{i\omega t}}{\rho_m c}\left[e^{-ikx} + e^{ikx}\right] \tag{6}$$

where: c – speed of sound.

Considering ideal travelling-wave engine, solution of pressure and velocity differential equation changes; thus, the final formulae for pressure distribution is indicated by Eq. (7):

$$p_1 = p_a e^{i\omega t} e^{-ikx} \tag{7}$$

Consequently, introducing Eq. (7) into Eq. (4), the distribution of velocity across the cross-section of the acoustic channel may be obtained [1]:

$$u_1 = \frac{p_a e^{i\omega t}}{\rho_m c} e^{-ikx} \tag{8}$$

For both standing- and travelling-wave engines, the ratio of acoustic pressure and velocity, states the acoustic impedance *Z*. Its phase represents the real phase shift between pressure and velocity of acoustic wave, generated in the regenerator [1].

In real cases, neither pure standing- nor travelling-wave conditions are present. Thus, while describing the acoustic field introduction of the superposition of a rightward travelling wave with standing wave component is useful. In such general case, an additional parameter, characterizing shifting from standing- to travelling-wave is present. Pressure field may be described using following dependence [1]:

$$p_1 = p_a e^{i\omega t}\left[\tau e^{-ikx} + (1-\tau)e^{ikx}\right] \tag{9}$$

where: τ - travelling wave ratio and τ = 0.5 denotes pure standing wave conditions, while τ = 1.0 denotes pure travelling wave case

Distribution of velocity may be obtained utilizing following formula [1]:

$$u_1 = \frac{p_a e^{i\omega t}}{\rho_m c}\left[\tau e^{-ikx} + (1-\tau)e^{ikx}\right] \tag{10}$$

General approach is especially useful in comparative analyses, since the change in parameter allows for smooth transition from standing-wave engine to travelling-wave engine. Furthermore, utilization of generalized formulae (Eq. (9) and Eq. (10)) allows to determine the operational parameters of the engine in intermediate states, when both transverse and stationary waves affect strongly the phenomenon.

Independently on the engine type, the average acoustic power, produced in regenerator of the length *Δx*, may be expressed as [1]:

$$\Delta\dot{E}_z = \left\{-\frac{1}{2}\omega\rho_m A\frac{\mathrm{Im}|-f_v|}{|1-f_v|^2}|U_1|^2 - \frac{1}{2}\frac{\gamma-1}{\gamma}\frac{\omega A\mathrm{Im}|-f_k|}{p_m}|p_1|^2 + \frac{1}{2}\frac{1}{T_m}\frac{\Delta T_m}{\Delta x}\mathrm{Re}\left[\frac{f_k-f_v}{(1-f_v)(1-\sigma)}p_1 U_1\right]\right\}\Delta x \tag{11}$$

where: f_v , f_k - cross-sectional averaged Rott's functions for set-of-plates geometry of regenerator, σ - Prandtl number of working medium, U_1 - volumetric mass flow induced by propagating acoustic wave.

The Rott's functions (*thermoviscous functions*) link convective heat transfer in the regenerator domain between solid and working gas, with geometry of the stack and properties of the fluid. These are known for number of geometries of the stack [1]. However, one of common shapes of these exchangers is set of parallel plates [1,8], as depicted in Figure 3b. Thus, such geometry of regenerator was assumed in the analysis input data.

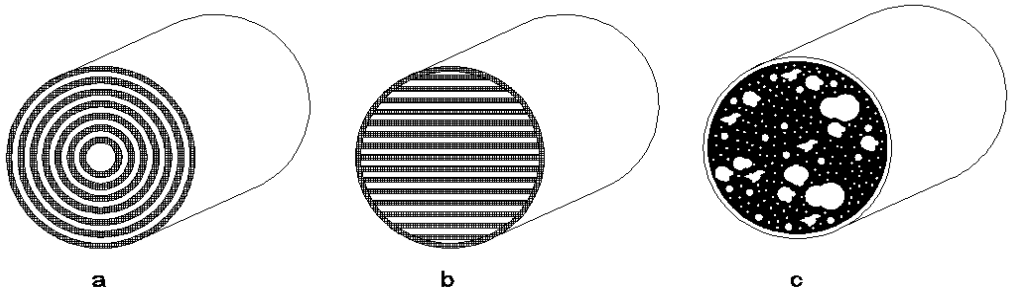

Fig. 3 Common geometries of the stack: a – set of thin-wall cylinders, b – set of parallel plates, c – porous body.

For this type of the stack, Rott's functions are defined by Eq. (12) and Eq. (13) [1]:

$$f_v = \frac{\tan h\left[(1+i)y_0{\delta_v}^{-1}\right]}{(1+i)y_0{\delta_v}^{-1}} \tag{12}$$

$$f_k = \frac{\tan h\left[(1+i)y_0{\delta_k}^{-1}\right]}{(1+i)y_0{\delta_k}^{-1}} \tag{13}$$

where: h - convective heat transfer coefficient for working gas flow inside the regenerator canals, δ_k - thermal penetration depth, δ_v - viscous penetration depth, y_0 - half of spacing between plates in the stack.

Thermal and viscous penetration depth are quantities introduced to the thermoacoustic devices analyses as estimation of the length of thermal and viscous boundary layers, respectively, affecting boundary phenomena in between solid part of regenerator and the working gas [8]. Thermal and viscous penetration depths are defined by Eq. (14) and Eq. (15), respectively [8].

$$\delta_k = \sqrt{\frac{2\alpha}{\omega}} \tag{14}$$

$$\delta_v = \sqrt{\frac{2\nu}{\omega}} \tag{15}$$

where: α - thermal diffusivity of working gas; ν - kinematic viscosity of working fluid.

The average heat flow, produced in the length of regenerator due to hydrodynamic transport may be expressed in the form of Eq. (16), according to Huifang *et al.* [1]:

$$\dot{Q} = \frac{|U_1|\rho_m c_p}{2\omega(1-\sigma^2)|1-f_v|^2}\Delta T_m \mathrm{Im}(f_k + \sigma f_v) - \frac{1}{2}\mathrm{Re}\left[p_1 U_1 \left(\frac{f_k - f_v}{(1+\sigma)(1-f_v)}\right)\right] \tag{16}$$

Energy efficiency of thermoacoustic device may be stated as ratio of acoustic power generated in the regenerator, to total heat flux derived to the system. Considering simple analytical representation of the device, concerning functioning of the regenerator as source of sound wave and heat flow produced along its domain, efficiency of the thermoacoustic engine may be indicated as follows:

$$\eta_Z = \frac{\Delta \dot{\mathrm{E}}_\mathrm{z}}{-\dot{Q} + \Delta \dot{\mathrm{E}}_\mathrm{z}} \tag{17}$$

On the basis of the formulae discussed, functioning of basic model of the thermoacoustic engine under varying conditions may be analyzed.

3. Simplified model analysis

To indicate changes in operational parameters with transistion from standing- to travelling-wave engine, generalized formulae for pressure and velocity distribution (Eq. (9) and (Eq. (10)) were used. In order to investigate functioning of the engine, certain initial parameters of the model were stated.

First, properties of the working gas were identified. According to Tijani *et al.* and others [4,7,8], best working media indicate low thermal conductance and high specific heat capacity. However, in number of cases, when the engine is designed to function under barometric pressure, ambient air is utilized as well [8]. Thus, dry air of initial temperature T_i=20°C and of barometric pressure was assumed as working gas in the engine modeled. Properties of the medium at assumed temperature and ambient pressure are indicated in Table 1.

Tab. 1. Properties of air at T_i assumed [13]

Density (kg/m^3)	**Specific heat (kJ/kg·K)**	**Thermal conductivity (W/m·K)**	**Kinematic viscosity (m^2/s)**	**Prandt number (-)**	**Thermal diffusivity (m^2/s)**
1.205	1.005	0.0257	$15.11\cdot10^{-6}$	0.713	$2.12\cdot10^{-5}$

Next, dimensions of the stack were introduced to the preliminary equations. Among these, the stack length, spacing between plates and average width of the plate are crucial for obtaining reliable results of the analysis. Values of the discussed parameters, assumed as input data for the analysis performed, are presented in Table 2.

Tab. 2 Selected dimension of the regenerator geometry

Length of the regenerator (m)	Average width of canal between plates (m)	Spacing between stack plates (m)
0.03	0.02	$0.50 \cdot 10^{-3}$

Further, several working parameters of the engine analysis were assumed. These parameters concern frequency of the sound wave, generated in the domain of regenerator, difference of temperature between heated and cooled edges of the regenerator (which ideally corresponds to difference in temperatures between hot and cold heat exchangers), mean temperature of the stack, and exact time of calculation of pressure and velocity distribution. Values of the chosen working parameters, assumed during analysis, are indicated in Table 3.

Tab. 3 Selected parameters of the engine assumed

Frequency of the generated sound wave (Hz)	Difference of temperature along the length of the regenerator (K)	Mean temperature of the working gas (K)	Time of calculation (s)
180.84	650.00 or 800.00	293.15	5.00

Finally, model of heat transfer between solid walls of regenerator and working medium has to be introduced. According to [1,4], due to possibly large pressure difference between pressure node and anti-node and low cross-sectional areas of canals in the stack, as well as influence of the entrance effect for short regenerators, working gas flow in the domain of regenerator may be assumed as turbulent flow. To simplify the analysis, influence of thermal radiation was neglected. Thus, pure convective heat transfer in the stack was assumed. One of the simplest convective heat transfer correlations for turbulent flow is the Dittus-Boelter correlation. Since, during gas oscillations, heat is transferred both to and from regenerator walls, the exponent of Prandtl number in this correlation was averaged and the classical Dittus-Boelter formula was stated as Eq. (18):

$$Nu = 0.023 Re^{0.8} Pr^{0.35} \tag{18}$$

where: *Nu* – Nusselt number, *Re* – Reynolds number, *Pr* – Prandtl number.

The analysis included investigation of two cases, of different values of temperature difference along the regenerator: this difference was equal to 650K in the first case and 800K in the second. For both cases, acoustic power generated by the engine and its energy efficiency for set of values of the τ parameter (in the range from 0.505 to 0.995) were calculated.

Acoustic power of the engine and its energy efficiency for lower value of ΔT_m as function of τ is indicated in the Figure 4. Power of the engine and its efficiency for the case of higher value of ΔT_m versus τ parameter is depicted in the Figure 5.

For both values of difference of temperatures along the regenerator ΔT_m, significant rise in the acoustic power of the engine with increase in the τ parameter value was visible. Increase of acoustic power on the τ coefficient visible on the figures is linear. Considering efficiency of the engine, for value of ΔT_m = 650K, slight drop in efficiency with rise in τ is visible. The same tendency was not observed for ΔT_m = 800K.

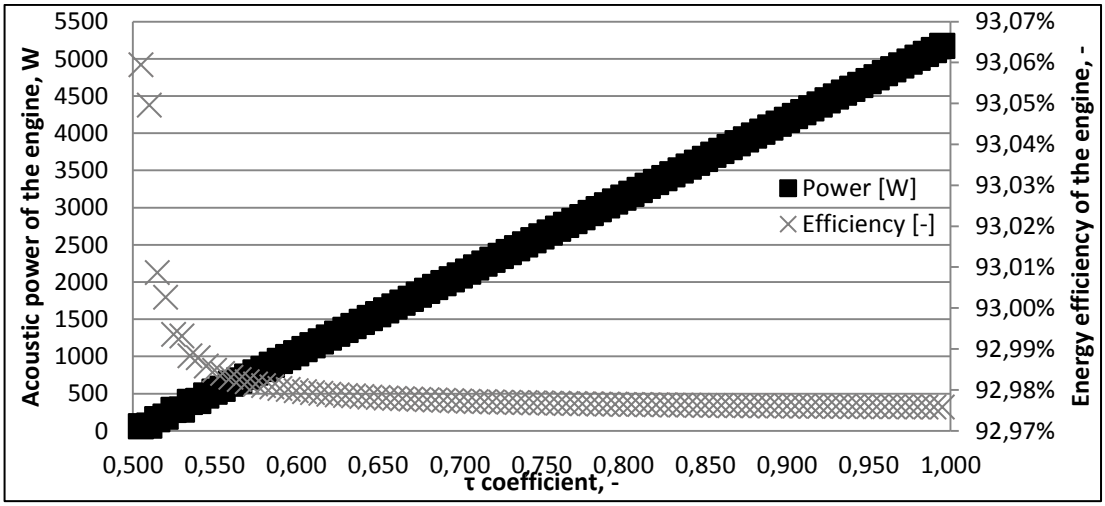

Fig. 4 Acoustic power and efficiency of the TA engine model for $\Delta T_m = 650K$.

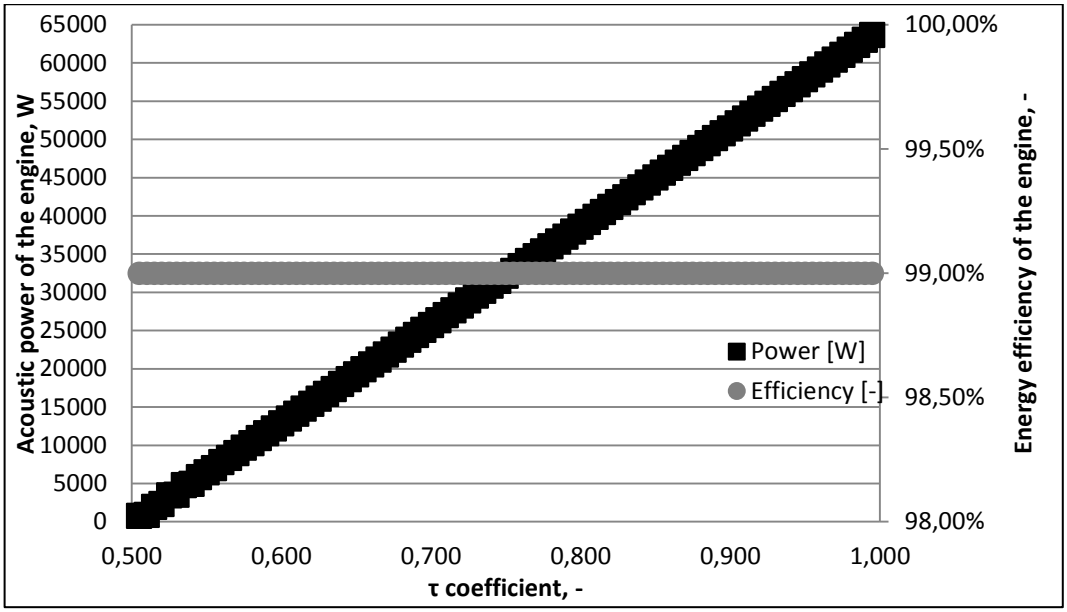

Fig. 5 Acoustic power and efficiency of the TA engine model for $\Delta T_m = 800K$.

4. Summary

Vital rise in the acoustic power of the engine with increase in the τ parameter value indicated better performance of the stack coupled with shifting from pure standing to pure travelling wave. This corresponds to results presented by Huifang *et al.* and Rossing [1,6]. However, increase observed was linear and did not correspond to experimental and numerical data derived [1]. Main cause of that fact is simplification of the thermoacoustic engine, introduced with basic analytical model. Since in the analysis performed, only regenerator is considered for thermoviscous phenomena, viscous losses coupled with boundary layer inside canals of the stack are insignificant. Viscous losses, stating significant part of total losses in thermoacoustic devices [4,8], rise with increase in velocity, affecting strongly power losses in the resonator, especially for travelling wave devices. Because in the basic mathematical model prepared, neither geometry of the resonator nor properties of its material were derived, power gained from the engine is limited only by part of losses, present in real devices and numerical models. Moreover, model presented does not take into account surface roughness of plates, forming

the stack, which influences the flow - and thus heat transfer conditions - in the domain of regenerator in constructed engines.

Decrease in efficiency with rise in τ for $\Delta T_m = 650K$ indicate the dependency of heat transport conditions within regenerator on change in hydrodynamic properties of fluid, passing through canals of the stack. However, since for $\Delta T_m = 800K$ efficiency did not change, increase in temperature difference ΔT_m over certain level does not lead to further significant change in hydrodynamic conditions in the stack. Thus, in that case, power losses in the regenerator are linearly dependent on temperature difference.

Values of energy efficiencies of the thermoacoustic engine obtained are relatively high and, thus, unrealistic. As in the case of acoustic power, this fact is caused by omitting number of significant losses, connected with acoustic power dissipation across the resonator, heat losses to ambient and imperfection of heat transfer in hot and cold heat exchangers. Several of those are highly dependent on pressure and velocity of the gas inside the tube of the engine [4,5], strongly reducing efficiency of real devices.

Despite of imperfections of the model described, results of the analysis indicate higher power of travelling wave engines, compared to standing wave engines of similar construction parameters. This proves better performance of the regenerator in the case of travelling wave devices. Since main operational parameters of thermoacoustic devices are highly influenced by performance of the stack [2,4], utilization of travelling wave may lead to vital rise in performance of thermoacoustic engines.

References

[1] K. Huifang, Z. Gang, L. Qing: Thermoacoustic effect of traveling-standing wave, *Cryogenics*, 50 (2010), pp. 450-458.

[2] G.W. Swift: Thermoacoustic engines, *The Journal of the Acoustical Society of America*, 84 (1988), pp. 1145-1180.

[3] J.R. Olson, G.W. Swift: Simlitude in thermoacoustics, *The Journal of the Acoustical Society of America*, 95 (1994), pp. 1405-1412.

[4] M.E.H. Tijani, J.C.H. Zeegers, A.T.A.M. de Waele: Design of thermoacoustic refrigerators, *Cryogenics*, 42 (2002), pp. 49-57.

[5] S. I. Sergeev: Fluid oscillations in pipes at moderate Reynolds numbers, *Mekhanika Zhidkosti i Gaza*, 1 (1966), pp. 168-170.

[6] T.D. Rossing *et. al*.: *Springer Handbook of Acoustics*, first edition, Springer Science+Business Media, 2007.

[7] S. Collard: Design and Assembly of Thermoacoustic Engine Prototype, Bechelor of Engineering Thesis, Helsinki Metropolia University of Applied Sciences, 2012.

[8] K. Grzywnowicz, L. Remiorz: Thermoacoustic cooling - numerical model of elementary device [in: Polish], *Rynek Energii*, 131 (2017), pp. 63-69.

[9] Air properties - Engineering Toolbox, https://www.engineeringtoolbox.com/air-properties-d_156.html, date of access: 20/11/2017.

Potential of Solar Energy in selected Countries from the MENA Region - A Review

Mohamed Mufid Hakim [1], Muhammad Yousif Gill [1]

[1]Department of Energy and Environmental Engineering, Silesian University of Technology, e-mail: mofeed.hakim@yahoo.com, myousif.gill@gmail.com

Abstract

The rising demand of energy in the MENA region with the increasing population means the Energy generation must expand. Most methods used in MENA are not environmental friendly and tend to be more expensive. Therefore it is very important to find some alternative way of generation which tends to be more environmental friendly and less expensive. Countries in this region present huge solar energy potential. In this paper we will talk about the potential of selected countries from the MENA region .We will also discuss the problems which they may face during the transition. At the end, previous and future solar projects in those countries are presented.

Keywords: MENA, solar projects, sustainable development, conventional methods, environment friendly, solar energy, future plans

1. Introduction

Countries in the MENA region present huge solar energy potential, as shown in the solar map in Figure 1.

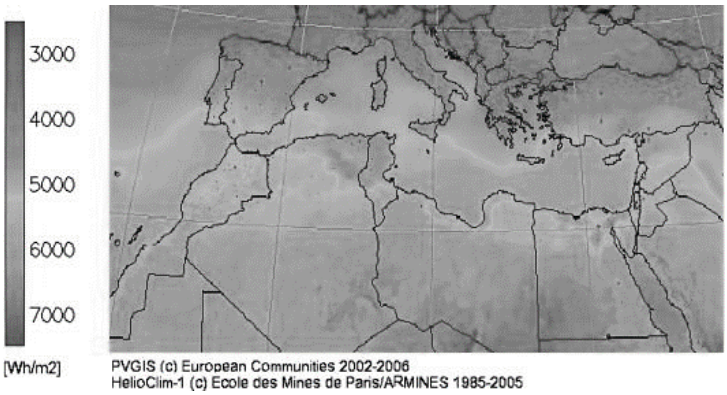

Fig. 1 Average daily solar radiation in the Meditation countries [1]

As evident the direct solar irradiance in the Middle East and North Africa (MENA) countries, is much higher than that of south Europe [1]. Furthermore, countries in MENA region have more deserts meaning no space restrictions, while some regions are very remote. The abundant space combined with the huge solar resources make this region one of the most promising areas for installation of Solar Energy plants for providing electricity, as the DESERTEC initiative describes [2]. Moreover, the methods used by countries in this are very conventional which produce harmful gasses such as CO_2, SO_2, and NOx which are the main sources of global warming.

Future energy systems need to be based on renewable energy technologies in order to minimize environmental impacts and account for the finite supply of fossil fuels. The energy vector that holds the most promise for future energy systems is hydrogen. There remain, however, several challenges that must be

addressed before a renewable hydrogen energy system can be implemented. The use of a carbon-based feedstock for hydrogen production in the near term cannot be avoided, but long-term solutions must be designed now to ensure energy needs are met in the future. The environmental, economic, and political reasons for the adoption of a renewable energy system emphasize the importance of its adoption [3].

For this we will be choosing four MENA countries and discuss them in three sections.

- Sate of the Market.
- Potential of Solar Energy.
- Previous and future Projects.

In the first section we will discuss about the geography of the country and its demands. Furthermore, we will discuss the main sources used by these countries and their impact on the environment.

In the second section we will discuss about the countries potential of solar energy mostly based on their location. In the third section we will give brief knowledge about the current and future projects of solar energy in the selected countries.

2. Presentation of the countries analyzed

UAE

- State of the Market

The UAE has become one of the most important spots in the world because of the economic growth and urbanization which results in increasing the energy demand. Figure 2 shows the factors that affect the energy consumption and environmental pollution in the UAE.

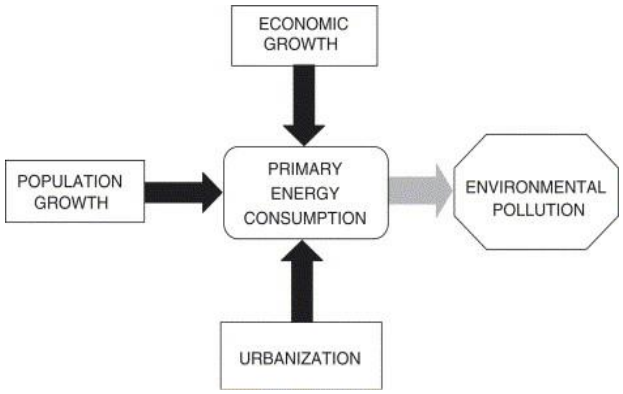

Fig. 2 Factors affecting the Energy demand and environment pollution

There are two main methods of energy production in the UAE namely crude oil and natural gas. According to energy information administration (EIA), the UAE's maximum crude oil production capacity is estimated to be around 2.0–2.5 million barrels per day (bbl/d), they have roughly 100 billion barrels of proven oil reserves which is nearly 10% of the world's crude oil supply. The UAE possesses about 215 trillion cubic feet of natural gas, which is ranked as the world's fifth-largest natural gas reserves after Russia, Iran, Qatar and Saudi Arabia [4].

Due to the low cost of energy, the energy consumption has increased dramatically in the last recent decades. Therefore, it is important to emphasise on the other energy generation sectors to have a balanced production from all resources while decreasing the pollution on the environment.

- Potential of Solar Energy

Since 2006, the UAE took part in the renewable energy, specifically the solar energy, because of the economic development and population growth. Most of the renewable energy projects are within the solar

energy due to the huge potential of solar energy with an annual average solar insolation exceeding 8.5 GJ/m^2 year [5]. The geographical position of the country makes it blessed with abundant resource of free energy besides the fossil fuels. They are able to take advantage of this opportunity to use it to produce clean and sustainable energy by using the photovoltaic panels and solar thermal energy technology for many different applications (off-grid and on-grid).

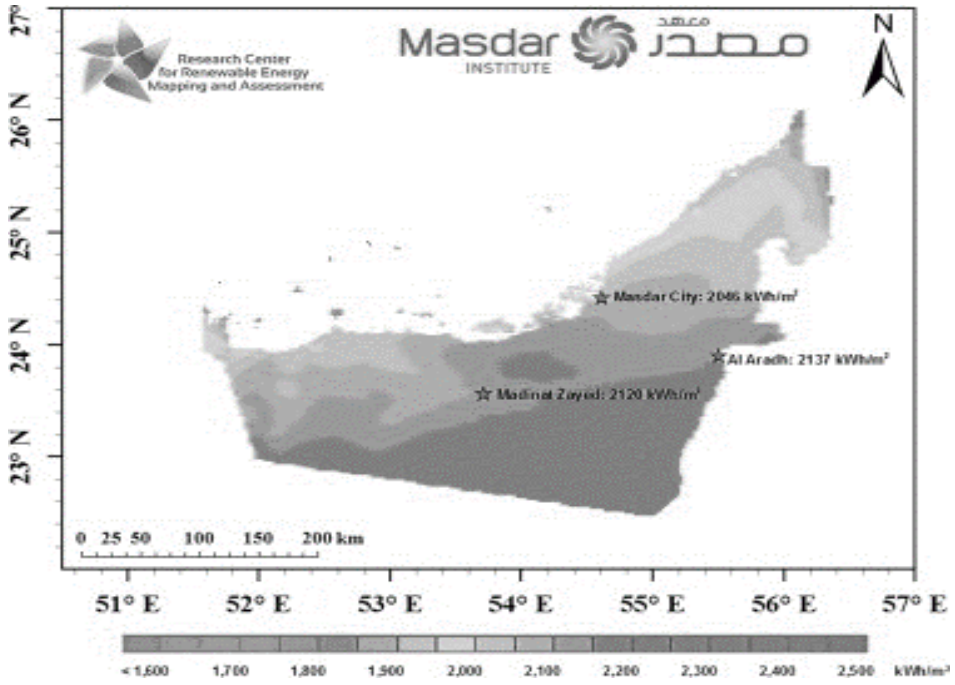

Fig. 3 Yearly GHI

- Previous and future projects
  - Solar rooftop plan (SRP)

This program is led by Masdar Institute in order to achieve the target of the UAE, which is to produce 7% of the energy production by 2020.

  - Masdar 10 MW PV power plant

This is the largest PV grid connected plant in the MENA region built in 2009 by ENVIROMENA. It includes crystalline Silicon PV modules (provide 5 MW) and CdTe thin films modules (provide 5 MW).

  - Shams 1 concentrated solar power plant

It is one of the world's largest concentrated solar power plants in the Middle East. it is a joint project between Masdar (60%), Total (20%), and Abengoa Solar (20%).

  - Sheikh Mohammed bin Rashid Al Maktoum solar park

This project is a mixture between PV and CSP, which is planned to be completed by 2030 with a total capacity of 1000 MW [6].

  - The concentrated PV testing facility (CPV)

It is a joint project between Masdar and ISFOC (Spain) that will test various concentrated PV (CPV) systems under Abu Dhabi environmental conditions. This project is being implemented in Masdar City. The CPV pilot project aims to connect 1 MW of CPV electricity generation to the electrical grid with a minimum power of 100 kW for each system tested. The reliability and the cost reduction of CPV is the main focus of this project.

- Masdar Institute

Masdar Institute was established in collaboration with the Massachusetts Institute of Technology as the R&D arm of the Masdar Initiative. It is a graduate level research-driven sustainability-focused university where a lot of research is conducted for supporting the renewable energy sector in the UAE.

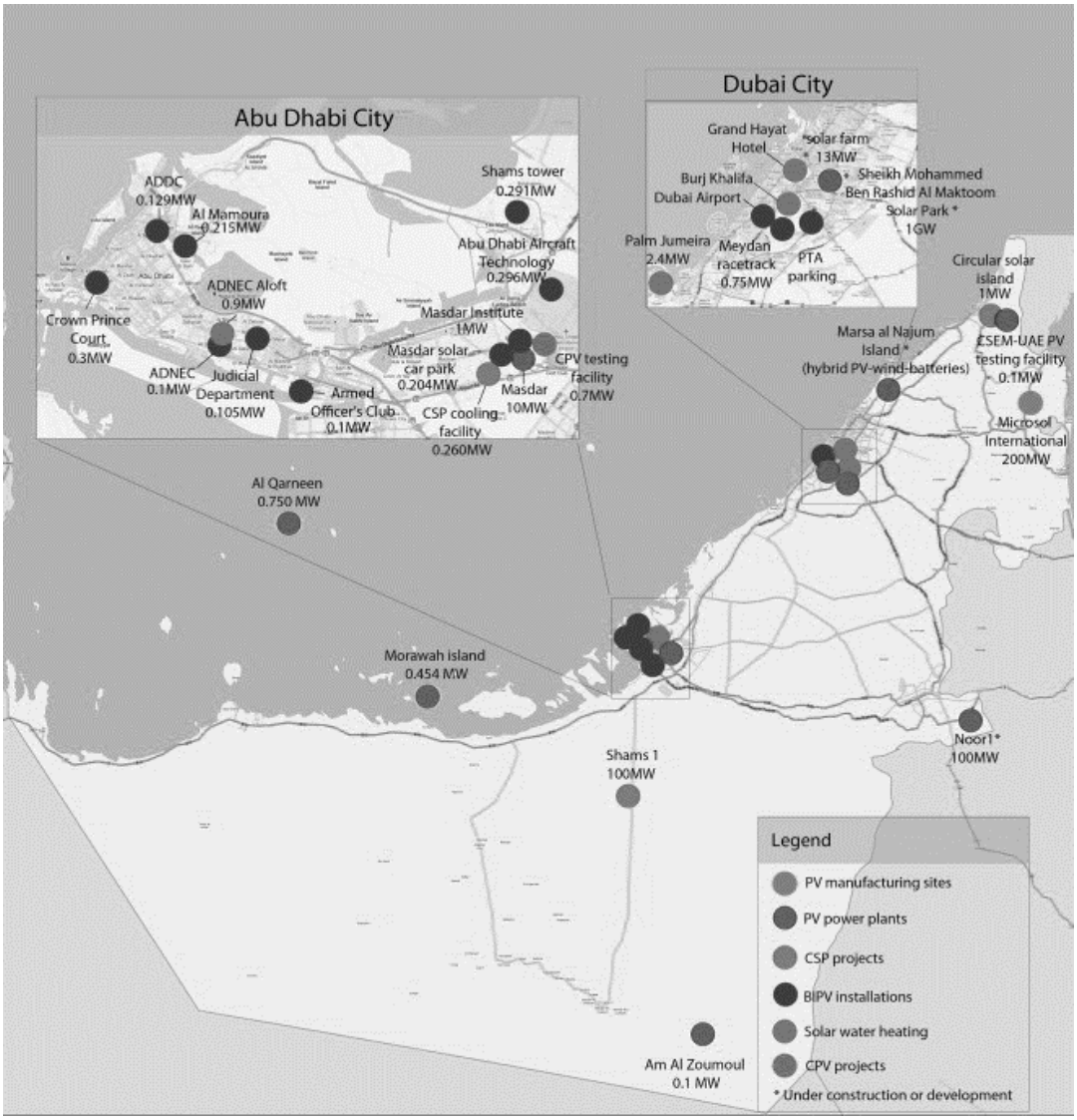

Fig. 4 Solar projects in the UAE [6].

Saudi Arabia

- State of the Market

Saudi Arabia is located in the middle-East with the population of 32.28 Million (as of 2016) and increasing rapidly. With rapidly growing industry Saudi Arabia will require huge amount of energy, as of now Peak loads reached nearly 24 GW in 2001 and are expected to approach 60GW by 2023. Saudi Arabia is one of the biggest oil exporters of the world, owing to this huge oil reserves Saudi's economy and energy consumption is hugely dependent on Fossil Fuels. Electricity productions of Saudi Arabia comes from these fossil fuels, 65% coming from Oil 27% from Natural Gas and 8% from steam [7].

Conventional methods of energy generation are the major contributor of production of harmful gasses and polluting the environment. Especially with the low quality methods of generation typical in Saudi Arabia emit a

variety of pollutants that contribute to public health problems. They produce harmful gasses such as CO_2, SO_2, and NO_x which are the main sources of global warming [8].

It is also MENA's largest oil consumer, one of the few major industrialized economies that produces a significant portion of its electricity through oil-burning plants. If Saudi Arabia doesn't curb its energy demand, institute energy efficiency requirements, and diversify its electricity generation profile, it could become an oil importer by 2030.

- Potential of Solar Energy

Saudi Arabia is fortunate enough to lie in "SUN BELT" , between latitudes 31°N and 17.5°N. Moreover, Average solar radiation in Saudi Arabia varies between a maximum of 7.004 kWh/m^2 at Bisha and a minimum of 4.479 kWh/m^2 at Tabuk. The southren part of Saudi Arabia seems to have more potential of Solar energy.The duration of sunshine varies between a maximum and minimum of 9.4 and 7.4 h/day. With an average daily sunshine duration of 8.89 h/day.

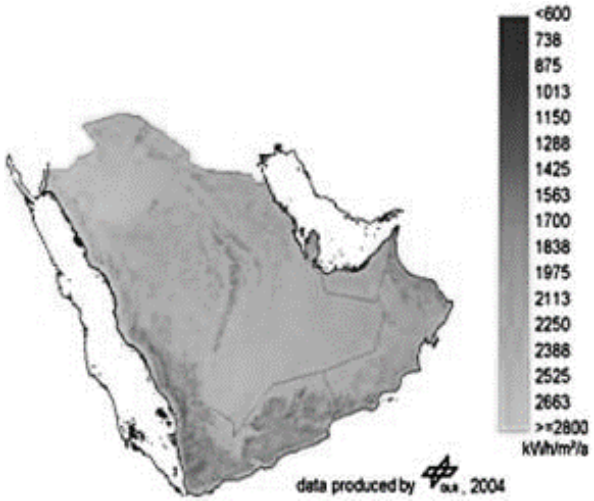

Fig. 5 Average Solar Radiation (kWh/m^2)

According to the study performed by Rahman and de Castro in 1995, they selected the top-ten locations of PV power plants according to solar irradiation [9].

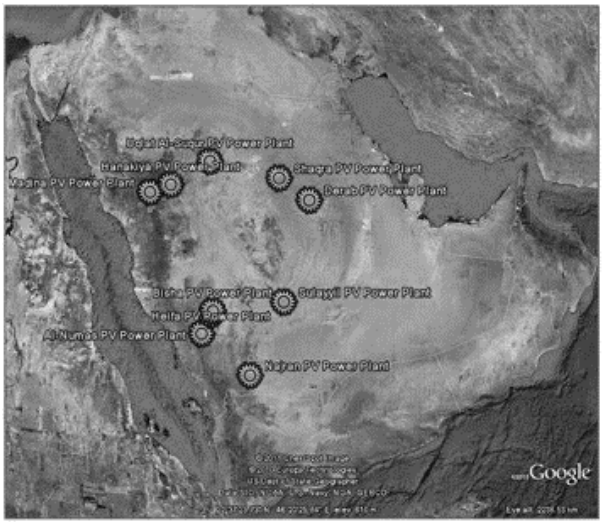

Fig. 6 Top-ten locations of PV power plants

- Previous and future projects

With the decreasing oil prices Saudi Arabia wants to decrease its dependency on oil by transforming the domestic consumption into Renewables, owing to the huge potential of Solars, it is keen to develop solar power industry. Saudi Arabia's first solar power plant was commissioned on October 2, 2011, on Farasan Island. It is a 500 kW fixed tilt photovoltaic plant. During the 2012 United Nations Climate Change Conference in Qatar Saudi-Arabia announced its target to receive third of its electricity demand from solar power with 41GW of solar capacity by 2032.

16 gigawatts (GW) of solar PV and 25 GW of concentrated solar power (CSP), both by 2032. In 2011, the Saudi Electricity Company (SEC) controlled roughly 51 GW of generating capacity, more than doubling since 2000, and projected to grow another 50 percent to 77 GW by 2020. Saudi Arabia is the world's largest oil producer, and 80 percent of its export and revenue come from the production and sale of hydrocarbon resources.

Morocco

- State of the Market

Morocco has a population of 30 million which is growing rapidly and becoming urban. They were mostly dependent on the imported crude oil and products of oil (97%) and hydro power (3-4%). Nowadays the diversity in the energy generation has luckily changed as by 2020 Morocco's annual electricity production will provide 38% from solar energy [10].

- Potential of Solar Energy

Morocco has an average solar power potential of over 5 kWh/m^2/day (3000 hours of sunshine per year). However, this abundant resource is still not utilized properly, the government is pushing to implement CSP and PV projects. There are also international collaboration with different countries like Germany and the UAE investing in Morocco to help them reach their target.

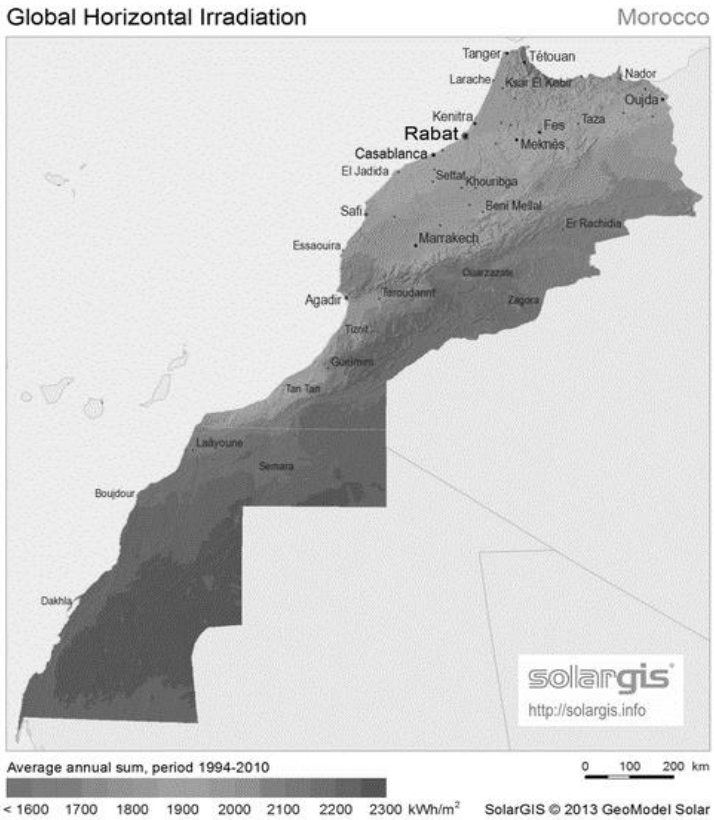

Fig. 7 GHI Morocco

- Previous and future projects

  Ouarzazate solar plant:

The entire Solar Project is planned to produce 580 MW, the projects consist of 5 stages (NOOR 1,2,3,4 and 5). The solar power is already competitive: the average cost of production at the Ouarzazate site (CSP) is 12 euro cents per kWh (source: KfW), and the price of the electricity produced at the PV power plant (Noor IV) will be 4.3 euro cents per kWh, among the lowest in the world.

The Programme to develop the Moroccan solar water heater market aims to encourage the purchase of solar water heaters through grants and standard loans, setting a target of 1.7 million m^2 of solar water heaters installed in households by 2020.

The Programme to develop the Moroccan solar water heater market aims to encourage the purchase of solar water heaters through grants and standard loans, setting a target of 1.7 million m^2 of solar water heaters installed in households by 2020.

Morocco has recently announced an ambitious plan for the development of Integrated Solar projects combined with combined cycle units [11]. The project would to a saving of 1 million Tons and 3.7 million tons of CO_2 emissions per year and aims to:

- Build 2000 MW of solar capacity by 2020 on five sites (Ouarzazate (500 MW), Ain Beni Mathar (400 MW), Foum Al Ouad (500 MW), Boujdour (100 MW), Sebkhat Tah (500 MW)). Table 2 [58] briefly describes the location, grid connection and water availability of each site and displays the approximate coordinates. These projects are to be based on two major technological variables: CSP and PV technologies.
- Provide access to energy for the general population at an affordable and competitive price.
- Achieve sustainable development through the promotion of renewable energy.
- Promote productivity and competitiveness.
- Strengthen regional integration through the opening up to EuroMediterranean energy markets and harmonizing energy legislation.

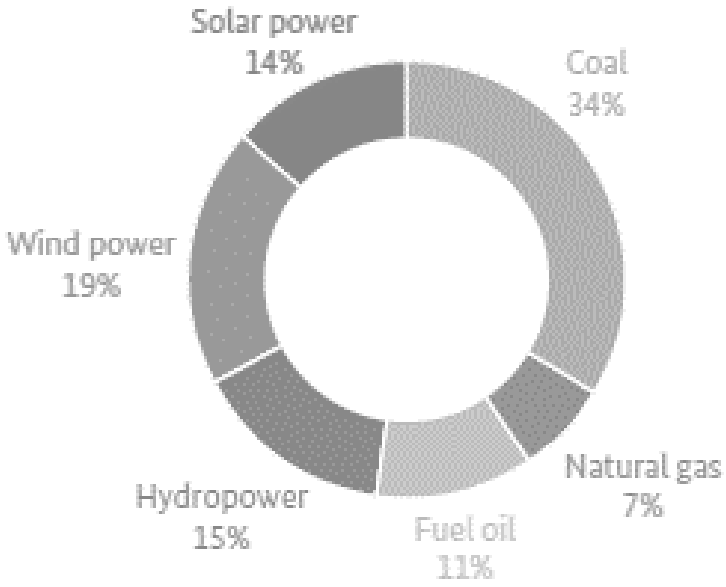

Fig. 8 Electricity generation capacity planned for 2020
(Source: ONEE)

Oman

- State of the Market

Oman is located in the middle-East with the population of 4.425 Million(as of 2016) and increasing rapidly.With rapidly growing indstry Oman will require huge amount of energy , as of now Peak loads reached nearly 6.83 GW in 2000 and increased to 18.51 GW by 2011. The main export of Oman is Petroleum products. Oil and gas contribute towards their economy. In 2012, 97.5% of electricity was generated at gas fired facilities whilst 2.5% amounted to diesel generation.

According to the annual Report of 2012 of the Authority for Electricity Regulation, Oman seeks to diversify the electricity generation and reduce its dependency on Petroleum products Convensional methods of energy generation are the major contributor of production of harmful gasses and polluting the environment.Especially with the low quality methods of generation typical in Oman emit a variety of pollutants that contribute to public health problems.They produce harmful gasses such as CO2, SO2, and NOx which are the main sources of global warming [12].

- Potential of Solar Energy

Oman is lucky enough to be located in the "SUN BELT" .The majority of the land in Oman receives daily solar radiations ranging between 5500–6000 Wh/m2/day and 2500–3000 Wh/m2/day in July and January, respectively. This shows that there is a very high potential of solar energy in Oman [13].

In addition, after reviewing solar radiation at 25 separate locations, the Engineering College of Sultan Qaboos University has identified that the three sites with the greatest solar energy potential are Marmul, Fahud and Sohar. Of these, the best choice would be a solar plant situated at Marmul which would produce an estimated 9,000MWh a year at a cost of US$210 MWh [14].

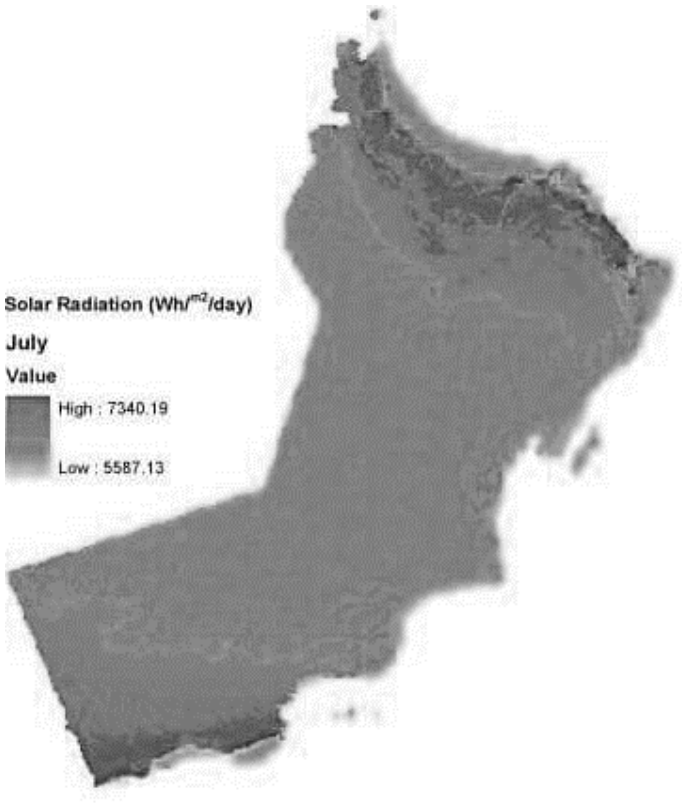

Fig. 9 Solar Radiation in Oman

- Previous and future projects

Oman seeks a smooth transition towards the renewables and reduce its dependency on oil. According to Ministry of Energy of Oman , 50% of the homes in Oman will be Solar power in the next five years.Oman's utility Oman Power and Water Procurement Company SAOC (OPWP) has issued a tender for PV solar plants having energy capacity of 200MW , this project will be completed by the end of 2022 [15].

- PDO in conjunction with GlassPoint Solar is building the largest solar plants in the world in terms of peak energy production. Miraah will be a 1,021 MW solar thermal facility in South Oman, harnessing the sun's rays to produce steam.
- Ningxia Zhongke Jiaye New Energy and Technology Management Co. and the Oman Investment Fund will jointly work to produce roof top solar panels which will contribute towards the energy generation of 1000 MW and this project will be completed by the end of 2019.

Conclusion

In this paper, a number of selected countries from the MENA region with the highest solar radiation potential among the world has been reviewed. Their energy market status, potential of generation from the solar energy and the future targets to be met by increasing the renewable energy share in their energy mix.

In all countries, to a greater or smaller extend, the lack of subsidies and the very cheap electricity or even gas prices have been the main barriers for increasing RES capacity. Energy security, environment protection, economic growth and social responsibility are the key elements of sustainable development. Those countires have achieved significant progress and took big steps toward a cleaner and sustainable future. The use of distributed generation based on solar energy can help significantly in improving, at competitive cost, the electrification rate with social benefits to the local population. Despite solar power becoming competitive with the wholesale price of electricity in many regions across MENA, additional cost reductions are needed to make solar electricity fully competitive against conventional power sources in the long term.

References

[1] The Desertec Initiative, http://www.desertec.org, (13-09-2017).

[2] I. Sakr F.A. Daghestani, W.R. Gocht, H.F. Mulki. Solar energy applications in the Arab world, *Proceedings of the International Seminar on appropriate technology in the fields of solar and wind energy applications*, Royal Scientific Society, Amman, Jordan, 1987.

[3] Solar Surges in the Middle East and North Africa, http://www.renewableenergyworld.com, (03/11/2017).

[4] US Department of Energy. Energy Information Administration, EIA. UAE country analysis briefs; February 2004. http://www.eia.doe.gov/emeu/cabs/uae.html , (03/11/2017).

[5] A. Kazim, T.N. Veziroglu. Utilization of solar-hydrogen energy in the UAE to maintain its share in the world energy market for the 21st century, *Renew Energy*, 2001, 24, pp. 259-274.

[6] A. Mokri, M. Aal Ali, M. Emziane. Solar energy in the United Arab Emirates: A review, *Renewable and Sustainable Energy Reviews*, 2013, 28, pp.340-375.

[7] W. Alnaser, N. AlnaserSolar and wind energy potential in GCC countries and some related projects, *Journal of Renewable and Sustainable Energy*, 2009, 1.

[8] A. Hepbasli, Z. Alsuhaibani, A key review on present status and future directions of solar energy studies and applications in Saudi Arabia, *Renewable and Sustainable Energy Reviews*, 2011 15(9), pp. 5021-5050.

[9] Presidency of Meteorology and Environment in Saudi Arabia. *General Environmental Law and Rules for Implementation*, 2001.

[10] S. Rahman, A. Castro. Environmental impacts of electricity generation: A global perspective *IEEE Trans. Energy Convers.*, 1995, 10 (2), pp. 307-314.

[11] Integrated Solar Energy Generation Project, Kingdom of Morocco. www.one.org.ma, (13-10-2017).

[12] C. Richts, The Moroccan solar plan—a comparative analysis of CSP and PV utilization until 2020. Faculty of Electrical Engineering and Computer Science, University of Kassel, 2012.
[13] Ministry of Finance, http://www.moneoman.gov.om/stat_book/2006/fscommand/english/ins/genin.htm, (09/11/2017).
[14] R.H.B. Exell Mapping solar radiation by meteorological satellite, *Renewable Energy Review Journal*, 1984, 6 (1).
[15] Oman's Renewable,http://www.nortonrosefulbright.com/knowledge/publications/75892/omans-renewable-energy-potential-solar-and-wind, date of access (4/12/2017).
[16] Ongoing Projects, Oman Gulf Comany, http://www.omangulf.com.om/Ongoing-Projects, date of access (01/12/2017).
[17] A., A. Saeed. Peak Load Forecast for Saudi Arabia Electric Power Generation. King Fahd University of Petroleum & Minerals, 1979.
[18] S.A. Al-Ajlan, A.M. Al-Ibrahim, M. Abdulkhaleq, F. Alghamdi. Developing sustainable energy policies for electrical energy conservation in Saudi Arabia, *Energy Policy*, 2006, 34, pp. 1556-1565.
[19] Inside MENA Countries' Solar Energy Plans, http://www.renewableenergyworld.com/articles , (01/12/2017).
[20] Al-Radady, A. Salman, M.K. Goknil. Study of air pollutants and their effects on the environment and public health in Yanbu industrial city, King Abdulaziz University, 1999.
[21] B. Brand. The Renewable Energy Targets of the MENA Countries: Objectives, Achievability, and Relevance for the Mediterranean Energy Collaboration, In Regulation and Investments in Energy Markets, edited by A. Rubino, M. Campi, V. Lenzi et I. OzTurk (Eds), pp. 89-100.

Implementation of waste materials from the energy sector in the construction industry

Kinga Klima [1], Natalia Czuma [1], Katarzyna Zarębska [1], Paweł Baran [1]

[1]Faculty of Energy and Fuels, AGH University of Science and Technology in Krakow, e-mail: kingaklima7@gmail.com, nczuma@agh.edu.pl, katarzyna.zarebska@agh.edu.pl, baranp@agh.edu.pl

Abstract

For several years, there has been an increasing interest in the protection of natural resources and minimization of the environment impoverishment in Poland and worldwide, which is why alternatives to conventional building materials have been sought. Nowadays, an ordinary Portland cement is the world's leading construction material and it is used in the amount of 4 million tonnes per year, with an annual growth rate is up to 4% per year. The main problem with Portland cement is its production, which is very energy-intensive and releases very large amounts of carbon dioxide into the atmosphere. In addition, the disposal of industrial waste such as fly ash, ground granulated blast-furnace slag or mining waste has become a major problem, because it requires a large usable area and has a huge impact on the environment. Geopolymers turn out to be one of the best solutions, because they can reduce CO_2 emissions into the atmosphere by 80% and thus contribute to reduce the global warming. From the last decade, geopolymers appear as the new building material and have a great potential to become an outstanding building product of good durability.

Keywords: : Geopolymers, natural resources, building materials, fly ash, industrial waste

1. Geopolymers

1.1. Structure

Geopolymers often determined as polysilanes are synthetic, amorphous, inorganic aluminosilicate polymers with specific composition and properties. They consist of long chains (copolymers) of aluminosilicon and silicon, stabilizing them with metal cations – most often sodium of potassium or lithium and bound water. In addition to polymeric chains, various phases can be found in the material, e. g. crystallized aluminosilicates of zeolite-type, unreacted aluminosilicate substrate or silicon oxide. The polymeric chain, the basic element of silane construction consists of four-layer structures SiO_4^{4-} and AlO_4^{5-} connected by oxygen atoms in two- or three-dimensional complex network(equation 1). The empirical formula describing geopolymers is as follows:

$$M_n[-(SiO_2)_z - AlO_2]_n \cdot wH_2O \tag{1}$$

where M denotes an alkali cation, n represents the degree of polycondensation, and z is the Si/Al ratio. It is important that the existence of complex spatial structures similar to cage structure makes them similar to those found in zeolites, and the main difference is lack of long-range order.

1.2. Properties of material

Properties of obtained building material in fact depend on the property of used components, their proportion and conditions of syntheses. With reference to the above, geopolymers to a considerable degree can differ between themselves. However, there are several features that are common to the whole group, among others short binding time. Already after four hours ripening in temperature of 20°C, they gain compressive strength within the limits of 20 MPa, and after 28 days from 70 to 100 MPa. Thanks to such features as high early strength, low shrinkage, resistance to high and low temperatures, as well as great corrosion resistance, they can

be used in many other construction fields. In addition, geopolymers are characterized by a low permeability comparable to natural granite, good fire and acid resistance, as well as lower shrinkage than Portland cement and good resistance to freezing and defrosting cycles [11,12]. Materials obtained from different raw materials showed recalled properties.

Geopolymers are presently developed and applied in 10 main classes of materials [2] :

- Waterglass-based geopolymer, Si:Al=1:0
- Kaolinite / Hydrosodalite-based geopolymer, Si:Al=1:1
- Metakaolin MK-750-based geopolymer, Si:Al=2:1
- Calcium-based geopolymer, Si:Al=1, 2, 3
- Rock-based geopolymer, 1< Si:Al<5
- Silica-based geopolymer, Si:Al>5
- Fly ash-based geopolymer
- Ferro-sialate-based geopolymer
- Phosphate-based geopolymer, $AlPO^{4-}$ based geopolymer
- Organic-mineral geopolymer

Moreover, various types of activators were used: sodium and potassium water glass, NaOH, KOH. It results that selection of raw material and activator has a significant impact on the reduction of production costs of materials.

1.3. Applications

The main proposed application of geopolymers is preparation of various types of building materials, and above all concrete containing a binder formed on the basis of aluminosilicate instead of classical cement. The building materials we have received include, among others facade panels, bricks, curbs, paving flags, cobblestones or decorative elements. Geopolymers are also used in some specific cases, where high geopolymers are required, and geopolymers have become standard material for fire protection in the aviation industry [4]. Geopolymers are also used in situations where high hardness is required very quickly. This is the case, e.g. in emergency runway repairs. Recently they have also been used as carrier material for utilization of toxic waste, and in particular radioactive substances [5].

1.4. Fabrication

Depending on the source material, geopolymers are obtained on the basis of blast-furnace cinder, volcanic tufa, perlite, fly ash, and iron minerals.

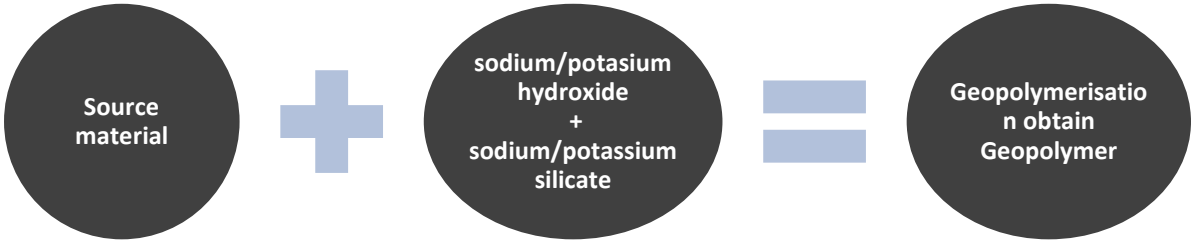

Fig. 1 The general manufacturing process, presented the following scheme

Selection and modification of both the base material and optimization of synthesis conditions is the essence of many studies. The process parameters determine the improvement of geopolymer properties, and it is also possible to obtain new, expected characteristics of dedicated building material.

The geopolymerization mechanism includes three main steps:

- Dissolution of silicon and aluminium atoms in raw material, generally metakaolin;
- Re-orientation of the ions in the solution;
- Poly-condensation reactions leading to the development of inorganic polymers

2. Applied materials

This work provides a literature review on the possibility of using fly ash and perlite expanded to the production of building materials with increased structural strength or insulation properties and fire-proof.

2.1. Fly Ash

Fly ash, which is a combustion product both of hard coal and lignite, is collected by electrostatic precipitators or fabric filters in coal-fired plants. The annual production of fly ash from coal combustion worldwide was about 800 Mtons, and only 20-30% was utilized. The possibility of production of the useful building material from waste material has hallmarks of environmental action. By definition, fly ash is finely gritted dust, consisting mainly of spherical, vitrified grains, obtained by burning coal dust, which has pucolane properties and contains primarily SiO_2 and Al_2O_3 in its composition, with a reactive SiO_2 content of at least 25% by weight. The properties of fly ash are determined by many factors, the most important are:

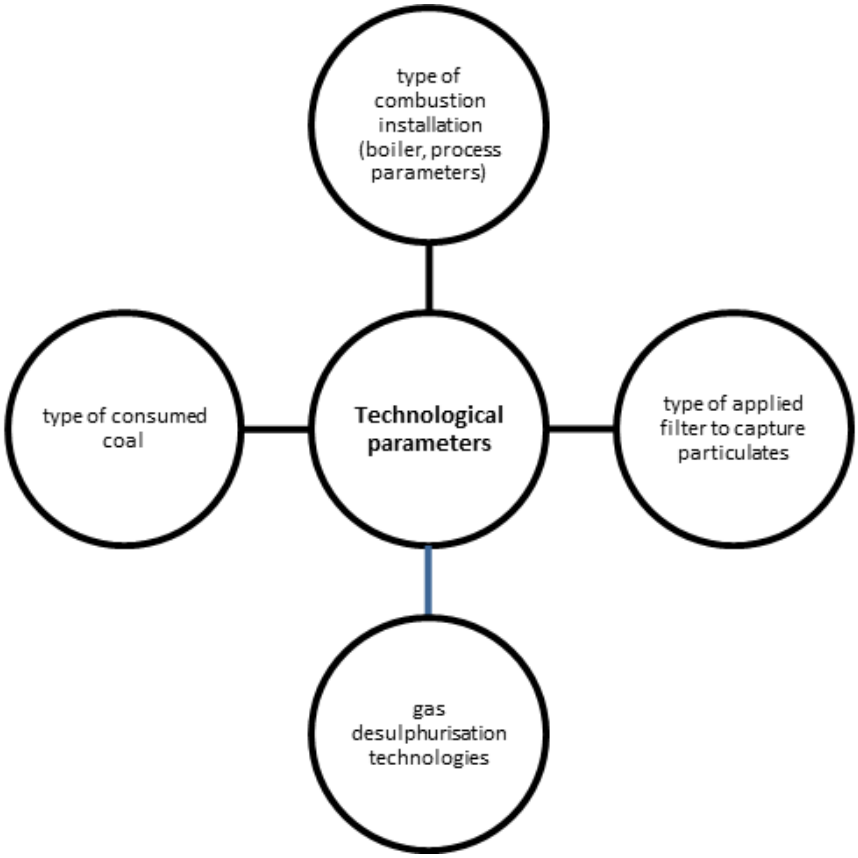

Fig. 2 The technological properties of fly ash

The most extensive applications for cement and concrete technologies are siliceous fly ash. The basic components of siliceous fly ash are: SiO_2 and Al_2O_3, Fe_2O_3, CaO, SO_3, MgO, Na_2O and K_2O, while undesirable components include not-consumed coal content and excessive calcium content. The diversified grain composition has a great influence on the ash water yield. Siliceous fly ash mainly consists of spherical particles with diameter of 3 to 40 μm; in addition the thick fractions include vitreous slag and quartz. Most of the methods

of this synthesis are based on mixing fly ash with aqueous solution of suitable silicate and strong alkali – usually with sodium or potassium hydroxide. The term of zeolite precursor for volatile ash mixtures activated in alkaline environments at high temperatures is often used in literature. The process takes into account the dissolution of active ash components in a strong alkaline solution, and then formation of the gel phase of aluminosilicates undergoes crystallization at high temperature. Literary data emphasize the important role of ash type in strength parameters of geopolymeric material. In the light of studies, ultrasonic siliceous ashes enable to obtain higher compressive strength values. However, the time and parameters of leaven ripening, i.e. temperature and time of heating and cooling the samples, should be taken into account. Parameters of hardened geopolymer balls compared with the leaven and the Portland cement base give comparable results, which has a promising influence on gradual displacement of cement by waste fly ash.

2.2. Perlite

Natural perlite is a glassy post-volcanic rock, from a minearological point of view. It is a transformed magma-like pouring rock made of volcanic glaze formed in ancient geological eras (volcanic rhythmic glaze). Hundreds of millions years ago, during the eruption of undersea volcanoes, the lava quickly stagnated in contact with water and closed its droplets, which today – hidden in a stagnant and sagging lava – constitute from 2 to 5% of its volume and determine the specific properties of this mineral. It is a hydrated acidic potassium-sodium aluminosilicate, containing also other elements. Its composition is mainly:

Tab. 1 Qualitative analysis of perlite

Composition	**%**
Silica SiO_2	70-75
Alumina Al_2O_3	12-15
Sodium oxide Na_2O	3-4
Potassium oxide K_2O	3-5
Iron oxide Fe_2O_3	0,5-2
Magnesium oxide MgO	0,2-0,7
Calcium oxide CaO	0,5-1,5

The amount of perlite consumption in Poland is difficult to estimate due to the lack of statistics, but with a high probability it can be assumed that it ranges between 4 and 6 thousand ton per year and continues an upward trend. In comparison, the global consumption of this raw material reaches over 3 million tons. The Polish economy "consumes" a little over 0.15% of this amount. In terms of thermal and acoustic insulation, they are one of the best building materials in the world. It is possible to prepare them with wet or semi-dry method from perlite and cement, or to produce as ready, dry blends for use on the site after mixing with water. Numerous studies on this material with X-ray fluorescence technique showed that this material is an amorphous volcanic glass, rich in silica and aluminum oxide, containing crystalline phases of among others quartz, calcite and biotite. Perlite, belonging to the group of thermally treated pucolane at a temperature of approximately 900^{o}C to remove pore water and produce bubbles that enable to increase the volume of material 10-15 times. After the process, perlite is called expanded, with white-beige color. Taking into account the perlite propagation properties in strongly alkaline environment, it is possible to obtain geopolymer with highly insulating properties, relatively low mass, good acoustic and fire resistant properties. Perlite paste treated with a strong 2-12M sodium or potassium alkali in the presence of water glass or alternatively with perhydrol, transforms into a mobile phase subjected to temperatures up to 100^{o}C.

Techniques of geopolymer synthesis obtained only on the basis of expanded perlite are still developed in numerous research units, currently used as an additive to Portland cement, in mixtures with fly ash and as heat-insulating mortars. Obtaining geopolymer from perlite characterized by high strength properties is quite a challenge due to the nature of base material and the need to modify synthesis conditions.

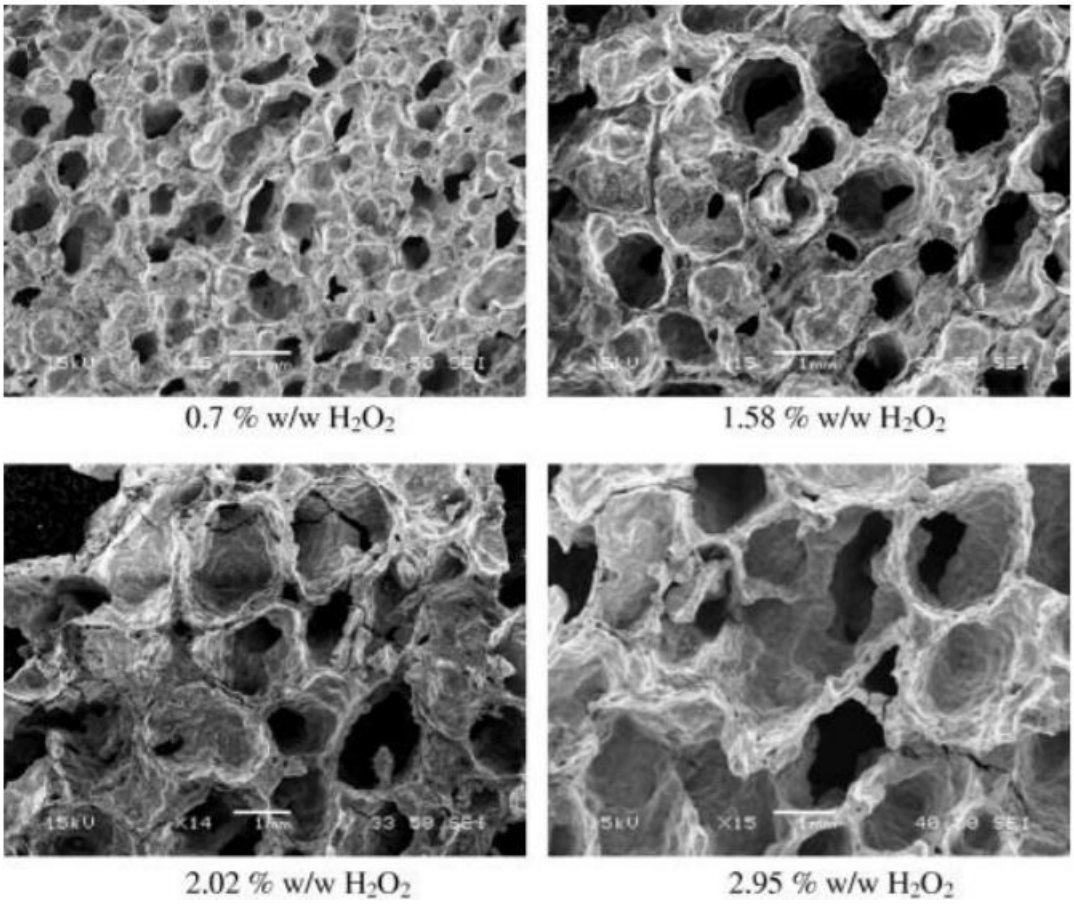

Fig. 3 SEM photos of foamy materials prepared with different H2O2 content in the geopolymeric paste [3]

3. Conclusions

Summing up, the reduction of carbon dioxide emission for geopolymer cements makes them a good alternative to the Portland cement, which is characterized by both higher emission and costs. Further development of geopolymer synthesis technology allows for production of materials with dedicated properties, which are not only a binder with strength parameters, but also thermally and acoustically insulated. In the case of natural insulating material – perlite, it is also possible to obtain refractory materials, which hypothetically can affect the quality and safety of newly formed construction structures. The technologies of utilization and modification of fly ash over recent years developed dynamically, which is related to both the synthesis of zeolite and geopolymers. These materials show good properties in acidic and strongly saline environments. At first used as admixtures to cement slurries, over time they became the basis for their preparation, and their similarity with the original Portland cement allows for reduction of production costs, emission of carbon dioxide to the atmosphere and waste disposal, included in the catalogue of waste. Dynamically conducted research may significantly improve and implement modern materials used in the construction industry.

References

[1] P. Pavithra , M. Srinivasula Reddy , P. Dinakar , B. Hanumantha Rao , B.K. Satpathy , A.N. Mohanty A mix design procedure for geopolymer concrete with fly ash" ,Journal of Cleaner Production 133 117-125, 2016.
[2] What is a geopolymer? Introduction https://www.geopolymer.org accesed 07.07.2017.
[3] V.Vaou, D.Panias „Thermal insulating foamy geopolymers from perlite" Minerals Engineering Volume 23, Issue 14, Pages 1146-1151, November 2010.
[4] Geopolymer Institute "Fire proof, heat resistant composites", 7 April 2006.

[5] D.C.Comrie, J.H. Paterson, D.J. Ritcey "Applications of geopolymer technology to waste stabilization" D. Code Consulting Ltd. 120 Traders Boulevard East Suite.
[6] T.Bakharev "Geopolymeric materials prepared using Class F fly ash and elevated temperature curing" - Cem. Concr. Res. 35: 1224-1232. 2005.
[7] M.Łach, K.Korniejenko, J.Mikuła „Thermal Insulation and Thermally Resistant Materials Made of Geopolymer Foams" Procedia Engineering, Volume 151, Pages 410-416, 2016.
[8] Fenghong Fan, Zhen Liu, , Guoji Xu, Hui Peng. C.S. Cai „Mechanical and thermal properties of fly ash based geopolymers" Construction and Building Materials Volume 160, Pages 66–81, 30 January 2018.
[9] M.Łach „J.Mikuła „Wytwarzanie i właściwości geopolimerów na bazie tufu wulkanicznego" Inżynieria Materiałowa, Vol. 35, nr 3, pages 270—276, 2014.
[10] K.Rajczyk, E.Giergiczny, M.Szota „Mikrostruktura i właściwości stwardniałych spoiw geopolimerowych z popiołu lotnego" Prace ICiMB nr 23, 79-89, ISSN 1899-3230, 2015.
[11] Z. Yunsheng S. Wei , L. Zongjin , Z. Xiangming , Eddie , C. Chungkong "Impact properties of geopolymer based extrudates incorporated with fly ash and PVA short fiber" Construction and Building Materials 22, 370–383, 2008.
[12] J. Davidovits „30 Years of Successes and Failures in Geopolymer Applications. Market Trends and Potential Breakthroughs." Geopolymer 2002 Conference, October 28-29, Melbourne, Australia, 2002.

Combustion Modelling of Circulating Fluidized Bed Furnace

Hafiz Umar Ali[1], Majid Ramzan[2], Muhammad Umar Hussain[2], Prof. Dr. Nasir Hayat[2]

[1]Silesian University of Technology, email: hafizumarali@gmail.com
[2]Mechanical Engineering, UET Lahore, e-mail: nasirhayat@uet.edu.pk

Abstract

Seven samples of coal available in various mines of Punjab were collected and their proximate and ultimate analyses were carried out. Higher Heating Values and Lower Heating Values of these samples were experimentally determined. A 12 MW (Loses=2MW) Circulating Fluidized Bed system has been designed based on these 7 samples to explore the possibility of coal based power generation in Punjab. Hydrodynamics and Combustion characteristics for Circulating Fluidized bed were specified. By using Microsoft Visio, temperature profile of CFB bed for these 7 samples was plotted. Moreover, the MATLAB code was also developed for temperature, Higher Heating Values and Lower Heating Values. Stoichiometric Calculations shows that Pakistani coal requires much more Lime stone for the Sulphur removal as compared to the standard Bituminous coal and it is suitable for small grid power plants. The result shows that there exists a variation among the sample in terms of Cyclone Temperature i.e. (T3). The best performance was shown by the sample 1 with Cyclone 423 ℃ for 0.462 Kg/s coal feed rate and 40% of Primary air (2.7Kg/s). Whereas the minimum value was found for sample 3 with Cyclone temperature 381℃ with their percentage decrease of 9.9%.

Keywords: Higher heating values, lower heating values, stoichiometric calculations, power, coal

1. Introduction

Electricity in Pakistan is a very common topic these days. Lack in power generation requires coal having less sulphur and nitrogen oxides contents. In our project, we designed a 12 MW circulating fluidized bed system and took 7 samples of coal from Punjab Province, specified their hydrodynamic and combustion characteristics, developed a matlab code for higher heating value, lower heating value and obtained results which are mentioned in the later sections of the article. The article is structured in the following sections:

- Introduction
- Methodology and Experimental setup
- Mathematical Modeling and result analysis

2. Methodology and experimental setup

The circulating fluidized bed (CFB) is a clean process with the ability to achieve lower emission of pollutants. By using this technology, up to 95% of pollutants will be absorbed before being emitted to the atmosphere. At the same time, the advantages of this technology outweigh the limitations, which made it favorable. However, the development of this technology is still at its early stages. With further R&D, this technology is predicted to bring numerous benefits to our society. Stationary or bubbling fluidized bed is the classical approach where the gas at low velocities is used and fluidization of the solids is relatively stationary, with some fine particles being entrained. On December 16, 1921 in Germany, Fritz Winkler introduced gaseous products of combustion into the bottom of a crucible containing coke particles; the event marked the beginning of a very important chapter of modem technology. Winkler saw particles lifted by the drag of the gas and the mass of particles looked like a boiling liquid (Squires, 1983). This little experiment initiated a new process called Fluidization.

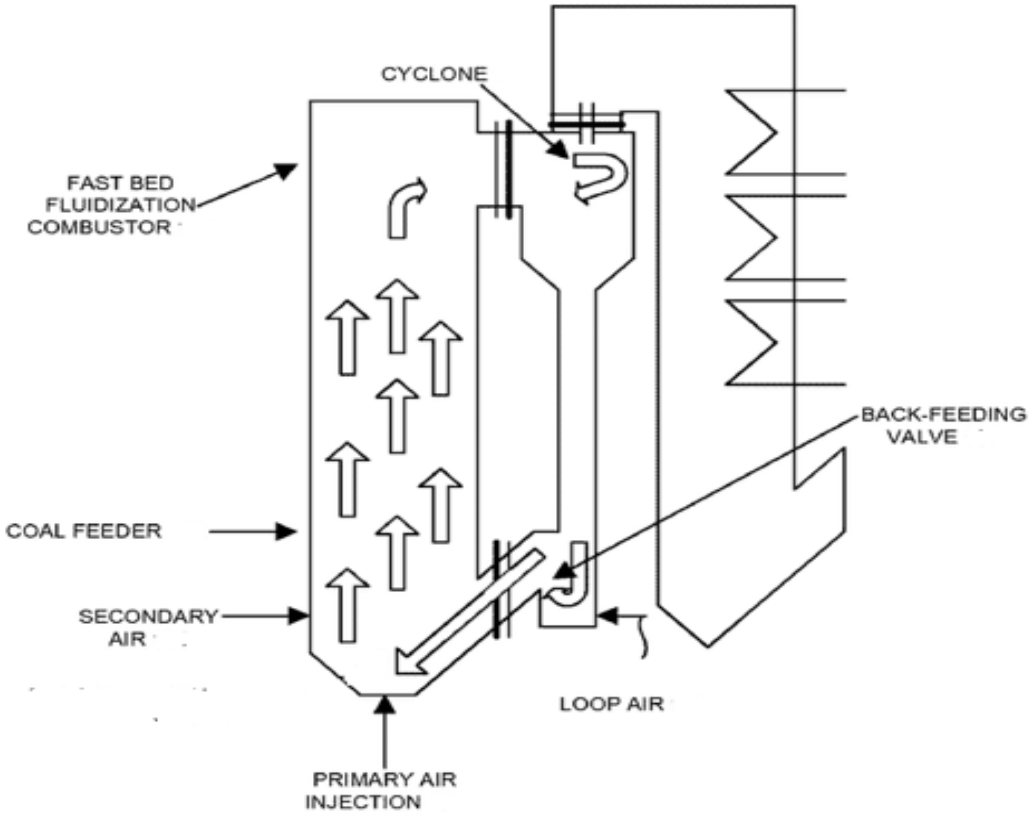

Fig.1 Schematic diagram of Fluidization process

3. Mathematical modelling and result analysis

Tab.1 Values of different parameters collected through samples

Sr No.	Symbols	Statements	Sample 1	Sample 2	Sample 3	Sample 4	Sample 5	Sample 6	Sample 7
1	C	Weight fraction of carbon in coal	0.48	0.449	0.3429	0.405	0.4547	0.3854	0.4375
2	N	Weight fraction of nitrogen in coal	0.0126	0.0094	0.0073	0.0064	0.008	0.0061	0.006
3	H	Weight fraction of hydrogen in coal	0.0434	0.0438	0.034	0.0429	0.0436	0.0381	0.0443
4	S	Weight fraction of sulphur in coal	0.08	0.0884	0.0785	0.072	0.0572	0.0678	0.0732
5	Mf	Moisture content of coal, kg/kg	0.0648	0.0687	0.0698	0.0867	0.0778	0.0381	0.0642
6	O	Weight fraction of oxygen in coal	0.1054	0.1225	0.1148	0.1466	0.1377	0.1008	0.130
7	ASH	Weight fraction of ash in coal	0.27	0.287	0.2322	0.3268	0.2948	0.2333	0.2553
8	Xinert	Weight fraction of inert in dry air	0.034	0.032	0.0274	0.0371	0.0349	0.0244	0.0265
16	Mda	Weight of dry air required per unit of coal, kg/kg	6.9734	6.5643	4.9873	5.8553	6.4139	5.6294	6.3410
17	Tda	Total dry air to be supplied to fire unit weight of coal, kg/kg	8.3681	7.8771	85.9848	7.0264	7.6967	6.7553	7.6092
18	Mwa	Weight of wet air required per unit of coal, Kg/Kg	8.4769	7.9795	6.0626	7.1177	7.7968	6.8431	7.7081
19	R	Calcium to sulfur molar ratio in the feed to the boiler	1.9146	1.9160	1.9054	1.8968	1.8701	1.8904	1.8985
20	Lq	Limestone Required per unit of weight of coal fired, kg/kg fuel	0.4685	0.4764	0.4207	0.3841	0.3009	0.3605	0.3909
21	Wf	Total weight of fly ash	9.1231	8.6380	6.6370	7.7666	8.4106	7.3596	8.3233
22	Ws	Total weight of sorbents	0.2157	0.2185	0.1907	0.1776	0.1380	0.1620	0.1767
23	HHV	Higher Heating value of fuel	2.1414e+04	2.0128e+04	1.5172e+04	1.7938e+04	1.9724e+04	1.7352e+04	1.9521e+04
24	LHV	Lower Heating value of fuel	2.0266e+04	1.8961e+04	1.4223e+04	1.6745e+04	1.8538e+04	1.6393e+04	1.8353e+04

The equations used in these calculations are as follows:

$$Mda = 11.53 \cdot \mathrm{C} + 34.34 \cdot (\mathrm{H} - \mathrm{O}/8) + 4.34 \cdot \mathrm{S} + \mathrm{ASH} \cdot \mathrm{S} \quad (1)$$

$$\mathrm{Tda} = \mathrm{Mda}.\,1.2 \quad (2)$$

$$\mathrm{Mwa} = \mathrm{Tda}.\,(1 + \mathrm{Xm}) \quad (3)$$

$$\mathrm{R} = \mathrm{r} - ((32/56).\,(\mathrm{Xm}/\mathrm{S})) \quad (4)$$

$$\mathrm{Lq} = (100.\,\mathrm{S}/32.\,\mathrm{Xcaco3}).\,\mathrm{R} \quad (5)$$

$$\mathrm{Wf} = \mathrm{Mwa} - 0.2315.\,\mathrm{Tda} + 3.66.\,\mathrm{C} + 9.\,\mathrm{H} + \mathrm{Mf} + \mathrm{Lq}.\,\mathrm{Xml} + \mathrm{N} + 0.25.\,\mathrm{S} + \mathrm{S}.\,3.025 + 0.15.\,\mathrm{ASH} \quad (6)$$

$$\mathrm{Ws} = 1.03.\,\mathrm{S}.\,\mathrm{Esorb} + 56.\,\big((\mathrm{Lq}.\,\mathrm{Xcaco3})(\mathrm{Esorb}.\,\mathrm{S}/32)\big) + 0.476.\,\mathrm{q}.\,\mathrm{Xmgco3} + \mathrm{Lq}.\,\mathrm{Xinert} \quad (7)$$

$$\mathrm{HHV} = 33823.\,\mathrm{C} + 144249.\,(\mathrm{H} - \mathrm{O}/8) + 9418.\,\mathrm{S} \quad (8)$$

$$\mathrm{LHV} = \mathrm{HHV} - 22604.\,\mathrm{H} - 2581.\,\mathrm{Mf} \quad (9)$$

4. Conclusions and discussions

For the Pakistani coal, that it can be used for small grid power plants as compared to the Standard Bituminous Coal because it is clear form the above results it will consume more Lime stone /Kg . Which certainly limits its use in large size operations as we need to feed 0.4 Kg of Lime stone for one 1Kg of coal entered so as we increase the size of the plant the coal feed rate increases and consequently we have to feed more and more Limestone to remove that Sulphur. As also the Sulphur removal action involves the Calcination reaction which in endothermic reaction so this reaction will consume energy from the heat released by the burning of the coal. So when we will increase the size of the Circulating Fluidized Bed Furnace power plant, heat loss will also increase. The values for the temperatures are low because of lower HHV of the fuel . Also we are getting lower values of temperatures for the Standard Bituminous Coal sample because we assumed many values during our calculations for the heat balance around the circulating fluidized bed furnace. The reason behind using the CFB furnace is the perfect mixing of the fuel particles with the air due to the continuous moment of the fuel particles in the furnace which increases combustion efficiency. Also high residence time enables CFB furnace to capture the Sulphur up to 90 % in the furnace which is not possible in any type of the furnace. It produces negligible amount of the NOx because of the Non-Stoichiometric combustion in the lower furnace which converts the atomic nitrogen to the molecular nitrogen which remains inert until the very high temperature. So it was concluded that Pakistani coal can be used for power Generation in CFB furnace but for low capacity power plants.

5. Acknowledgment

For acknowledgement, I would like to mention my Dean of Mechanical Engineering Department Prof. Dr. Nasir Hayat, and my other colleagues namely Majid Ramzan and Muhammad Umar Hussain from University of Engineering and technolgy Lahore, Pakistan.

References

[1] P. Basu, Combustion and gasification in fluidized beds. CRC press, 2006.

[2] Furusawa, T. Shimizu (1988). "Analysis of Circulating Fluidized Bed Combustion Technology and Scope for Future Development," in Circulating Fluidized Bed Technology II, P. Basu and J. F. Large, eds., Pergamon Press, Oxford, pp. 51-62.

[3] Weiss, J. Scholer, and F. N. Fett (1988). "Mathematical Modeling of Coal Combustion in a Circulating Fluidized Bed Reactor," Circulating Fluidized Bed Technology II, Ed. P. Basu & J.F. Large, Pergamon Press, Oxford, pp. 289-298.

[4] B. Costa, D. Faille, O. Lamquet, C. Marchiondelli, S. Spelta. Dynamique modeling of a 250 Mwe CFBboiler, 16th Inter. Conf. On FBC, Reno, Nevada, may 2000.

[5] P. Basu, P.K.Haider (1989)."A New Concept for Operation of a Pulverized Coal-fired Boiler using Circulating Fluidized Bed Firing," Trans, of ASME, J. of Engineering for Gas Turbines and Power, 111, pp. 626-630.

[6] J. Biswas, L. E. Leung (1987). "Applicability of Choking Correlations for Fast-Fluid Bed Operation," Powder TechnoL, 51, pp. 179180.

[7] P. A Jones, T. J. Hellen and Friedman (1989). "Determination of Heat Loss due to Surface Radiation and Convection from the CFB Boiler at NUCLA," Proc. 10th FBC Conference, A. Manaker, ed., pp. 10471052.

[8] Chen W, Jiang P (2011) Design and operation of CFB with compact separator. In: PowerGen Asia 2011 Conference Proceedings. Kuala Lumpur, Malaysia, 27-29 Sep 2011, 9 pp (Sep 2011).

Authors Index

Published by Department of Technologies and Installations of Waste Management, Silesian University of Technology

This release is an activity of InnoEnergy Clean Fossil and Alternative Fuels Energy M.Sc. program students.

The following publication consists of articles presented during the Environmental Protection and Energy Conference at Silesian University of Technology in Gliwice, 2017

ISBN 978-83-950087-1-9

Clean Alternative

POLITECHNIKA ŚLĄSKA

KTiUZO

eit InnoEnergy
Knowledge Innovation Community